

Schlumberger

Reservoir and Production Fundamentals



FOREWORD

The study of Petroleum Engineering covers a broad spectrum of geology, physics and applied mathematics spanning the geological processes by which hydrocarbons are formed and accumulated into reservoirs, the properties of reservoir rocks and the behavior of formation oil, water and gases during the process of extraction.


This booklet was distilled from the mass of literature available on the subject with the objective of providing the incoming engineer with an overall view of the industry and with the fundamentals of reservoir and production that a Schlumberger general field engineer requires.

The reservoir and wells are interacting elements of a composite system in which the well provides access to the reservoir and is the means by which measurements (and our revenues) are made. Considerable emphasis is placed on well performance and testing as these are areas of direct involvement with our Production logging and well completion services.

With the advent of computer log processing, field integrated log analysis has become possible and reservoir mapping of reserves is a developing extension of our logging activities into reservoir management.

The study of fractured reservoirs would normally be considered beyond the scope of an introductory petroleum engineering course. However, due to the great importance of this unconventional type reservoir to Middle East oil production, Chapter 10, written by Prof. Van Gold Racht of the University of Trondheim, has been included summarizing the subject.

We would like to thank Manfred Wittmann and Dr. G. Stewart of EHS Marketing PR for their help in reviewing the draft of this booklet.



J. Aitken
MEA July 1980

CONTENTS

Chapter

Page

<u>1.- Introduction</u>	1-1
A. Conditions favorable for hydrocarbon reservoir formation	1-1
B. Oil field units of measurement	1-2
C. SI oilfield units	1-3
<u>2.- Geology and hydrocarbon accumulations</u>	2-1
A. Introduction (geological terminology)	2-1
B. Historical geology	2-2
C. Structure of the earth	2-4
D. Classification of rocks	2-7
E. The origin and habitat of oil	2-11
F. Hydrocarbon reservoirs	2-13
G. Sub-surface mapping	2-16
H. Reservoir temperature and pressure	2-17
<u>3.- Reservoir Fluid behaviour</u>	3-1
A. Classification of oil and gas	3-1
B. Phase behaviour in hydrocarbon reservoirs	3-4
C. Reservoir fluid properties	3-11
1) source of fluids data	3-11
2) compressibility of gases	3-12
3) conversion factors between surface and downhole volumes	3-16
a) gas formation volume factor, B_g	3-17
b) oil formation volume factor, B_o	3-19
c) water formation volume factor, B_w	3-23
4) fluid density correlations	3-24
5) viscosity correlations	3-26
D. Rock compressibility	3-28
E. Appendix - Fluid Conversion Charts	3-29
<u>4.- Reservoir Rock properties</u>	4-1
A. Porosity	4-1
B. Permeability	4-3
C. Measurement of permeability	4-6
D. Measurement of porosity	4-8
E. Measurement of capillary pressure (mercury injection)	4-9

<u>5.- Surface-tension-wettability-capillarity-saturation</u>	5-1
A. Surface tension	5-1
B. Wettability	5-3
C. Capillarity	5-4
D. Repartition of saturation in reservoir rocks	5-6
E. Irreducible water saturation	5-7
F. Displacement pressure	5-8
G. Displacement of oil	5-9
H. Residual oil	5-11
I. Relations between permeabilities and fluid saturations	5-13
J. Relative permeability - Saturation correlations	5-15
<u>6.- Reservoir drive mechanisms</u>	6-1
A. Oil reservoirs	6-1
B. Solution gas drive reservoirs	6-2
C. Gas cap expansion drive reservoirs	6-3
D. Water drive reservoirs	6-4
E. Discussion of recovery efficiency (including gravity drainage)	6-5
<u>7.- Well performance</u>	7-1
A. Nomenclature and model for ideal cylindrical flow	7-1
B. Radius of drainage	7-4
C. Well pressure drawdown	7-5
D. Productivity index and specific productivity index	7-5
E. Formation damage	7-6
F. Formation improvement	7-8
G. Skin factor	7-8
H. Skin damage in perforated completions	7-9
I. Inflow production relation - IPR	7-10
J. Evaluation of a formation treatment with IPR	7-11
K. Composite IPR of multi-zone completion	7-12
L. Cross flow between zones	7-13
M. Water cut vs. production rate	7-14
N. Performance of flowing oil wells	7-15
O. Simulator - single well model	7-20
<u>8.- Reservoir Estimates</u>	8-1
A. Volumetric methods	8-1
B. Calculation of the reserve	8-2
C. Uncertainty in reservoir estimates	8-3
D. Field integrated log analysis and reservoir mapping services	8-6
1) Normalization of data	8-8
2) Gridding and mapping	8-9
3) Monitoring fluid interface changes	8-9
E. Reservoir estimates - material balance methods	8-10
1) Material balance - gas reservoirs	8-10
2) Generalized material balance - oil reservoirs	8-13

<u>9.- Well testing and pressure transient analysis</u>	9-1
A. The DST (drill stem testing)	9-1
B. LTT (long term production test) of oil wells	9-4
C. Test procedures for high capacity gas wells	9-6
D. RFT - The wireline formation tester	9-10
E. Transient test techniques and analysis	9-11
F. Drawdown behavior	9-15
G. Pressure buildup analysis	9-18
1) Horner's method	9-19
2) MDH (Miller, Dyes, Hutchinson method)	9-22
H. Remarks concerning slope and shape of pressure drawdown curves	9-24
<u>10.- Fractured reservoirs</u>	10-1
A. Introduction	10-1
B. A physical description of a fractured reservoir	10-2
C. A comparison of conventional and fractured reservoir performance	10-3
D. Idealized model of a fractured reservoir	10-7
E. Description of the fracture process	10-8
F. Porosity and permeability	10-10
1) Determination of porosity	10-10
2) Permeability determination	10-11
G. Production mechanisms in the fractured reservoir	10-12
H. Discussion of displacement mechanisms	10-15
I. Steady state flow towards the well	10-17
J. Transient flow	10-19
1) Warren and Root method	10-19
2) Pollaird method	10-21
K. Appendix - Mathematical derivation of Warren and Root method	10-23
<u>11.- Appendix</u>	
A. Nomenclature - Practical oilfield units and symbols	11-1
B. Conversion factors between Practical oilfield units, Metric S.I. and other measures	11-3
C. Miscellaneous oil field conversions	11-12
D. Physical constants and values	11-13

INTRODUCTION

1

A. Conditions favorable for hydrocarbon reservoir formation

Three basic requirements must be fulfilled to accumulate oil and gas in a commercially exploitable reservoir.

First, the reservoir rock must possess sufficient void space, called porosity, to contain the oil and gas. Secondly, there must be adequate connectivity, or permeability, of the pore spaces to allow transportation of the fluids over large distances under reasonable gradients of pressure. Third, a sufficient quantity hydrocarbons must be accumulated into a trap of impervious cap rock which prevents upward migration of the oil and gas from the source beds, forming a petroleum reservoir.

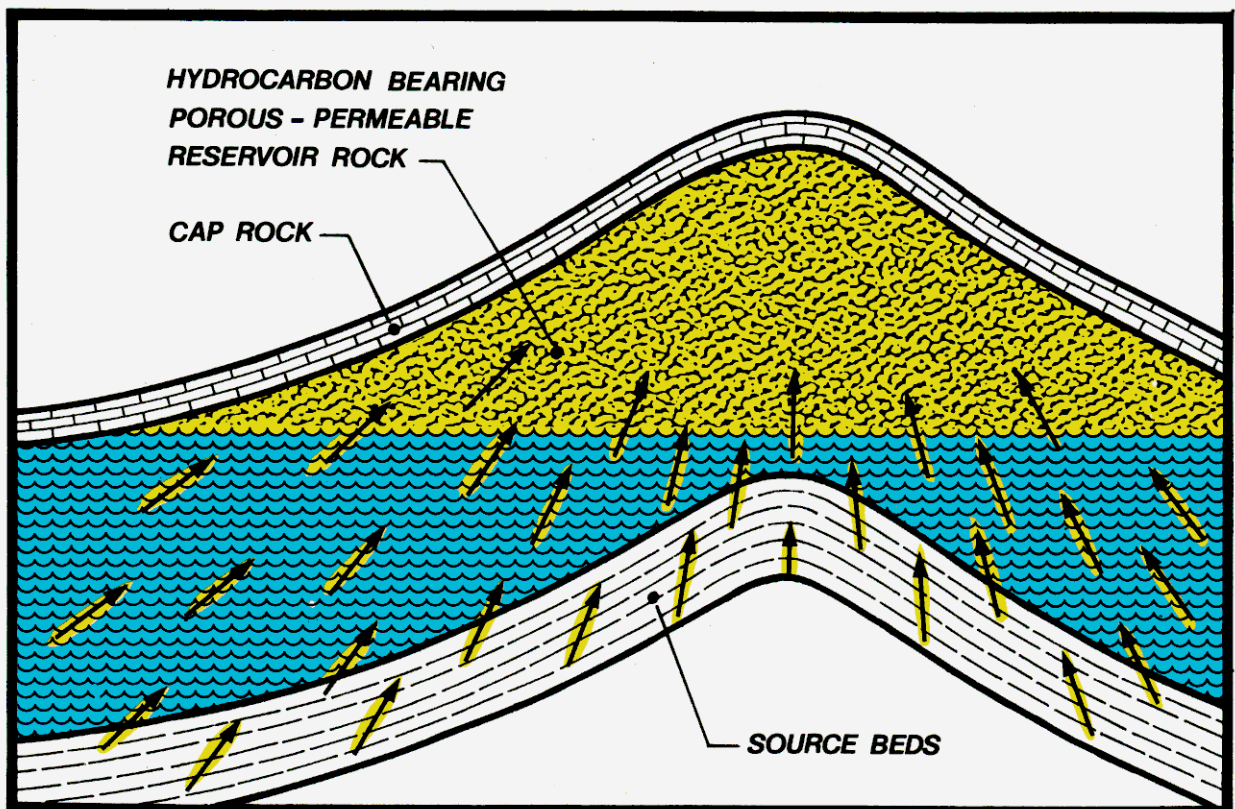


Fig. 1-1. Accumulation of oil and gas into a reservoir.

B. Oilfield units of measurement

Thus far no industry-wide standardization of units has occurred and a mixture of metric mks, cgs, SI, and "practical oilfield units" with its API barrels, cubic feet of gas and psi units are used.

It is expected that all countries will eventually standardize on metric SI* system of measurements. Standardization within the Petroleum industry, with only very minor variations in detail, has been launched in England, Canada and the U.S. Progress is slow however, and the preponderance of technical literature available today uses the "practical oilfield units" established by the AMIE (American Institute of Mining and Petroleum Engineering) in 1958.

Table 1-1 below compares units and quantities most frequently encountered in oil field practice.

Quantity	Practical Oilfield Unit	Coherent SI Unit
Volume, liquid	STB, stock tank barrel measured at 60°F, 14.65 psia	m ³ , cubic metre measured at 15°C, 1 atm = 101.35 kPa
Volume, gas	scf, standard cubic foot measured at 60°F, 14.65 psia	m ³ , cubic metre measured at 15°C, 1 atm
Production rate, liquid	STB/D, stock tank barrel per day	m ³ , cubic metre per second
Production rate, gas	scf/D, standard cubic feet per day	m ³ , cubic metre per second
Gas-oil ratio	scf/B, standard cubic feet per stock tank barrel	m ³ /m ³ , dimensionless
Pressure	psi, pounds per square inch	Pa, pascal = newton per square metre
Temperature, absolute	°R, degree Rankine	K, Kelvin
Time	hr., hour	s, second
Formation thickness	ft., feet	m, metre
Viscosity	cp, centipoise	Pa-s, pascal-second
Permeability	md, millidarcy	μm ² , square micrometre

Table 1-1. Comparison of units used in the oilfield.

* S.I. is the official abbreviation, in all languages, for the International System of units (le Système International d'unités)

C. A brief description of SI oilfield units

(Condensed from Technical Review article "Metrification in North America," Vol. 26 No 4)

SI is a coherent unit system of units and measures, essentially an up-graded version of mks, and is based on the meter, kilogram, second, ampere, kelvin, mole and candela. A list of SI base and supplementary units is given below :

Quantity	Unit Name	Unit Symbol	Remarks
BASE UNITS			
length	meter, or metre	m	U.S. spelling is "meter". Canadian and ISO (International Organization for Standardization) spelling is "metre".
mass	kilogram	kg	This is the only base unit having a prefix. In SI the "kilogram" is always a unit of mass, never a unit of weight or force.
time	second	s	The "second" is the base unit, but in practice other time units are allowable.
electric current	ampere	A	
thermodynamic temperature	kelvin	K	Note lower-case k in "kelvin", but cap K for unit symbol. No degree sign is used with "kelvin".
amount of substance	mole	mol	
luminous intensity	candela	cd	
SUPPLEMENTARY UNITS			
plane angle	radian	rad	These angular units are designated by ISO to be dimensionless with respect to the base quantities.
solid angle	steradian	sr	

Table 1-2. SI base and supplementary units.

Additional units obtained from base and supplementary units with a conversion factor of unity, are called "derived coherent units" - a list of examples is given in Table 1-4.

Table 1-3 lists prefixes for SI unit symbols used for multiples and sub-multiples. Note that some SI prefixes, conflict with those used with practical oilfield units.

For example, SI, "k" and "M" ("kilo" and "mega") correspond to $\times 1000$ and $\times 1\,000\,000$, whereas "M" and "MM", or "m" and "mm", have been used in the oil industry to designate "thousands" and millions of volume units of gas.

One inconvenience of the SI system is that many common oilfield quantities, pressure, production rate, permeability etc. must be expressed in unfamiliar unit multiples - which are not yet industry-wide standardized.

Multiplication Factor	SI Prefix for Unit Name	SI Prefix for Unit Symbol	Pronunciation (U.S.)
10^{18}	exa	E	ex' a (as in about)
10^{15}	peta	P	as in petal
10^{12}	tera	T	as in terrace
10^9	giga	G	jig' a (a as in about)
10^6	mega	M	as in megaphone
10^3	kilo	k	as in kilowatt
10^2	hecto	h	heck'toe
10	deka	da	deck'a (a as in about)
10^{-1}	deci	d	as in decimal
10^{-2}	centi	c	as in centipede
10^{-3}	milli	m	as in military
10^{-6}	micro	μ	as in microphone
10^{-9}	nano	n	nan'oh (an as in ant)
10^{-12}	pico	p	peek'oh
10^{-15}	femto	f	fem'toe (fem as in feminine)
10^{-18}	atto	a	as in anatomy

Table 1-3. SI unit prefixes.

For more complete information on use of SI units in well logging, refer to Technical Review Vol. 26, No 4.

Unless otherwise noted, practical oilfield units are used in this booklet. Nomenclature and a conversion factor table is given in the appendix, chapter 11.

Quantity	Unit Name	Unit Symbol	Expressed in Terms of Other Derived SI Units	Expressed in Terms of Base- and Supplementary-Unit Symbols
absorbed dose (of ionizing radiation)	gray (replaces the rad)	Gy	J/kg	$\text{m}^2 \cdot \text{s}^{-2}$
acceleration, linear	meter per second squared	m/s^2		$\text{m} \cdot \text{s}^{-2}$
activity (of radionuclides)	becquerel (replaces the curie)	Bq		s^{-1}
angular acceleration	radian per second squared	rad/s^2		$\text{rad} \cdot \text{s}^{-2}$
angular velocity	radian per second	rad/s		$\text{rad} \cdot \text{s}^{-1}$
area	square meter	m^2		m^2
capacitance (electrical)	farad	F	C/V	$\text{m}^{-2} \cdot \text{kg}^{-1} \cdot \text{s}^4 \cdot \text{A}^2$
charge (electrical)	coulomb	C	A · s	$\text{s} \cdot \text{A}$
conductance (electrical)	siemens* (replaces the mho)	S	A/V	$\text{m}^{-2} \cdot \text{kg}^{-1} \cdot \text{s}^3 \cdot \text{A}^2$
conductivity (electrical)	siemens per meter	S/m		$\text{m}^{-3} \cdot \text{kg}^{-1} \cdot \text{s}^3 \cdot \text{A}^2$
current density	ampere per square meter	A/m^2		$\text{A} \cdot \text{m}^{-2}$
density (mass)	kilogram per cubic meter	kg/m^3		$\text{kg} \cdot \text{m}^{-3}$
electromotive force	volt	V	W/A	$\text{m}^2 \cdot \text{kg} \cdot \text{s}^{-3} \cdot \text{A}^{-1}$
energy	joule*	J	N · m or W · s	$\text{m}^2 \cdot \text{kg} \cdot \text{s}^{-2}$
entropy	joule per kelvin	J/K		$\text{m}^2 \cdot \text{kg} \cdot \text{s}^{-2} \cdot \text{K}^{-1}$
field strength (electrical)	volt per meter	V/m		$\text{m} \cdot \text{kg} \cdot \text{s}^{-3} \cdot \text{A}^{-1}$
force	newton	N		$\text{m} \cdot \text{kg} \cdot \text{s}^{-2}$
frequency	hertz	Hz		s^{-1}
heat capacity	joule per kelvin	J/K		$\text{m}^2 \cdot \text{kg} \cdot \text{s}^{-2} \cdot \text{K}^{-1}$
heat, quantity of	joule*	J		$\text{m}^2 \cdot \text{kg} \cdot \text{s}^{-2}$
illuminance	lux	lx	lm/m^2	$\text{m}^{-2} \cdot \text{cd} \cdot \text{sr}$
inductance	henry	H	V · s/A (= Wb/A)	$\text{m}^2 \cdot \text{kg} \cdot \text{s}^{-2} \cdot \text{A}^{-2}$
luminance	candela per square meter	cd/m^2		$\text{cd} \cdot \text{m}^{-2}$
luminous flux	lumen	lm		$\text{cd} \cdot \text{sr}$
magnetic field strength	ampere per meter	A/m		$\text{A} \cdot \text{m}^{-1}$
magnetic flux	weber	Wb	V · s	$\text{m}^2 \cdot \text{kg} \cdot \text{s}^{-2} \cdot \text{A}^{-1}$
magnetic flux density	tesla	T	Wb/m ²	$\text{kg} \cdot \text{s}^{-2} \cdot \text{A}^{-1}$
magnetic permeability	henry per meter	H/m		$\text{m} \cdot \text{kg} \cdot \text{s}^{-2} \cdot \text{A}^{-2}$
neutron capture cross section	per meter (i.e., square meter per cubic meter)	1/m	m^2/m^3	m^{-1}
permittivity	farad per meter	F/m		$\text{m}^{-3} \cdot \text{kg}^{-1} \cdot \text{s}^4 \cdot \text{A}^2$
potential, potential difference (electrical)	volt	V	W/A	$\text{m}^2 \cdot \text{kg} \cdot \text{s}^{-3} \cdot \text{A}^{-1}$
power	watt	W	J/s	$\text{m}^2 \cdot \text{kg} \cdot \text{s}^{-3}$
pressure	pascal*	Pa	N/m ²	$\text{m}^{-1} \cdot \text{kg} \cdot \text{s}^{-2}$
quantity of electricity (charge)	coulomb	C		$\text{s} \cdot \text{A}$
radiant flux	watt	W	J/s	$\text{m}^2 \cdot \text{kg} \cdot \text{s}^{-3}$
radiant intensity	watt per steradian	W/sr		$\text{m}^2 \cdot \text{kg} \cdot \text{s}^{-3} \cdot \text{sr}^{-1}$
resistance (electrical)	ohm	Ω (cap omega)	V/A	$\text{m}^2 \cdot \text{kg} \cdot \text{s}^{-3} \cdot \text{A}^{-2}$
resistivity (electrical)	ohm meter or ohm-meter**	$\Omega \cdot \text{m}$		$\text{m}^3 \cdot \text{kg} \cdot \text{s}^{-3} \cdot \text{A}^{-2}$
specific heat capacity	joule per kilogram kelvin	J/(kg · K)		$\text{m}^2 \cdot \text{s}^{-2} \cdot \text{K}^{-1}$
stress	pascal*	Pa	N/m ²	$\text{m}^{-1} \cdot \text{kg} \cdot \text{s}^{-2}$
thermal conductivity	watt per meter kelvin	W/(m · K)		$\text{m} \cdot \text{kg} \cdot \text{s}^{-3} \cdot \text{K}^{-1}$
velocity	meter per second	m/s		$\text{m} \cdot \text{s}^{-1}$
viscosity, dynamic	pascal second or pascal-second	Pa · s	N · s/m ²	$\text{m}^{-1} \cdot \text{kg} \cdot \text{s}^{-1}$
viscosity, kinematic	square meter per second	m^2/s		$\text{m}^2 \cdot \text{s}^{-1}$
voltage	volt	V	W/A	$\text{m}^2 \cdot \text{kg} \cdot \text{s}^{-3} \cdot \text{A}^{-1}$
volume	cubic meter	m^3		m^3
wave number	(cycles) per meter	1/m		m^{-1}
work	joule*	J	N · m	$\text{m}^2 \cdot \text{kg} \cdot \text{s}^{-2}$

*Pronounce "siemens" like "seamen's", pronounce "pascal" to rhyme with "rascal", pronounce "joule" to rhyme with "pool".

**The "ohm meter squared per meter", sometimes used to designate the resistivity unit in the past, is definitely discarded.

Table 1-4. Examples of SI coherent derived units.

Quantity	Coherent SI Units	Allowable Units for Logging and Related Use	Comments and Conversions	Quantity	Coherent SI Units	Allowable Units for Logging and Related Use	Comments and Conversions
Acceleration, linear	m/s ² (meter per second squared)	m/s ² mm/s ² Gal (gal)	1 ft/s ² = 0.3048* m/s ² 1 Gal = 1 cm/s ² The "gal" and "milligal" are special units used in geodetic and gravity work to express the acceleration due to gravity. The internationally accepted value of acceleration due to gravity is 9.806 65 m/s ² = 32.1740 ft/s ² . Actual value will vary with latitude, densities of surrounding rocks, and depth.	Distance	m (meter)	km	1 mi = 1.609 344* km 1 naut. mi = 1.852* km
Angle, plane	rad (radian)	rad mrad (milliradian) μrad (microradian) ° (degree) ' (minute) " (second)	1° = 0.017 453 29 rad (ANSI prefers the "unit degree" with decimal divisions.)	Energy	J (joule) Pronounce "joule" to rhyme with "pool"	J	1 Btu = 1.055 056 kJ 1 eV (electronvolt) = 1.602 19 × 10 ⁻¹⁹ J = 16.0219 aJ
Area	m ² (square meter)	km ² ha (hectare) dm ² cm ² mm ²	1 ha = 10,000 m ² = 1 hm ² The "hectare" is used for land measure.	Flow Rate, mass	kg/s (kilogram per second)	kg/s	1 lbm/s = 0.453 59 kg/s ("lbm" is "pound mass")
Conductance	S (siemens) (1 S = 1 A/V)	S	1 mho = 1 Ω ⁻¹ = 1* S The "mho" is replaced by the "siemens".	Flow Rate, volumetric	m ³ /s (cubic meter per second)	m ³ /s m ³ /min m ³ /h m ³ /d L/s	1 BPD = 0.158 987 m ³ /d (For standard conditions, see "Gas Volume" and "Oil Volume".)
Conductivity	S/m (siemens per meter)	S/m mS/m	"mS/m" replaces "mmho/m" on induction-log conductivity curves.	Force	N (newton) 1 N = 1 kg/s ²	N	1 lbf (pound force) = 4.448 22 N 1 kgf (kilogram force) = 9.806 65* N Note: The kilogram is NEVER used as a unit of force in SI.
Density	kg/m ³ (kilogram per cubic meter)	kg/m ³ Mg/m ³	1 lbm/ft ³ = 16.085 kg/m ³ ("lbm" is "pound mass") 1 g/cm ³ = 1000 kg/m ³ = 1 Mg/m ³	Gamma Ray Intensity		API Unit	
Depth, bed thickness, tool length, macro-spacing (and invasion depth)	m (meter)	m	1 ft = 0.3048* m 1 yd = 0.9144* m	Gas-Oil Ratio	m ³ /m ³ (dimensionless)	Std. m ³ /m ³ at specified standard conditions	1 scf/bbl (standard cubic foot per barrel) = 0.180 117 5 std. m ³ /m ³ . (See Gas Volume.)
Diameter of hole, bit or casing size, mud-cake thickness, microspacing, tool diameter	m (meter)	mm	1 in. = 25.4* mm	Gas volume	m ³ (cubic meter)	m ³ at specified standard conditions	1 scf (standard cubic foot at 60° F and 14.65 psi) = 2.817 399 × 10 ⁻² m ³ (at 15°C and 1 atm = 101.325 kPa)
				Gravity: See Relative Density			
				Interval transit time	s/m (second per meter)	μs/m (microsecond per meter)	1 μs/ft = 3.280 840 μs/m
				Length (see Depth, Diameter, Distance)			
				Mass	kg (kilogram)	t (metric ton or tonne)** Mg kg g mg ** In Canadian French "tonne" may refer to 2000-lb ton.	1 t = 1 Mg (megagram) 1 lbm avoirdupois (pound mass avoirdupois) = 0.453 592 4 kg.
				Mud Weight (see also Density)	kg/m ³ (kilogram per cubic meter)	kg/m ³ Mg/m ³	1 lbm/U.S. gal = 119.826 4 kg/m ³ 1 lbm/U.K. gal = 99.776 33 kg/m ³

*Exact value

Table 1-5. Allowable SI units and conversions.

GEOLOGY & HYDROCARBON ACCUMULATIONS

2

A. Introduction from "Handbook of Natural Gas Engineering".

Study of the nature of the earth's crust and of its ability to accumulate petroleum under pressure constitutes an important background for the engineer in the producing branch of the natural gas industry. Geology treats all phases of the earth's history, including the processes by which reservoirs were created. Man is fortunate that many of the processes which produced the earth's crust are still in evidence to permit a reconstruction of methods by which most reservoirs were formed.

There are several branches of geology and of related earth sciences. Their nomenclature makes frequent use of such terms as *geo* - earth, *petra* - rock, *lithos* - stone, and suffixes like *log* - science or discourse, *graphy* - description. Physical geology is a study of the processes affecting the earth's surface, such as action of wind, water, ice, and atmosphere. Historical geology endeavors to trace the events in the history of the earth, including the processes responsible for the earth's crust. The origin of life and the evolution of plant and animal forms are included. Structural geology treats the methods by which the position and shape of the various members of the earth's crust are determined, and studies forces which have brought about both the surface and subsurface structures. *Stratigraphy* covers the character, sequence relationship, distribution, and origin of sedimentary rocks.

Several branches deal with the recognition of rock according to type and age. The study of rocks to determine their character and constitution is termed *lithology*. *Paleontology* and *micropaleontology* classify information on life in past geologic ages by studies of fossils and microfossils. *Mineralogy*, *petrography*, and *petrology* deal with the physical properties, chemical properties, classification, and identification of minerals or rocks and with their genesis.

Sedimentation is the process of depositing solids at the bottom of a fluid, and the term is in frequent use to describe methods of depositing particles of rock from bodies of water. *Sedimentary* rocks are rocks that have been deposited by this process. Essentially all petroleum is contained in sedimentary rock. *Geohydrology*, or groundwater geology, combines the principles governing water movement through porous media and the geology of the earth's crust with respect to the ability of the various strata to conduct water.

Geophysics is the application of the principles of physics to problems of the earth. The study of the transmission of shock waves generated either from natural causes, such as earthquakes, or by explosions of dynamite is an example. These principles are utilized in the seismic method of searching for structures. The reflection of elastic waves at the interface between layers of rock with different physical properties permits the mapping of the interface.

Other methods of making physical measurements at the earth's surface to find the nature of its subsurface employ the magnetic field, the gravitational field, and the electrical properties of the earth, principally its electric resistivity. These methods usually depend upon anomalies or irregularities in the earth's crust.

Geochemistry is the application of the principles of chemistry to the study of the earth. The search for petroleum by analysing soils for hydrocarbons is considered a geochemical method. The physical chemistry of molten rock and the chemistry of its disintegration and recrystallization are included.

B. Historical Geology

Historical geology reconstructs the successive events in the history of the earth since it was in a molten condition. Geologic time scales have been devised to indicate the periods of time during which various layers of the earth's surface were formed. The point at which cooling of the earth's surface led to water precipitation marks the beginning of the sedimentary processes in geological time.

Figure 2-1 presents the geologic time scale divided into eras, periods, and epochs. Visualizing the transition which have occurred over the approximately 4,500 million years of the earth's existence is difficult, for persons who individually live less than 100 years and who collectively have a recorded history of 5,000 years, to comprehend.

When water condensed on the surface of the earth, the high areas were subjected to rain and the low areas were inundated. The power of wind and water to extract and carry sediment is primarily responsible for the nature of the immediate surface of the earth's crust.

The erosion of mountains and the filling of seas go on continuously. The mountains would all be worn down and the seas all full of sediment if it were not for the changes in elevation (uplifts and submergences) of areas on the earth's surface.

Era	Period	Epoch	Millions of years ago ¹
	Quaternary	Recent Pleistocene	1
Cenozoic	Tertiary	Pliocene Miocene Oligocene Eocene Paleocene	65
Mesozoic	Cretaceous Jurassic Triassic		135 180 230
Paleozoic	Permian Pennsylvanian Mississippian Devonian Silurian Ordovician Cambrian		280 310 345 400 425 600
Precambrian	The 4½ billion years now estimated for the age of the earth makes the length of the Precambrian time far exceed that of later eras.		

Fig. 2-1. Geological time scale.

Geologists have mapped the earth to show the present outcrops of sedimentary rock as well as the positions of the seas during geologic periods. The pre-Cambrian Eras cover the time span from the formation of the earth up to approximately 500 million years ago. The rocks formed during these eras are of three characters.

- (1) Igneous : Products of solidification of molten material
- (2) Metamorphic: Rock that changed its character by solution, heat, and pressure
- (3) Sedimentary: Composed of the detritus of previous rock

Common examples of igneous rock are granite, which has solidified slowly within the earth's crust, and lava, which solidifies rapidly on the surface. Schist and gneiss were formed by metamorphic processes that occur with heat, pressure and time. Sedimentary rocks include sandstone, limestone, dolomite, and shale.

The Cambrian period is the first in which the sediments show evidence of life such as marine fossils. Oil and gas are produced from deposits ranging in age from early Cambrian through the Pliocene epoch of the Tertiary, a span of 500 million years.

C. Structure of the earth

The internal structure of the earth is revealed by analysis of earthquake waves as they are reflected and refracted by concentric layers of material with differing density and rigidity.

The core, extending to a radius of 2200 miles from the center of the earth, is composed of nickel-iron with an average density of 10.7 gm/cc. The inner core is solid while the outer core is liquid.

Surrounding the core is an 1800 mile thick mantle, largely composed of iron silicates whose density, averaging 4.0 gm/cc, varies with depth. The mantle is plastic except for the outer 400 miles or so which is solid.

The crust or lithosphere, composed of the more common variety of rocks, varies in thickness from about 25 miles under the continents to 7 miles beneath the ocean basins.

The crust is of insignificant thickness when compared to the core and mantle. It consists of:

- A basaltic layer overlying and floating on the mantle. It is rich in lime, iron and magnesia with a density of 2.9g/cc.
- A second lighter granitic layer, rich in silica and alkalis of 2.7g/cc density, resting on the basaltic layer and forming the continents.

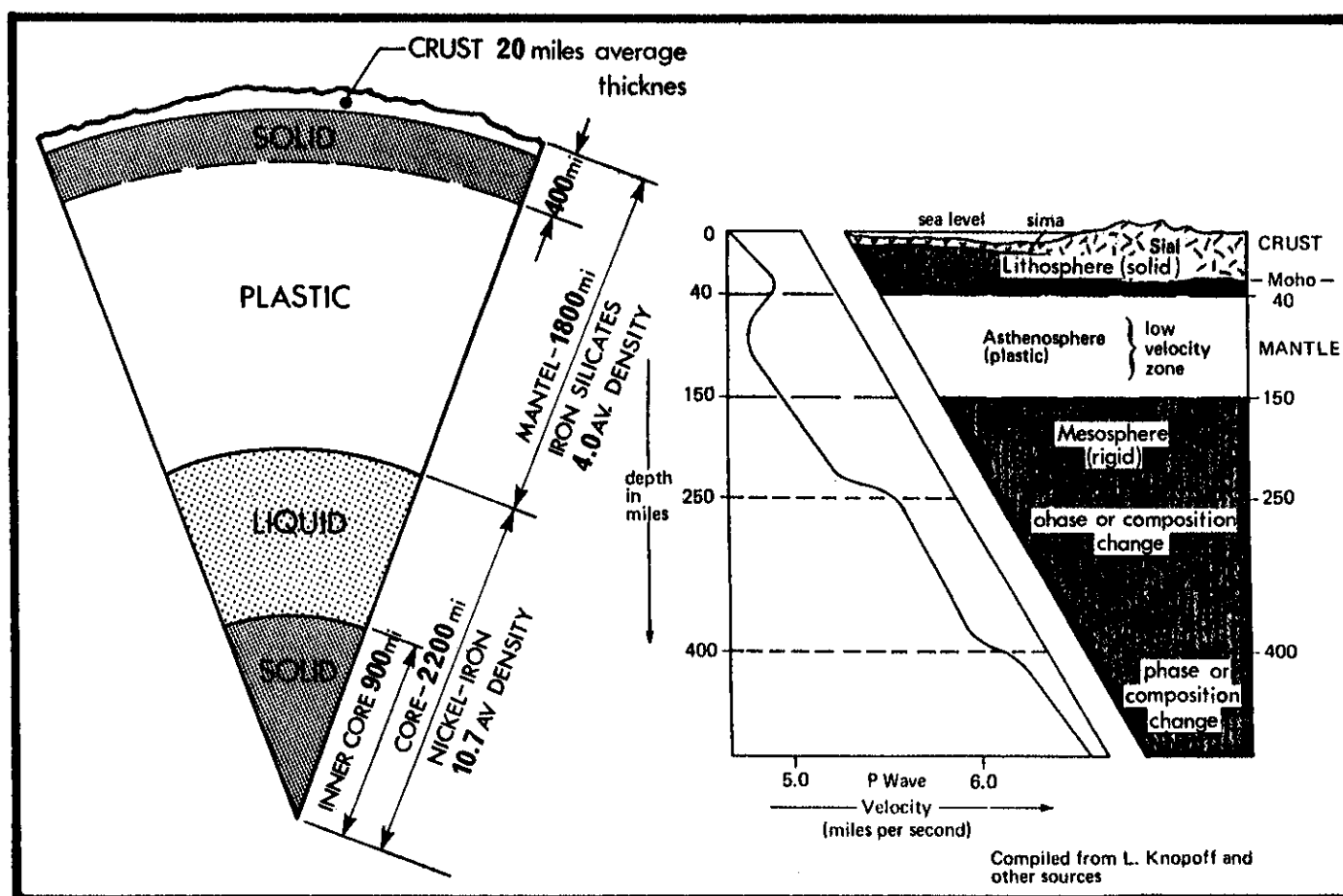


Fig.2-2. Cross section the earth
From Mears, The Changing Earth

Fig.2-3. Detail structure of crust
from earthquake wave analysis
From Mears, The Changing Earth

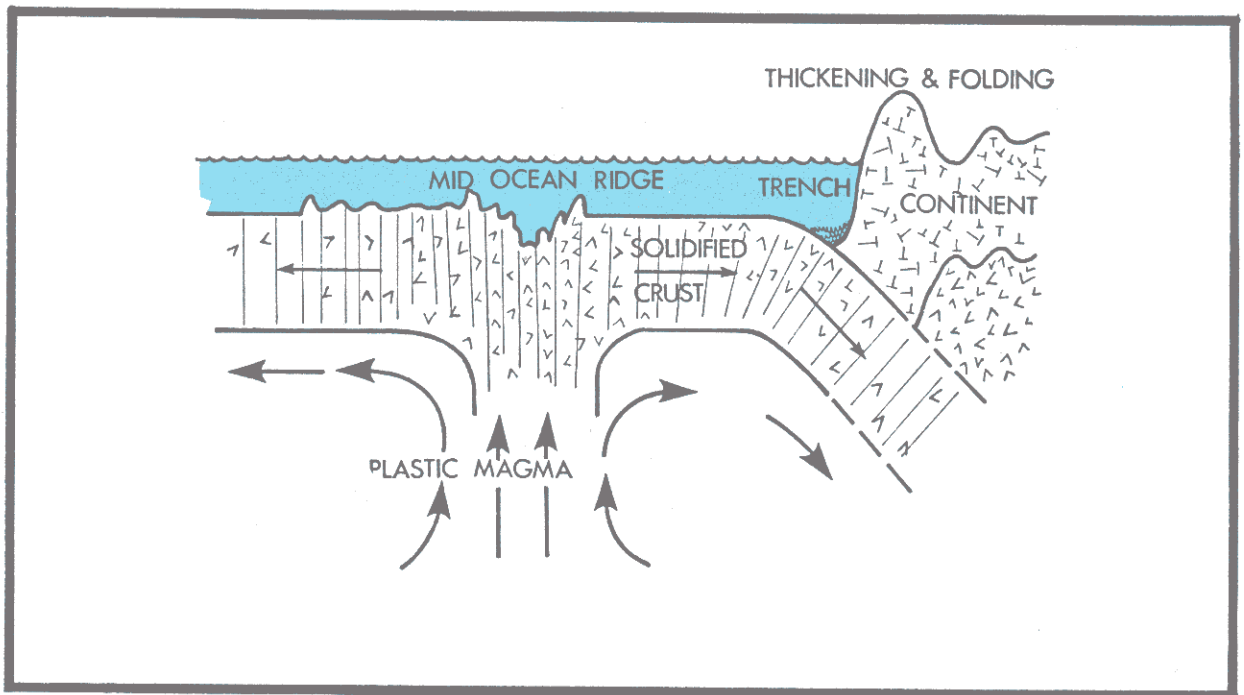


Fig. 2-4. Mechanism of tectonic plate movements -
From Mears "The Changing Earth"

Driven by density differences due to unequal heating, convection currents circulate in the plastic mantle.

Uplifting magma breaks through the crystal layer forcing a rift into which the upwelling material solidifies as it surfaces, becoming a mid-ocean ridge.

As new material is continuously added at the rift, the crust spreads, and the continental land masses are rafted apart.

Compressional forces caused by lateral plate movements cause thickening and folding of the crust until faulting occurs, and one plate overrides the other, driving it back into the mantle where it is remelted.

It is now generally accepted that this mechanism caused the break up of the continents from a single land mass 200 million years ago.

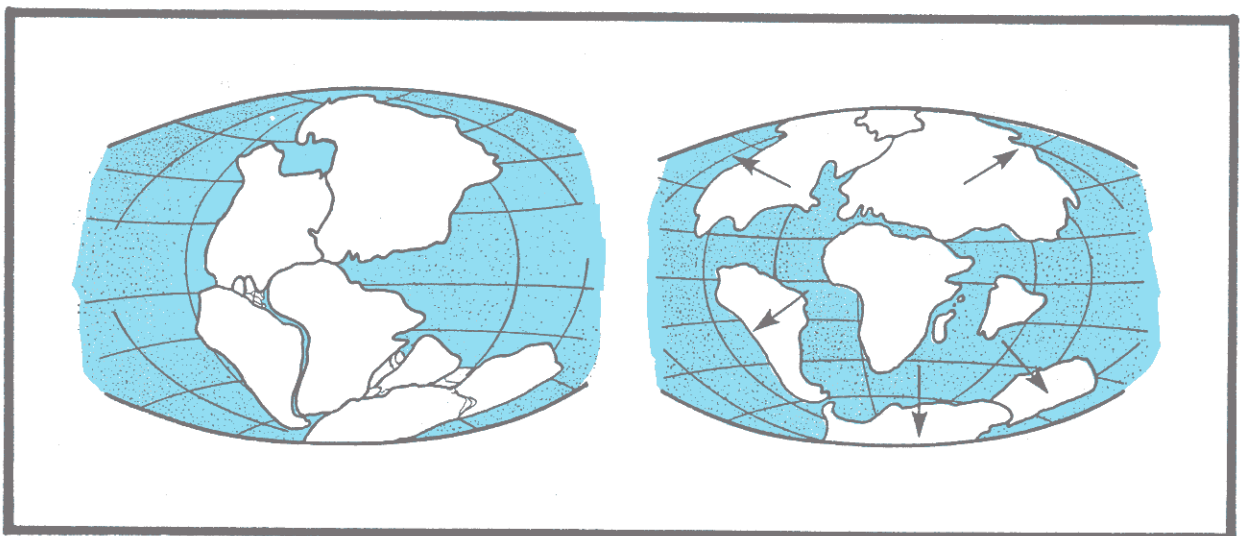


Fig. 2-5. Break-up of the Continents - From Scientific American

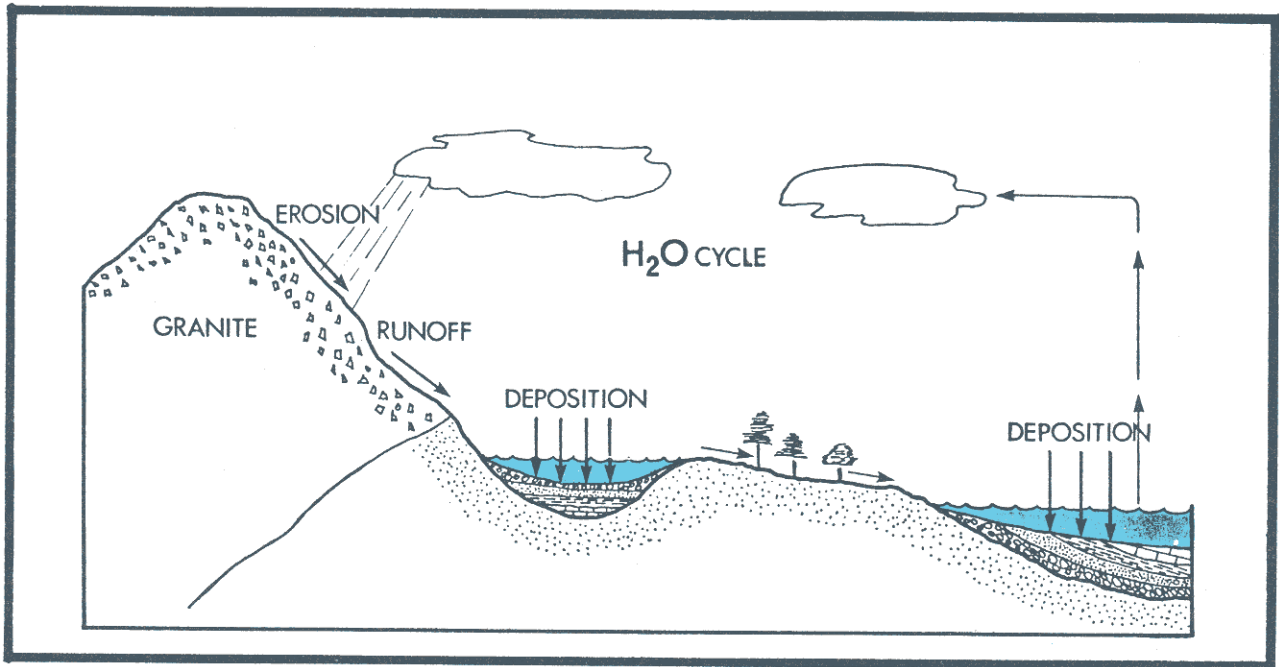
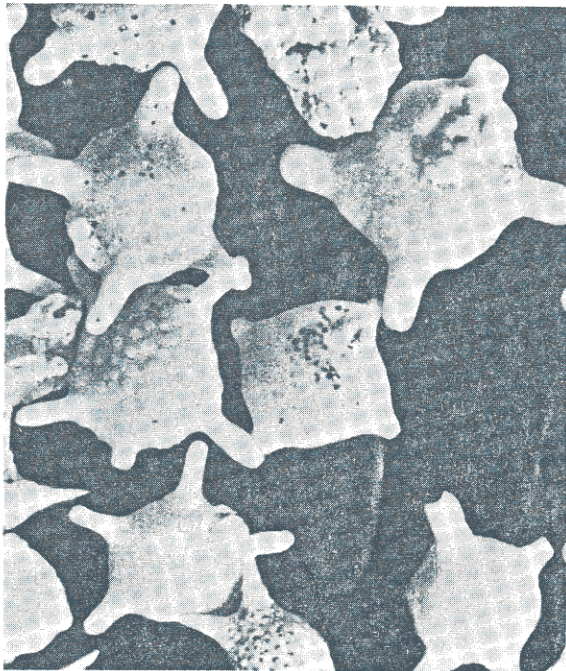


Fig. 2-6. Erosion of mountains/transport/deposition of sediments

Mechanical forces act to break down gniess and granite from boulders to cobbles, pebbles, gravel, and smaller particles. Chemical weathering transforms feldspars into clays, releasing quartz grains which become sand. The great abundance of quartz sand is due to the fact that quartz grains are extremely durable.

Sands are also composed of feldspar and carbonate particles - the limy coral reef sand shown below is one such form.



Limy coral - reef sand



Grains of quartz beach sand

Fig. 2-7. Sand particles - From Kuenen-Scientific American

D. Classification of rocks

Rocks are classified into three groups :

- igneous
- sedimentary
- metamorphic

- 1) Igneous rocks comprise 95% of the earth's crust. They originate from the solidification of molten material emanating from below the earth's surface.

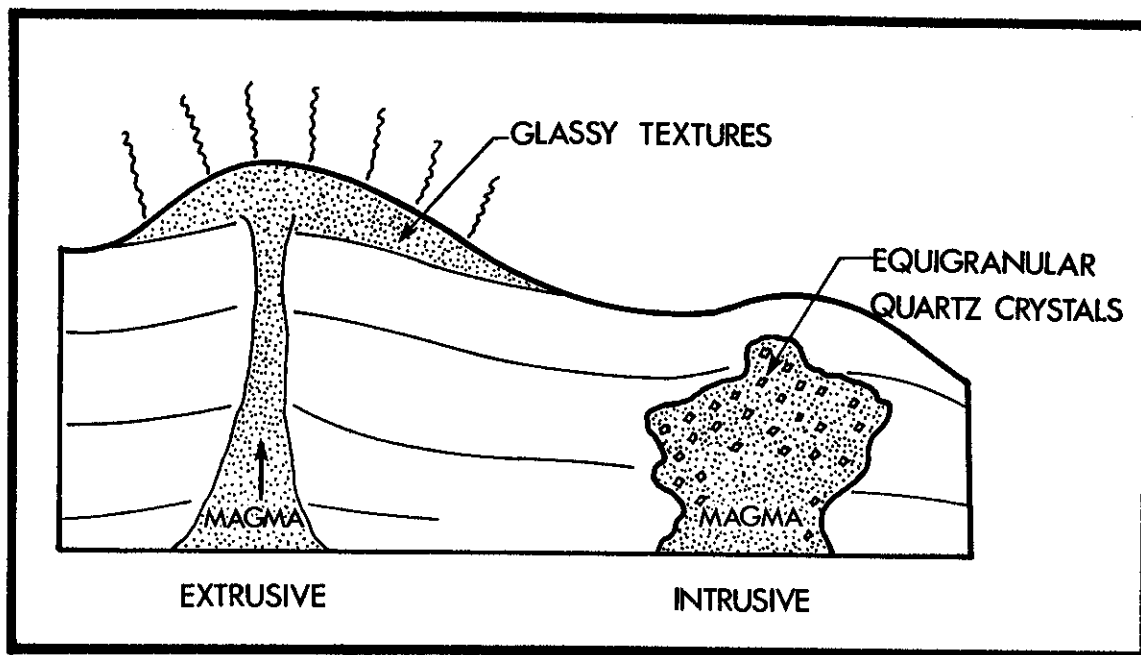


Fig. 2-8. Igneous rock formation - From Mears, The Changing Earth

Volcanic igneous rocks are often glassy in texture as rapid cooling of magma does not allow time for the formation of crystals.

Plutonic igneous rocks are formed in slower cooling intrusive magmas which allows the time needed for the atoms to arrange themselves into a crystalline grain structure.

Almost (95%) of granitic rocks are plutonic (CRYSTALLINE texture.) The size of the grains is controlled by the cooling rate, the largest grains corresponding to slowest cooling rates.

Granite is made up of three principal materials in roughly equal proportions : quartz (SiO_2), sodium feldspar ($\text{Na Al Si}_3\text{O}_8$) and potassium feldspar ($\text{K Al Si}_3\text{O}_8$).

2) Sedimentary rocks

Sedimentary rocks are formed from the materials of older up-lifted formations which have been broken down by erosion and transported by wind and water to lower elevations, where they are deposited.

The grain size of quartz sand is determined during the crystallization process by the rate of magma cooling into granite.

The grains are rounded off to some extent by rolling before the wind and polished during transport by running off in streams and rivers to the point of deposition.

Consolidation of sands, silts, pebbles, and clays by the pressure of many thousands of feet of overlying sediments, and cementation by precipitates from percolating waters act to convert these materials into sandstones, siltstones, and conglomerates.

Sedimentary rocks may be classified into two groups, clastic (the rocks of detrital origin previously mentioned) and nonclastic. Sediments which are of biochemical or chemical precipitate origin are non-clastic.

CLASTIC ROCKS - FORMED FROM DEBRIS OF OLDER ROCKS

ROCK TYPE	PARTICLE DIAMETER
CONGLOMERATE	PEBBLES - 2 TO 64 mm
SANDSTONE	SAND - .06 TO 2 mm
SILTSTONE	SILT - .003 TO .06 mm
SHALE	CLAY - LESS THAN .003 mm

NONCLASTIC - MOSTLY OF CHEMICAL OR BIOCHEMICAL ORIGIN

ROCK TYPE	COMPOSITION
LIMESTONE	CALCITE - CaCO_3
DOLOMITE	DOLOMITE - $\text{CaMg}(\text{CO}_3)_2$
SALT	HALITE - NaCl
GYPSUM	GYPSUM - $\text{CaSO}_4 \cdot 2\text{H}_2\text{O}$
CHERT	SILICA - SiO_2
COAL	CHIEFLY CARBON

Fig. 2-9. Sedimentary rock classification

Carbonate rocks

The carbonates, limestone, dolomite and chalk comprise about 20% of all sedimentary rocks.

Limestone, composed mainly of the mineral calcite (CaCO_3) may be concentrated by an accumulation of the shells and skeletons of marine animals or by direct precipitation from mineral saturated waters. In either case the carbonate ions were dissolved from older formations by passing waters.

Precipitated accumulations occur in lake bottoms and in shallow seas where mineral-laden waters are cooled, decreasing the solubility. Fine calcite crystals form and fall to bottom where the beds are compacted by the weight of overlying sediments, and with time crystal growth may continue, forming dense consolidated rocks.

Dolomite is the double carbonate of calcium and magnesium. When dolomitization (the conversion from limestone by replacement of calcium by magnesium) occurs, a shrinkage of the matrix is observed.

Matrix porosities and permeabilities of carbonate rocks are typically low. While formation of pits, vugs, channels and other cavities add to the storage capacity, most prolific hydrocarbon bearing carbonates are highly fractured.

Chalk is a soft form of limestone which has high porosity and low permeability.

Calcareous sandstones are formed by wave action, breaking coral or shell into sand-sized particles which are subsequently re-cemented.

Many rocks are a mixture of sand and carbonates.

Evaporites

The evaporites include rock salt, anhydrite, and gypsum, all of which are precipitated by the evaporation of water.

3) Metamorphic rocks

Metamorphic rocks, the third genetic group of rocks, are formed from other sedimentary deposits by alteration under great heat and/or pressure.

- marble, is metamorphized limestone
- hornfels, is converted from shale or tuff
- gneiss, with a texture and composition similar to granite but is metamorphically consolidated.

Oil and gas are not usually found in igneous or metamorphic rocks as both are so non-porous that hydrocarbons can not accumulate or be extracted from them. The few exceptions are where oil and gas have seeped from near-by sedimentary formations through cracks or fractures into them.



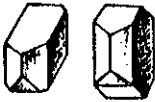



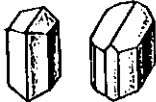

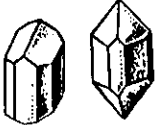
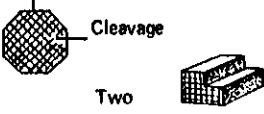


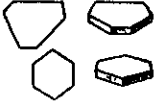
Hardness Specific Gravity MINERAL Chemical Composition	COMMON CRYSTALS Color	CLEAVAGE and fragments	USES
H = 7 Sp.G = 2.67 QUARTZ SiO_2	 Pure-clean, colorless Impure-pink, purple black etc.	 None-shatters	Crystals in electrical and electronic work Radio quartz Optical lenses & prisms Window glass
H = 6 Sp.G = 2.5-2.9 FELDSPAR GROUP Sodium: Potassium- Calcium Aluminum silicates	 Light colored: white pink, grey, cream	 Two directions	Glazes and Flux enamels for ceramics
H = 2-2.25 Sp.G = 2.76-3 MICA Complex: Potassium Aluminum, Iron, Magnesium silicates	 Clear, whitish brown, black, purple	 Parallel, excellent One direction	In electrical and electronic equipment Heat-proof windows
H = 5-6 Sp.G = 29-3.4 HORNBLENDE (AMPHIBOLE GROUP) Complex: Potassium Magnesium, Aluminum Sodium silicates, Iron	 Dark: green to black	Crystal faces  Fragments Two dir.	Some fibrous members of amphibole group used as asbestos
H = 5-6 Sp.G = 3.2-3.6 AUGITE (PYROXENE GROUP) Generally like hornblende	 Dark: green, black, brown	Crystal faces  Cleavage Two	
H = 3 Sp.G = 2.72 CALCITE CaCO_3	 Usually colorless or white, Other tints common	 Three	Optical Prisms (transparent crystals) Range finders Microscopes
H = 1-2.5 Sp.G = 2-2.6 CLAY GROUP Complex: Aluminum silicates combined with water	 Pure: white Impure: wide range of colors		Bricks Pottery, china Drilling mud Paper slicks

Fig. 2-10. Summary chart of general properties of some of the commonest rock-forming minerals - From Mears, The Changing Earth.

SEDIMENTARY MINERALS		MINERAL	COMPOSITION	Apparent Log Density	Average Δt	ϕ_N^* (GNT) p.u.	γ -Ray Deflection (APIU)	Apparent K ₂ O%		
		Calcite	CaCO ₃	2.710	47.5	0	0	—		
		Dolomite	CaMg (CO ₃) ₂	2.876	43.5	4	0	—		
		Quartz	SiO ₂	2.648	55.5	-4	0	—		
SEDIMENTARY FORMATIONS		Limestone	(e.g., when $\phi = 10\%$)	2.540	62	10	5-10	0		
		Dolomite	(e.g., when $\phi = 10\%$)	2.683	58	13.5	10-20	0		
		Sandstone	(e.g., when $\phi = 10\%$)	2.485	65.3	3	10-30	0		
		Shale		2.2-2.75	70-150	25-60	80-140	2-10		
EVAPORITES		NON-RADIOACTIVE	Halite	NaCl	2.032	67	0	0	—	
			Anhydrite	CaSO ₄	2.977	50	0	0	—	
			Gypsum	CaSO ₄ • 2H ₂ O	2.351	52.5	49	0	—	
			Trona	Na ₂ CO ₃ • NaHCO ₃ • 2H ₂ O	2.100	65	40	0	—	
		RADIOACTIVE	Sylvite	KCl	1.863	74	0	~500	63.0	
			Carnallite	KCl • MgCl ₂ • 6H ₂ O	1.570	78	65	200	17.0	
			Langbeinite	K ₂ SO ₄ • 2MgSO ₄	2.820	52	0	275	22.6	
			Polyhalite	K ₂ SO ₄ • MgSO ₄ • 2CaSO ₄ • 2H ₂ O	2.790	57.5	15	180	15.5	
			Kainite	MgSO ₄ • KCl • 3H ₂ O	2.120	—	45	225	18.9	
		OTHER MINERALS		Sulfur**		2.030	122.0	<0 (15.5")	0	
				Lignite		0.7-1.5	140-170	↑ Higher than 50% ↓	0	
				Bituminous Coal		1.3-1.5	110-140		0	
Anthracite Coal				1.4-1.8		0				

* ϕ_N = Apparent Limestone Porosity from a Neutron Log.
** $\phi_{NPF} (\text{calitraz}) = 0$.

Fig. 2-11. Petrophysical properties of common sedimentary materials

E. The origin and habitat of oil

Many hypotheses concerning the origin of oil (and/or gas) have been advanced over the years. Currently, the most favored one is that oil is formed from Phytoplankton (tiny floating plants) and to a lesser degree from Algae and Foraminifera. These die, fall to the bottoms of seas and lakes, and form oozes rich in organic material. They are most abundant in near-shore areas, where rivers carry off nutrients from the land masses. These areas are also the regions of greatest sedimentation.

If such oozes are overlain by fine sediments and are at such a depth that anaerobic bacteria can live in them, these bacteria busily remove oxygen, nitrogen, phosphorus, and sulfur from the oozes, leaving them richer in hydrogen and carbon. It is important that the mother oozes are at a depth in the water below zero oxygen level; otherwise not only the source material but the petroleum itself is destroyed by oxidation.

As deposition of sediments progresses, depending upon water velocities, the fine sediments will be overlain by coarser ones, which, in turn are overlain by fines, etc. Eventually the oil is squeezed from the oozes into the porous reservoir materials.

Until about 20 years ago it was commonly believed that the source materials had to be deposited in a marine environment (seas, oceans). But lake sediments can be just as promising as sea-floor sediments, provided the depths are right. Many oil fields in various parts of the world are producing from ancient lake beds.

Most of world's larger oil reservoirs are found on the continental shelves of ancient seas, however.

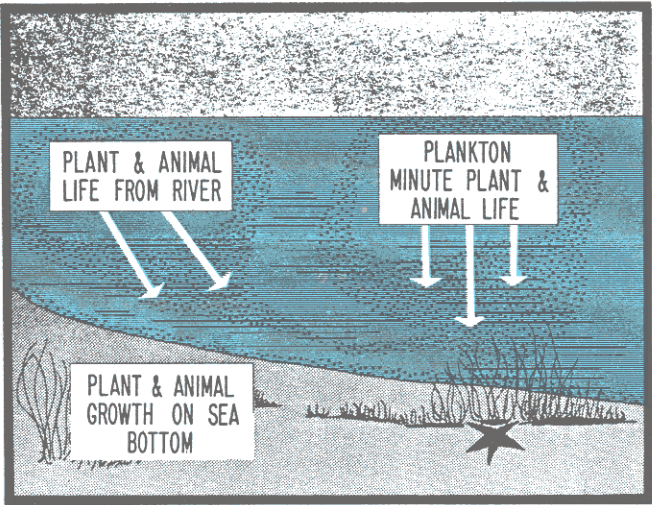


Fig. 2-12. Sources of organic material - From Clark - Elements of Petroleum Reservoirs.

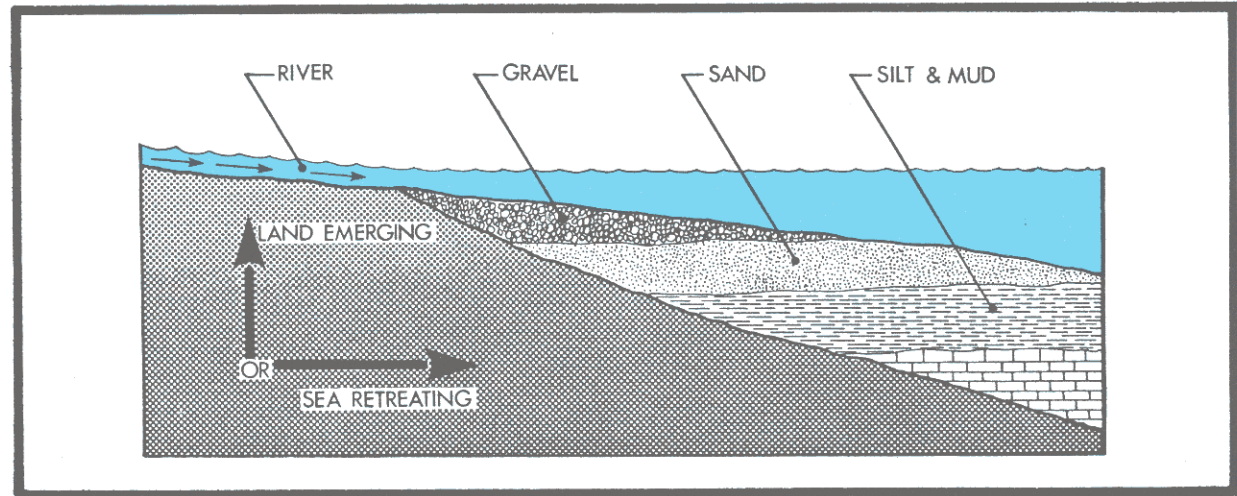


Fig. 2-13. Offlap process - beds formed by retreating sea or land emerging. (regression)

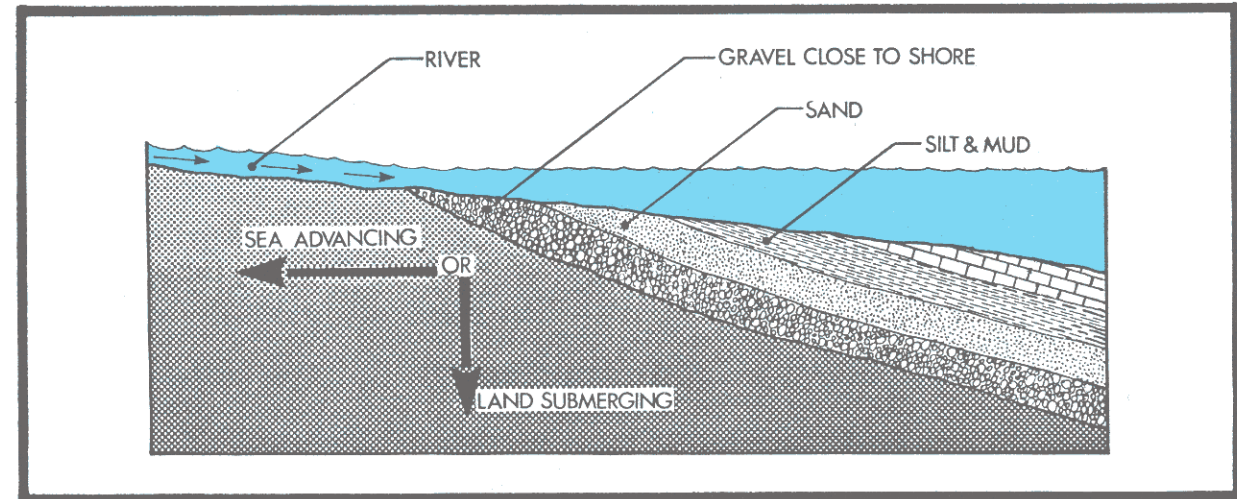


Fig. 2-14. Onlap process-beds formed by advancing sea or submerging shoreline. (transgression)

F. Hydrocarbon reservoirs

Petroleum deposits will be found only in those areas where geological conditions combine to form and trap them.

Hydrocarbons, being less dense than water, migrate upward from the source beds until they escape at surface, or an impervious barrier is encountered.

Oil and gas accumulates in partially sealed structures by expelling water from the porous rock. That part of the trap which contains hydrocarbons is called the reservoir.

Generally water underlies the hydrocarbons in a trap. An aquifer is a water bearing formation which is hydraulically connected to the reservoir.

Both oil and gas are formed together in varying proportions in the source beds and a gas cap is often found above the oil in the reservoir. Traps do at times act to segregate oil and gas which were formed together so that they accumulate in different reservoirs.

The principal classifications of petroleum-reservoir-forming traps are as follows :

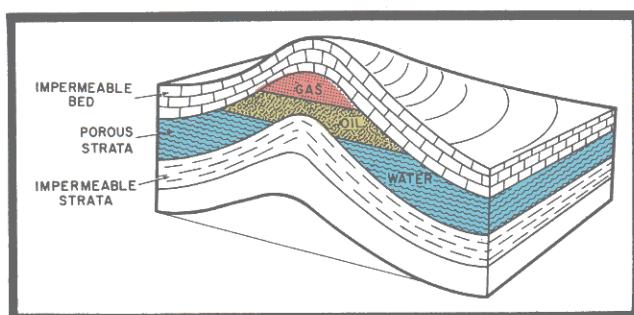


Fig. 2-15. Dome structure. Oil and gas migrate upward from source beds until trapped by the impermeable cap rock.

Domes and Anticlines

Domes and Anticlines are formed by uplifting and folding of the strata. When viewed from above the dome is circular in shape, whereas the anticline is an elongated fold.

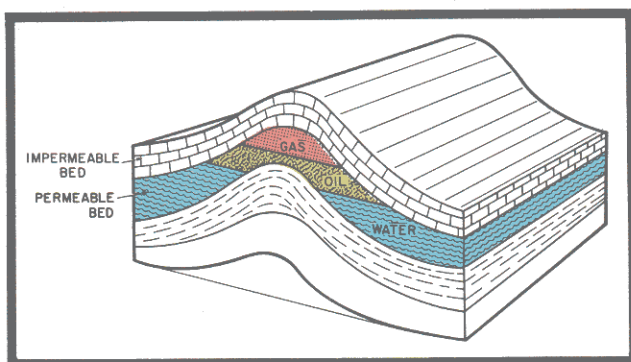


Fig. 2-16. Oil and gas accumulation in an anticline.

Salt Domes and Plug Structures

This commonly occurring geological structure is caused by the intrusion from below of a salt mass, volcanic material, or serpentine. In pushing up or piercing through the overlying strata the intrusion may cause the formation of numerous traps in which petroleum may accumulate.

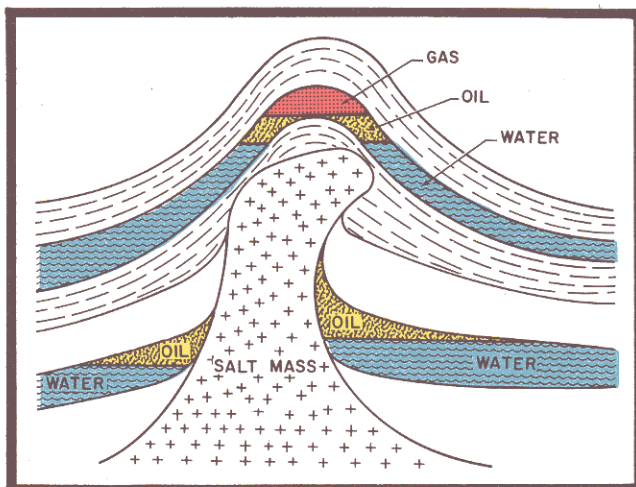


Fig. 2-17. Hydrocarbon accumulation associated with a piercement salt dome.

Structure Associated with Faulting

Reservoirs may be formed along the fault plane where the shearing action has caused an impermeable bed to block the migration of oil and gas through a permeable bed.

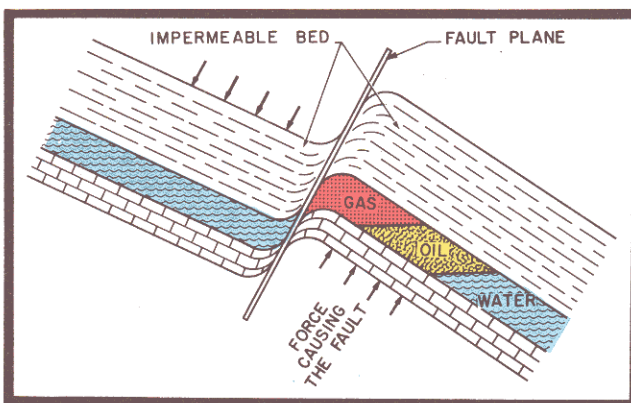


Fig. 2-18. Trap formed by a fault.

Structure with Unconformity

This type of structure can be formed where more recent beds cover older, inclined formations that have been planed off by erosion. A reservoir may be formed where oil and gas is trapped by an impermeable overlying layer.

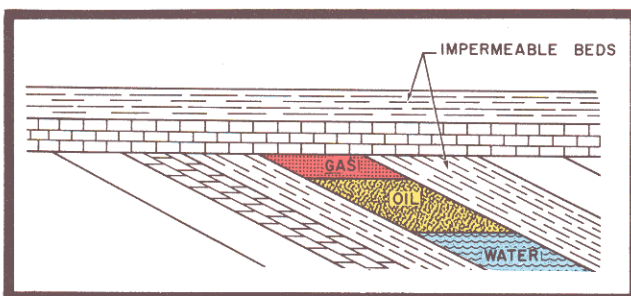


Fig. 2-19. Oil and gas trapped under an unconformity.

Lenticular Reservoirs

Oil and gas may accumulate in pockets of porous permeable beds, or traps formed by pinch-outs of the porous beds, within an impermeable bed.

Lens-type reservoirs are formed where sand was deposited along an irregular coastline or by filling in an ancient river bed or delta. Similar productive zones occur in various porous sections in thick impermeable limestone beds.

Pinch-outs may occur near the edge of a basin where the sand progressively "shales out" as the edge of the basin is approached. In river-deposited sand bars, shale-out frequently occurs within a few hundred feet.

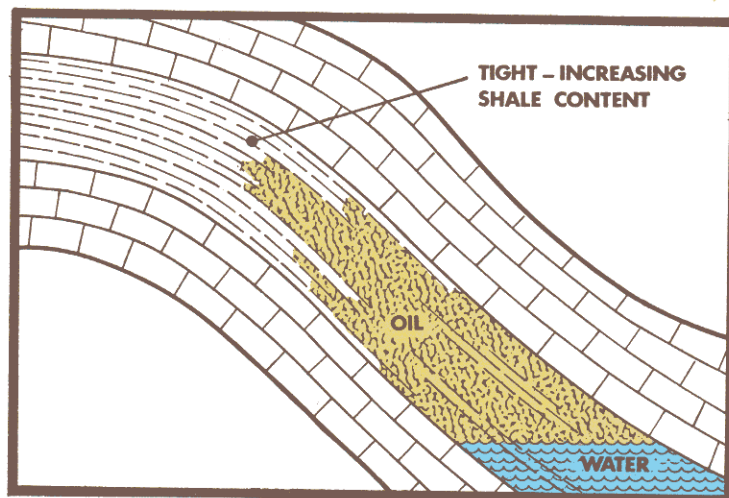


Fig. 2-20. Upper bounds of the reservoir formed by change in permeability of a sand.

G. Sub-surface mapping

A Structural map is a sub-surface contour map made by connecting points of equal elevations. In the example below, contours are from seismic data and correspond to the top of the cap rock.

An isopacheous map shows the contours of the inner surface of the cap rock with equal thicknesses of pay. Generally the zero is taken at the oil/water contact. Logs and seismic maps may be used to prepare early isopach maps, with increasing dependence on log data as the field is developed.

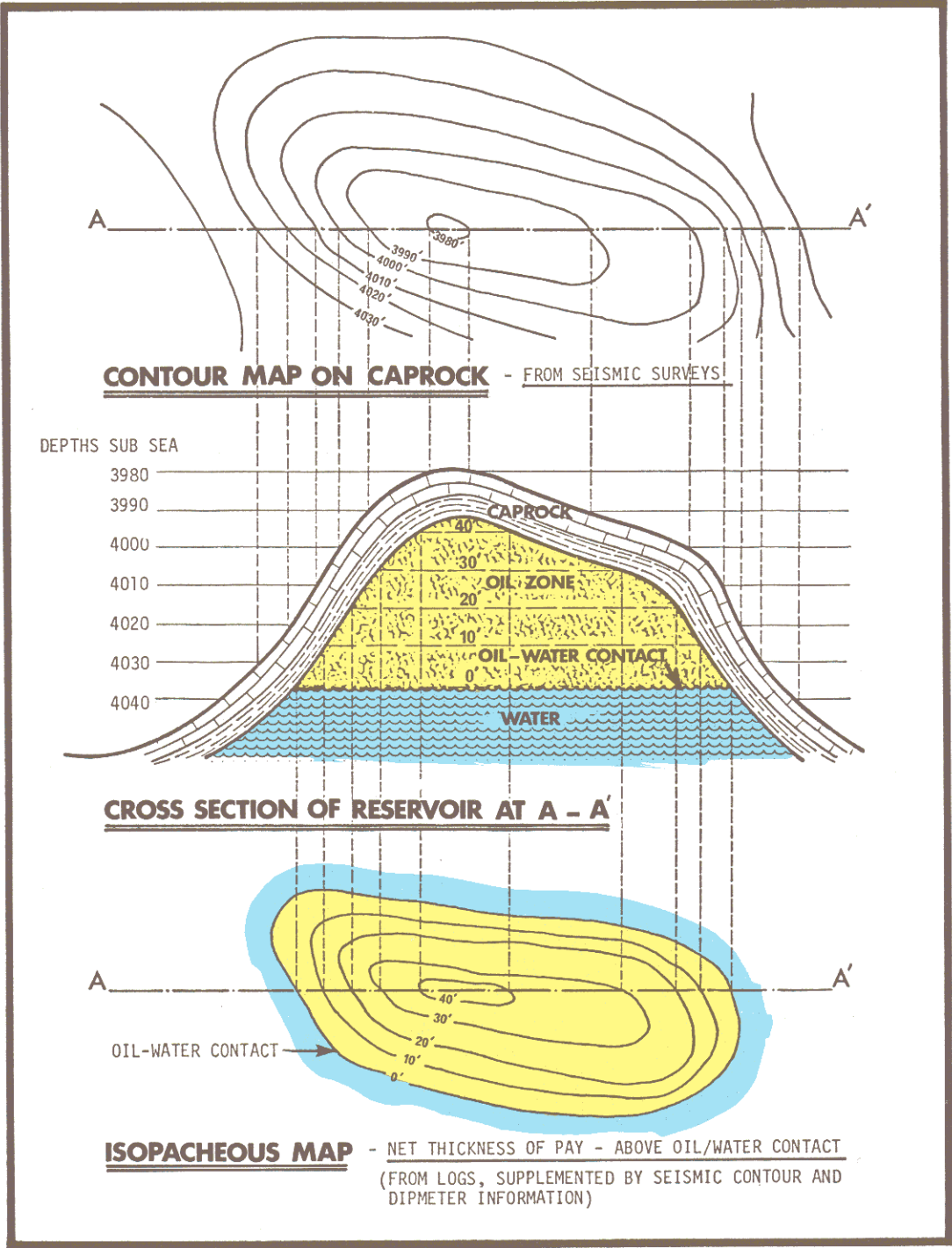


Fig. 2-21. Sub-surface mapping.

H. Reservoir Temperature and Pressure-

1.- Normal Pressures

Hydrocarbon accumulations occur in partially sealed structures where the upward migration of oil and gas from the source beds is blocked by an impermeable barrier.

As hydrocarbon accumulates, formation water is expelled from the porous reservoir rock.

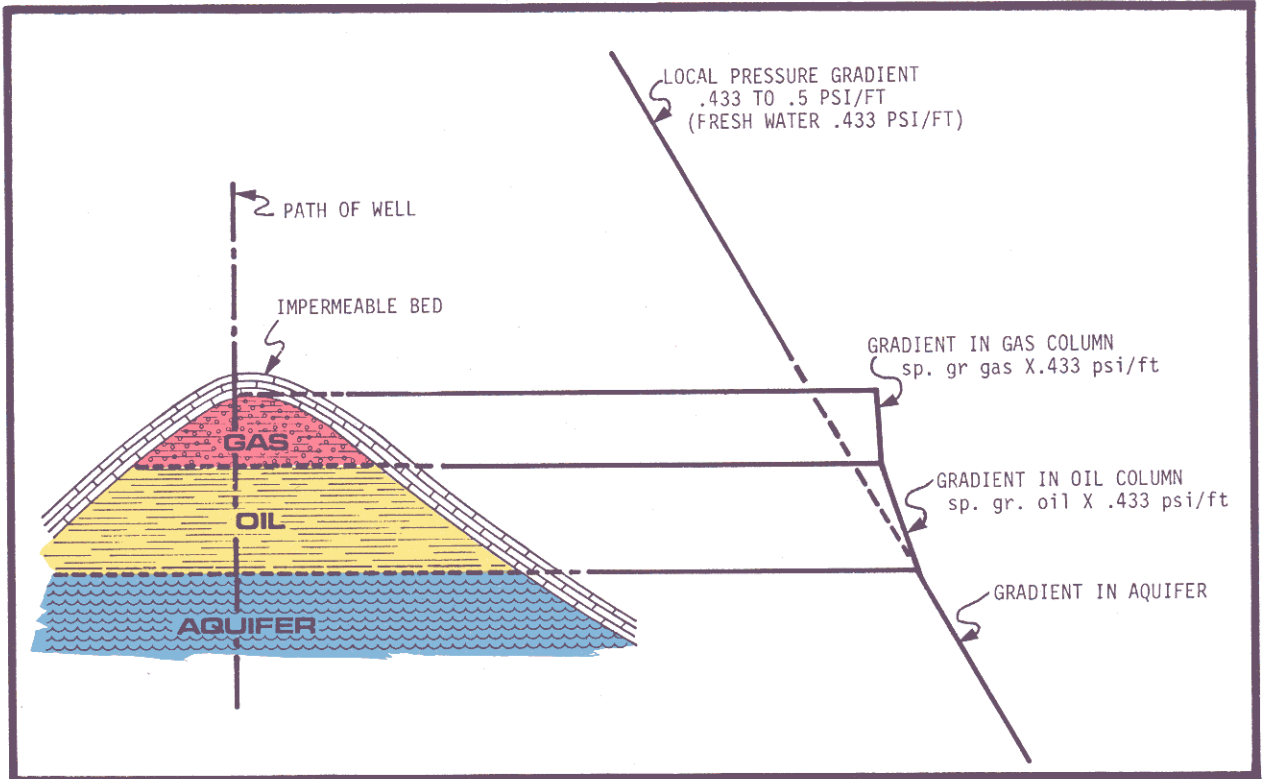


Fig. 2-22. "Normal" pressure distribution from surface through a reservoir structure.

Unless subsequent tectonic movements completely seal the reservoir, the underlying waters are contiguous and pressures in the aquifer will approximate to some local or regional hydrostatic gradient. That is in a water column, the pressure at any depth is approximated by :

$$P = h G_w$$

where: h , is the depth
 G_w is the pressure gradient.

Although ground waters are saline, temperatures increasing with depth tend to reduce the water density and a common "normal" value of G_w is .433 psi/ft (.1 kg/cm²/m), which is approximately a fresh water gradient.

Gradients within the range .43 to .5 psi/ft are considered normal.

Pressure at the top of a hydrocarbon bearing structure, higher than the hydrostatic gradient extrapolated from the hydrocarbon/water contact, is expected because of the lower density of hydrocarbon compared with water. Even in thick gas bearing zones this situation does not lead to dangerously abnormal pressures.

2.- Abnormal Pressures

Under certain depositional conditions, or because of earth movements which close the reservoir structure, fluid pressures may depart substantially from the normal range.

Abnormal pressures can occur when some part of the overburden load is transmitted to the formation fluids. Abnormal pressures corresponding to gradients of .8 psi/ft to .9 psi/ft and approaching the geostatic gradient (generally taken as approximately equivalent to 1.0 psi/ft) may occasionally be encountered and can be considered dangerously high.

3.- Reservoir Temperature

Reservoir temperatures will conform to the regional or local geothermal gradient, a normal value being 1.6° F/100 ft.

Because of the large thermal capacity of the rock matrix which comprises in the order of 80% of the bulk reservoir volume and the very large area for heat transfer, conditions within the reservoir may be considered isothermal in most cases.

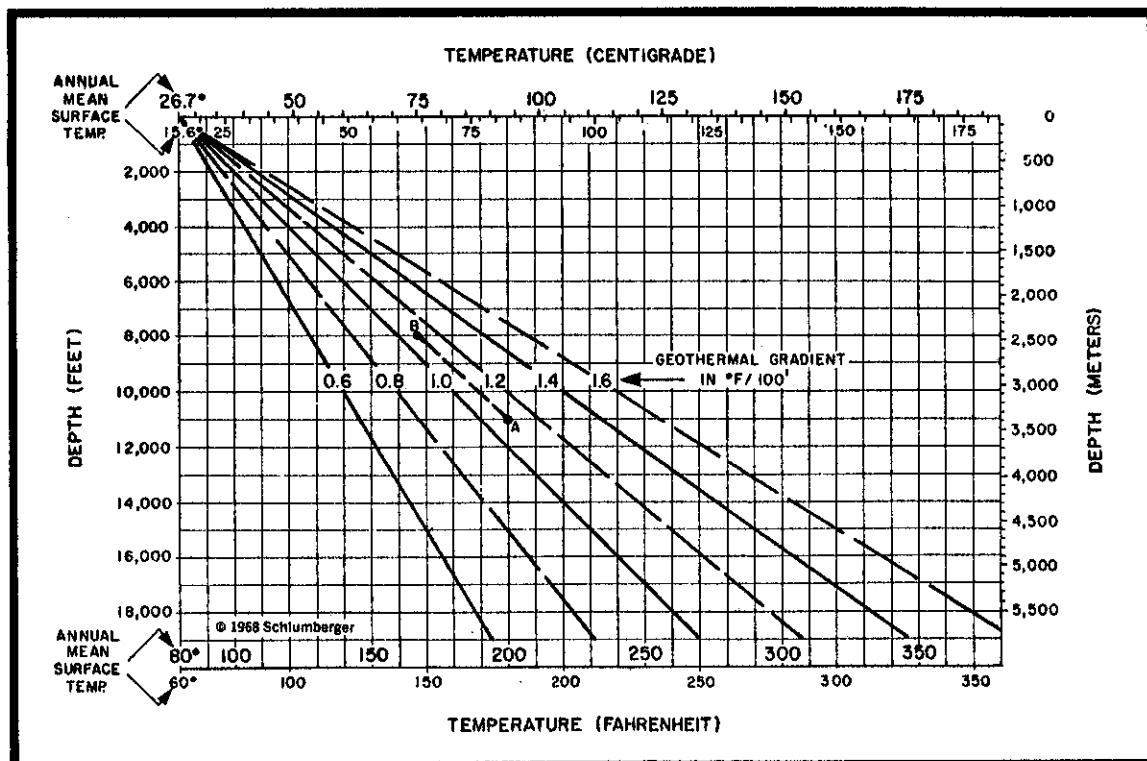


Fig. 2-23. Estimation of formation temperature.

RESERVOIR FLUID BEHAVIOR

3

A. Classification of oil and gas

What are oil and gas ? - Petroleum consists predominantly of paraffin series ($C_n H_{2n+2}$) hydrocarbons together with lesser quantities of cyclic hydrocarbons naphthalenes ($C_n H_{2n}$) and aromatics ($C_n H_{2n-6}$) mixed together in varying proportions.

The chart below classifies reservoir hydrocarbons into categories giving typical ranges for composition, gravity, and GOR.

There are no definite demarkations between the categories, which often vary in definition according to local usage. In general oils contain a higher fraction of heavy molecules, while at the other end of the scale, methane and other light molecules predominate in gases.

	<u>GOR RANGE</u>	<u>API GRAVITY</u>	<u>TYPICAL COMPOSITION</u>					
			C ₁	C ₂	C ₃	C ₄	C ₅	C ₆₊
1) DRY GAS	∞ (no liquid)		.9	.05	.03	.01	.01	.01
2) WET GAS	1B/100 MCF	50 ⁰ - 70 ⁰						
3) CONDENSATE	5 TO 100MCF/B	50 ⁰ - 70 ⁰	.75	.08	.04	.03	.02	.08
4) VOLATILE OIL	3000 CF/B	40 ⁰ - 50 ⁰	.6-.65	.08	.05	.04	.03	.2-.15
5) BLACK OIL OR DISSOLVED GAS SYSTEMS	100-2500 CF/B	30 ⁰ - 40 ⁰	.44	.04	.04	.03	.02	.43
6) HEAVY OIL	0	20 ⁰ - 25 ⁰	.20-.03	.02	.02	.02	.02	.75
7) TAR & BITUMEN	0	10 ⁰	-	-	-	-	-	.90

Fig. 3-1. Classification and composition of reservoir hydrocarbons

Classification of oil

Crude oil chemistry is quite complex and a typical crude may contain several thousand different compounds belonging to 18 different hydrocarbon series. A complete chemical analysis of crude oils, in terms of compounds present, is a difficult, if not impossible task and, less complete types of analyses (e.g. by the amounts of lumped elements present) are often not useful for determining its physical characteristics.

Difficulty in classifying oils by the chemical composition of their constituents has led to widespread use of simpler, less technical classifications.

One classification widely used distinguishes between "paraffin base" and "asphalt-base" oils. In the former, the paraffins predominate, and such an oil, when cooled to low temperatures, yields an appreciable amount of light-colored wax that is not readily attacked by acids or dissolved by ether, chloroform, carbon bisulfide.

Asphaltic oils after slow distillation yield a lustrous, solid residue, usually jet black in color, which exhibits conchoidal fracture and which dissolves in the previously mentioned solvents.

The distinction between paraffin-base and asphalt-base oils serves only as a broad classification. Most asphaltic oils contain traces of solid paraffins, and most paraffin oils will produce some asphaltic residue. Some oils, said to be of "mixed base", respond to the two tests above in equal degree.

Often times the only classification made on crude oils is by its specific gravity, a procedure which has the advantage of being easy to measure using a float type hydrometer.

API gravity is an expanded inverse scale given by the relation :

$$^{\circ}\text{API} = \frac{141.5}{\text{S.G. (at } 60^{\circ}\text{ F)}} - 131.5$$

Classification of gases

Natural gas typically consists of .6 to .8 methane with the remainder made up primarily of the heavier gaseous hydrocarbons C_2 , C_3 , C_4 and C_5 . Exceptionally, natural gases have been found to contain as little as 7% methane.*

Nitrogen, carbon dioxide, hydrogen sulfide, and helium when present in small amounts are considered as impurities. However, when present in sufficiently large quantities, H_2S and He may be exploited commercially. N_2 and CO_2 do not contribute to the heat value of the gas and if present in large amounts, the gas may not burn. CO_2 and H_2S with water are corrosive and cause embrittlement of ferrous material, while the latter is a highly poisonous gas.

Chemical analysis of gases and volatile hydrocarbons, up to C_5 or C_6 , is relatively easy and inexpensive to perform by low-temperature fractional distillation, mass spectroscopy or chromatography. The results are reported in mole fraction which may be multiplied by the corresponding molecular weight to find the composition by weight.

Classification of natural gas by specific gravity, which is the ratio of the density of the gas to the density of an equal volume of air at the same temperature, is invariably available as it is easily measured at the well site with a simple balance.

* Titusville, Pa.

Field State Formation Depth, ft.	Hugoton Oklahoma, Texas Permian dolomite 3,000	Austin Michigan Stray sand 1,200	Leduc Gas Cap D-3 Alberta Devonian 5,000	Viking, Kinsella Alberta Cretaceous sand —	West Cameron, Blk 149 Louisiana (Gulf) Miocene sand 7,150
Mole percentage:					
Nitrogen, N ₂	15.5	7.3	7.41	0.24	
Carbon dioxide, CO ₂	—	—	0.72	2.26	0.30
Helium, He	0.58	0.4			
Methane, CH ₄	71.51	79.74	72.88	88.76	96.65
Ethane, C ₂ H ₆	7.0	9.1	9.97	4.76	2.05
Propane, C ₃ H ₈	4.4	2.8	5.09	2.67	0.47
Isobutane, C ₄ H ₁₀	0.29	0.1	0.72	0.42	0.08
n-Butane, C ₄ H ₁₀	0.70	0.4	1.76	0.21	0.09
Isopentane, C ₅ H ₁₂	0.02	0.1	0.99	0.38	0.03
n-Pentane, C ₅ H ₁₂	—				0.02
Hexanes, C ₆ H ₁₄	—	0.05	0.46	0.30	0.31
Heptane+	—	0.01			
	100.00	100.00	100.00	100.00	100.00

From Handbook of Natural Gas Engineering (Katz), McGraw-Hill

Table 3-1. Composition of Natural Gases.

Field	Leduc D-2	Leduc D-3	Paloma	Oklahoma City, Wilcox Oklahoma	Rodessa	Keokuk	Schuler (Jones sand) Arkansas
State or province	Alberta	Alberta	California	Oklahoma	Louisiana	Oklahoma	Arkansas
Reservoir:							
Depth, ft.	5,000	5,300	10,600	6,200	5,950	4,026	7,600
Pressure, psia	1,774	1,908	4,663	2,630	2,600	1,455	3,520
Temperature, °F	149	153	255	132	192	130	198
Mole percentage:							
Nitrogen, N ₂	—	—	—	—	—	—	1.00
Carbon dioxide, CO ₂	—	—	—	—	—	—	0.80
Methane, CH ₄	28.6	30.3	55.8	37.7	40.88	25.60	42.85
Ethane, C ₂ H ₆	10.9	13.1	5.81	8.7	4.53	8.88	6.60
Propane, C ₃ H ₈	9.4	9.4	6.42	6.3	2.60	12.41	4.10
Isobutane, C ₄ H ₁₀	2.5	1.8	1.31	1.4	1.25	1.93	
n-Butane, C ₄ H ₁₀	4.4	4.9	3.97	3.0	1.82	7.56	3.64
Pentanes, C ₅ H ₁₂	4.8	4.5	3.67	3.3	3.48	5.53	3.10
Hexanes, C ₆ H ₁₄	39.4	36.0	2.61	39.6	4.43		3.83
Heptane+	—	—	20.41	—	41.01	38.09	34.08
	100.0	100.0	100.00	100.0	100.00	100.00	100.00
Molecular weight, heptanes+	201	193	237	225	220	195	243
Specific gravity as liquid, heptanes+	0.840	0.840	0.891	0.840	0.824	0.839	0.8759

From Handbook of Natural Gas Engineering (Katz), McGraw-Hill

Table 3-2. Analysis of Reservoir Oils Containing Dissolved Gases.

B. Phase behaviour of hydrocarbon fluids

Hydrocarbon accumulations are invariably associated with formation waters that exist in the hydrocarbon zone as interstitial water, and as aquifers which lend energy to the production process.

Commonly, two or three different fluid phases* exist together in the reservoir. Any analysis of reservoir behaviour depends on the P-V-T (pressure, volume, temperature) relationships for the co-existing fluids.

It is customary to represent the phase behaviour of hydrocarbon reservoir fluids on the P-T plane showing the limits over which the fluid exists as a single phase and the proportions of oil and gas in equilibrium over the two phase P-T range.

1) Phase behaviour of a single-component system

Single-component* hydrocarbons are not found in nature; however it is beneficial to observe the behaviour of a pure hydrocarbon substance under varying pressure and temperature to gain insight into more complex hydrocarbon systems under similar conditions. As an example of the behaviour of a pure hydrocarbon substance as temperature and pressure are varied, the PVT cell shown at the upper left of Fig. 3-2 is charged with ethane at 60°F and 1000 psia. Under these conditions, ethane is in the liquid state.

If the cell volume is increased while holding the temperature constant at 60°F throughout, it will be found that the pressure falls rapidly until the first bubble of gas appears. This is called the bubble point. Further increase of cylinder volume does not reduce the pressure provided temperature is held at 60°F, although heat must be added to the system to maintain a constant temperature. The gas volume increases at this constant pressure until the point is reached where all of the liquid is vaporized. This is called the dew point. The ethane gas expands with further increase of cylinder volume at 60°F as pressure decreases hyperbolically.

A series of similar expansions can be performed at various constant temperatures from which the three-dimensional chart of Fig. 3-3 can be constructed. The locus of bubble points obtained at various temperatures projected on the pressure-temperature plane is a line, called the vapor pressure curve. At pressures above the vapor pressure curve ethane exists in the liquid phase, and beneath it in the gaseous phase.

The vapor pressure curve for single-component systems terminates at the critical point. As the critical point is approached the properties of the gas and liquid phases approach each other, and they become identical at the critical point.

Figure 3-3 shows a three-dimensional diagram of ethane illustrating the ranges of temperature and pressure it may exist as single phase gas or liquid and as a two phase mixture in equilibrium.

This same information is also conveyed on the P-T plane as shown to the left. Note that in this diagram of a single-component system the bubble point and dew point lines coincide and is called the vapor pressure curve. The vapor pressure curve terminates at the critical point.

* A fluid phase being defined, for our purposes, as a physically distinct and separable part of the system; oil, gas, or water.

* A component is any pure chemical substance—nitrogen, methane, butane, water etc. A component may exist in more than one phase i.e. liquid water, water vapor, or as ice.
By vapor we mean gas which is close to or co-existing with its liquid form.

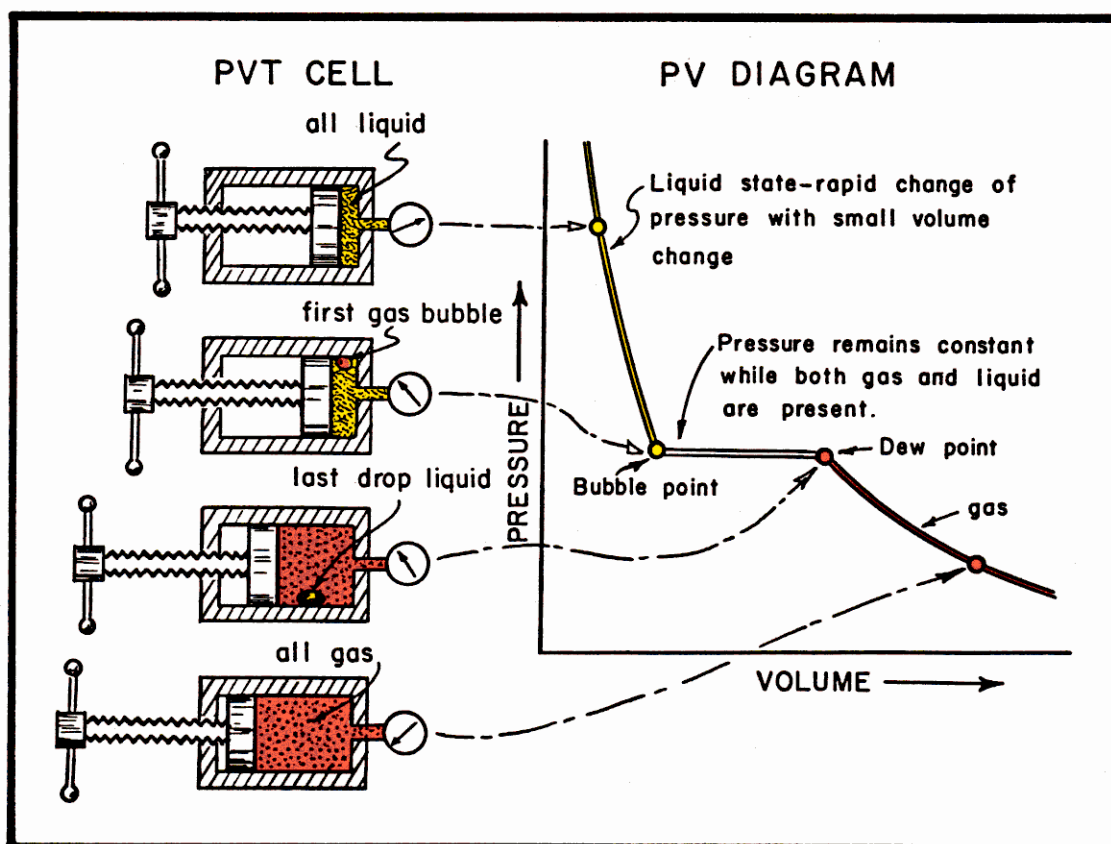


Fig. 3-2. Phase behaviour of a single-component hydrocarbon

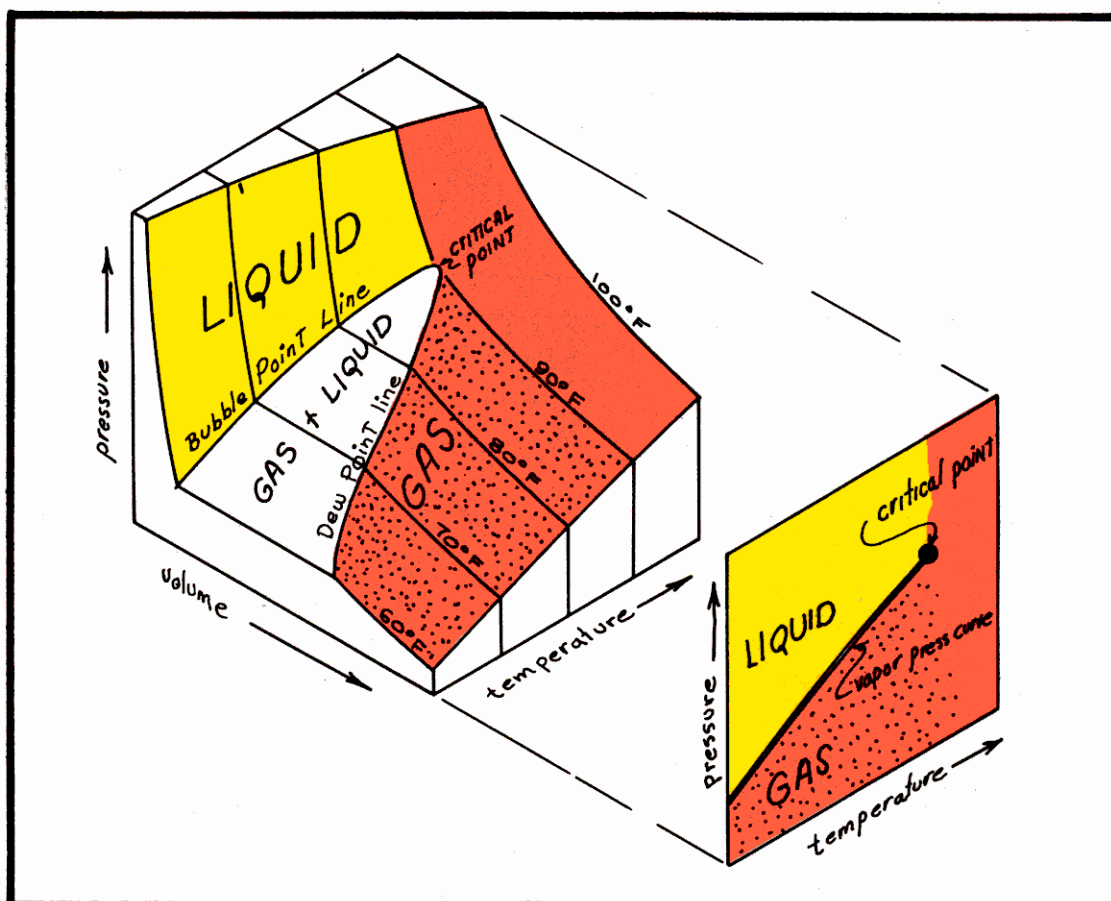


Fig. 3-3. Three-dimensional diagram of single-component system.

Fig. 3-4 shows the densities of the liquid and vapor that co-exist in the two-phase region between bubble point line and dew point line. Points A and B respectively represent the densities of liquid and vapor at temperature T_1 . As temperature increases liquid density decreases and vapor density increases, until they become identical at the critical point.

It has been found that the average density of the liquid and vapor

$\frac{D_l + D_v}{2}$ results in a straight line plot.

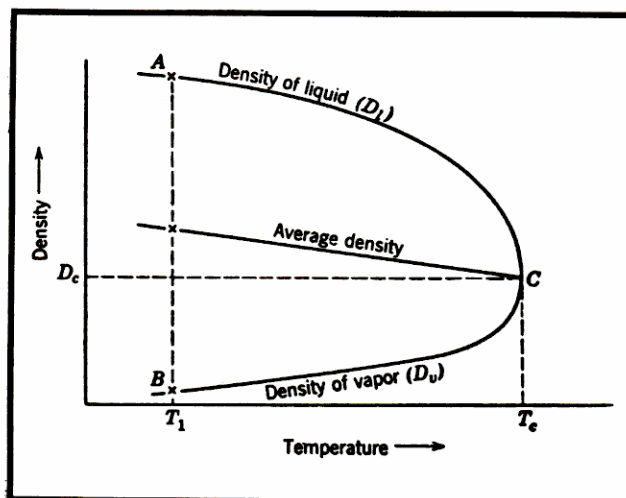


Fig. 3-4. Typical diagram of densities vs temperature in two-phase region (From Burcik)

2) Phase behaviour of multi-component systems

Consider the phase behaviour of a 50:50 mixture of two pure hydrocarbon components on the P-T plane shown in figure 3-5.

The vapor pressure and bubble point lines do not coincide but form an envelope enclosing a broad range of temperatures and pressure at which two phases (gas and oil) exist in equilibrium.

The dew and bubble point curves meet at the critical point, which is defined as that temperature and pressure at which liquid and vapor (gas) phases have identical intensive properties-density, specific volume etc.

Fluid above the bubble point is in the liquid state and fluid below the dew point line is gas : in the space enveloped between the two lines, liquid and gas are in equilibrium.

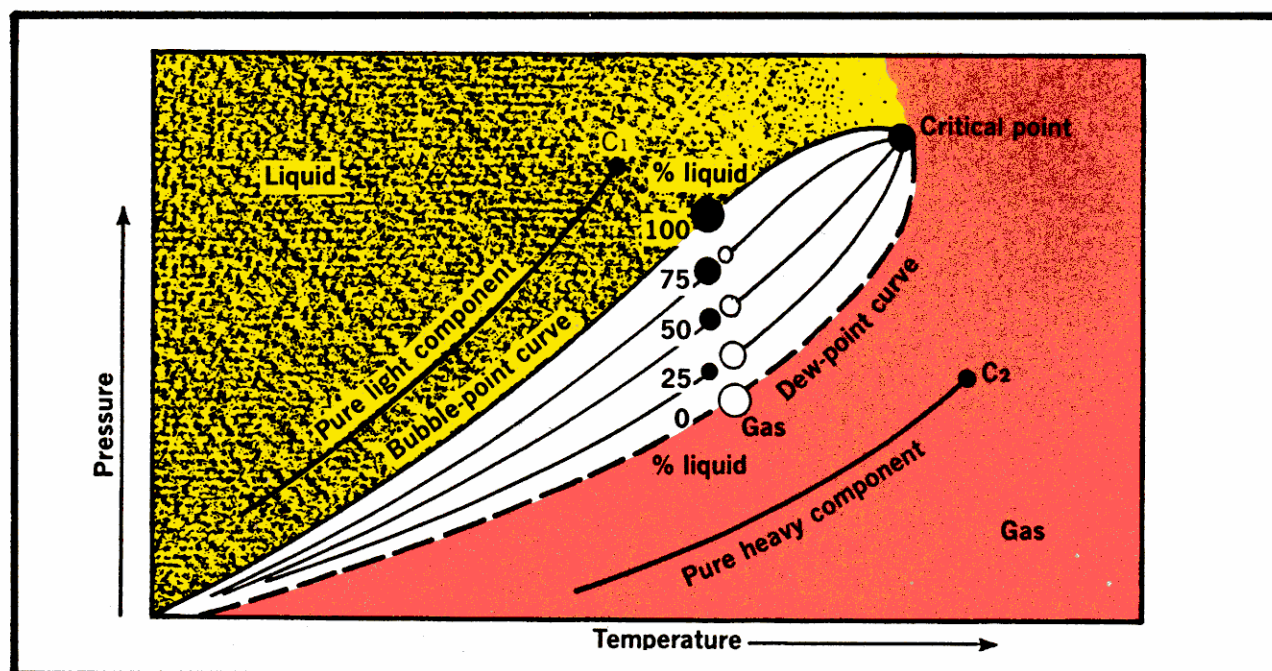


Fig. 3-5. Vapor pressure curves for two pure components and phase diagram for a 50:50 mixture of the same components. (Elements of Petroleum Reservoirs.)

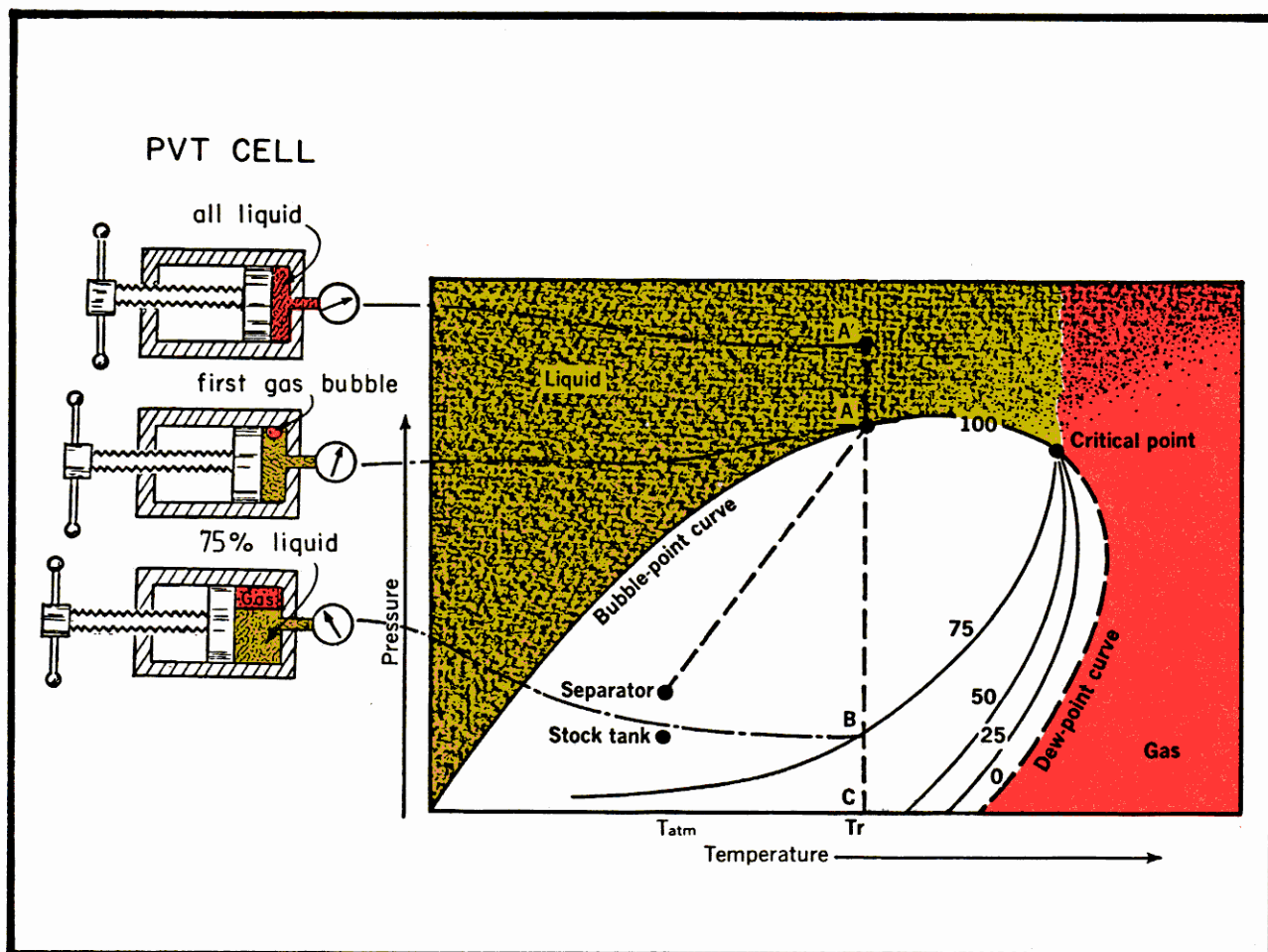


Fig. 3-6. Phase diagram of low shrinkage oil.

a) Phase diagram of a low shrinkage reservoir fluid

The shape of the two-phase envelope and its position on the P-T diagram is determined by the chemical composition and amount of each constituent present. Each reservoir fluid has a unique phase diagram.

Figure 3-6 is a phase diagram typical of a low shrinkage reservoir fluid.

Fluid at reservoir temperature and pressure at point A' exists as under-saturated liquid. If a sample of this fluid is expanded in a PVT cell at reservoir temperature T_r , from A', the bubble point pressure will be reached at A. This is approximately the path that fluids follow in moving horizontally through the reservoir to the well bore.

A continued expansion at T_r , yields increasing percentage of gas and decreasing percentage of oil in the PVT cell until at point B there remains 75% oil.

The path from A to the pressure and temperature the separator is operated at is shown by a dashed line and indicates the fractions of gas and oil recovered at separator conditions.

A further reduction in pressure between the separator and stock tank conditions results in some loss of gas at the tank vent and a corresponding reduction in oil volume - see figure 3-7.

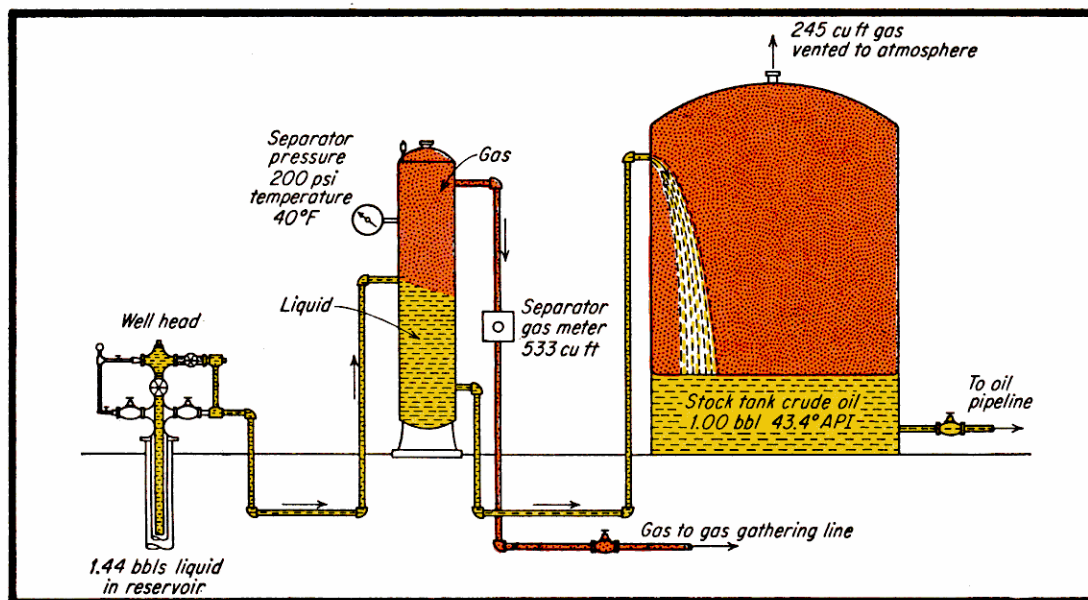


Fig. 3-7. Operation of separator on well producing crude oil with dissolved natural gas.

b) Phase diagram of retrograde condensate reservoir fluid

The phase diagram 3-8 typifies the behaviour of a retrograde reservoir. Fluid at point A' is above critical temperature and is therefore classified as gas. On reduction of pressure at constant temperature from point A', the dew point line is crossed at A and liquid begins to condense from the reservoir gas.

If the pressure and temperature are reduced from A along the dashed line path to separator condition, the diagram shows that 25% of liquid is recovered at this point. On further reduction of pressure to atmospheric pressure only about 2% of liquid remains.

The recovered liquid is termed "condensate" or "distillate" which is simply oil, generally light in color and low in specific gravity.

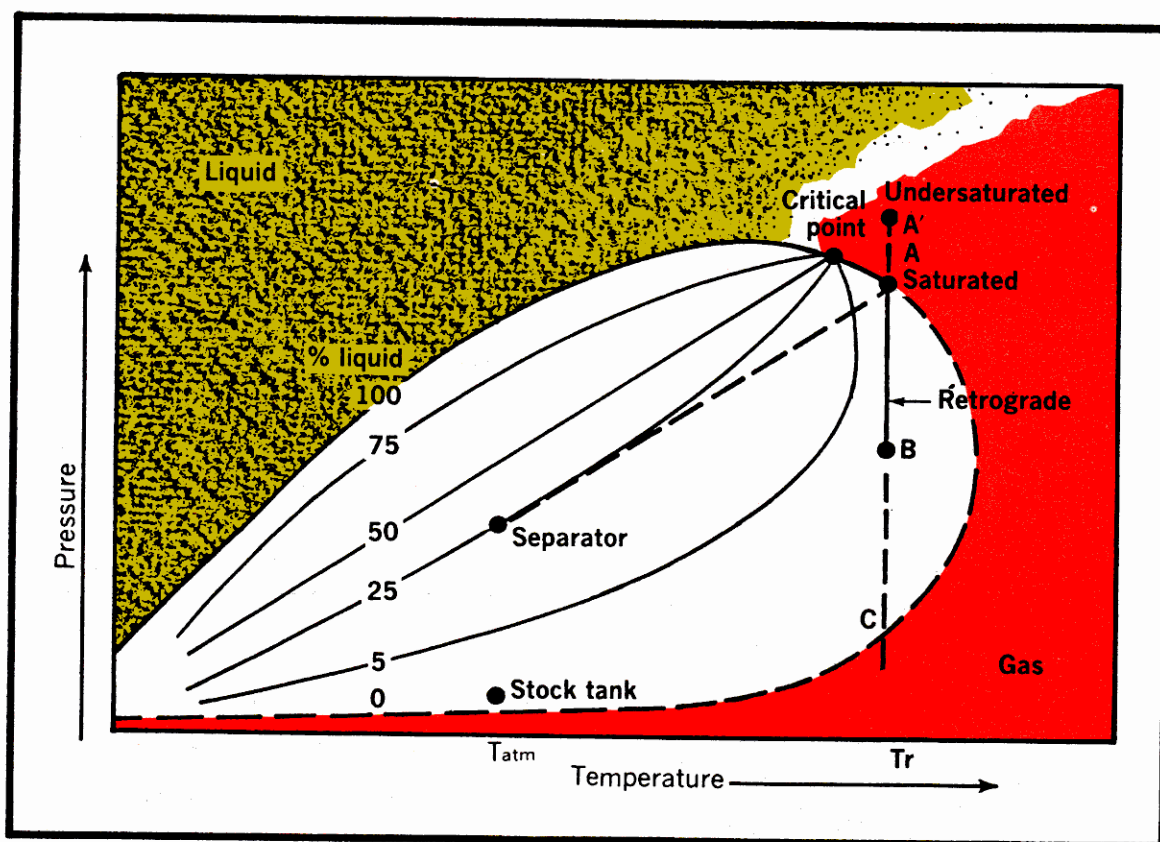


Fig. 3-8. Phase diagram of retrograde condensate gas.

c) Phase diagram of a dry gas reservoir fluid

The phase diagram given in Fig. 3-9, on the pressure-temperature plane, typifies the behaviour of a dry gas reservoir. If the pressure and temperature are reduced from the original reservoir conditions at point A to standard stock tank conditions (60°F and 14.7 psia)* there is no liquid recovery and the reservoir fluid remains completely in the gaseous phase during the process.

* psia = pounds per square inch absolute

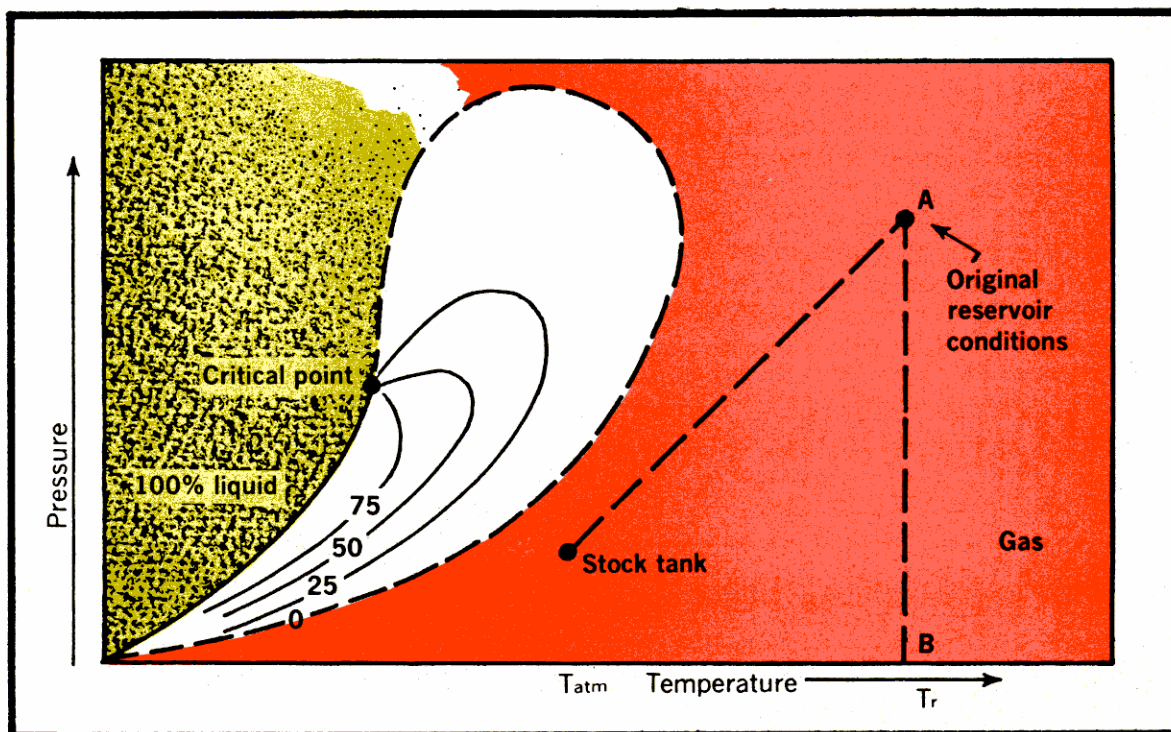


Fig. 3-9. Phase diagram of dry gas. (Elements of Petroleum Reservoirs.)

d) Phase diagram of a wet gas reservoir fluid

Fluid that exists above its critical temperature as gas in reservoir conditions, but produces a small quantity of liquid condensate on reduction to separator/stock tank conditions, may be termed "wet gas". A typical phase diagram for a wet gas is shown in figure 3-10.

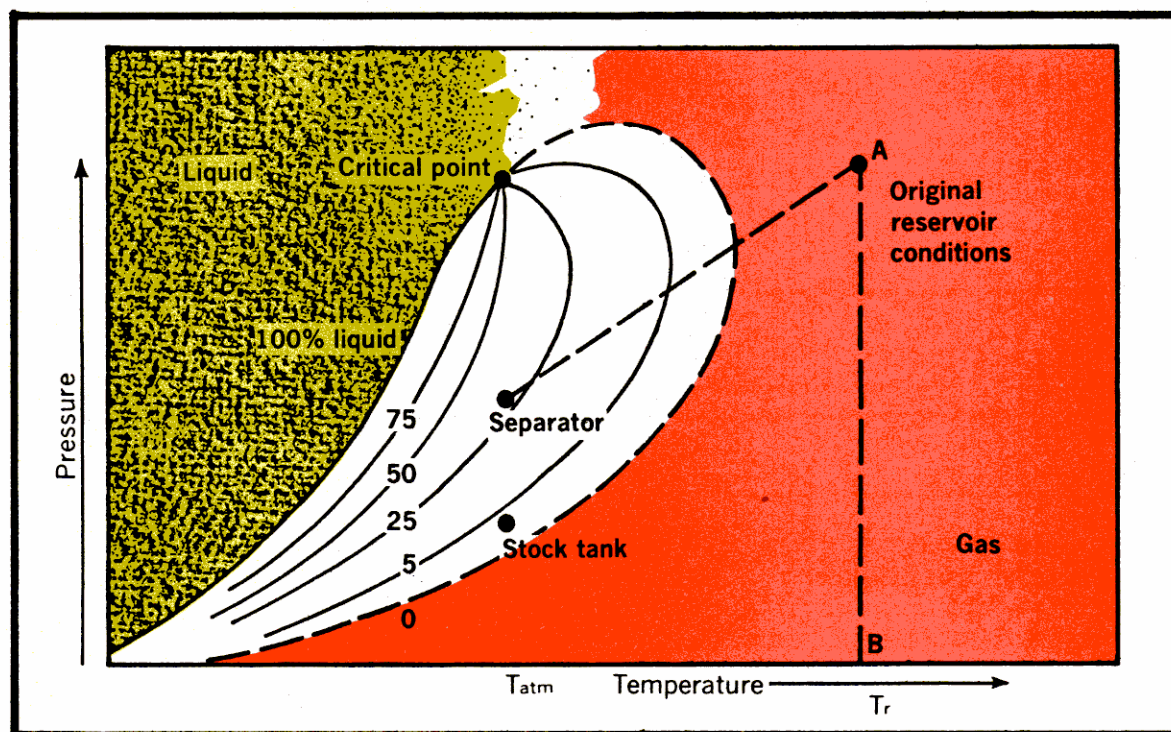


Fig. 3-10. Phase diagram of wet gas. (Elements of Petroleum Reservoirs.)

C. Reservoir fluid properties

An exact knowledge of a reservoir fluids physical properties including compressibility is needed to predict reservoir performance and interpret well test data and production logs.

1.- There are three possible sources of data :

a) Laboratory measurement made on a representative reservoir fluid sample :

- 1) The sample may be taken with a PST or wire line bottom hole sampling tool - This is the best and most costly method, and requires considerable care to assure a truly representative sample.
 - well to be shut in (or slightly opened just before sampling)
 - pressure during sampling should remain above the bubble point
 - leakage or segregation during transfer must be avoided
 - an average of three samples assures reliability
- 2) Sample of oil and gas taken at the separator and recombined at producing GOR in the lab.
 - flowrates must be stable
 - gas vented at stock tank must be included in the total GOR

b) Charts of correlated or "average" properties usually made on a basis of specific gravity are used in absence of measured data.

- results with oil volume factor, solubility are subject to larger errors, particularly if the composition varies appreciably from the correlation model
- gas volume factors are generally accurate to within 1% for hydrocarbon gases with less than 5% impurities. Exceptionally error may reach 2 or 3%.

c) In situ measurement with production tools.

The relative densities of oil/water/gas fluid columns can be measured in situ using a Gradiomanometer in the shut in well. An accurate determination of these densities requires a well calibrated bottom hole pressure gauge such as the Hewlett-Packard quartz pressure gauge.

Where direct laboratory PVT measurements are not available, it may be necessary to use charts to estimate fluid properties.

Use of the "Fluid Conversion Charts" given on the following pages should be made with the understanding that they are correlations or estimates of average physical properties with specific gravity, temperature and pressure, while the true fluid behaviour depends on chemical composition of the constituents.

The application at hand dictates which sources of data may be used. Obviously, reservoir predictions made by material balance methods, can be no better than the fluids data used. On the other hand, use of a gas volume factor based on specific gravity correlations is probably better than needed to convert a downhole spinner flowmeter volumetric rates to surface conditions.

2) Compressibility of gases

a) Ideal gas behaviour :

The ideal gas law may be expressed :

$$pV = nRT$$

where :

METRIC UNITS-CGS

p = absolute pressure of gas in atmospheres
 V = volume occupied by gas in cc
 n = number of gram-moles of gas (grams of gas/molecular weight)
 R = 82.05 (gas constant)
 T = absolute temperature in degrees Kelvin
 ($^{\circ}\text{K} = 273 + ^{\circ}\text{C}$)

API UNITS

p = absolute pressure of gas in psia (psia = 14.7 + gauge pressure)
 V = volume occupied by gas in cu ft
 n = number of lb-moles of gas (lbs of gas/molecular weight)
 R = 10.71 (gas constant)
 T = absolute temperature in degrees Rankine
 ($^{\circ}\text{R} = 460 + ^{\circ}\text{F}$)

To find the volume occupied by a quantity of gas when the conditions of temperature and pressure are changed from State 1 to State 2 we note that $n = pV/RT = \text{a constant}$, so that:

$$\frac{p_1 V_1}{T_1} = \frac{p_2 V_2}{T_2}$$

where :

p_1 and p_2 are absolute pressures in States 1 and 2
 T_1 and T_2 are absolute temperatures in States 1 and 2
 V_1 and V_2 are volumes in States 1 and 2.

Boyles law is $pV = p'V'$ at constant temperature.

Charles law is $\frac{V}{T} = \frac{V'}{T'}$ at constant pressure.

b) Deviation factor for natural gases

Most gases show considerable deviation from ideal behaviour at elevated temperatures and pressures. The compressibility factor "Z", which is a function of the gas composition, pressure, and temperature, is used to modify the ideal-gas law. The law now takes the form :

$$\frac{p_1 V_1}{Z_1 T_1} = \frac{p_2 V_2}{Z_2 T_2}$$

where :

p_1 and p_2 are absolute pressures at States 1 and 2

V_1 and V_2 are volumes at States 1 and 2

T_1 and T_2 are absolute temperatures at States 1 and 2

Z_1 and Z_2 are compressibility correction factors at States 1 and 2.

The generalized chart of figure 3-11 can be used to approximate the compressibility factor Z, of any gas after first reducing it to a "corresponding state".

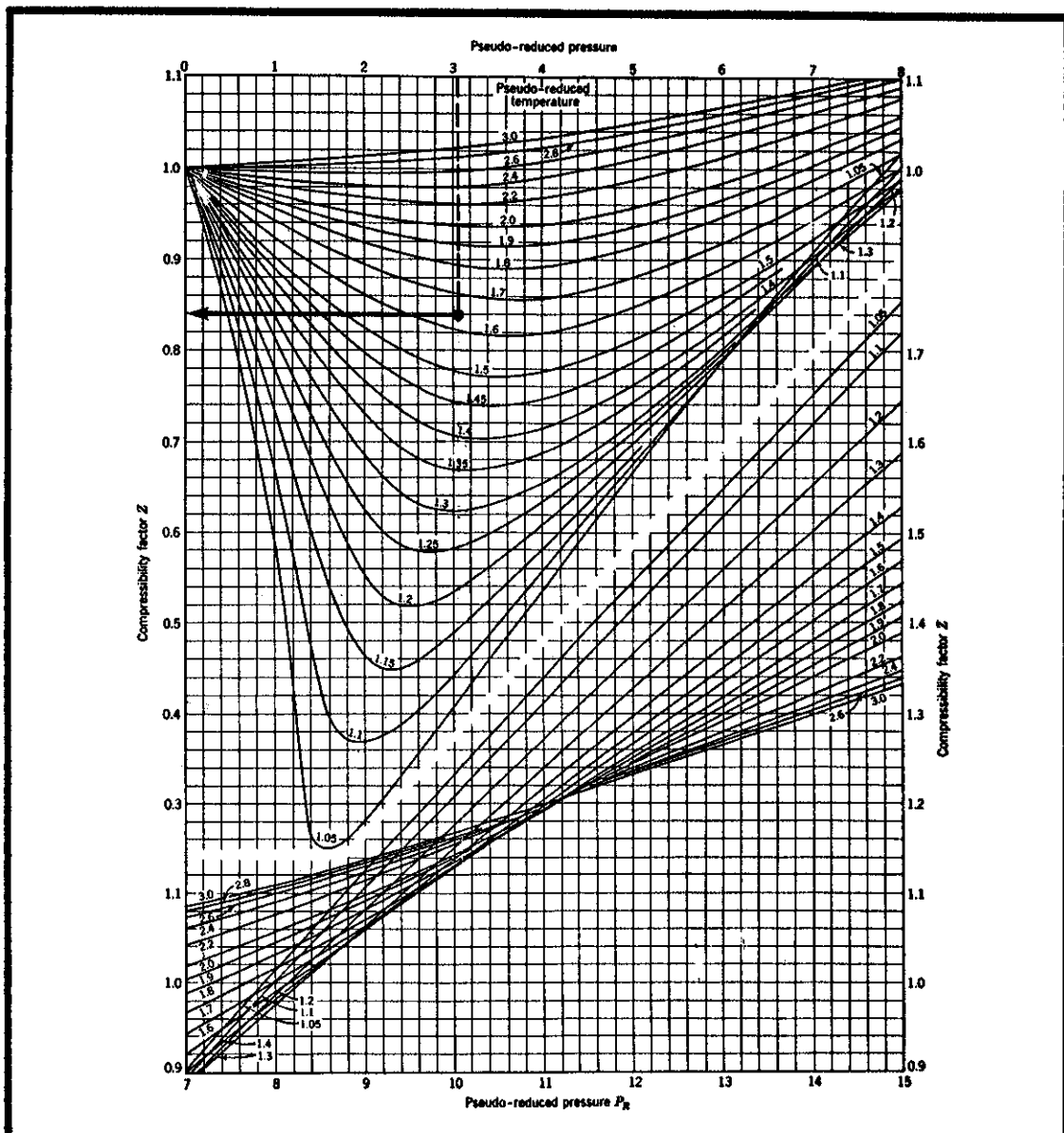


Fig. 3-11. The compressibility factor for natural gases as a function of pseudoreduced pressure and temperature.

Fluids are in a corresponding state, with respect to the critical state, the reference, when any two variable properties have the same ratio of reduced values.

$$T_R = \frac{T}{T_C} \quad , \quad P_R = \frac{P}{P_C} \quad , \quad V_R = \frac{V}{V_C}$$

- 1) For pure substances, the critical temperature and pressure is found from a table of physical properties.
- 2) For mixtures of known composition the "pseudo critical" pressure and temperature is calculated by taking the mole average of the individual constituent values.

$$\text{i.e. } P_{pc} = \sum Y_1 P_{c1} + Y_2 P_{c2} \dots$$

$$T_{pc} = \sum Y_1 T_{c1} + Y_2 T_{c2} \dots$$

where :

Y_1 = mole fraction of component 1
 P_{c1} = critical pressure of component 1
 T_{c1} = critical temperature of component 2

1	2	3	4	5	6
Component	Mole Fraction	Individual Absolute Critical Temperature T_c °R	Product Col 2 x Col 3	Individual Absolute Critical Pressure p_c psia	Product Col 2 x Col 5
CH ₄	0.8319	344.2	286.3	673	560
C ₂ H ₆	0.0848	550.3	46.7	710	60.2
C ₃ H ₈	0.0437	666.3	29.1	617	27.0
i-C ₄ H ₁₀	0.0076	735.0	5.59	529	4.02
n-C ₄ H ₁₀	0.0168	765.6	12.86	551	9.26
i-C ₅ H ₁₂	0.0057	829.0	4.73	483	2.75
n-C ₅ H ₁₂	0.0032	845.5	2.71	490	1.57
C ₆ H ₁₄	0.0063	914.1	5.76	440	2.77
Pseudocritical Temperature			393.75	Pseudocritical Pressure	667.57

Table 3-3. Computation of Pseudocritical Temperature and Pressure of a Natural Gas.

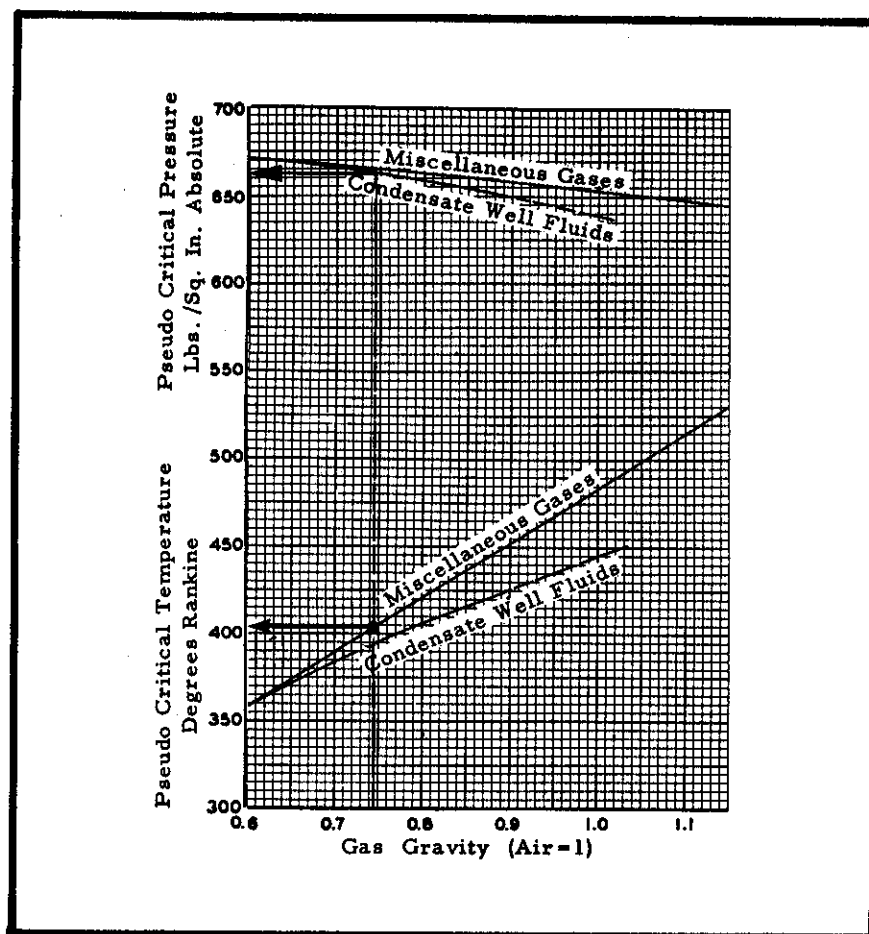


Fig. 3-12. Pseudocritical properties of natural gases.

Example :

Find compressibility factor Z for a .75 gravity gas at 2000 psig, 150°F .

1.- From figure 3-12, $P_c = 665$ psi and $T_c = 405^{\circ}\text{R}$

2.- Reduced temperature and pressures :

$$T_{PR} = \frac{T}{T_{pc}} = \frac{460+150}{405} = 1.63$$

$$P_{PR} = \frac{P}{P_{pc}} = \frac{2000 + 14.7}{665} = 3.03$$

3.- Entering chart figure 3-11 with $T_{PR} = 1.63$ and $P_{pc} = 3.03$, we find $Z = 0.84$.

3) Conversion factors between surface and downhole volumes

Conversion of downhole volumes (or volumetric rates) of oil, gas, and water to equivalent volumes at surface conditions is made so frequently that it is convenient to use conversion factors which account for the overall changes due to solubility and compressibility.

Before a discussion of volume factors, let us define the units commonly used to measure hydrocarbon volumes.

Oil volume measurement

The unit of measurement of oil is the API barrel or the cubic meter at stock tank conditions - conventionally 60°F (15.5°C) and 14.7 psia (1 atmosphere).

Gas measurement

Gas is measured in standard cubic feet scf, or in cubic meters at the same reference conditions 60°F, 14.7 psia.

Gas oil ratio

Gas oil ratio R , (sometimes abbreviated GOR) is the ratio of gas production to oil production - both measured at standard conditions 60°F, 14.7 psia. Units are standard cubic feet/stock tank barrel, scf/B or cubic meters gas per cubic meter of oil m^3/m^3 . As there are 5.6 cubic feet in a barrel.

$$\text{scf/B} \div 5.6 = m^3/m$$

The basic surface/downhole volumetric relationships shown diagrammatically in figure 3-13 should be kept firmly in mind when dealing with fluid conversions.

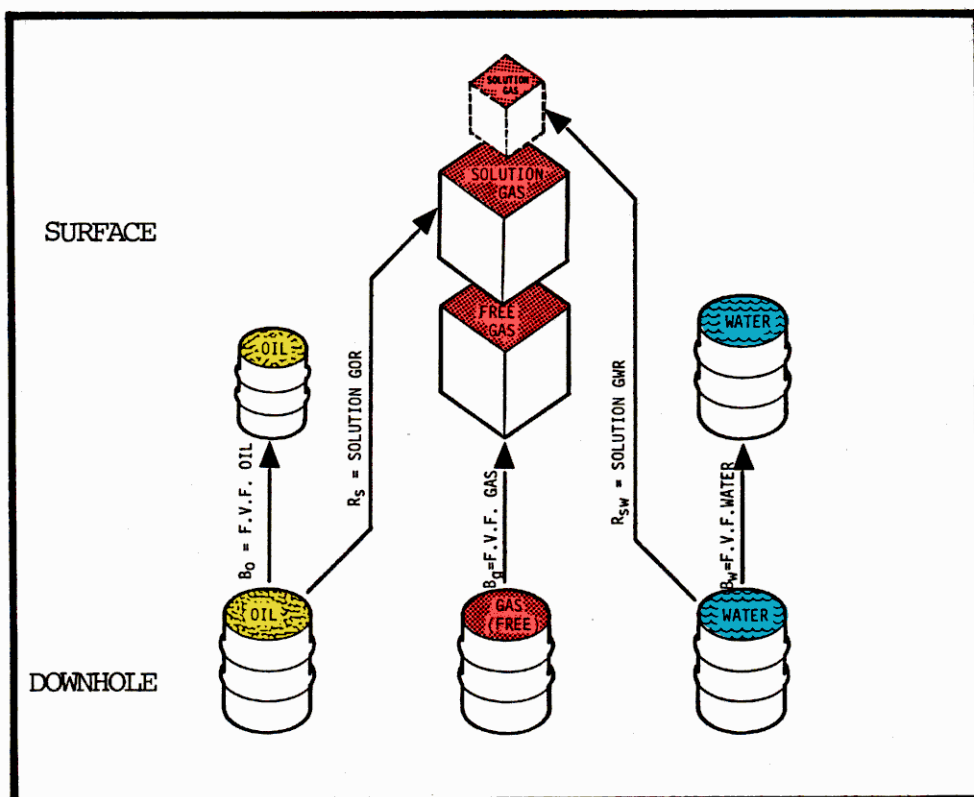


Fig. 3-13. Relationships between surface and downhole volumes - dissolved gas system.

Formation volume factors are designated by the letter B with a suffix denoting the fluid phase concerned.

Formation volume factor, defined below, is a function of fluid composition and the pressure/temperature difference between the downhole and reference state.

$$\text{Formation Volume Factor} = \frac{\text{Volume at downhole conditions}}{\text{Volume at reference conditions}}$$

Figure 3-13 shows that the total gas at surface is the sum of the solution gas evolved from the downhole liquids plus free gas produced independently from the oil. The gas volume factor accounts for expansion of free gas.

Oil shrinks in volume between downhole/surface conditions primarily as a result of the solution gas evolved. A typical range of B_o is 1.2 for low GOR oil to 1.4 or higher for the more volatile oils.

Solubility of gas in water is low and the combined effects of reduction in temperature, pressure and loss of solution gas has a small (but for some purposes important) effect on B_w .

a) Gas Formation Volume Factor, B_g

$$B_g = \frac{\text{Volume at downhole temp. and pressure}}{\text{Volume at } 60^\circ\text{F, } 14.7 \text{ psia}} \quad \text{is scf/B or m}^3/\text{m}^3$$

The gas formation volume factor may be known from PVT measurements on a gas sample, or it might be calculated using the relation :

$$\frac{P_1 V_1}{Z_1 T_1} = \frac{P_2 V_2}{Z_2 T_2}$$

then

$$B_g = \frac{V_2}{V_1} = \frac{P_1 T_2 Z_2}{P_2 T_1 Z_1}$$

where conditions 1 are standard and conditions 2 are bottom hole.

Charts based on the relationship and correlations between Z and specific gravity, pressure and temperature have been established to simplify calculations.

The following example illustrates use of these charts (Figure 3-14.)

Find the volume occupied by 400 scf of gas when $\gamma_g = 0.70$, $T_{wf} = 200^\circ\text{F}$, and $p_{wf} = 2,000$ psia.

Using Fig 3-14 (lines drawn in) this is solved as follows:

1. Select the group of temperature lines for $\gamma_g = 0.70$. Entering on the abscissa at 2,000 psia, go vertically to the 200°F line, then move left to the ordinate value of 125 for $1/B_g$.

$$\frac{1}{B_g} = 125 = \frac{V_{gsc}}{V_{gwf}} = \frac{400 \text{ scf}}{V_{gwf}}$$

$$2. \quad V_{gwf} = \frac{400}{125} = 3.2 \text{ cu ft}$$

EXAMPLE — Interpolation needed.

Find the volume occupied by 600 scf of gas where: $\gamma_g = 0.74$, $T_{wf} = 175^\circ\text{F}$, and $p_{wf} = 2,000$ psia.

Using Fig 3-14 (lines not drawn in) this is solved as follows:

1. Select the group of temperature lines for $\gamma_g = 0.70$. Entering on the abscissa at 2,000 psia, go vertically to the 175°F position, then move left to the ordinate value of 133 for $1/B_g$.
2. Select the group of temperature lines for $\gamma_g = 0.80$. Entering on the abscissa at 2,000 psia, go vertically to the 175°F position, then move left to the ordinate value of 138 for $1/B_g$.
3. The interpolation between the $1/B_g$ values is solved as follows:

γ_g	$\frac{1}{B_g}$
0.70	133
0.74	X
0.80	138

$$\frac{1}{B_g} = 133 + 0.4 \times (138 - 133) = 135$$

$$4. \quad \frac{1}{B_g} = 135 = \frac{V_{gsc}}{V_{gwf}} = \frac{600 \text{ scf}}{V_{gwf}}$$

$$V_{gwf} = \frac{600}{135} = 4.44 \text{ cu ft}$$

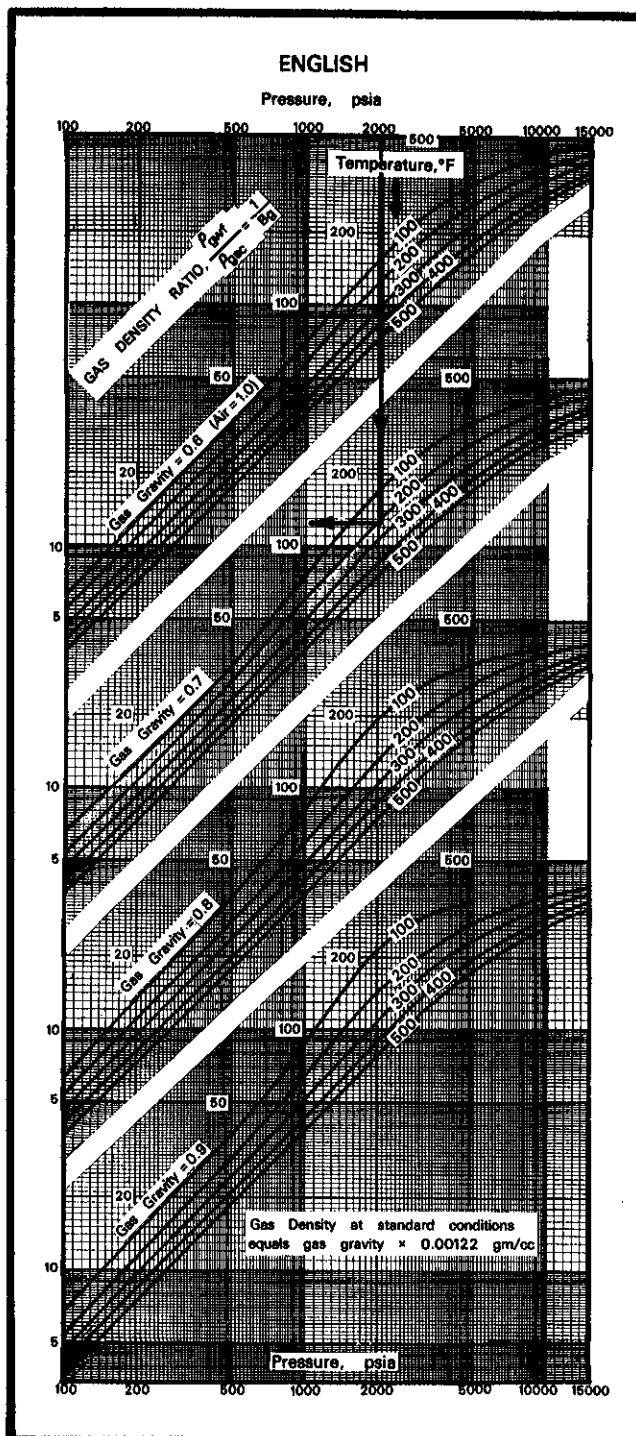


Fig. 3-14 (Chart Fg-1): $1/B_g$ as a function of γ_g , T_{wf} , and p_{wf} (after Standing and Katz)

b) Formation Volume Factor of oil, B_o

$$B_o = \frac{\text{Volume of oil (including dissolved gas at downhole conditions)}}{\text{Volume of oil at reference conditions } 60^\circ\text{F, } 14.7 \text{ psia}}$$

The formation volume factor of an oil is best determined by PVT measurement on a reservoir fluid sample.

Figure 3-15 is a typical plot of PVT data for an undersaturated oil. From 8000 psig to the bubble point pressure at 6350 psig, the B_o increase is due to expansion of the undersaturated oil.

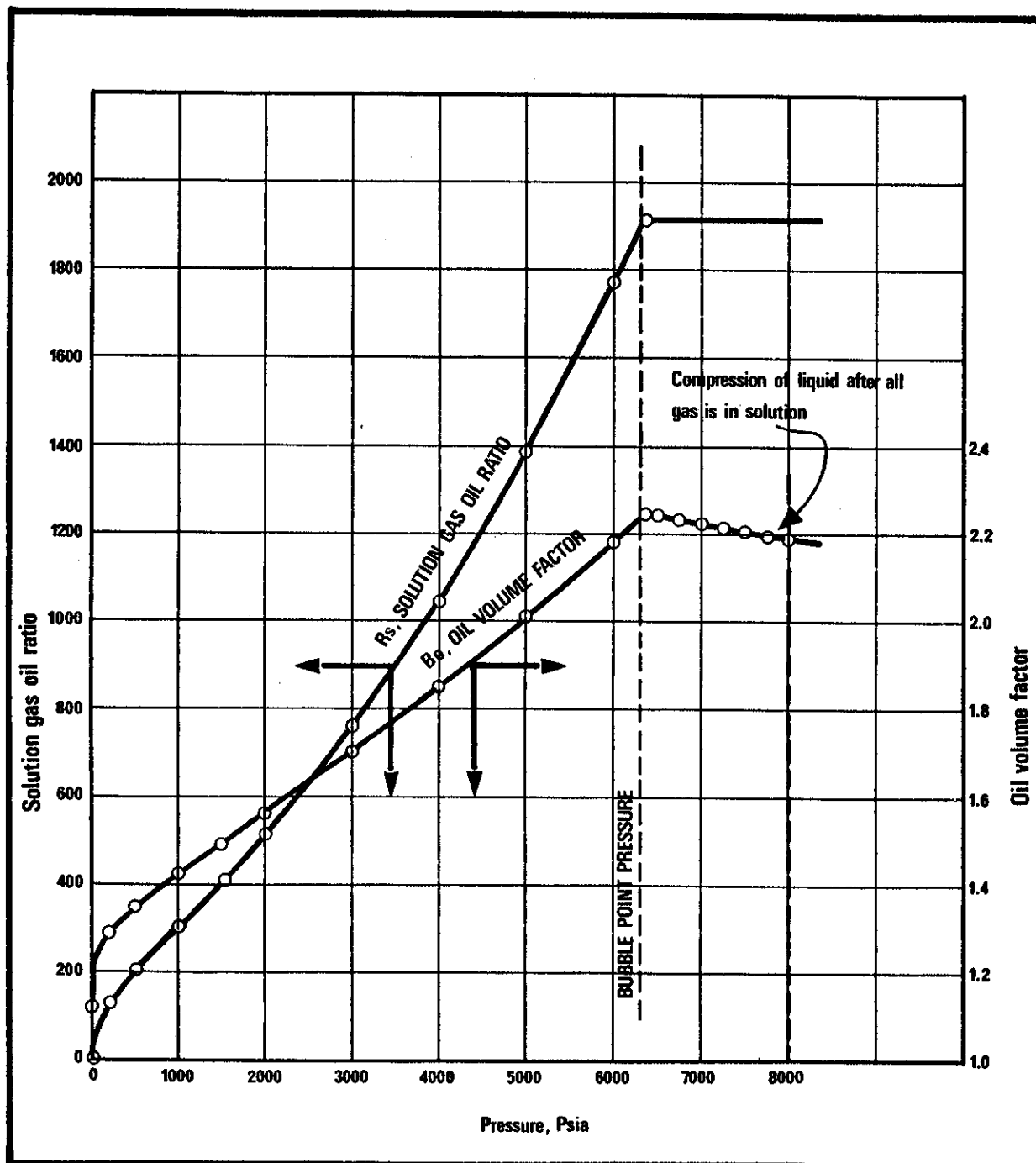


Fig. 3-15. Typical PVT data for differential vaporization of an undersaturated oil at constant temperature (305°F).

On expansion from 6350 psi to atmospheric pressure increasing amounts of gas are liberated. Note that the R_g , the amount of gas in solution is almost directly proportional to the system pressure.

B_o , being dependent essentially on the amount of dissolved gas increases with pressure up to the bubble point, where all of the available gas is dissolved and then decreases at a rate determined by the liquid compressibility.

Solubility and volume factor correlations

Solubility of natural gas in oil is dependent on the composition of the hydrocarbons, the temperature, and pressure applied.

Figure 3-16 (chart Fgo-1) can be used to estimate bubble point pressure, P_b , and R_{sb} , the amount of gas which will dissolve in a given amount of oil at this pressure and temperature.

EXAMPLE — Fig. 3-16

Find the bubble-point pressure, p_b , under the following conditions:

$$\begin{aligned} q_{osc} &= 600 \text{ B/D} \\ q_{gsc} &= 240 \text{ Mcf/D} \\ T_{wf} &= 180^\circ\text{F} \\ \gamma_g &= 0.75 \\ \gamma_o &= 40^\circ \text{ API} \end{aligned}$$

The solution is as follows:

1. $R = \frac{240,000 \text{ cf/D}}{600 \text{ B/D}} = 400 \text{ cf/B}$
2. Take $R_{sb} = R$; that is, the solution gas-oil ratio at bubble-point pressure is defined as being equal to the producing gas-oil ratio. The assumption is implicit that, for all practical purposes, all the dissolved gas has come out of solution when standard conditions are reached.
3. On the nomograph (Fig. 3-16) draw a line from the temperature ($T_{wf} = 180^\circ\text{F}$) through the solution gas-oil ratio at bubble-point pressure ($R_{sb} = 400 \text{ cf/B}$) to Point **a** on Line A.
4. Draw a line from the gas gravity ($\gamma_g = 0.75$) through the oil gravity ($\gamma_o = 40^\circ \text{ API}$) to Point **b** on Line B.
5. Connect Points **a** and **b** and read the answer: $p_b = 1,560 \text{ psia}$.

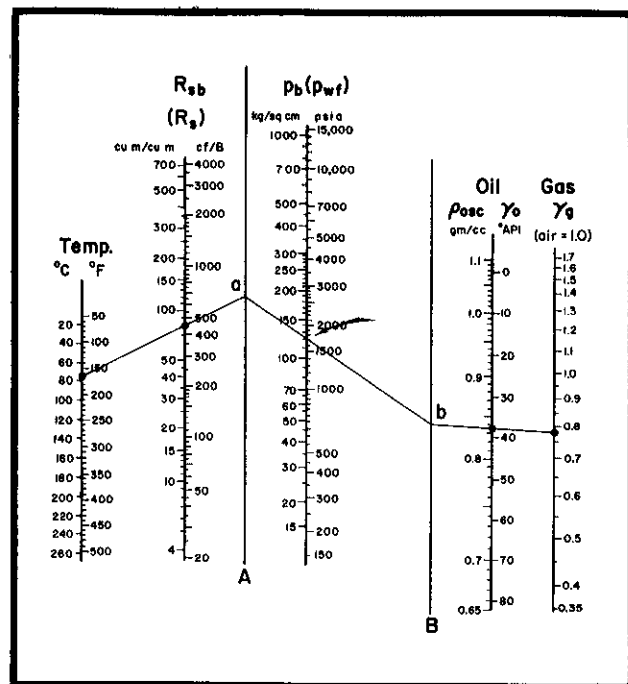


Fig. 3-16 (Chart Fgo-1): Nomograph relating R_{sb} to p_b , T_{wf} , γ_g , and γ_{osc} (or ρ_{osc}) for "average" conditions. Can be used to find p_b if R_{sb} is known, or vice versa.

EXAMPLE

Find R_{sb} , the solution gas-oil ratio at bubble-point pressure, under the following conditions:

$$\begin{aligned} p_b &= 900 \text{ psia} \\ T_{wf} &= 140^\circ\text{F} \\ \gamma_g &= 0.7 \\ \gamma_o &= 40^\circ \text{ API} \end{aligned}$$

This is solved using Fig. 3-16 lines not drawn in), as follows:

1. From right to left: draw a line through $\gamma_o = 40^\circ$ and $\gamma_g = 0.7$ to locate a point on Line B.
2. From that point, draw a line through $p_b = 900 \text{ psia}$ to Line A.
3. From there, draw a line to $T_{wf} = 140^\circ\text{F}$.
4. Read the answer:

$$R_{sb} = 220 \text{ cf/B}$$

Estimation of B_o at P_b

B_{ob} , the oil formation volume factor at bubble point pressure is estimated from figure 3-17 (Chart F_{go}) by entering the gas gravity γ_g , the solution gas oil ratio at bubble point pressure R_{sb} , and the temperature.

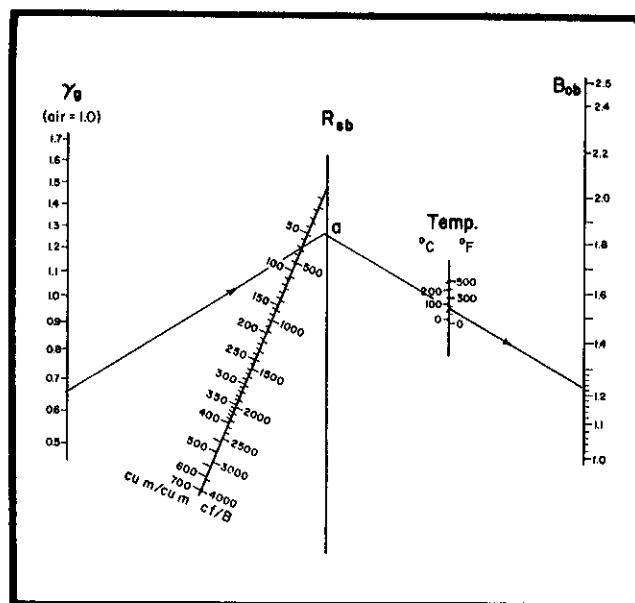


Fig. 3-17 (Chart Fgo-4): Nomograph to find

B_{ob} scales calibrated in both English and metric units.

EXAMPLE — Nomograph Solution

Find B_{ob} under the following conditions:

$$R_{sb} = 400 \text{ cf/B}$$

$$T_{wf} = 180^\circ\text{F}$$

$$\gamma_g = 0.65$$

$$\gamma_o = 45^\circ \text{ API}$$

Using Fig. 3-17 the solution is:

1. Draw a line from the gas gravity (γ_g) of 0.65 through the solution gas-oil ratio at bubble-point pressure (R_{sb}) of 400 cf/B to Line A.
2. Draw a line from Point **a** through T_{wf} (180°F) to B_{ob} at 1.24.

Estimation of oil volume factor above bubble point pressure

The formation volume factor reaches a maximum value at P_b when all of the available gas is in solution.

If the pressure is increased beyond bubble point, and there is no more gas to be driven into solution, a reduction in oil volume results.

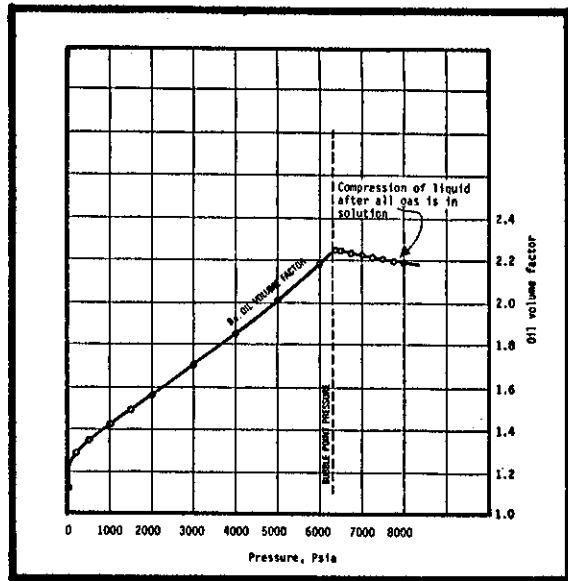


Fig. 3-18 Oil FVF (B_o) as a function of pressure (general).

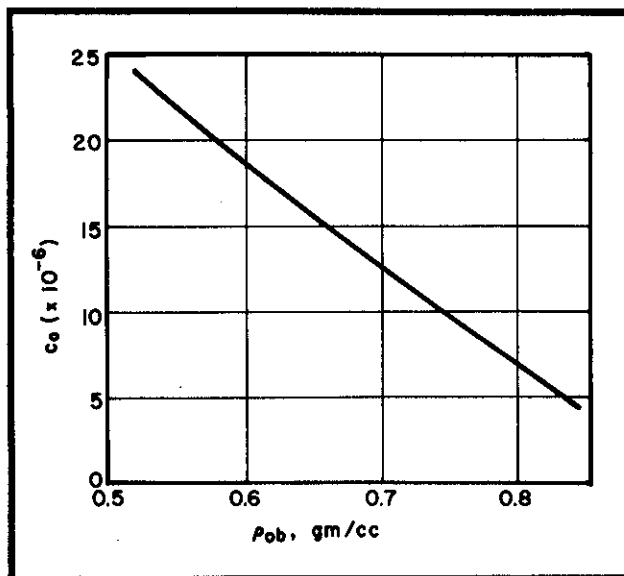


Fig. 3-19 " c_o " as a function of ρ_{ob} for "average" oils (after Calhoun)

The oil compressibility factor (C_o) is a function of the density of the oil at bubble point pressure (P_{ob}) - see figure 3-19.

For undersaturated oil, the equation relating B_o to B_{ob} is :

$$B_o = B_{ob} [1 - C_o(P_{wf} - P_b)]$$

Nomograph of figure 3-20 (chart Fgo-5) may be used to solve this equation.

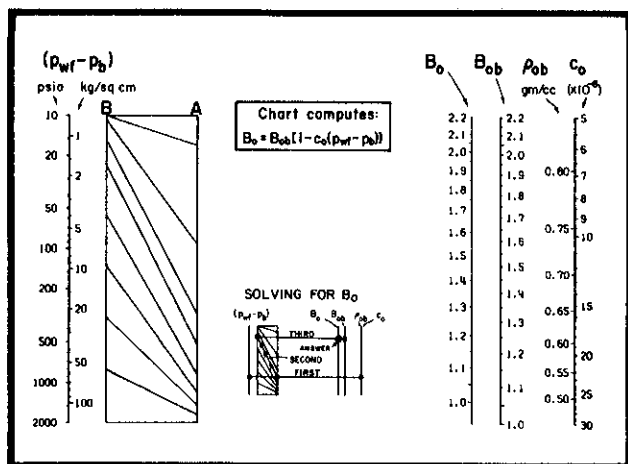


Fig. 3-20 (Chart Fgo-5): Nomograph to find B_o .
Needed: p_{wf} , p_b , c_o (or ρ_{ob}), and B_{ob} .

EXAMPLE — Undersaturated Oil

Find B_o under the following conditions:

$$\begin{aligned} B_{ob} &= 1.22 \\ \rho_{ob} &= 0.66 \text{ gm/cc} \\ p_{wf} &= 3,000 \text{ psia} \\ p_b &= 2,000 \text{ psia} \end{aligned}$$

The solution is as follows:

- From Fig 3-19 $c_o = 15 \times 10^{-6}$
- $B_o = B_{ob} (1 - c_o (p_{wf} - p_b))$
 $B_o = 1.22 (1 - (15 \times 10^{-6}) (3,000 - 2,000))$
 $= 1.20$

c) Formation volume factor of water, B_w

Dissolved gases and salts affect the compressibility of water, hence B_w . However, the solubility of natural gas in water and brine is small and the effect on compressibility can be neglected for small changes of pressure and temperature and B_w taken as unity.

For large changes in pressure and temperature, B_w may be found from figure 3-21, for either pure or natural gas saturated water.

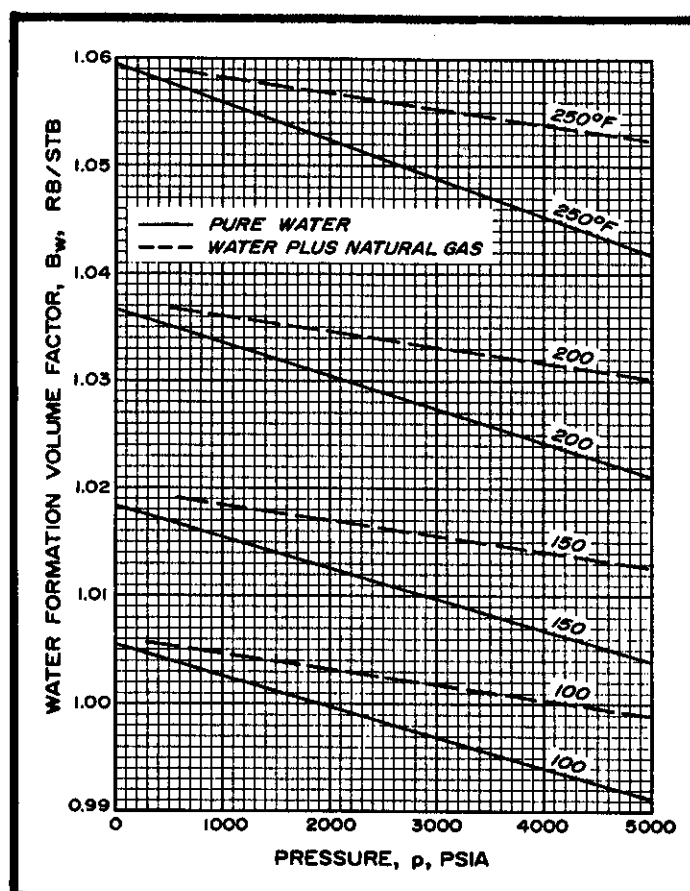


Fig. 3-21 - Formation volume factor of pure water and a mixture of natural gas and water. (Data of Dodson and Standing.)

4) Fluid density correlationsa) **GAS DENSITY**

1. **Gas specific gravity**, γ_g , is widely used in the oil industry to characterize natural gases. Gas specific gravity is defined as the ratio of the density of gas to the density of air, both at standard conditions.

$$\gamma_g = \frac{\rho_{gsc}}{(\rho_{air})_{sc}}$$

The weight of any volume of a gas can be determined by multiplying the volume of gas times γ_g times ρ_{air} . The density of air at standard conditions is 0.001223 gm/cc or 0.0762 lb/cu ft.

2. The **density** of gas at any temperature and pressure can be found from the gas formation volume factor, B_g :

$$\frac{1}{B_g} = \frac{\rho_{gwt}}{\rho_{gsc}}$$

$$\rho_{gwt} = \gamma_g (0.001223) \times \frac{1}{B_g} \text{ (gm/cc)}$$

EXAMPLE

Find the weight of 500 scf of gas with

$$\gamma_g = 0.55$$

This is solved as follows:

$$\text{Weight} = V_g \times \rho_{air} \times \gamma_g$$

$$\text{Weight} = 500 \text{ cu ft} \times 0.0762 \text{ lb/cu ft} \times 0.55 = \mathbf{20.95 \text{ lbs}}$$

EXAMPLE

Find the density of a gas at standard conditions when:

$$\gamma_g = 0.70$$

Solution:

$$\rho_g = \gamma_g \times \rho_{air}$$

$$\rho_g = 0.7 \times 0.001223 \text{ gm/cc} = \mathbf{0.000856 \text{ gm/cc}}$$

EXAMPLE

Find the density of a gas when:

$$\gamma_g = 0.70$$

$$p_{wt} = 2,000 \text{ psia}$$

$$T_{wt} = 200^\circ\text{F}$$

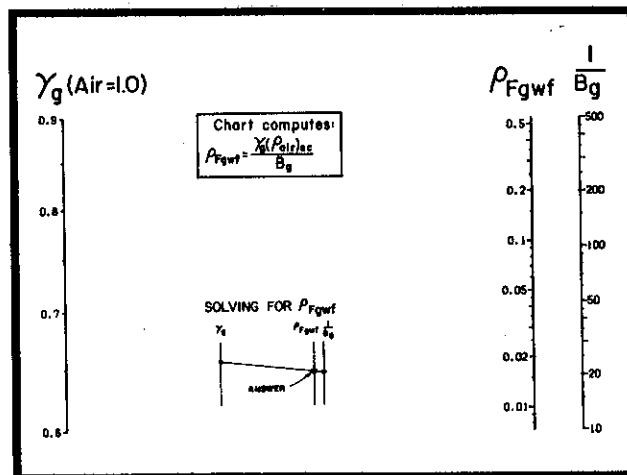


Fig. 3-22 (Chart Fg-5): Nomograph for solving the equation:
 $\rho_{gwt} = \gamma_g (0.001223) (1/B_g)$.

Solution:

1. From Fig 3-14 and as shown in a previous example, $1/B_g = 125$.

2. $\frac{1}{B_g} = \frac{\rho_{gwt}}{\rho_{gsc}}$ (from paragraph 2, above).

3. $\rho_{gwt} = \gamma_g \times 0.001223 \times (1/B_g)$.
 $\rho_{gwt} = 0.7 \times 0.001223 \text{ gm/cc} \times 125 =$
 $\mathbf{0.107 \text{ gm/cc}}$

or:

2. Using the nomograph in Fig 3-22 **Chart Fg-5**, construct a line from $\gamma_g = 0.7$ to $(1/B_g) = 125$ to obtain:

$$\rho_{gwt} = \mathbf{0.11 \text{ gm/cc}}$$

b) OIL DENSITY, ρ_o

At standard conditions the density of oil is equal to the weight divided by the volume; or, in equation form:

$$\rho_{osc} = W_{osc} / V_{osc}$$

At well-flowing conditions the density of oil is still equal to the weight divided by the volume. It is, however, not quite straightforward because the weight of the oil has been increased by dissolved gas, and the volume of the oil has been increased by the oil formation volume factor:

$$\rho_{owf} = \frac{W_{osc} + W_{dis.gas}}{V_{osc} \times B_o}$$

or

$$\rho_{owf} = \frac{\rho_{osc} + \rho_{air} \gamma_g R_s}{B_o}$$

In English units:

$$\rho_{owf} = \frac{\rho_{osc} + 0.001223 \gamma_g \left(\frac{R_s}{5.615} \right)}{B_o}$$

$$\rho_{ob} = \frac{\frac{141.5}{131.5 + \gamma_o} + 0.0002178 \gamma_g R_{sb}}{B_o} \text{ gm/cc}$$

And at bubble-point pressure, p_b , as used in determining c_o :

$$\rho_{owf} = \frac{\frac{141.5}{131.5 + \gamma_o} + 0.0002178 \gamma_g R_{sb}}{B_{ob}} \text{ gm/cc}$$

Note that the 0.001223 is the density of air in gm/cc, and the 5.615 is the necessary conversion factor to convert the English units of cf/B into B/B. The $141.5 / (131.5 + \gamma_o)$, of course, converts γ_o in °API to ρ_{osc} in gm/cc.

In metric units the above equations would simplify to:

$$\rho_{owf} = \frac{\rho_{osc} + 0.001223 \gamma_g R_s}{B_o}$$

and

$$\rho_{ob} = \frac{\rho_{osc} + 0.001223 \gamma_g R_{sb}}{B_{ob}} \text{ gm/cc}$$

EXAMPLE — English units

Find ρ_{owf} in the following situation:

$$\begin{aligned} \gamma_o &= 30^\circ \text{ API} \\ \gamma_g &= 0.75 \\ R_s &= 350 \text{ cf/B} \\ B_o &= 1.21 \end{aligned}$$

The solution is as follows:

$$\begin{aligned} 1. \rho_{osc} &= \frac{141.5}{131.5 + 30.0} = 0.876 \\ 2. \rho_{owf} &= \frac{\rho_{osc} + 0.0002178 \gamma_g R_s}{B_o} \\ 3. \rho_{owf} &= \frac{0.876 + 0.0002178 \times 0.75 \times 350.0}{1.21} \\ &= \mathbf{0.771 \text{ gm/cc}} \end{aligned}$$

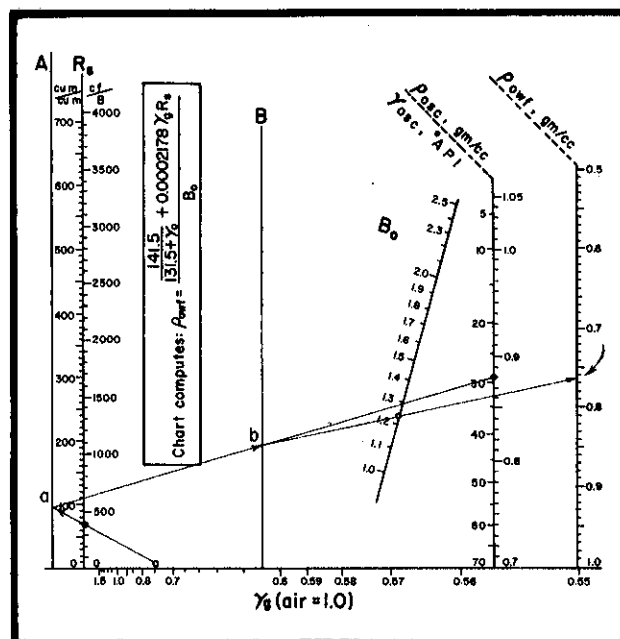


Fig. 3-23 - (Chart Fgo-6): Nomograph to find ρ_{owf} . Needed: R_s , γ_g , γ_o , and B_o .

An alternate solution is with Fig 3-23 **Chart Fgo-6**), the nomograph for determining ρ_{owf} .

1. Draw a line from $\gamma_g = 0.75$ through $R_s = 350$ cf/B to Line A.
2. Draw a line from Point **a** to $\gamma = 30^\circ$ API and establish Point **b**.
3. Draw a line from Point **b** through $B_o = 1.21$ to the answer, $\rho_{owf} = \mathbf{0.77 \text{ gm/cc}}$.

EXAMPLE — Metric units

Find ρ_{ob} in the following situations:

$$\begin{aligned} \rho_{osc} &= 0.84 \text{ gm/cc} \\ \gamma_g &= 0.65 \\ R_{sb} &= 100 \text{ cu m/cu m} \\ B_{ob} &= 1.26 \end{aligned}$$

The solution is:

$$\begin{aligned} 1. \rho_{ob} &= \frac{\rho_{osc} + 0.001223 \gamma_g R_{sb}}{B_{ob}} \\ \rho_{ob} &= \frac{0.84 + 0.001223 \times 0.65 \times 100}{1.26} \\ &= \mathbf{0.730 \text{ gm/cc}} \end{aligned}$$

c) WATER DENSITY, ρ_w

The density of gas-free water is a function of temperature, pressure, and water salinity. A nomograph of this relationship is shown in Fig. 3-24 (**Chart Fw-1**). As the solubility of gas in water (R_{sw}) is small, the effect of the dissolved gas is ignored, and this chart is used for the density of water at any R_{sw} .

EXAMPLE

Find the density of water under the following conditions:

$$C_{NaCl} = 90,000 \text{ ppm}$$

$$T_{wf} = 200^\circ\text{F}$$

$$p_{wf} = 2,000 \text{ psia}$$

Using Fig. 3-24 the solution is as follows:

1. Starting from $C_{NaCl} = 90,000$ ppm, draw a line through $T_{wf} = 200^\circ\text{F}$ to Point **a**.
2. Starting from $p_{wf} = 2,000$ psia, draw a line through Point **a** to water density (ρ_{wtf}), of **1.035 gm/cc**.

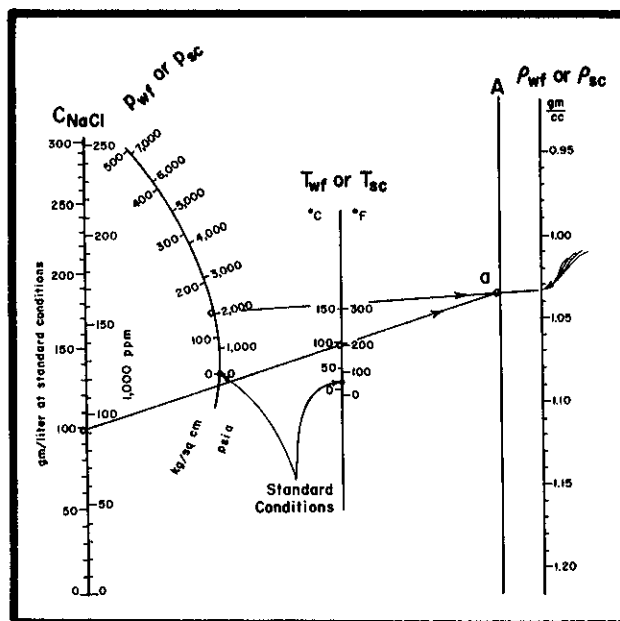


Fig. 3-24 - (**Chart Fw-1**): Nomograph to find ρ_{wtf} . Needed: C_{NaCl} , T_{wf} , and p_{wf} .

5) Viscosity correlations

a) GAS VISCOSITY

At elevated temperatures and low pressures, low-gravity gases closely resemble "perfect" gas in their behavior, while at low temperatures and high pressures, the heavier gases resemble liquids.

The charts in Fig. 3-25 (**Chart Fg-6**) give gas viscosity as a function of temperature and pressure, for gases of five different gravities.

Note that above about 1,500 psi, an increase in temperature *decreases* the gas viscosity, while below that point increasing the temperature *increases* the viscosity.

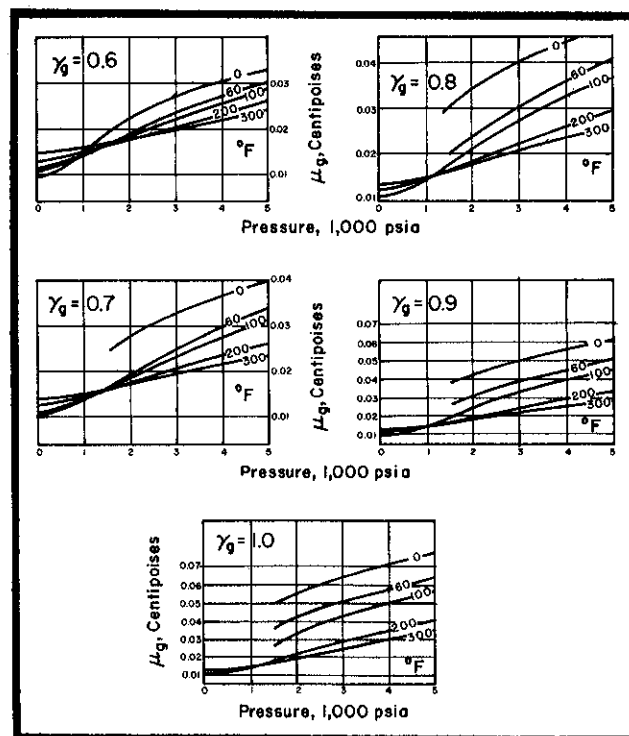


Fig. 3-25 - (**Chart Fg-6**): Gas viscosity, μ_{gwf} , as a function of γ_g , T_{wf} , and p_{wf} (courtesy Oil and Gas Journal).

b) OIL VISCOSITY, μ_o

The viscosity of a crude oil decreases with a temperature increase and with an increase of dissolved gas.

Heavier oils are generally more viscous than lighter oils of the same hydrocarbon base.

The question of which viscosity units are to be used may be rather confusing since there are several different systems used in the oil field. The *centipoise* is the unit used throughout this document.

The charts given in Fig. 3-26 (Chart Fgo-7) correlate crude oil viscosity with stock-tank oil gravity, temperature, and solution gas-oil ratio at or below bubble-point pressure. If the pressure on the oil is above bubble-point pressure its viscosity is increased by the amount given by the correction curve.

EXAMPLE

Find the oil viscosity in centipoises, in the following situation:

$$\begin{aligned}\gamma_o &= 30^\circ \text{ API} \\ T_{wf} &= 200^\circ \text{ F} \\ p_b &= 1,700 \text{ psia} \\ p_{wf} &= 2,700 \text{ psia} \\ R_{sb} &= 400 \text{ cf/B}\end{aligned}$$

Referring to Fig. 3-26 (English units), the solution is made as follows:

1. Start on the ordinate at 30° API .
2. Go right to 200° F .
3. Drop to the R_{sb} value of 400 cf/B.
4. Go left to read 1 cp, the viscosity at bubble-point pressure, and, along the way, note the Point D.
5. Drop vertically from Point D to the abscissa. Read a viscosity gradient of 0.07 cp/1,000 psi. This figure is used only when $p_{wf} > p_b$, which is the case in this problem. The increase in viscosity is from the value obtained on the ordinate (Step 4), so that:

$$\mu_o = 1.0 \text{ cp} + \frac{0.07}{1,000 \text{ psia}} (p_{wf} - p_b)$$

$$\mu_o = 1.0 \text{ cp} + \frac{0.07}{1,000 \text{ psia}} (2,700 - 1,700) = 1.07 \text{ cp}$$

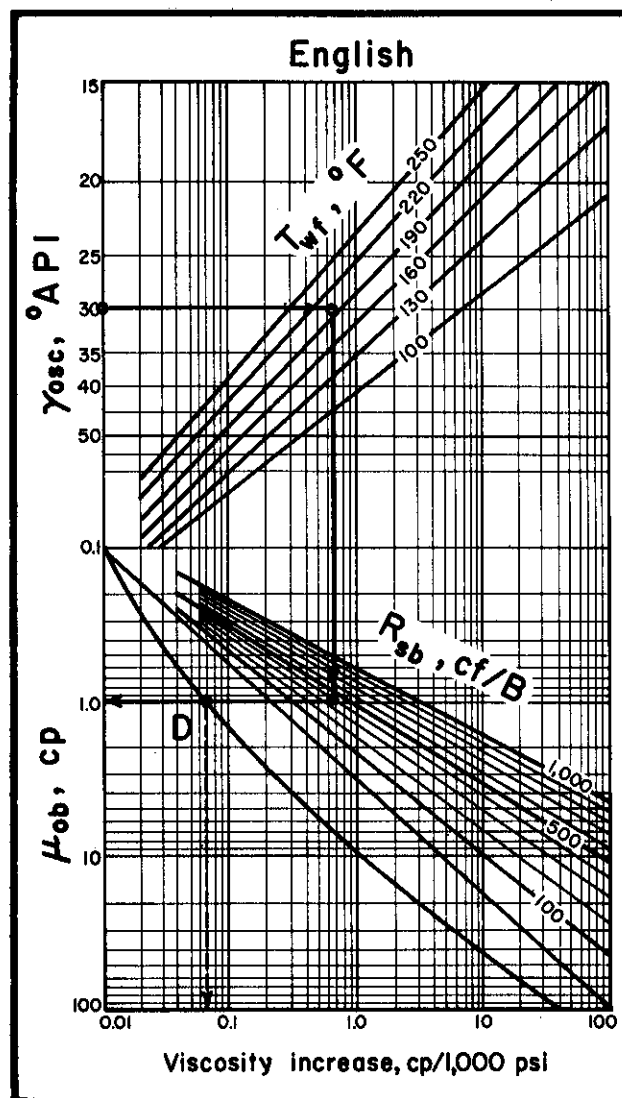


Fig. 3-26 (Chart Fgo-7): μ_{ob} as a function of γ_{os} , T_{wf} , and R_{sb} (and viscosity increase where $p_{wf} > p_b$).

c) WATER VISCOSITY, μ_w

The viscosity of water is primarily a function of temperature and water salinity. Fig. 3-27 (Chart Fw-2) shows this relationship.

EXAMPLE

Find the viscosity of water under the following conditions:

$$C_{NaCl} = 150,000 \text{ ppm}$$

$$T_{wf} = 200^\circ\text{F}$$

Using Fig. 2-19, the solution is:

$$1. \mu_w = 0.43 \text{ cp}$$

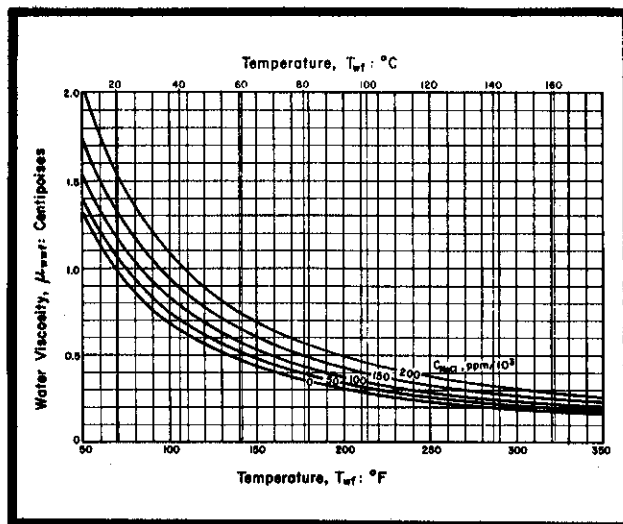


Fig. 3-27. Water viscosity vs. temp and concentron of NaCl

d) VISCOSITY OF MIXTURES

The viscosity of a water-in-oil emulsion may be many times that of either the water or the oil. As a practical limit, however, the viscosity of a water-in-oil emulsion does not exceed 5 cp.

D. Rock pore-volume compressibility

While fluid pressure in the reservoir rock pore space decreases with depletion, the lithostatic pressure on the matrix remains essentially constant. This causes the pore-volume and rock bulk volume to decrease with depletion.

Correlations of Hall and Knaap, Figure 3-28, have been used extensively in the literature, however these correlations do not apply over a very wide range of reservoir rocks. They may be used only to give order of magnitude estimates for the more consolidated rocks but not for friable sandstone.

Formation compressibility is best measured in the laboratory for the reservoir rock being studied.

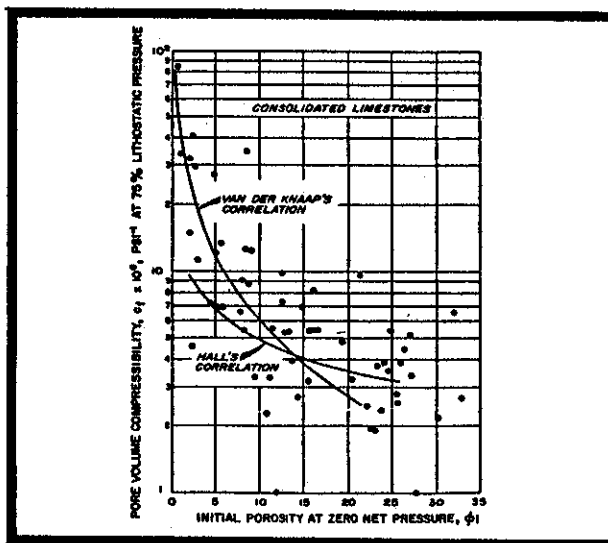


Fig. 3-28. Pore-volume compressibility - limestone

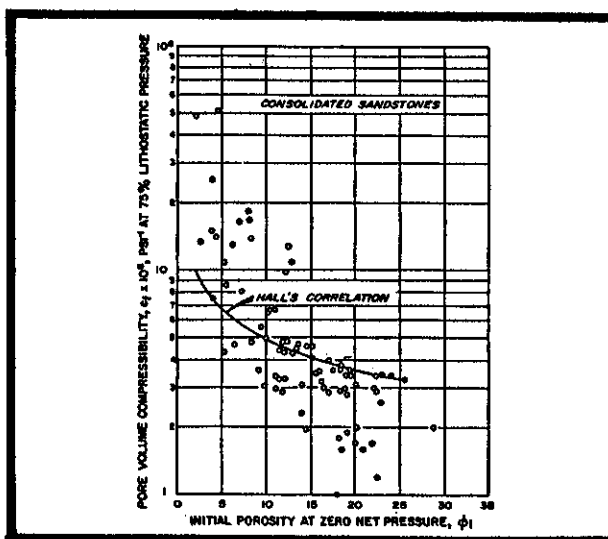


Fig. 3-29. Pore-volume compressibility - sandstone

E. Appendix - SCHLUMBERGER FLUID CONVERSION CHARTS

<u>CHART CODE</u>	<u>TO FIND</u>		<u>NEED:</u>	<u>Page</u>
Fg-1	$1/B_g$	p_{wf}, T_{wf}, γ_g	3-30
Fg-2	T_{gc}, p_{pc}	γ_g	3-31
Fg-3	z	p_{pr}, T_{pr}	3-32
Fg-4	$1/B_g$	p_{wf}, T_{wf}, z	3-33
Fg-5	ρ_{Fgw}	$\gamma_g, 1/B_g$	3-34
Fg-6	μ_g	p_{wf}, T_{wf}, γ_g	3-35
Fgo-1	p_b (or R_s)	R_{sb} (or p_b), T_{wf}, γ_g and γ_o (or ρ_{osc})		3-36
Fgo-2	k	p_{wf}, p_b	3-37
Fgo-3	B_{ob}	$R_{sb}, \gamma_g, \gamma_o, T_{wf}$ (English only)		3-38
Fgo-4	B_{ob}	R_{sb}, γ_g, T_{wf} (English or metric)		3-39
Fgo-5	B_o	p_{wf}, p_b, c_o (or ρ_{ob}), B_{ob}		3-40
Fgo-6	ρ_{owf}	γ_g, R_s, γ_o (or ρ_{osc}), B_o	3-41
Fgo-7	μ_{ob} (and μ_o increase, if p_{wf} is greater than p_b)	γ_{osc} (ρ_{osc}), T_{wf}, R_{sb}	3-42
Fgw-1	Solution Gas-Water ratio		3-43
Fw-1	Densities of NaCl solutions		3-44
Fw-2	Water viscosity		3-45

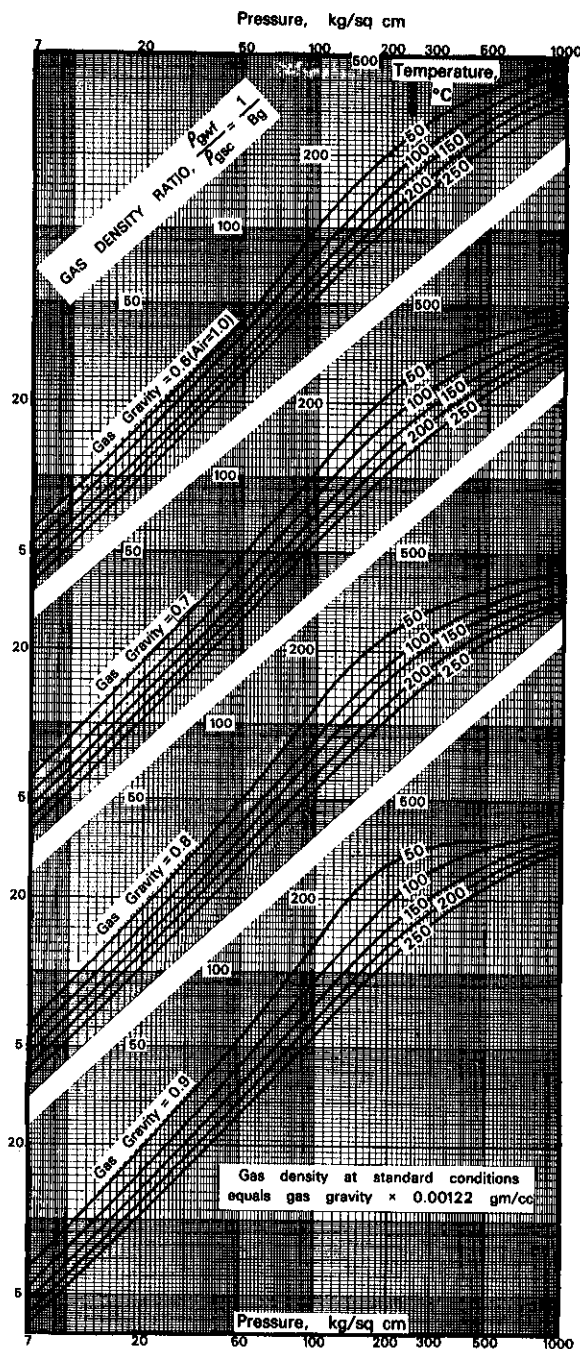
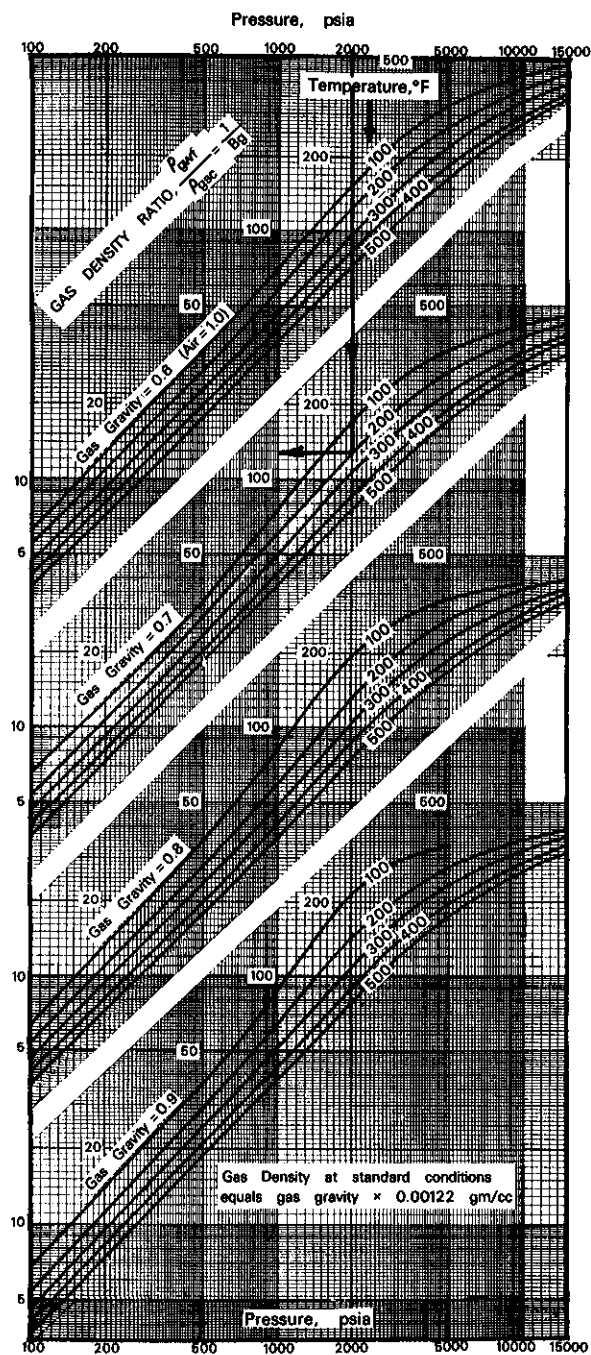
Schlumberger

GAS FORMATION VOLUME FACTOR

After Standing and Katz, Ref. 3.

ENGLISH

METRIC

Find V_{gwf} .

Given: $V_{gsc} = 400$ cu ft
 $\gamma_g = 0.70$
 $T_{wf} = 200^\circ\text{F}$
 $P_{wf} = 2,000$ psia

1. Select " $\gamma_g = 0.70$ " section. Enter abscissa at 2,000 psia, go vertically to 200°F .2. Go left to $\frac{1}{B_g} = 125$.

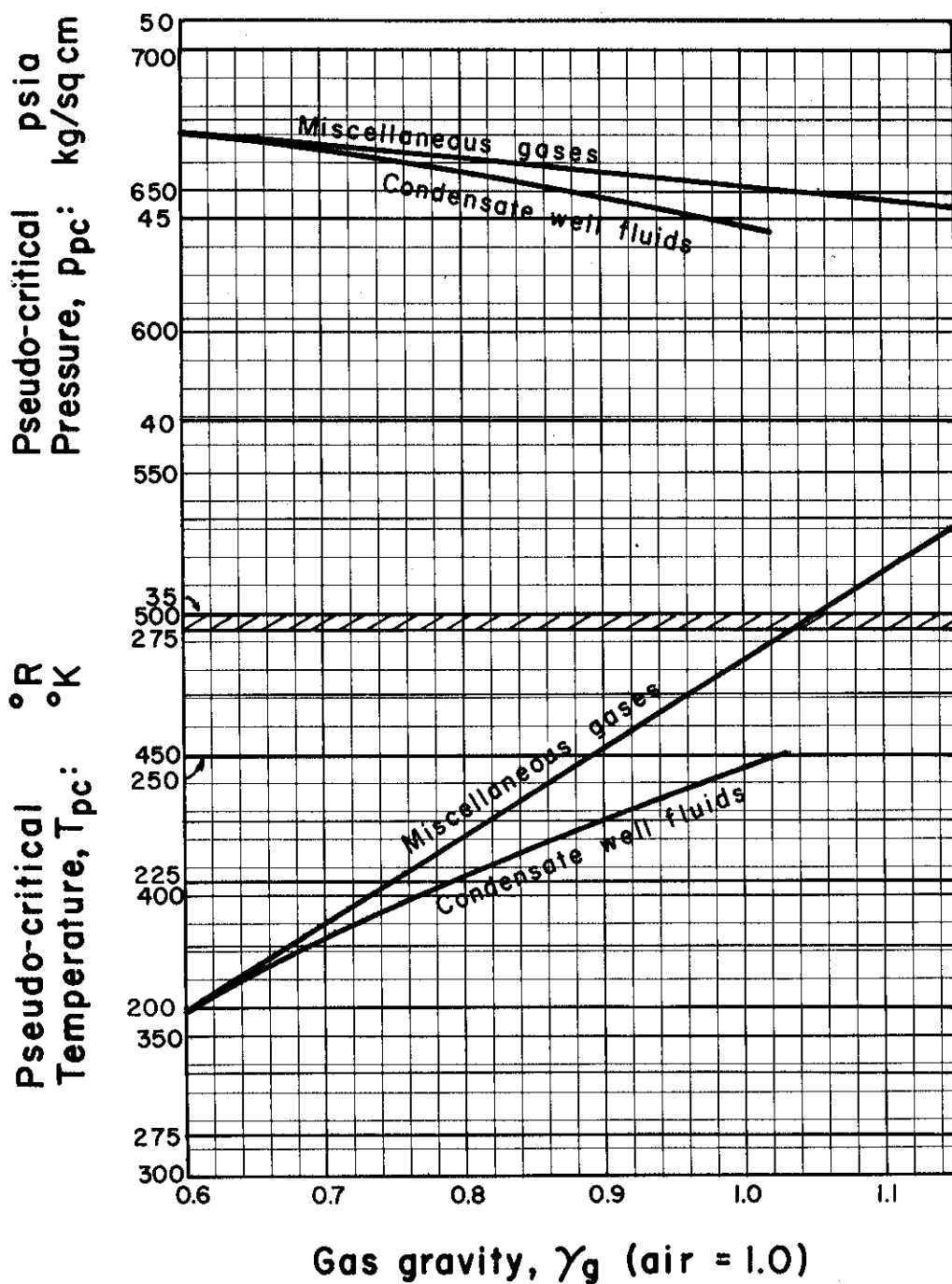
$$3. \frac{1}{B_g} = 125 = \frac{V_{gsc}}{V_{gwf}} = \frac{400}{V_{gwf}}$$

$$V_{gwf} = 3.2 \text{ cu ft}$$

Schlumberger

PSEUDO-CRITICAL NATURAL GAS PARAMETERS

After Brown et al, Ref. 4.



Find T_{pc} and p_{pc} .

Given: $\gamma_g = 0.75$, average gases

1. Enter abscissa at 0.75. Go up to:

$T_{pc} = 406^\circ R$

and

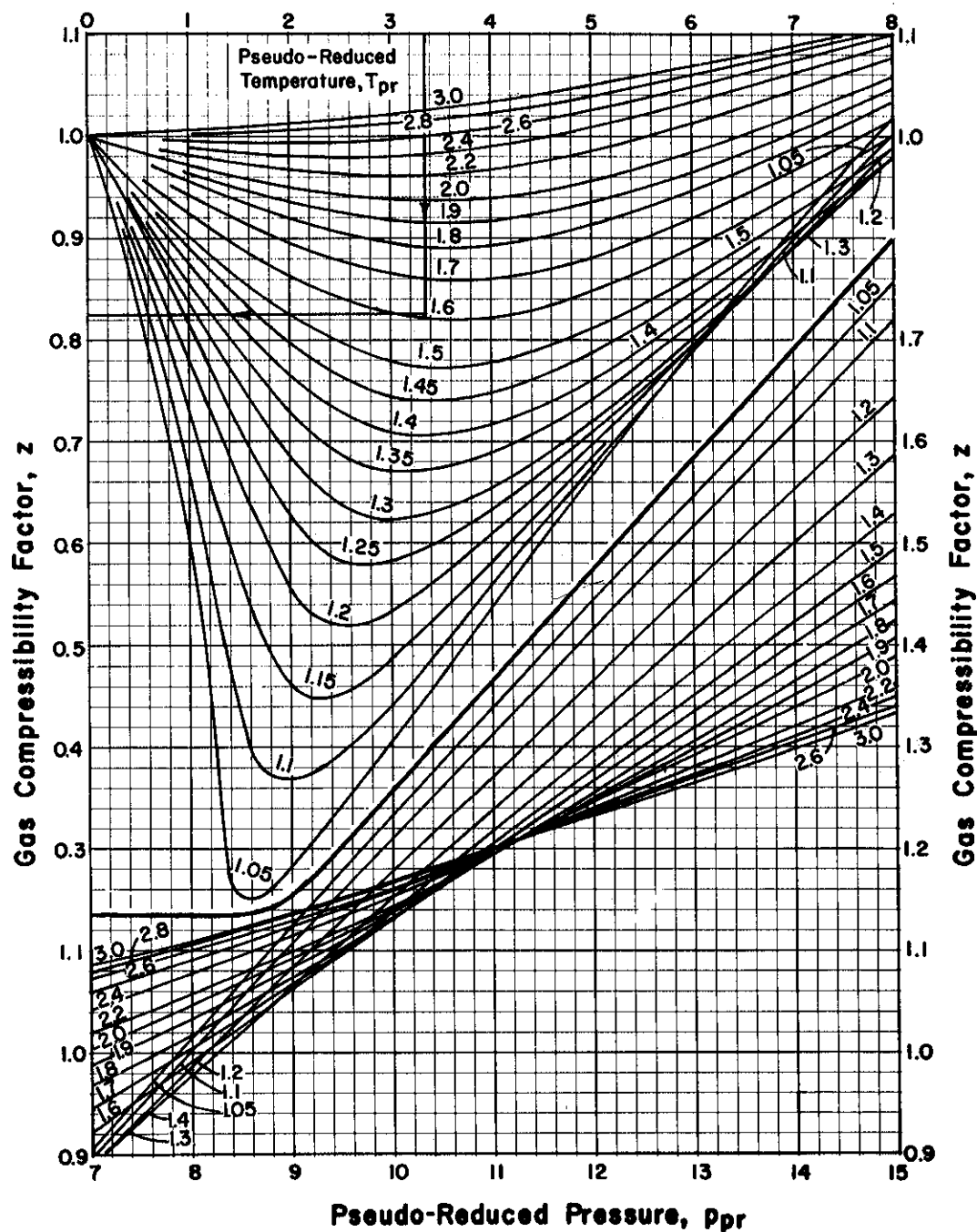
$p_{pc} = 664 \text{ psia}$

Chart fg-3

Schlumberger

NATURAL GAS DEVIATION FACTOR

After Standing and Katz, Ref. 3.

Pseudo-Reduced Pressure, p_{pr} Find z .Given: $P_{wf} = 2,000$ psia $P_{pe} = 650$ psia $T_{wf} = 200^\circ\text{F}$ (660°R) $T_{pe} = 410^\circ\text{R}$

1. $p_{pr} = P_{wf}/P_{pe} = 2,000/650 = 3.07$.
2. $T_{pr} = T_{wf}/T_{pe} = 660/410 = 1.61$
3. Enter abscissa (top) at 3.07 (p_{pr}). Go down to T_{pr} of 1.61, between 1.6 and 1.7 lines.
4. $z = \mathbf{0.828}$

Schlumberger

GAS FORMATION VOLUME FACTOR (Nomograph)

© 1974 SCHLUMBERGER

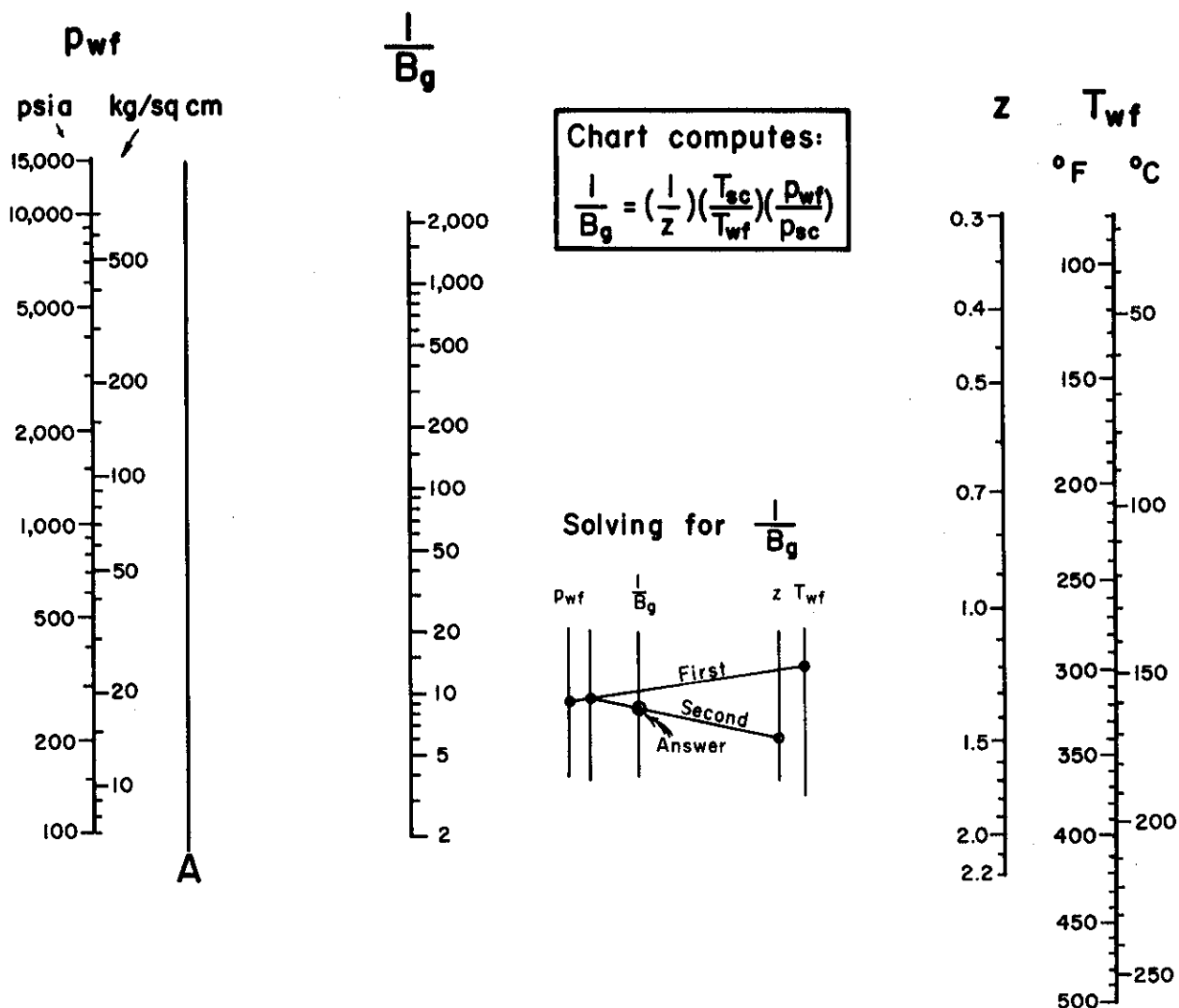
Find $1/B_g$.Given: $p_{wf} = 140$ kg/sq cm $T_{wf} = 93^\circ\text{C}$ $z = 0.828$ 1. Enter p_{wf} scale at 140 kg/sq cm. Follow lines as in small diagram.2. $1/B_g = 135$

Fig-4

Schlumberger

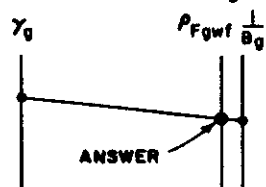
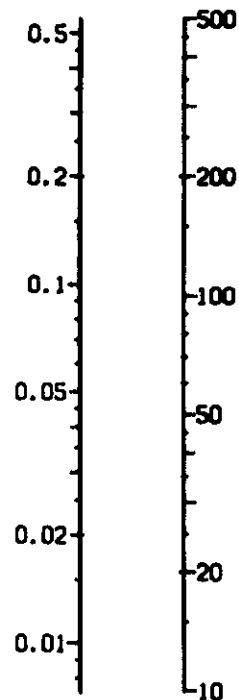
GAS DENSITY

© 1974 SCHLUMBERGER

 γ_g (Air=1.0)

Chart computes:

$$\rho_{Fgwf} = \frac{\gamma_g(\rho_{air})_{sc}}{B_g}$$

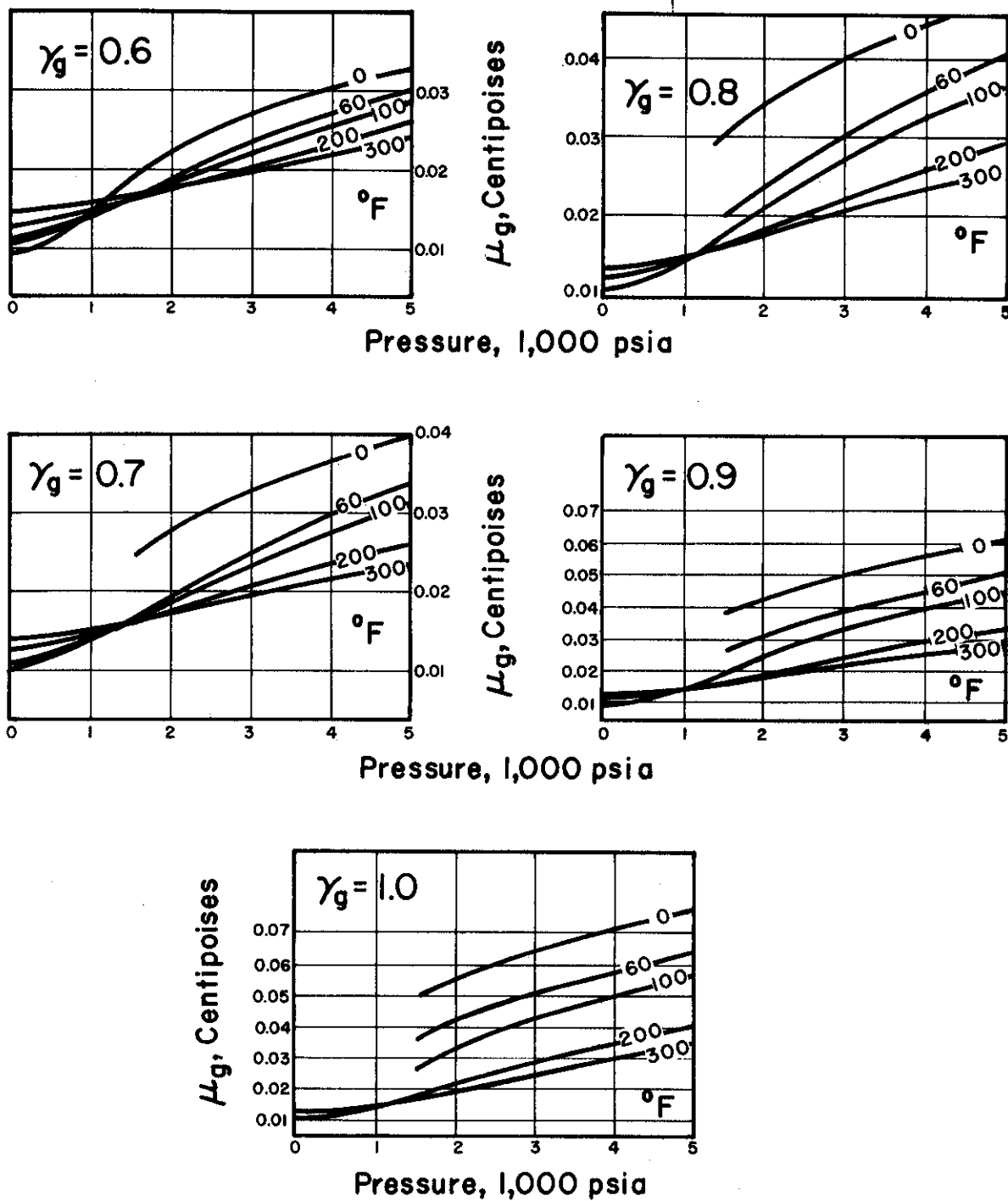
SOLVING FOR ρ_{Fgwf}  ρ_{Fgwf} $\frac{1}{B_g}$ Find ρ_{Fgwf} ,Given: $\gamma_g = 0.75$ $1/B_g = 140$

1. Connect $\gamma_g = 0.75$ and $1/B_g = 140$, as in small diagram.
2. $\rho_{Fgwf} = 0.13 \text{ gm/cc}$.

Schlumberger

GAS VISCOSITY

Courtesy of Oil and Gas Journal, May 12, 1949.

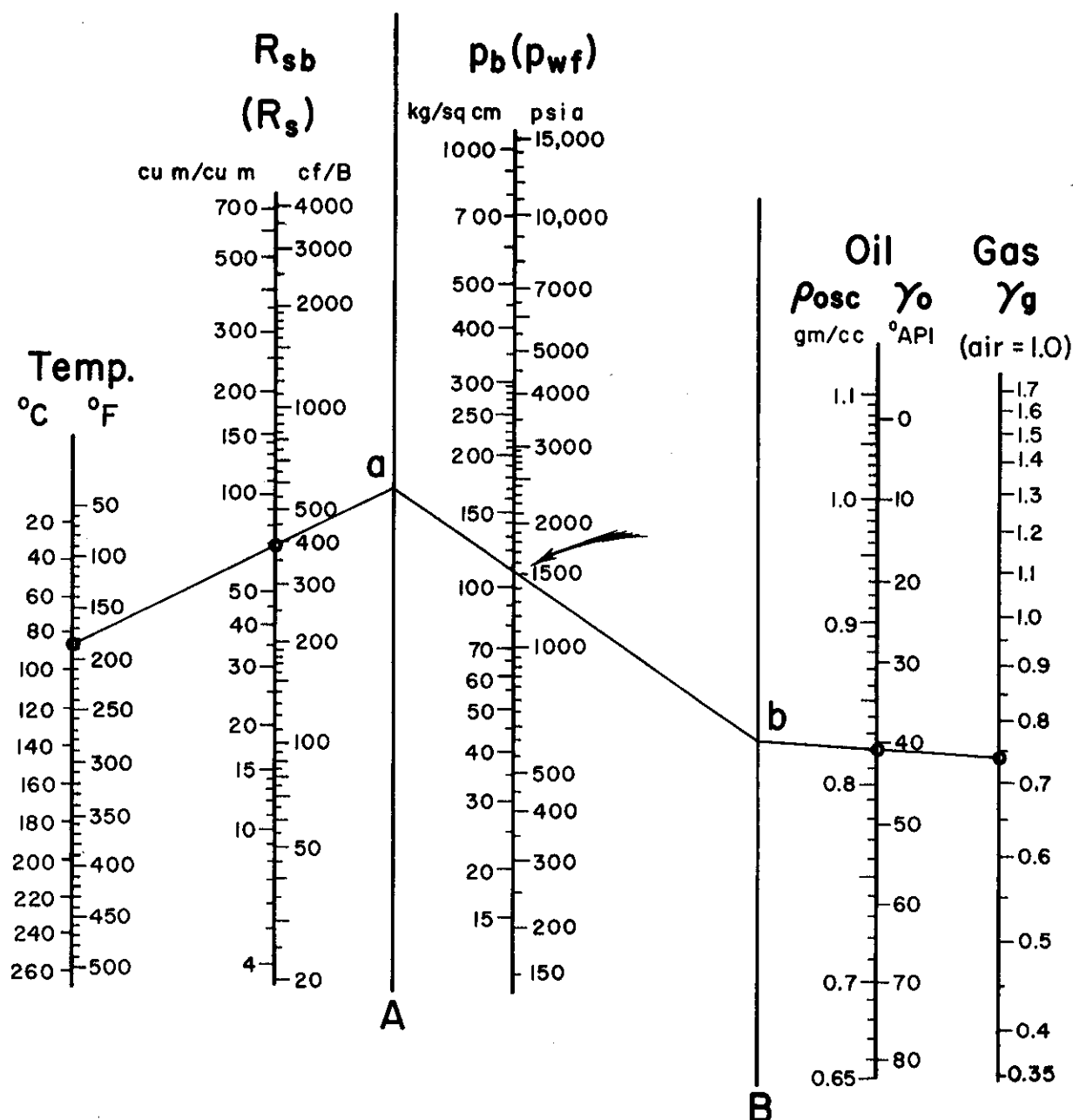
Find μ_{gwf} .Given: $\gamma_g = 0.70$ $p_{wf} = 2,000$ psia $T_{wf} = 200^\circ\text{F}$

1. Enter $\gamma_g = 0.70$ chart at $p_{wf} = 2,000$ psia.
2. Go up to $T_{wf} = 200^\circ\text{F}$.
3. $\mu_{gwf} = 0.018$ centipoises.

Schlumberger

BUBBLE-POINT PRESSURE

© 1974 SCHLUMBERGER

Find p_b .Given: $T_{wf} = 180^\circ\text{F}$ $q_{osc} = 600 \text{ B/D}$ $q_{gsc} = 240 \text{ Mcf/D}$ $\gamma_g = 0.75$ $\gamma_o = 40^\circ \text{API}$

$$1. \quad R = \frac{240,000 \text{ cf/D}}{600 \text{ B/D}} = 400 \text{ cf/B.}$$

2. $R_{sb} = R$, since the field-usage definition of p_b stipulates given flow rates of oil and gas, taken here to be q_{osc} and q_{gsc} (above).

3. On the nomograph, locate Point **a** by a line through $T_{wf} = 180^\circ\text{F}$ and $R_{sb} = 400$.

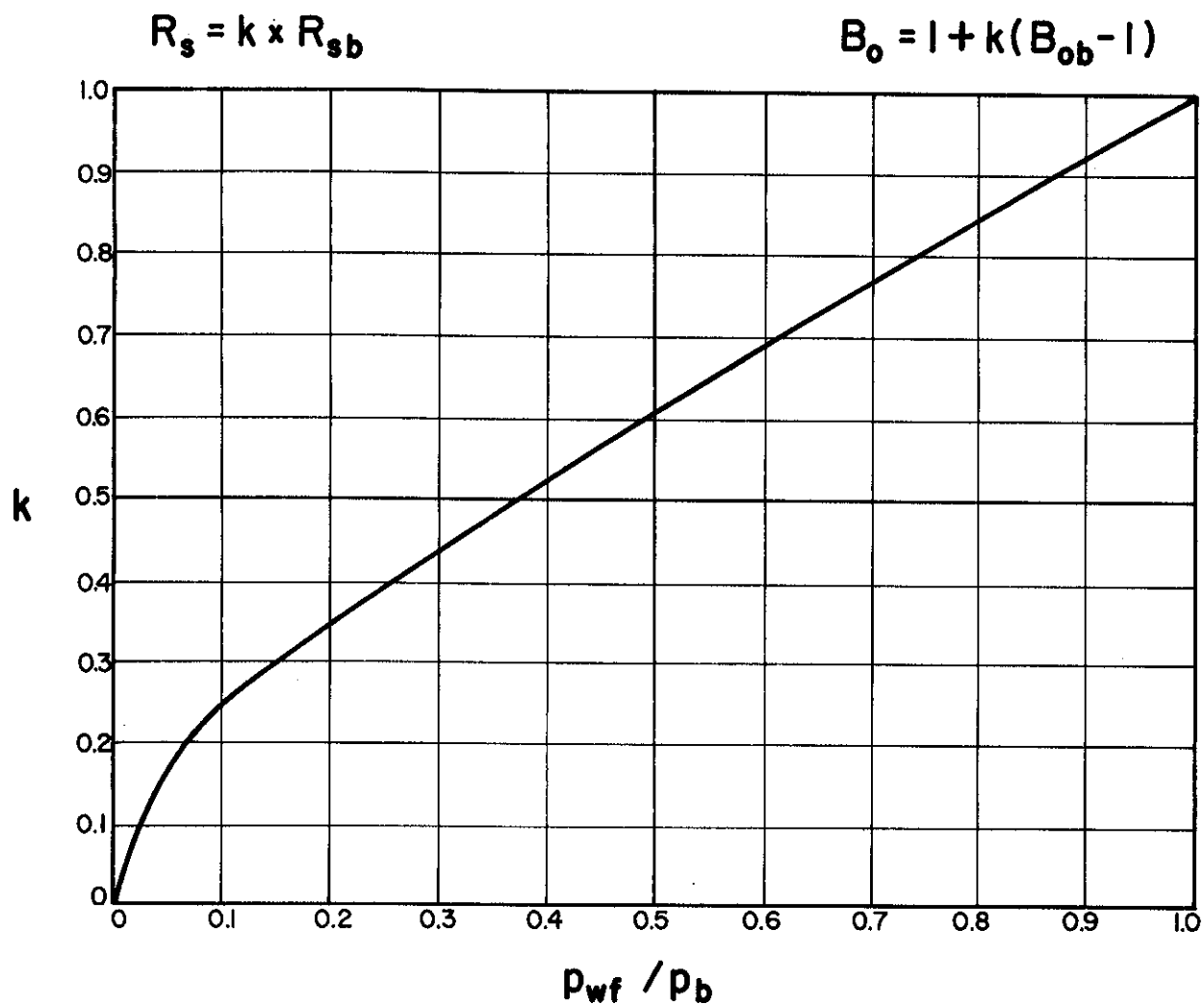
4. Locate Point **b** by a line through $\gamma_g = 0.75$ and $\gamma_o = 40^\circ \text{API}$.

5. Connect **a** and **b**: $p_b = 1,560 \text{ psia}$.

Schlumberger

SOLUTION GOR CORRECTION FACTOR

© 1974 SCHLUMBERGER



Find k.

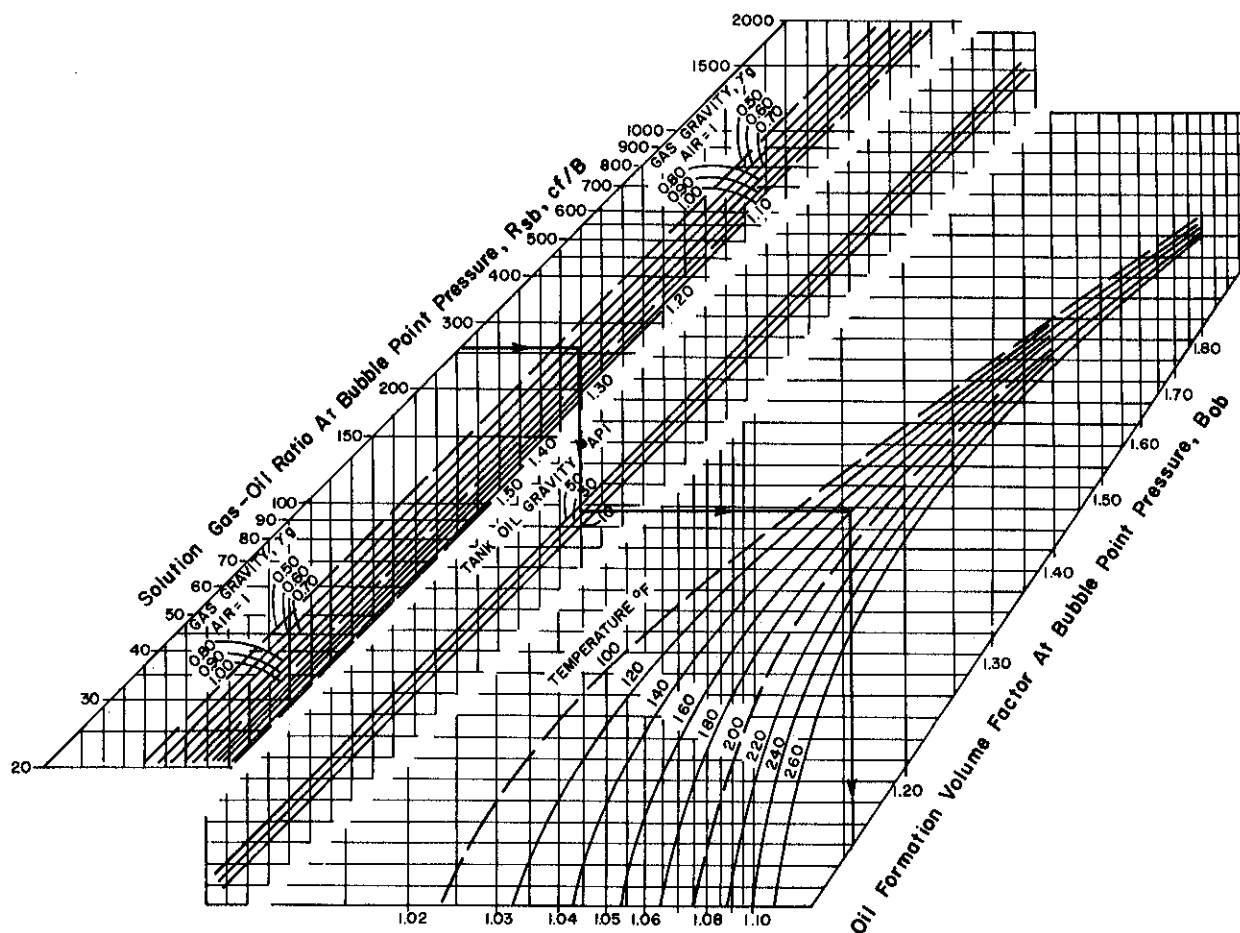
Given: $p_{wf} = 250 \text{ kg/sq cm}$ $p_b = 185 \text{ kg/sq cm}$

1. $p_{wf}/p_b = 0.74$.
2. Enter abscissa at 0.74.
3. $k = \mathbf{0.810}$.

Schlumberger

FORMATION VOLUME FACTOR AT p_b , OIL

After Standing, Ref. 6.

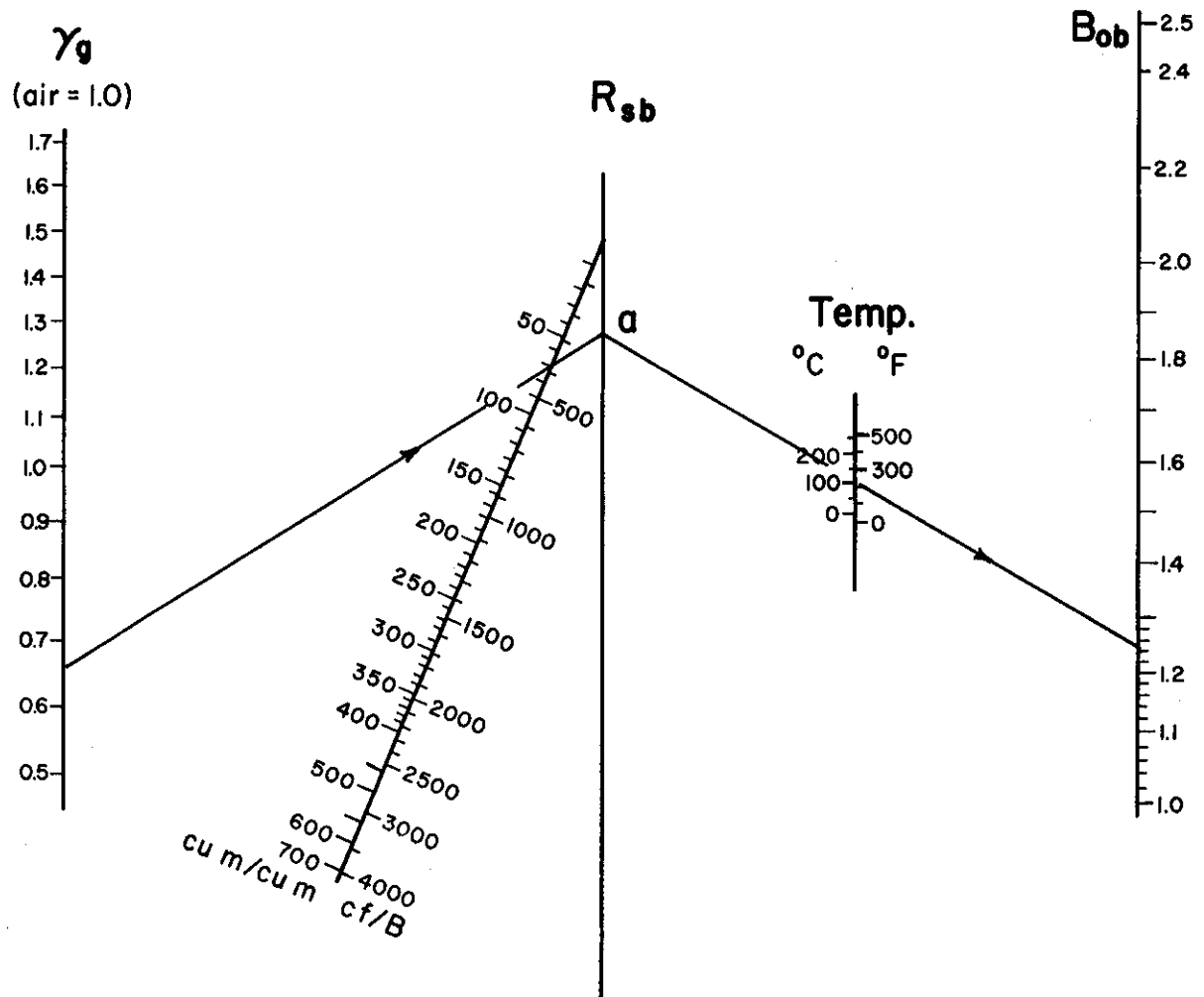
Find B_{ob} .Given: $R_{sb} = 260$ cf/B $T_{wf} = 160^\circ\text{F}$ $\gamma_g = 0.7$ $\gamma_o = 36^\circ\text{API}$

1. Enter upper left scale at $R_{sb} = 260$.
2. Go right to $\gamma_g = 0.7$.
3. Go down to $\gamma_o = 36$.
4. Go right to $T_{wf} = 160$.
5. Go down to the answer:
 $B_{ob} = 1.155$

Schlumberger

FORMATION VOLUME FACTOR AT p_b , OIL (Nomograph)

© 1974 SCHLUMBERGER

Find B_{ob} .Given: $R_{sb} = 400 \text{ cf/B}$ $T_{wf} = 180^{\circ}\text{F}$ $\gamma_g = 0.65$ $\gamma_o = 45^{\circ} \text{ API}$

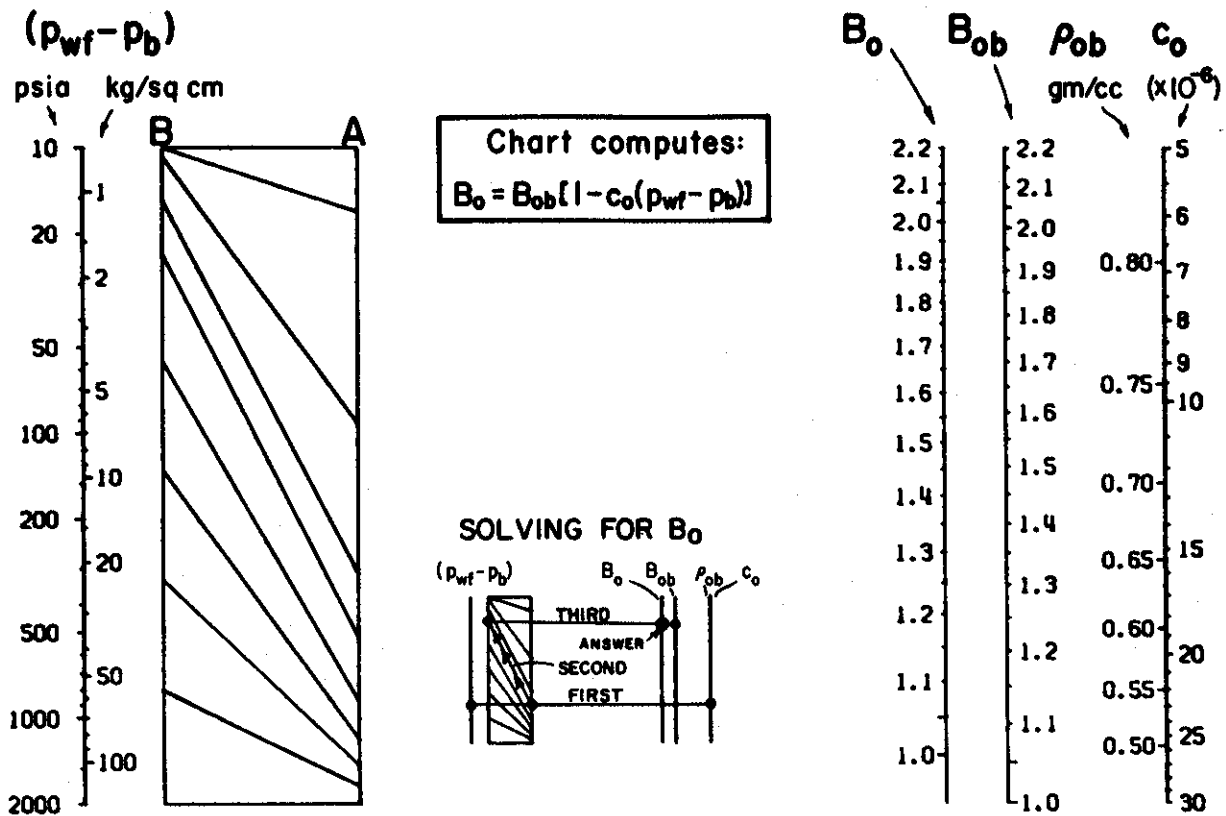
1. Locate Point **a** by line through $\gamma_g = 0.65$ and $R_{sb} = 400$.
2. Draw a line from **a** through $T_{wf} = 180^{\circ}\text{F}$, to the answer:
 $B_{ob} = 1.24$

Fig-4

Schlumberger

FORMATION VOLUME FACTOR, OIL

© 1974 SCHLUMBERGER

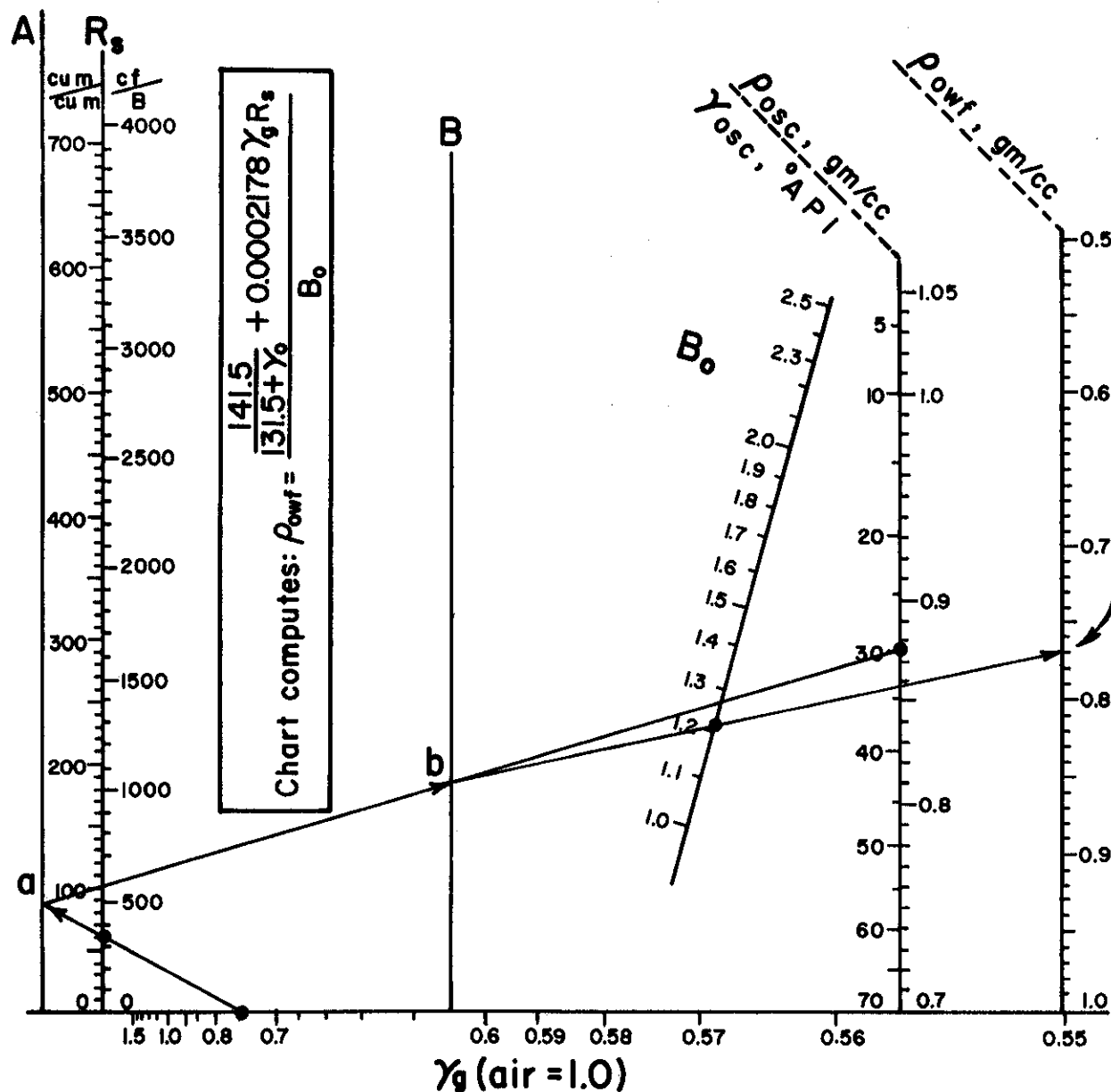
Find B_o .Given: $B_{ob} = 1.22$ $\rho_{ob} = 0.66 \text{ gm/cc}$ $p_{wf} = 3,000 \text{ psia}$ $p_b = 2,000 \text{ psia}$

1. Since $p_{wf} > p_b$, oil is undersaturated. Connect $p_{wf} - p_b = 1,000 \text{ psia}$ to $\rho_{ob} = 0.66$. Mark the point so located, as shown in small diagram.
2. Move this point as shown, following trend lines.
3. Connect this point to $B_{ob} = 1.22$ and read:
 $B_o = 1.20$

Schlumberger

OIL DENSITY AT WELL CONDITIONS

© 1974 SCHLUMBERGER



Find ρ_{owf} .

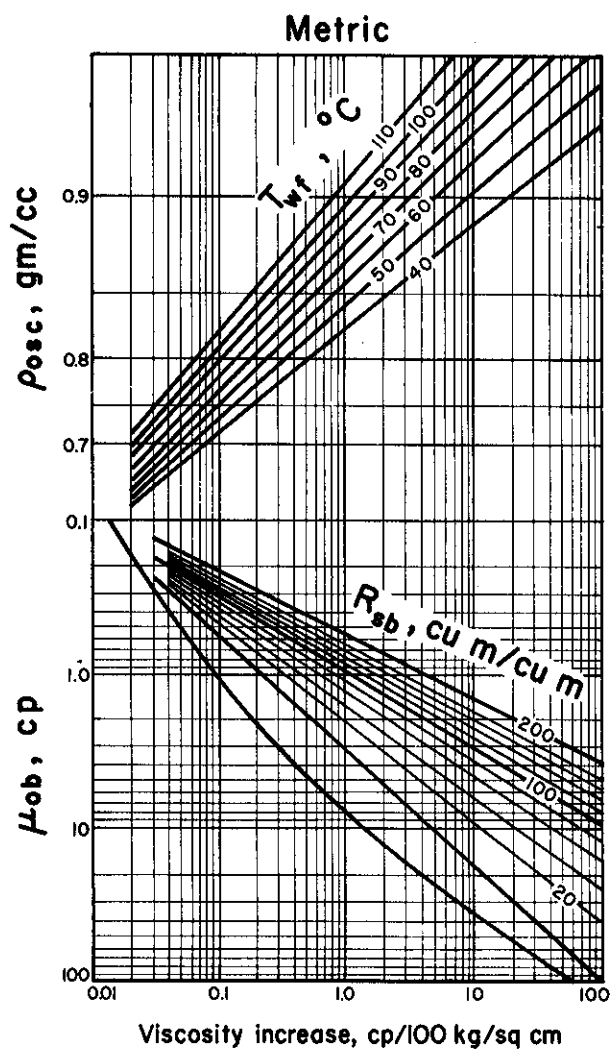
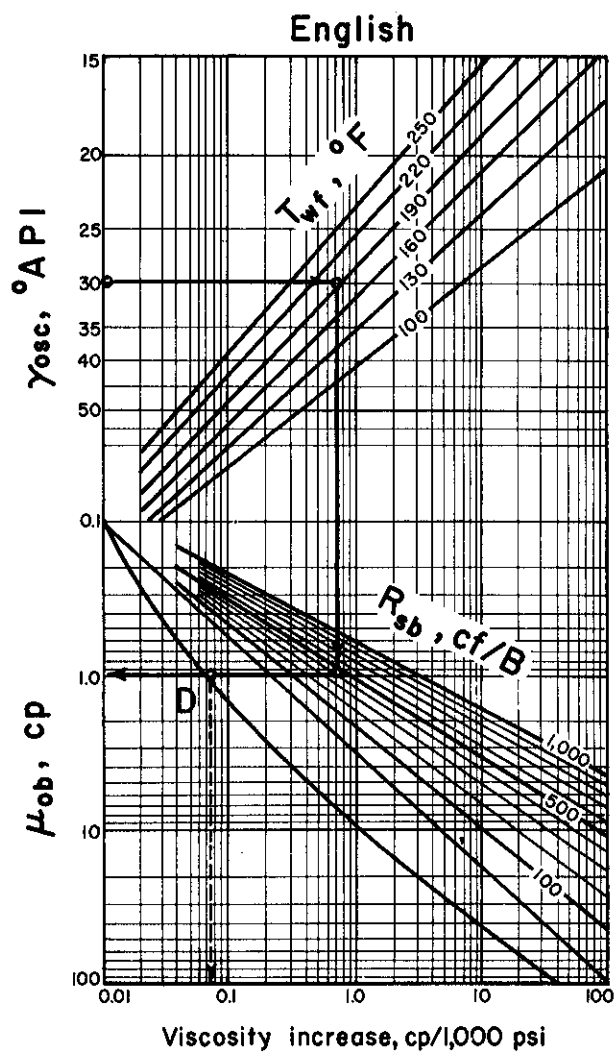
Given: $\gamma_o = 30^\circ \text{ API}$
 $\gamma_g = 0.75$
 $R_s = 350 \text{ cf/B}$
 $B_o = 1.21$

1. Locate Point **a** by a line from $\gamma_g = 0.75$ through $R_s = 350$.
2. Locate Point **b** by a line from Point **a** to $\gamma_o = 30^\circ \text{ API}$.
3. Draw a line from Point **b** through $B_o = 1.21$.
 $\rho_{owf} = 0.77 \text{ gm/cc}$

Schlumberger

OIL VISCOSITY

© 1974 SCHLUMBERGER

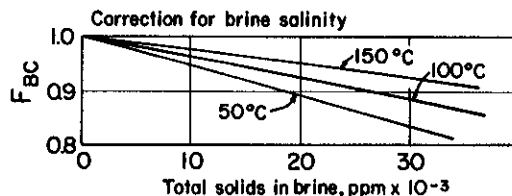
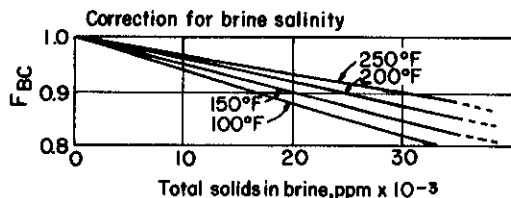
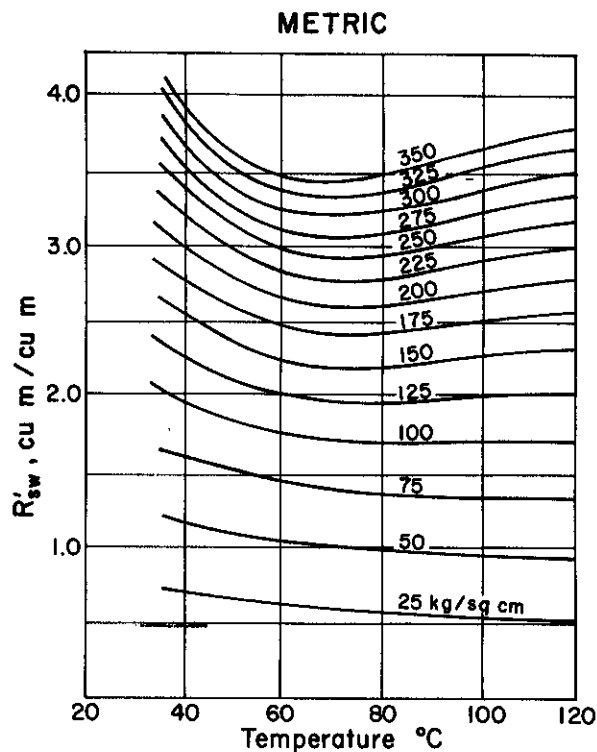
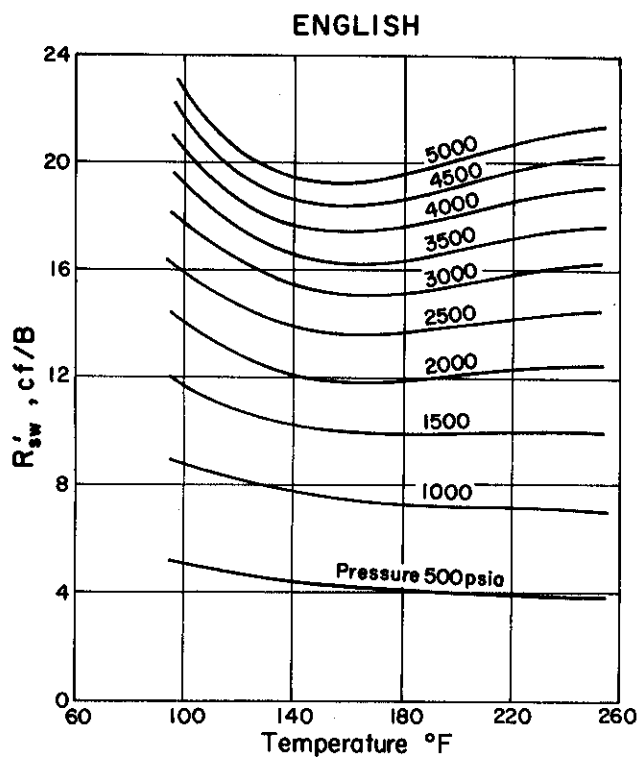
Find μ_{owf} .Given: $\gamma_o = 30^\circ \text{API}$ $T_{wf} = 200^\circ\text{F}$ $p_b = 1,700 \text{ psia}$ $p_{wf} = 2,700 \text{ psia}$ $R_{sb} = 400 \text{ cf/B}$

1. Enter ordinate at $\gamma_{osc} = 30^\circ \text{API}$.
2. Go right to $T_{wf} = 200$.
3. Go down to $R_{sb} = 400$.
4. Go left to answer, locating Point D on the way: $\mu_{ob} = 1.0 \text{ centipoise}$.
5. Since $p_{wf} > p_b$, $\mu_{owf} > \mu_{ob}$. From Point D, go down to read: viscosity increase = $0.07 \text{ cp/1,000 psi}$.
6. $\mu_{owf} = \mu_{ob} + \Delta\mu(p_{wf} - p_b)/1,000 = 1.0 + 0.07(2,700 - 1,700)/1,000 = 1.07 \text{ centipoises}$.

Schlumberger

SOLUTION GAS-WATER RATIO

After Dodson and Standing, Ref. 2.



Find R_{sw} .

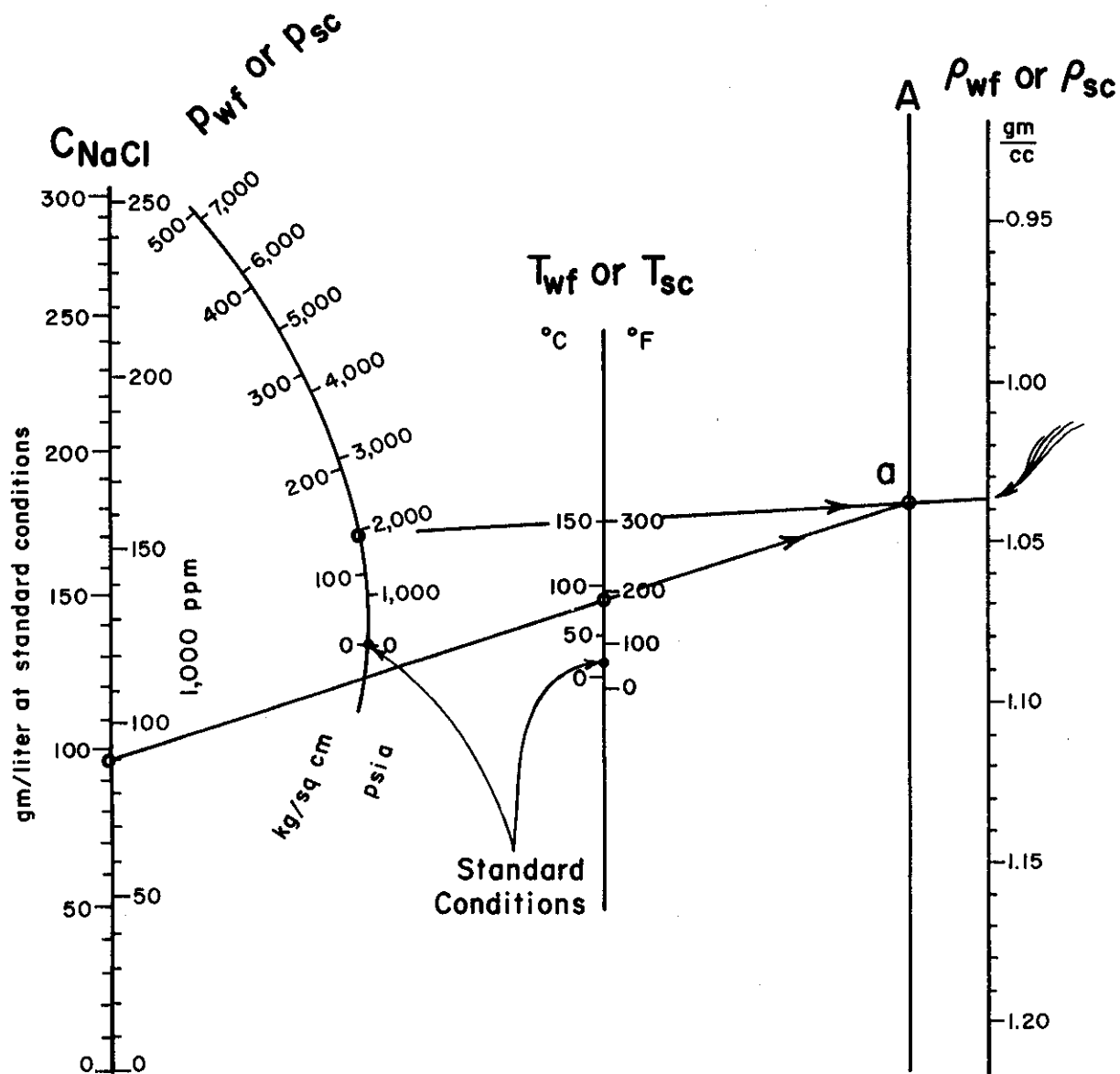
Given: $T_{wt} = 180^\circ\text{F}$
 $p_{wt} = 3,400$ psia
 $C_{NaCl} = 20,000$ ppm

1. (Top) Enter the abscissa at $T_{wt} = 180$.
2. Go up to $p_{wt} = 3,400$.
3. Read $R'_{sw} = 16$ cf/B.
4. (Bottom) Enter the abscissa at 20 (20,000 ppm). Go up to $T = 180$. Read $F_{BC} = 0.91$.
5. $R_{sw} = R'_{sw} F_{BC} = 16 \times 0.91 = 15$ cf/B.

Schlumberger

DENSITIES OF NaCl SOLUTIONS

© 1974 SCHLUMBERGER

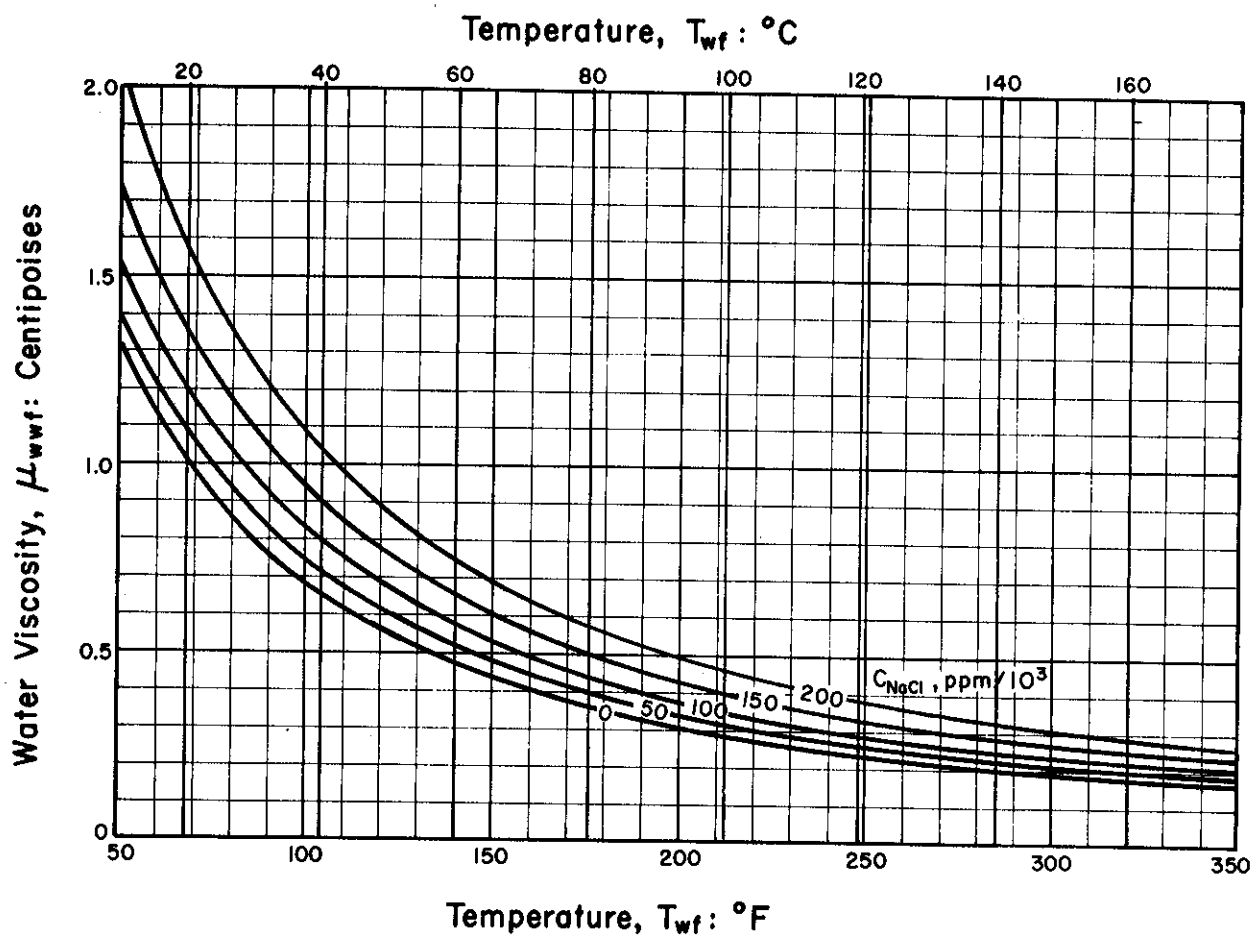
Find ρ_{wvf} .Given: $C_{NaCl} = 90,000$ ppm $T_{wf} = 200^\circ F$ $p_{wf} = 2,000$ psia

1. Locate Point **a** by a line from $C_{NaCl} = 90,000$ through $T_{wf} = 200$.
2. Draw a line from $p_{wf} = 2,000$ through **a**. Read: $\rho_{wvf} = 1.032$ gm/cc.

Schlumberger

WATER VISCOSITY

© 1974 SCHLUMBERGER

Find μ_{wvf} .Given: $C_{NaCl} = 150,000$ ppm $T_{wf} = 200^\circ\text{F}$

1. Enter abscissa at $T_{wf} = 200$.
2. Go up to $C_{NaCl} = 150,000$.
3. $\mu_{wvf} = \mathbf{0.43\text{ cp}}$.

RESERVOIR ROCK PROPERTIES

4

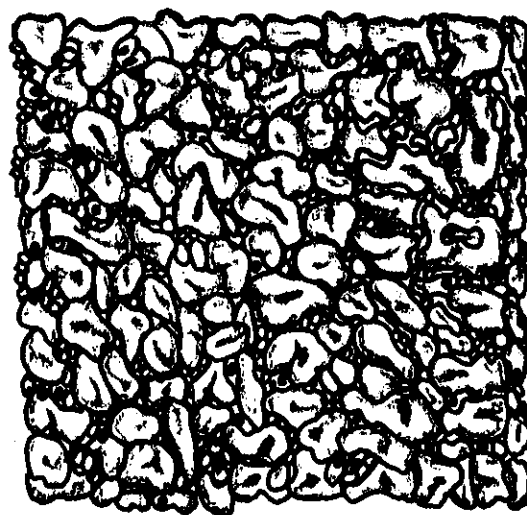
To form a commercial reservoir of hydrocarbons, any geological formation must exhibit two essential characteristics. These are a capacity for storage and a transmissivity to the fluid concerned, i.e. the reservoir rock must be able to accumulate and store fluids, and when development wells are drilled it must be possible for those reservoir fluids to flow through relatively long distances under small potential gradients.

A. Porosity

The void spaces in reservoir rocks are, for the most part, the intergranular spaces between the sedimentary particles. Porosity is defined as a percentage or fraction of void to the bulk volume of the rock. While the proportion of void can be calculated for regular arrangements of uniform spheres, as shown on the left, the porosity of reservoir rocks must be determined by direct measurement on core samples in the laboratory or estimated in situ by well log analysis.



Porosity of rombohedrally packed spheres - 26%



Grain sorting, silt, clay and cementation affect sandstone porosity

Fig. 4-1. Intergranular porosity.

Processes subsequent to sedimentation (cementation, re-crystallization, solution, weathering, fracturing), can modify substantially the proportion and distribution of void space. In reservoir engineering, only the interconnected or effective porosity is of interest since this is the only capacity which can make a contribution to flow. Pore spaces initially present but subsequently sealed off by cementation or re-crystallization effects are of no interest.

Primary porosity refers to the void spaces remaining after sedimentation of the granules in the matrix and hence is a matrix porosity.

Secondary porosity is the contribution from pits, vugs, fractures and other discontinuities in the bulk volume of the matrix. The contribution of secondary porosity to the overall bulk porosity is generally small yet it can lead to dramatic increases in bulk permeability.

Dual porosity systems

From the reservoir engineering point of view, the distinguishing factor between primary and secondary porosity is not the mode of occurrence but the very different flow capacity where an interconnected secondary porosity system is present. This is called a dual porosity system.

As shown in figure 4-2, the porosity of reservoir rocks may range from about 5% of bulk volume to about 30% of bulk volume, the lower porosity range normally being of interest only in dual porosity systems.

It will normally be possible to distinguish any effects of dual porosity if the "coarse" system has a flow capacity about two orders of magnitude greater than that of the "fine" system. With lesser contrasts, behaviour is virtually indistinguishable from single porosity systems with some heterogeneity. In this situation generally only porosities greater than about 10% are likely to be of commercial interest, the lower porosities generally being of interest only when a dual system is clearly definable.

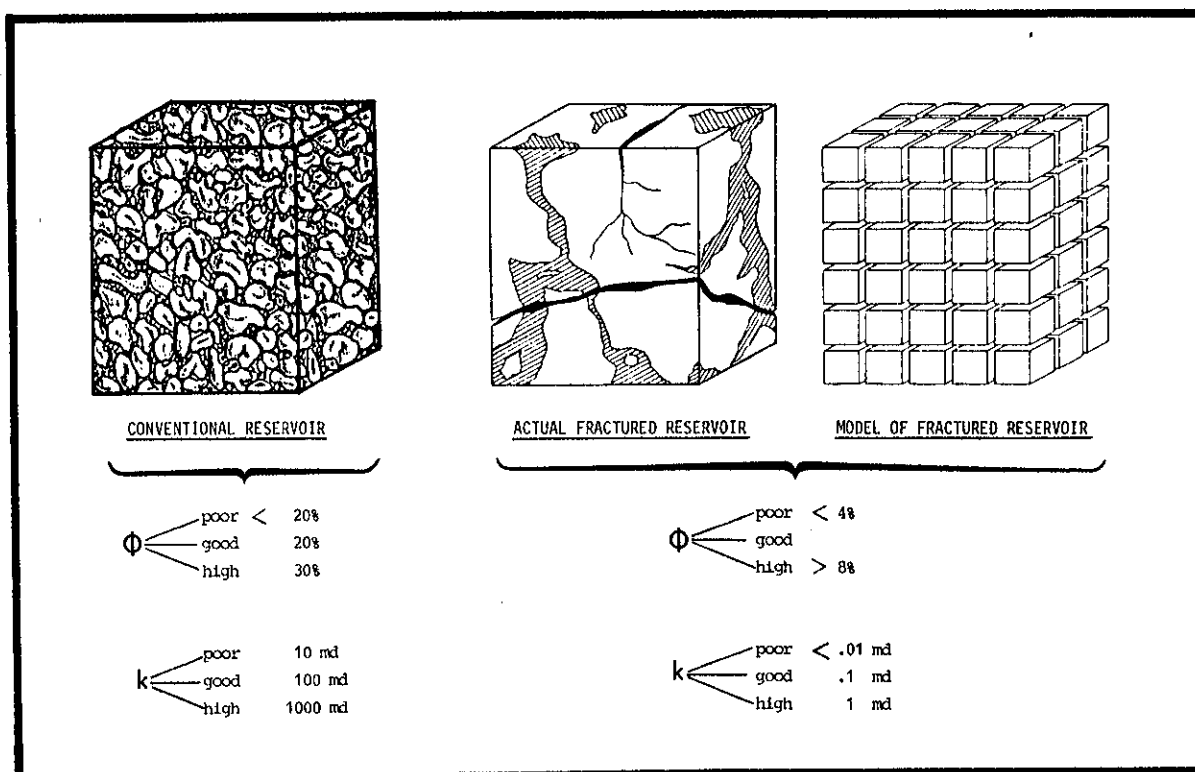


Fig. 4-2. Range of matrix porosity and permeability of commercial interest of conventional and fractured - dual porosity systems.

B. Permeability

The permeability of a rock is a measure of its specific flow capacity and can be determined only by a flow experiment. Since permeability depends upon continuity of pore space, there is not any unique relation between the porosity of a rock and its permeability, (except that a rock must have a non-zero porosity if it is to have a non-zero permeability).

Henry Darcy experimented with filtration of water through unconsolidated sand beds about 1856. The results of Darcy's studies, for horizontal flow, can be written in differential form :

$$v = \frac{k}{\mu} \frac{dp}{dL}$$

This is the defining equation for the measurement of permeability by flow measurement. The unit of proportionality k , between velocity and pressure gradient, is the coefficient of permeability and is usually measured in Darcy.

Note that the coefficient of permeability k , is a rock characteristic independent of the fluid used for its measurement.

1) Practical definition of the Darcy

In the oil industry permeability is expressed in Darcy units. A rock has a permeability of 1 Darcy if a pressure gradient of 1 atm/cm induces a flow rate of 1 cc/per square cm. of cross-sectional area of a liquid viscosity 1 cp. The Darcy is large for a practical unit, and the millidarcy is more commonly used.

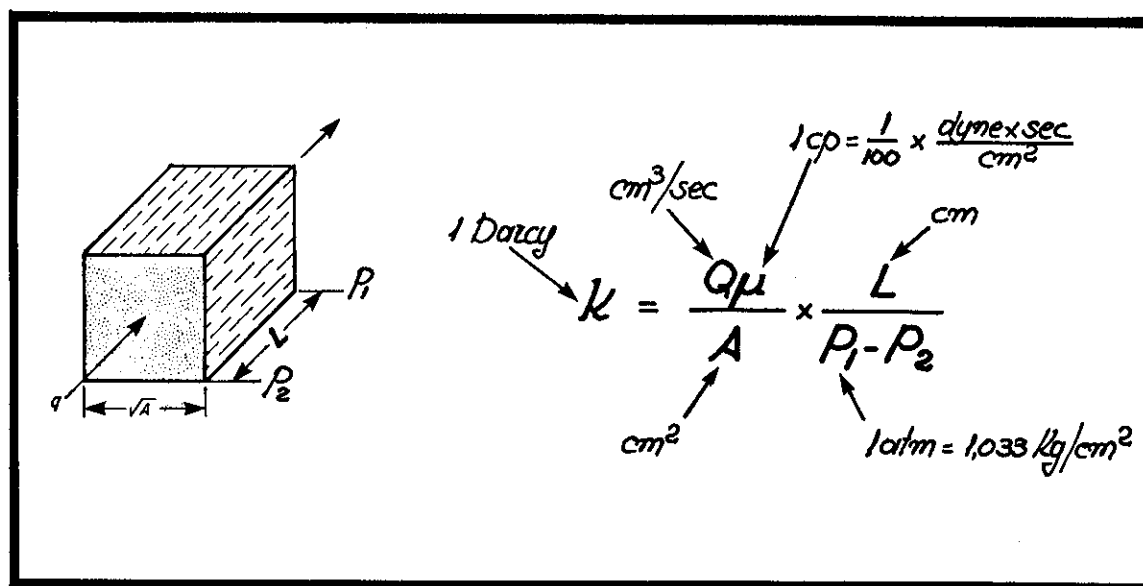


Fig. 4-3. Definition of a Darcy.

The Darcy thus defined, is a mixed unit which may eventually be replaced by a new SI unit.

It can be demonstrated as follows that k has the units of length^2 and that 1 Darcy is equal to $1\mu\text{m}^2$.

$$k = \frac{V\mu L}{\Delta P} = \frac{\frac{L}{T} \times \frac{FT}{L^2} \times L}{\frac{F}{L^2}} = L^2$$

where : L = Length
 F = Force
 T = Time

Evaluating 1 Darcy in cgs units :

$$1 \text{ Darcy} = \frac{\frac{\text{cm}}{\text{sec}} \times \frac{1}{100} \times \frac{\text{dyne sec}}{\text{cm}^2} \times \text{cm}}{1,033 \times 981000 \frac{\text{dyne}}{\text{cm}^2}} = 10^{-8} \text{ cm}^2 \text{ or } 1 \mu\text{m}^2$$

2) Factors affecting permeability

While grain size has a negligible effect on the porosity of a rock, this parameter has a predominant effect on permeability. This is so because grain size controls the total wetted surface. Each grain has a wetted surface surrounding it where fluid velocity is always zero, and shearing friction is formed between this zero velocity layer and any passing fluids. Thus more pressure energy is consumed in moving a given quantity of fluid through a fine granular pack (with its larger wetted surface and correspondingly higher frictional losses) than through a coarse granular pack of equal porosity.

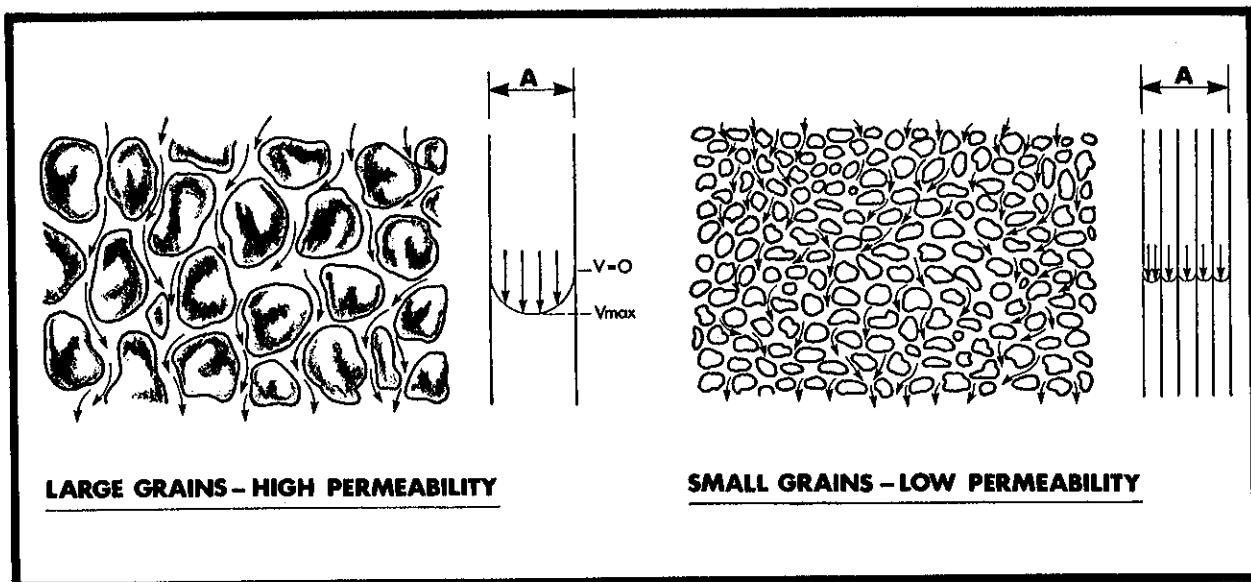


Fig. 4-4. Effect of grain size on permeability.

As an example of the effect of grain size on wetted surface, compare the wetted surface of a 1 m^3 rectangular conduit with a 1 m^3 rectangular conduit filled with .1 mm diameter sand grains.

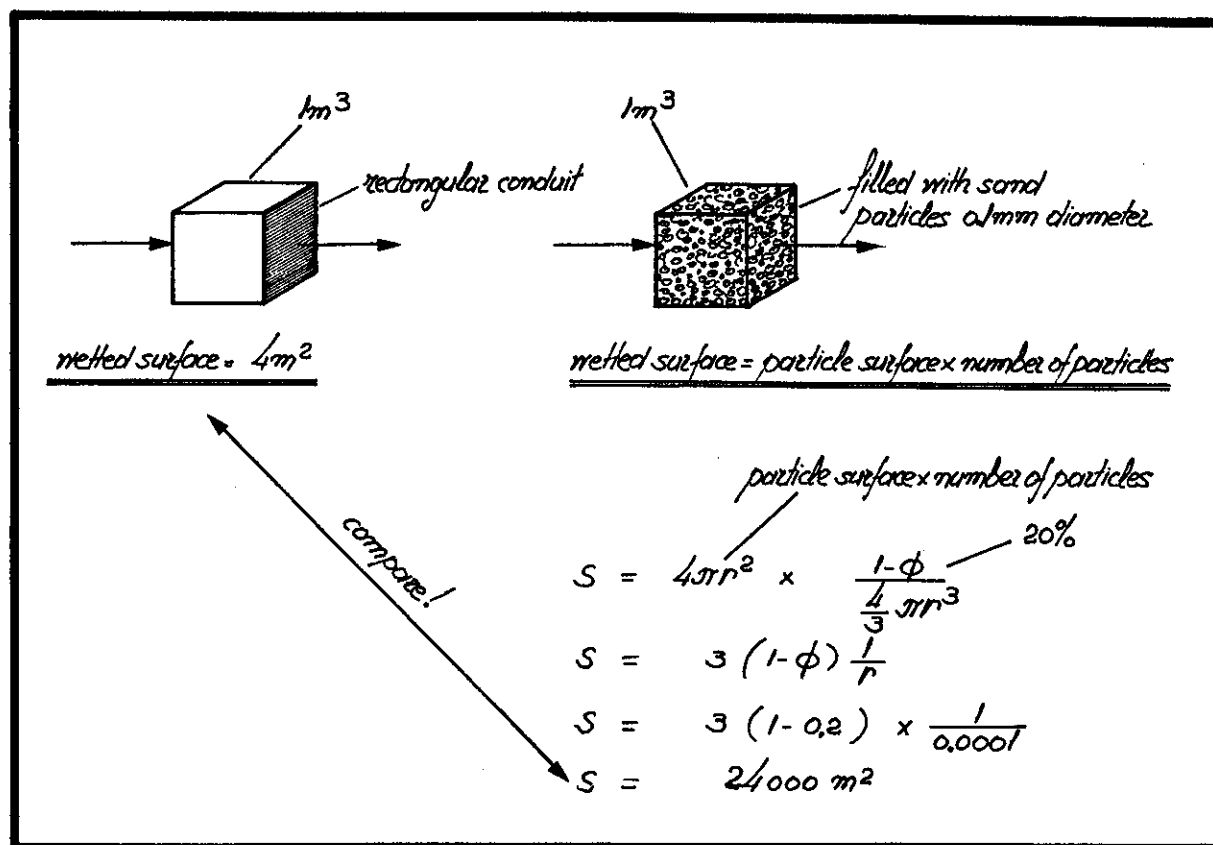


Fig. 4-5. Example illustrating effect of grain size on wetted surface.

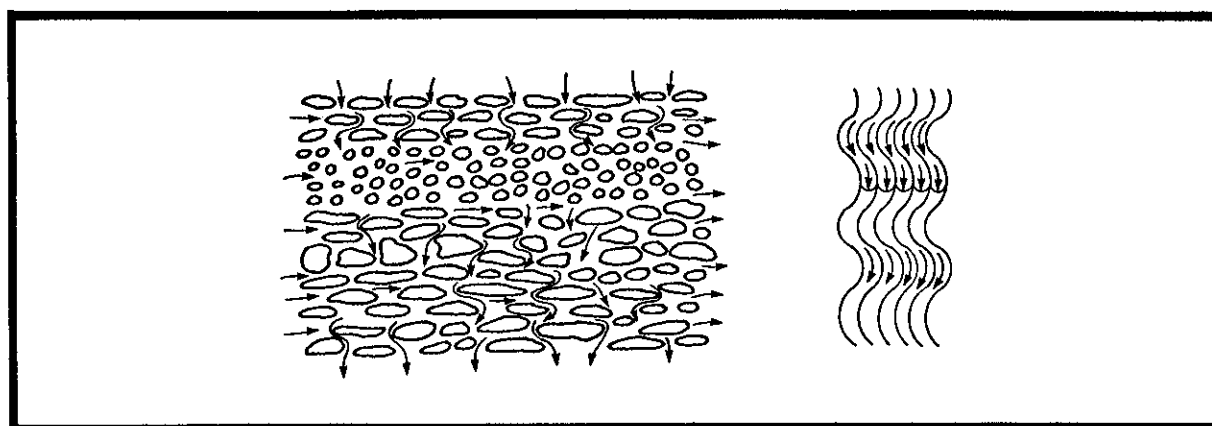


Fig. 4-6. High horizontal-low vertical permeability.

Granular sorting, silting, clay inclusions, and processes subsequent to sedimentation mentioned previously, such as solution, cementation, weathering, and fracturing all act to influence both the porosity and permeability of a rock.

C. Measurement of permeability

Permeability can be measured by passing a fluid of known viscosity through a cylindrical core cut from the rock (axis parallel to the bedding plane) of known dimensions and measuring the pressure drop and flow rate.

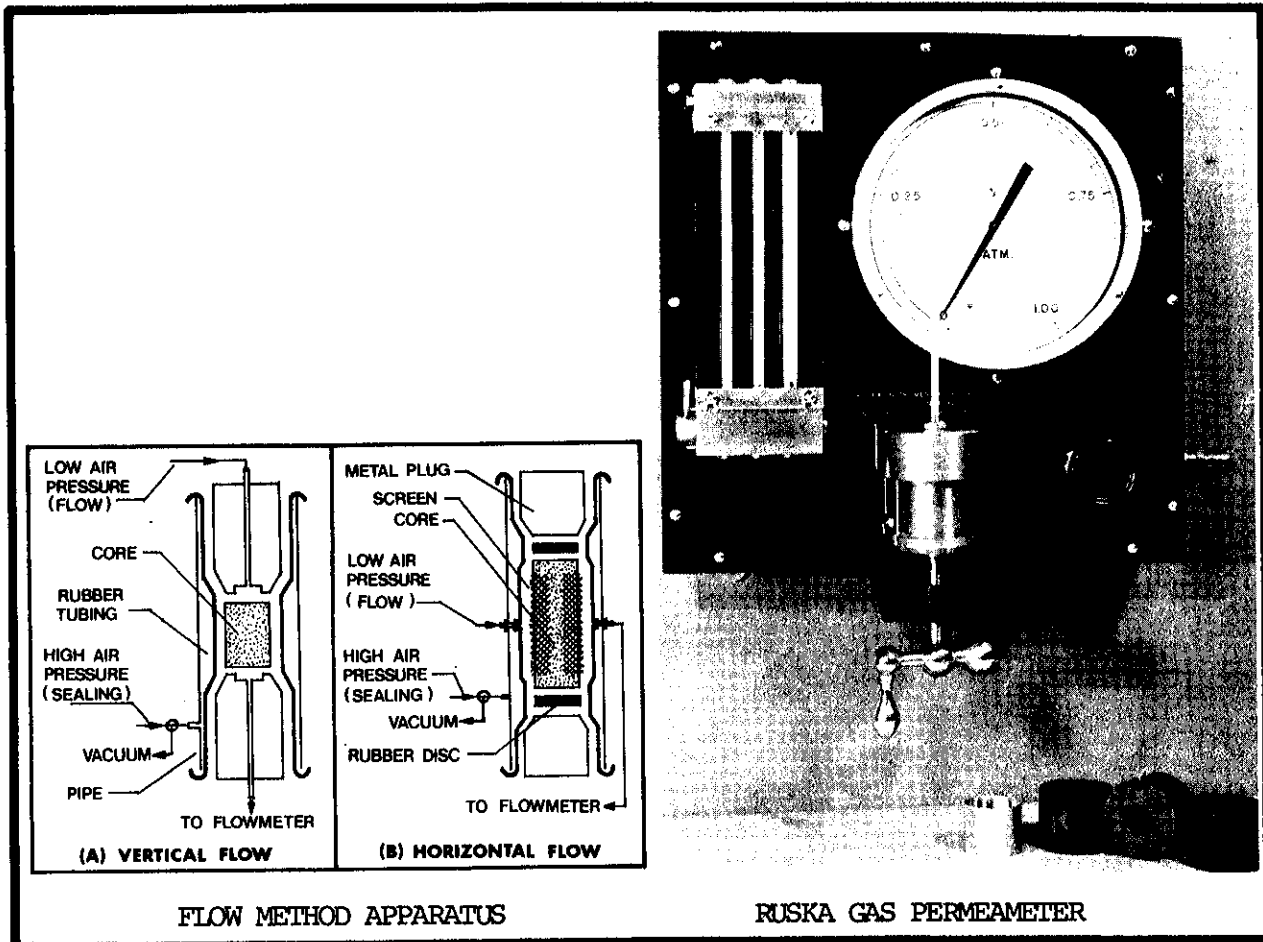


Fig. 4-7. Laboratory apparatus for measurement of permeability.

The permeability of a core specimen is most easily measured using gas (nitrogen or air) at pressures of about 1 atmosphere. As the volumetric flow rate varies with the pressure along the flow path, gas flow rates g , measured at mean core pressure $(P_1 + P_2) / 2$ have to be corrected to Q , the flow rate at the reference pressure for the measurements, P_b . This is done as follows :

From Boyle's law :

$$Q = g \frac{(P_1 + P_2)}{2}$$

or :

$$g = \frac{2QP_b}{P_1 + P_2}$$

substituting g for Q in the Darcy equation for linear flow, $k = \frac{Q \mu L}{(P_1 - P_2) A}$

we find :

$$k = \frac{2QL\mu P_b}{A(P_1^2 - P_2^2)} \quad \text{in Darcy's where :}$$

Q = gas flow rate, at reference pressure cm^3/sec
 L = length of core, cm
 μ = gas viscosity, cp
 A = areas of core, cm^2
 P = absolute press. atm .

Subscript 1 = upstream press.
 2 = downstream press.
 b = base pressure for
 gas measurement

It may be noted that flow rates for liquids through porous media are proportional to $P_1 - P_2$ while they vary with $P_1^2 - P_2^2$ for gases.

Klinkenberg effect

While permeability is a characteristic of the rock and independent of the fluid used, gas flow data must be corrected for its behaviour in the very fine pore passages where the mean free path of the gas molecule approaches the passage dimension.

Klinkenberg derived the following expression to correct gas permeabilities.

$$k_g = k_l \left(1 + \frac{b}{P_m} \right)$$

where : k_g = permeability to gas
 k_l = permeability to liquid
 P_m = mean pressure on gas $\left(\frac{P_1 + P_2}{2} \right)$
 b = constant for gas - liquid systems

A plot of the reciprocal of the mean pressure $\left(\frac{P_1 + P_2}{2} \right)$ vs. permeability at several pressures extrapolates at $\frac{1}{P} = 0$, to the liquid permeability.

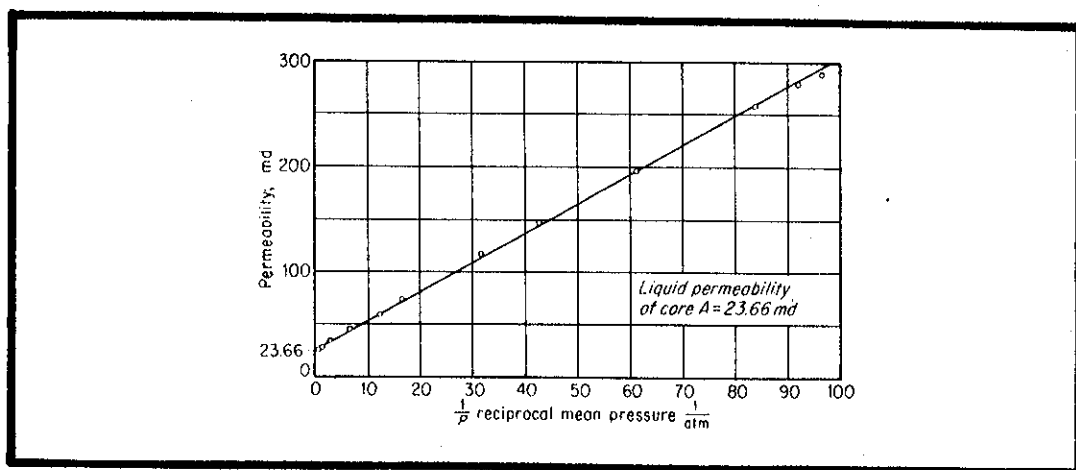


Fig. 4-8. Permeability of core sample A to air at various pressures. (After Klinkenberg).

D. Measurement of porosity

The definition of porosity requires that both the bulk volume and either pore or matrix volumes of the rock sample be determined.

The bulk volume of a rock sample is readily measured by mercury displacement. Where a porometer instrument is used, the volume can be read directly from the metering plunger's micrometer scale.

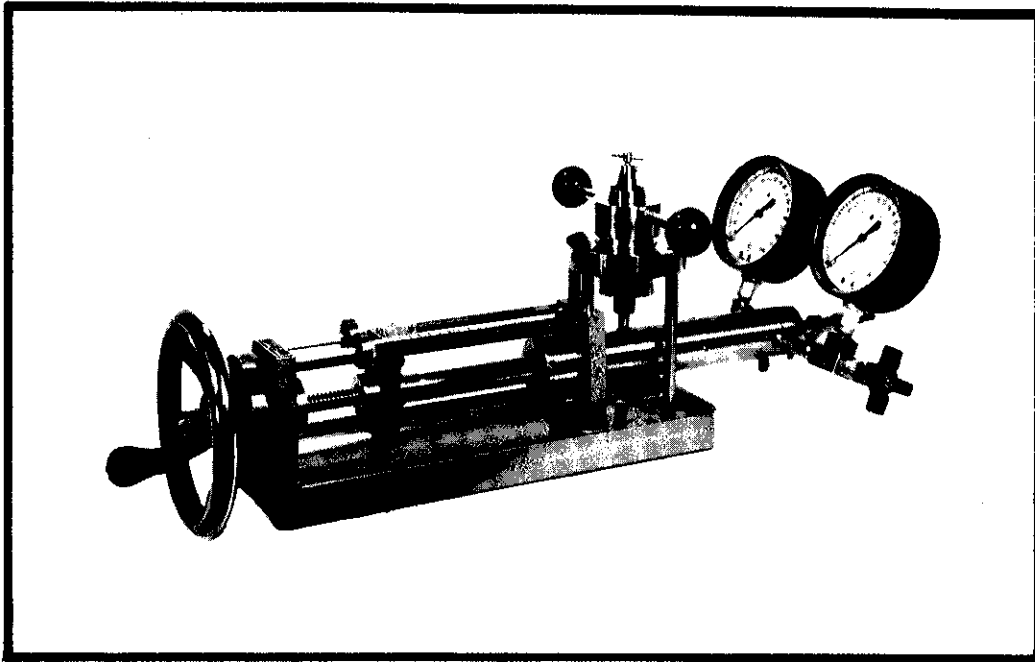


Fig. 4-9. RUSKA Universal porometer.

The pore volume can be determined by various means :

- 1) The rock sample evacuated and weighed, then saturated in brine or other fluid and re-weighed.

$$\% \text{ POROSITY} = \frac{\text{weight of fluid injected}}{\text{density of injected fluid} \times \text{core bulk volume}} \times 100$$

Excess fluid adhering to sample surface or excessive drainage from the pore spaces during weighing affect accuracy of the measurement.

- 2) In the Boyles law method of measurement, using the instrument shown above, the pore volume can be found by compressing a fixed volume of air from P_1 (usually one atmosphere) to a reference pressure P_2 (usually 2 atmospheres) and noting the volume change. Then the procedure is repeated with the rock sample in the chamber. The matrix volume may be calculated from the volumetric changes between P_1 and P_2 .

Since the sample has been penetrated only by air it can be used for additional core analysis tests.

- 3) Pore volume can be quickly and easily measured by injecting mercury under high pressure using a precision volumetric mercury pump.

With low porosity, fine pore structure systems, high pressures may be necessary to approach 100% displacement, and corrections for mercury and steel vessel compressibility may become necessary. At pressures of 6,000 psi - 10,000 psi, attainable with standard equipment, most of the pore space contributing to flow is occupied.

E. Measurement of capillary pressure by mercury injection

Using the same equipment to inject measured volumes of mercury at a series of pressures a mercury capillary pressure curve, which is related to the water capillary pressure curve may be obtained.

Although oil/water or air/water experiments can be conducted to determine capillary pressure vs. saturation relationships, these may be very prolonged because of the long times required to reach equilibrium at low water saturations.

The conventional method for measuring capillary pressures is therefore an accelerated method, using the injection of mercury (a strongly non-wetting fluid), into an evacuated core sample at high pressure.

The mercury capillary pressures can be converted into oil-water or gas-water capillary pressures, through the factors :

$$\frac{P_{\text{oil/water}}}{P_{\text{mercury}}} = \frac{(\sigma \cos \theta)_{\text{oil/water}}}{(\sigma \cos \theta)_{\text{mercury}}} \quad (1:14)$$

$$\frac{P_{\text{gas/water}}}{P_{\text{mercury}}} = \frac{(\sigma \cos \theta)_{\text{gas/water}}}{(\sigma \cos \theta)_{\text{mercury}}} \quad (1:5)$$

where σ is the surface tension and θ the contact angle which will be discussed in the next chapter.

Through the use of capillary pressure data, the theoretical saturation existing at any level above the hydrocarbon water contact can be determined, and the extent and importance of any transition zone evaluated.

Samples which have been subjected to mercury injection can not be used for further laboratory tests.

SURFACE TENSION

WETTABILITY, CAPILLARITY,

SATURATION &

FLUID DISPLACEMENT

5

The repartition of hydrocarbons and connate water in the reservoir at initial conditions and during depletion is strongly dependent on the interfacial forces which act between the fluids and the rock matrix. Any proper understanding of fluid behaviour in reservoir rocks begins with a grasp of the principles of surface tension, wettability, and capillarity.

A. Surface tension

The apparent film which separates two immiscible fluids, such as air-water is caused by unequal attractive forces of molecules at the interface.

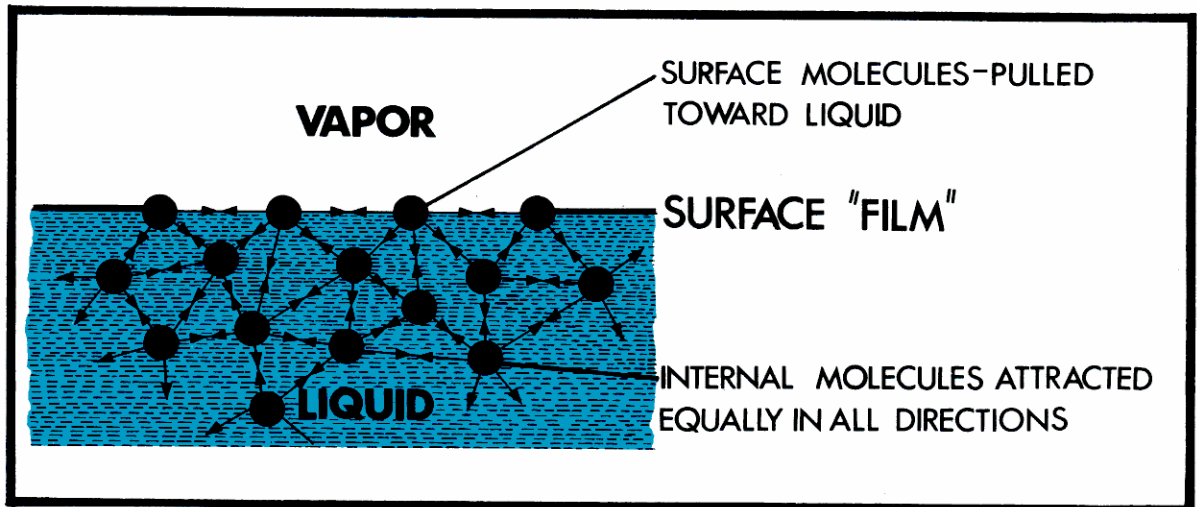
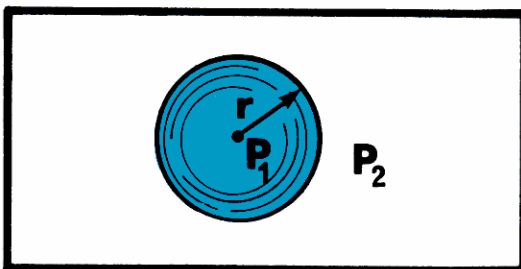


Fig. 5-1. Apparent surface film caused by imbalance of molecular forces

It is because of these attractive forces that a bubble contracts into spherical form. It can be shown theoretically and experimentally that a pressure difference must exist across any curved fluid interface - the smaller the radius the greater is the pressure on the concave side.

The pressure in a bubble having a single phase boundary is given by :



$$P_1 - P_2 = \frac{2\sigma}{r} \quad \text{in dynes where :}$$

σ = surface tension, dynes/cm
 r = bubble radius, cm
 P = pressure, dynes/cm²

Fig. 5-2. Pressure in a bubble.

Measurement of surface tension

Surface tension can be determined by the ring method in which the force, F , required to break the two annular films is measured.

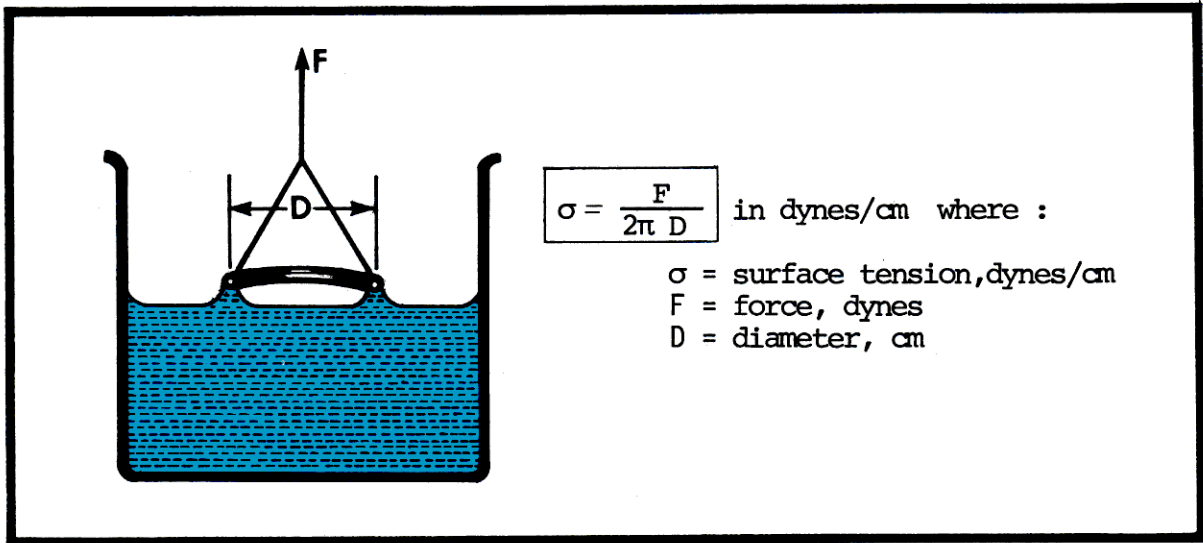


Fig. 5-3. Measurement of surface tension by ring method.

Surface tensions between some common fluids and air at 20° C are given below :

Water	72.6 dynes/cm
Benzene	28.9
Cyclohexane	25.3
N-hexane	18.4
N-octane	21.8

The interfacial tension between water and oil at 20° C \approx 30 dynes/cm.

Interfacial tension between a liquid and its vapor decreases with temperature increase until at the critical point, surface tension is zero and differentiation between fluid/vapor phases ceases to exist.

B. Wettability

The tendency of one fluid to displace another from a solid surface is determined by the relative wettability of the fluids to the solid.

If the work of the adhesion of fluid A is greater than the work of adhesion of fluid B, then fluid A will displace fluid B from the surface until an equilibrium contact angle θ is attained.

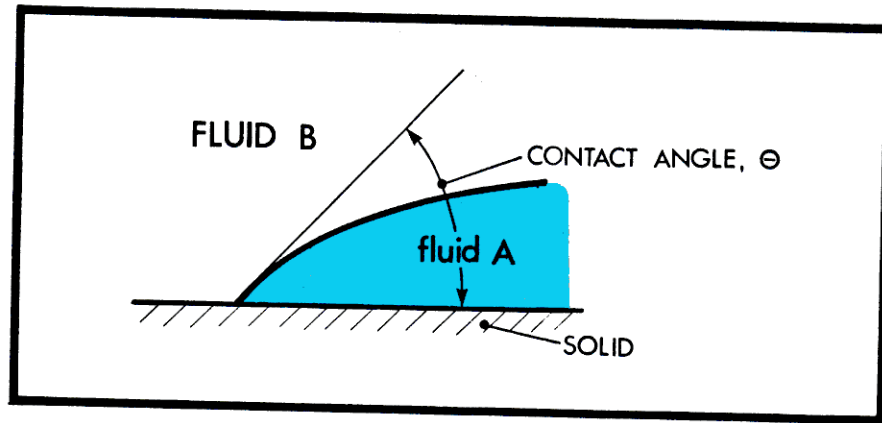


Fig. 5-4. Contact angle as a measure of wettability.

The contact angle may be used as a method of expressing wettability. If the contact angle measured through liquid A is acute, the meniscus between the liquids will be concave towards B, and liquid A will displace liquid B from a solid surface (powder or granular pack). Liquid A is said to be a wetting phase with respect to the solid surface and liquid B.

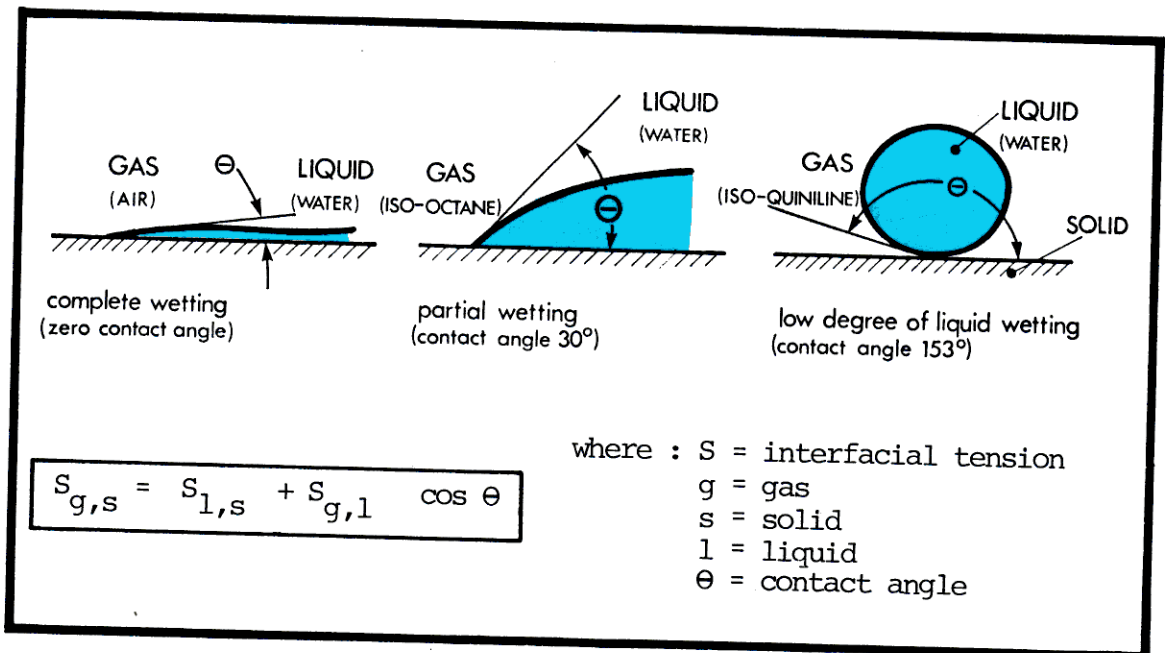


Fig. 5-5. Contact angle as a measure of wetting.

C. Capillarity

When liquid wets the surface of a fine bore glass capillary tube, surface tension around the periphery of the contact pulls the liquid interface up the tube until an equilibrium is reached with the downward force due to the liquid column height.

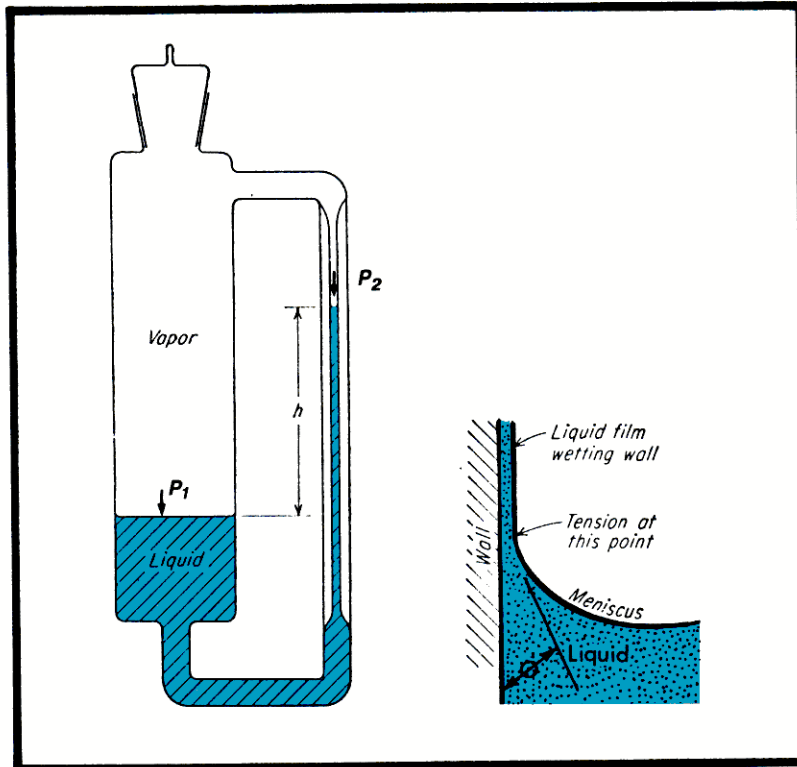


Fig. 5-6. Capillary rise

The equation expressing this pressure equilibrium is given by :

Surface tension X periphery = column hydrostatic pressure

$$\cos \theta \sigma (2\pi r) = \pi r^2 h (p_L - p_V) g$$

where : σ = surface tension, dynes/cm
 r = radius of tube, cm
 h = capillary rise, cm
 p_L = density of liquid, grams/cu cm
 p_V = density of vapor, grams/cu cm
 g = acceleration due to gravity, 980.6 cm/sec²
 θ = contact angle between liquid and solid
 $\cos \theta = -1$ when $\theta = 180^\circ$, for complete wetting

A pressure P_2 applied above the liquid in the capillary sufficient to lower the meniscus to the same level (pressure P_1) as in the reservoir is equal to the capillary pressure, P_C . That is, the capillary pressure $P_C = P_2 - P_1$ in this condition of equilibrium.

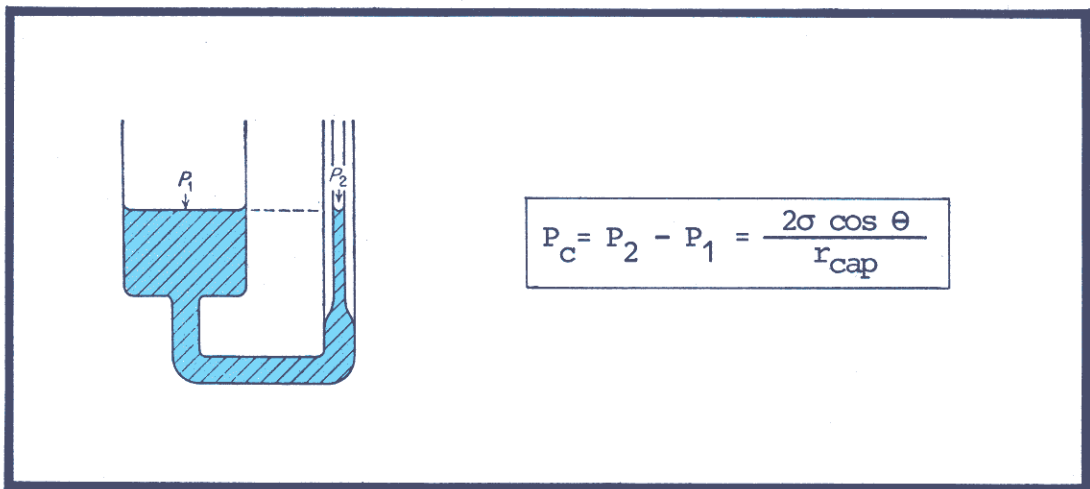


Fig. 5-7. Measurement of capillary pressure by depression of rise

Capillary pressure between spherical particles

Capillary pressure between the wetting and non wetting fluids at the contact between spherical grains can be expressed in terms of the two principal radii of curvature of the meniscus, R_1 and R_2 .

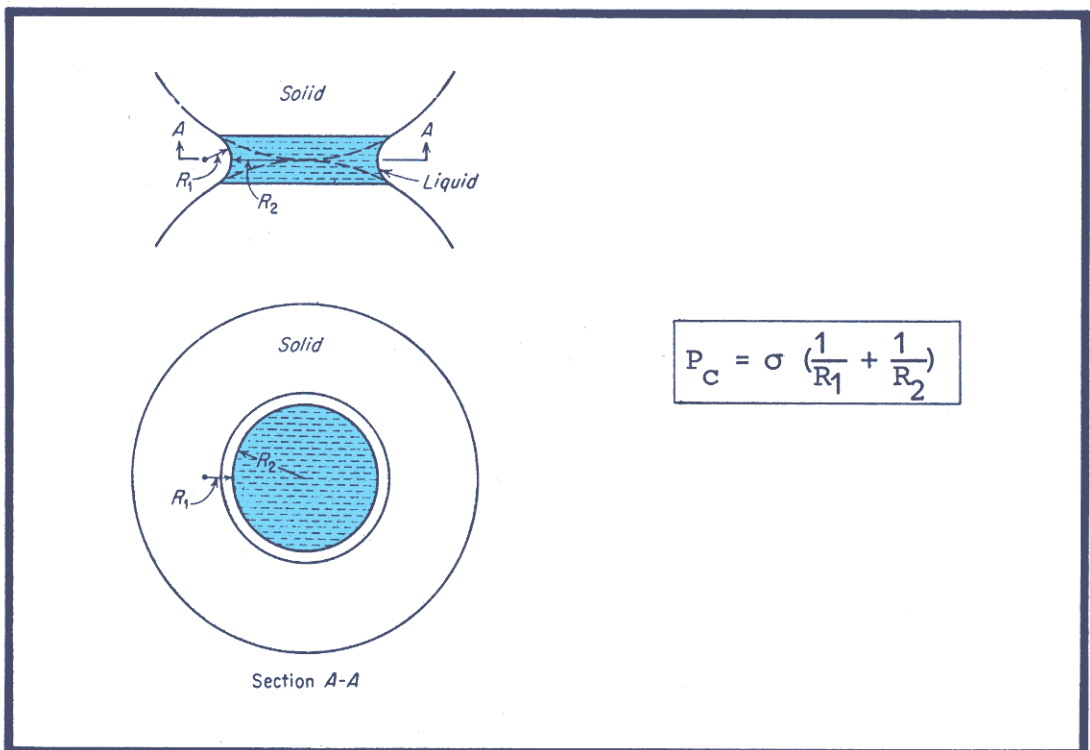


Fig. 5-8. Capillary pressure and radii of curvature of meniscus

D. Repartition of saturation in reservoir rocks

During deposition, reservoir rocks are completely saturated and water wet.

As hydrocarbons migrate and accumulate in the reservoir rock, a portion of this connate water is displaced.

Both silica, SiO_2 and calcite CaCO_3 have a strong tendency to remain water wetted. Therefore, connate water may only be displaced by hydrocarbons migrating into the reservoir to the extent of attaining an equilibrium when the pressure arising from fluid density differences is equal to the capillary pressure between the fluid phases at a particular level.

Taking a hypothetical water contact, where water saturation is 100%, the pressure difference between the phases at some elevation "h" above this level, will be :

$$P_O - P_W = g h (P_W - P_O)$$

This pressure difference, which is equal to the capillary pressure, obviously increases with height above the hydrocarbon - water contact and a gradient in the capillary pressure implies a gradient in the water saturation above the hydrocarbon.

If at some elevation, the water phase becomes discontinuous, then the water saturation (S_{wir}) becomes essentially constant, and independent of the pressure difference between the phases.

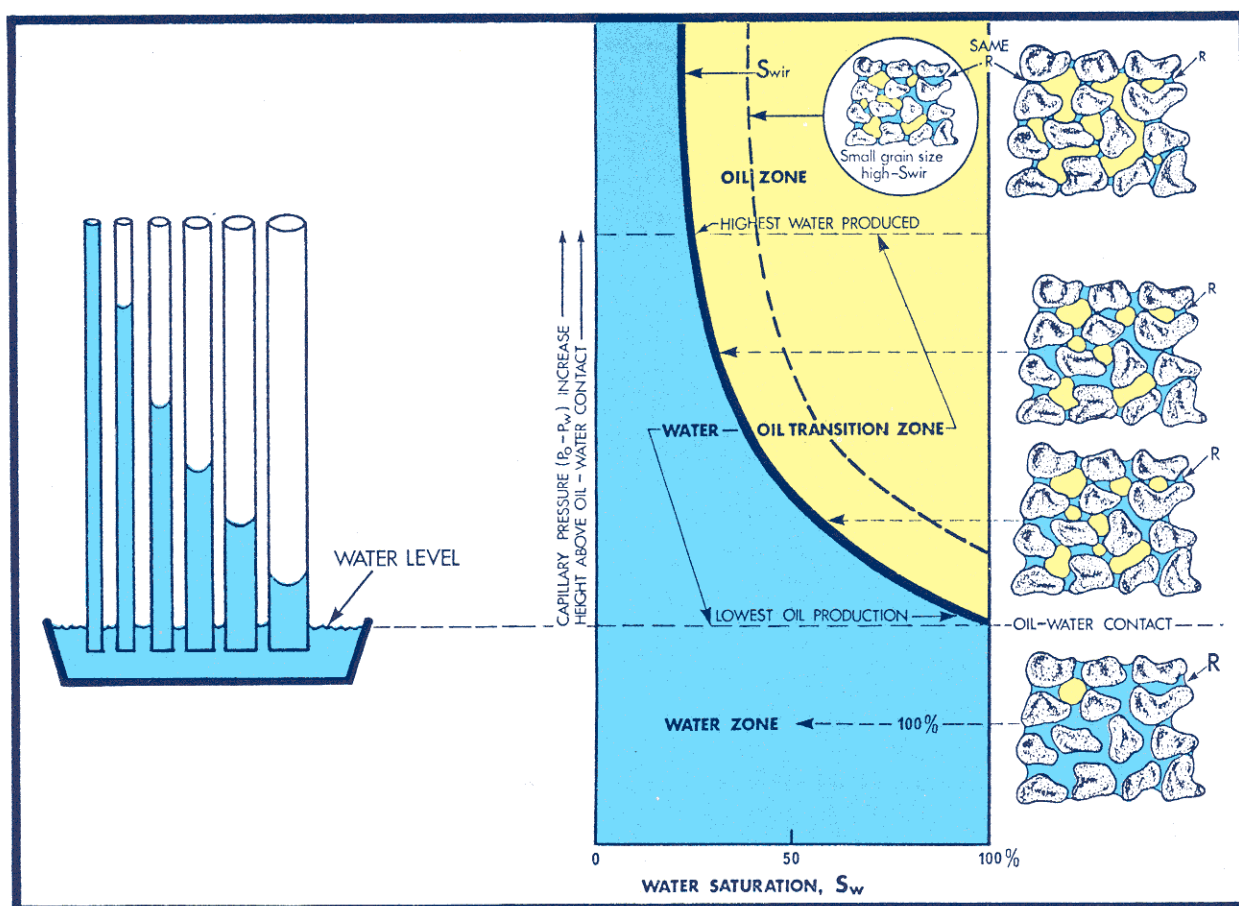


Fig. 5-9. Comparison of fluid rise in a capillary tube bundle of varying diameters illustrates the distribution of saturation in the transition zone above an oil/water contact.

E. Irreducible water saturation

The minimum saturation that can be induced by displacement is one in which the wetting phase becomes discontinuous. In a packing of uniform spheres this would correspond to a state wherein the wetting phase would exist as pendular rings at sphere contacts. The minimum saturation corresponds to the smallest mean radius of curvature, and maximum capillary pressure. Since the wetting phase will become discontinuous at some finite capillary pressure (corresponding to $\sigma(\frac{1}{R_1} + \frac{1}{R_2})$ for a single contact of two equal spheres) there will always be some irreducible water saturation—a saturation which cannot be reduced by displacement by a non-wetting phase, no matter how great a pressure is applied to the system. As shown below grain size has a strong influence on the irreducible water saturation.

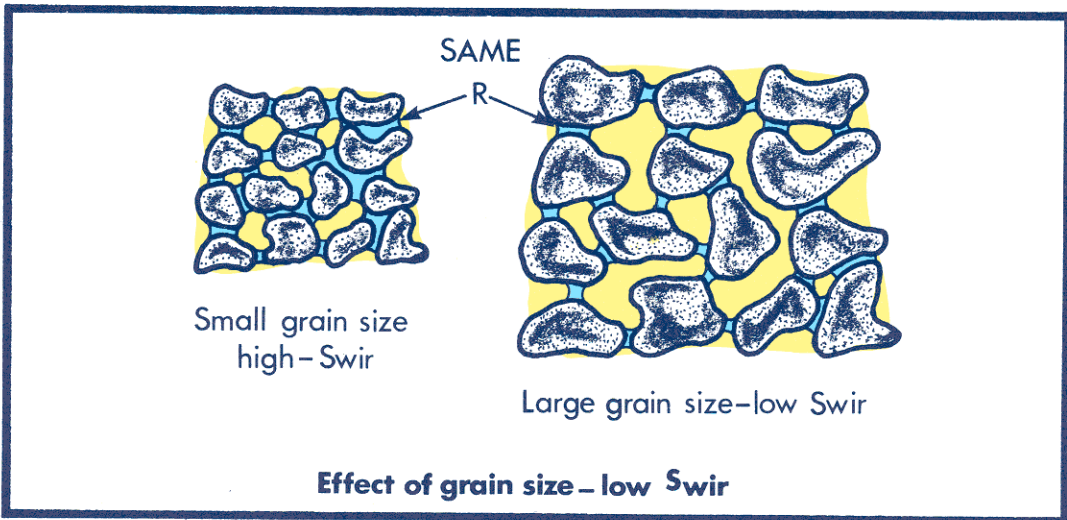


Fig. 5-10. Shape of the capillary pressure vs. saturation curve.

At higher wetting phase saturations, the mean radius of curvature increases, and the capillary pressure decreases. For idealized systems it is possible to establish an explicit relation between capillary pressure and saturation, but this is not possible for more complex natural porous media. The nature of the interstices, particularly in carbonates, and the clay content of sands has an important effect on connate water saturation.

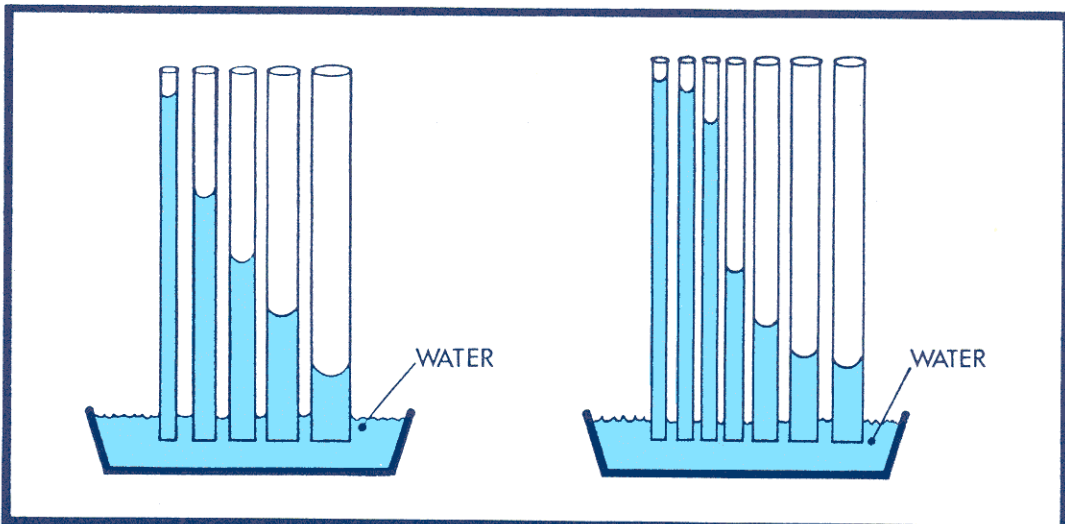


Fig. 5-11. Shape of capillary curve through the transition zone is strongly affected by the distribution of grain size.

F. Displacement pressure

Before a non-wetting phase can penetrate a capillary tube or porous medium that is saturated with a wetting phase, some minimum threshold pressure must be exerted.

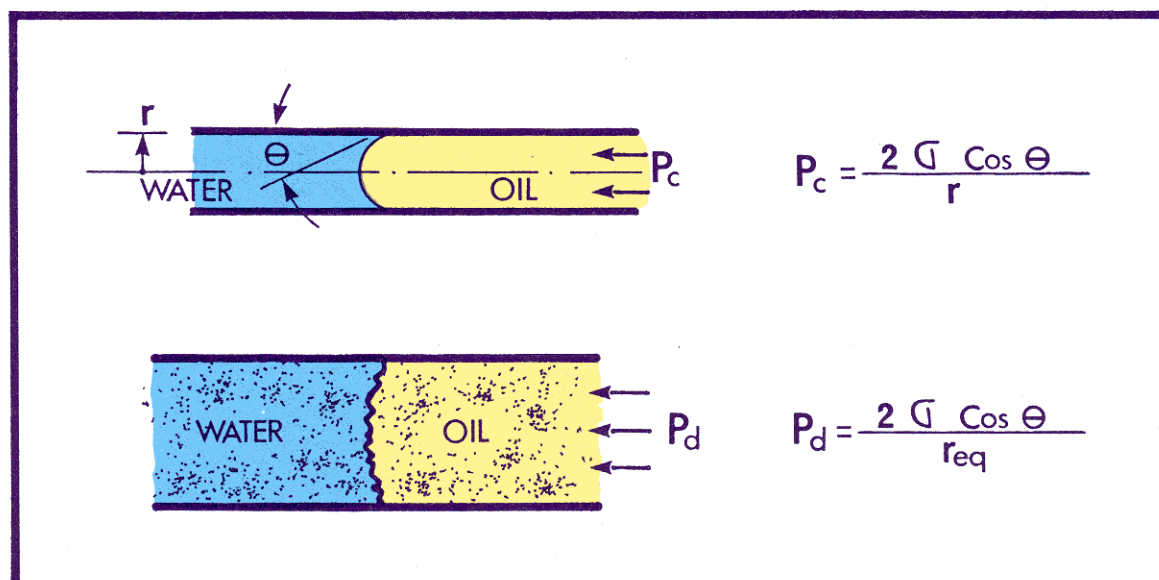


Fig. 5-12. Comparison of displacement from a capillary tube and granular packs.

To displace water (the wetting phase) from a single capillary tube, a pressure slightly higher than the capillary pressure must be applied to the oil (non-wetting phase).

Likewise, to displace water from a granular pack a pressure greater than the threshold must be applied to the oil. Displacement pressure is controlled by the size of the pore openings, r_{eq} as defined by the relation given in figure 5-12.

G. Displacement of oil

The mechanisms affecting the original repartition of hydrocarbons which have migrated into the reservoir have been discussed earlier. It is now useful to examine qualitatively the mechanisms by which accumulated hydrocarbons can be displaced from elementary pore channels of reservoir rock.

Water tends to displace oil in a piston like fashion, moving first close to the rock surface where it is aided by capillary forces in squeezing oil from the smaller channels.

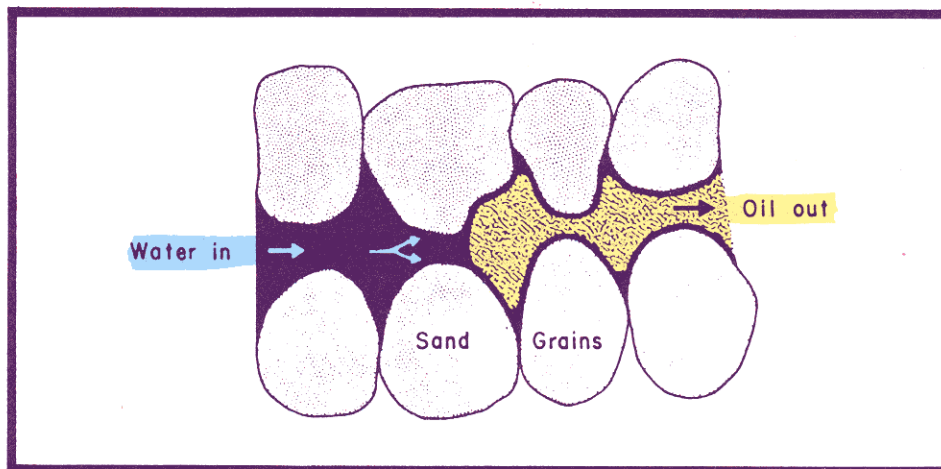


Fig. 5-13. Natural displacement of oil by water in a single pore channel. (Courtesy Journal of Petroleum Technology - June, 1958).

Gas, being more mobile tends to move easily along the center of the larger pore channels leaving oil behind in the smaller channels.

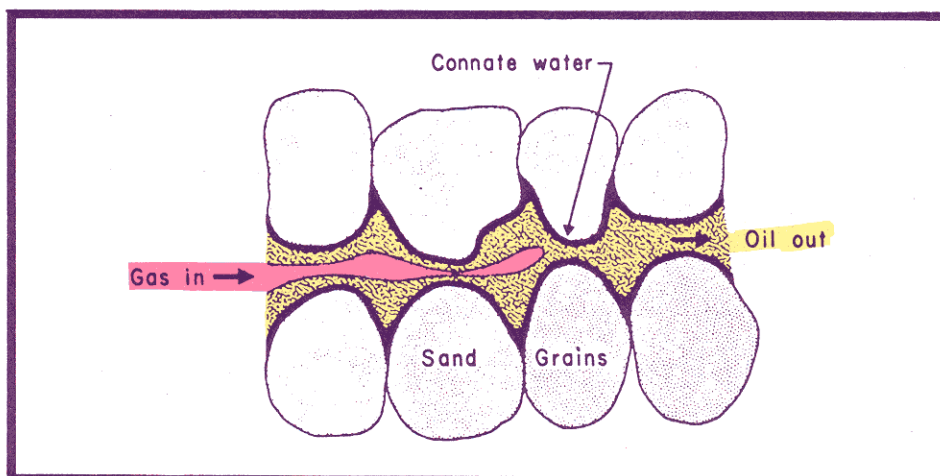


Fig. 5-14. Natural displacement of oil by gas in a single pore channel. (Courtesy Journal of Petroleum Technology - June, 1958).

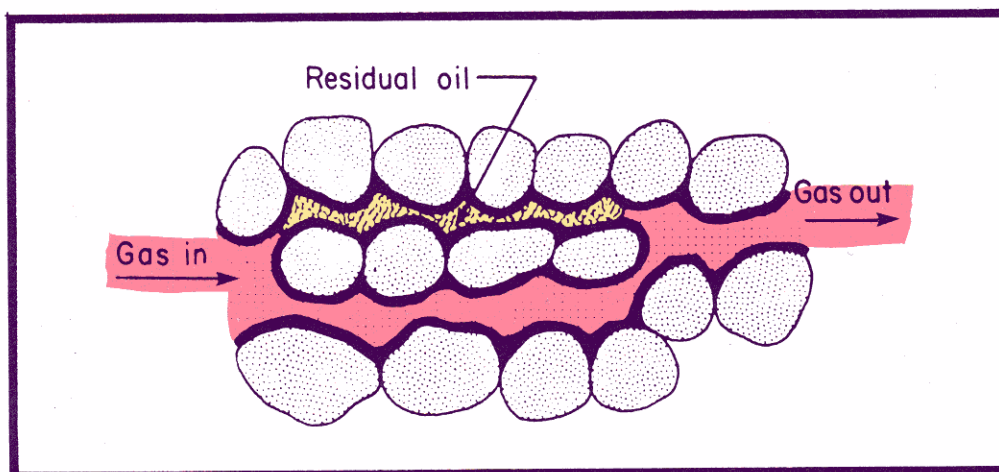


Fig. 5-15. Gas displaces oil first from high permeability pore channels. Residual oil occurs in lower permeability pore channels. (Courtesy Journal of Petroleum Technology - June, 1958).

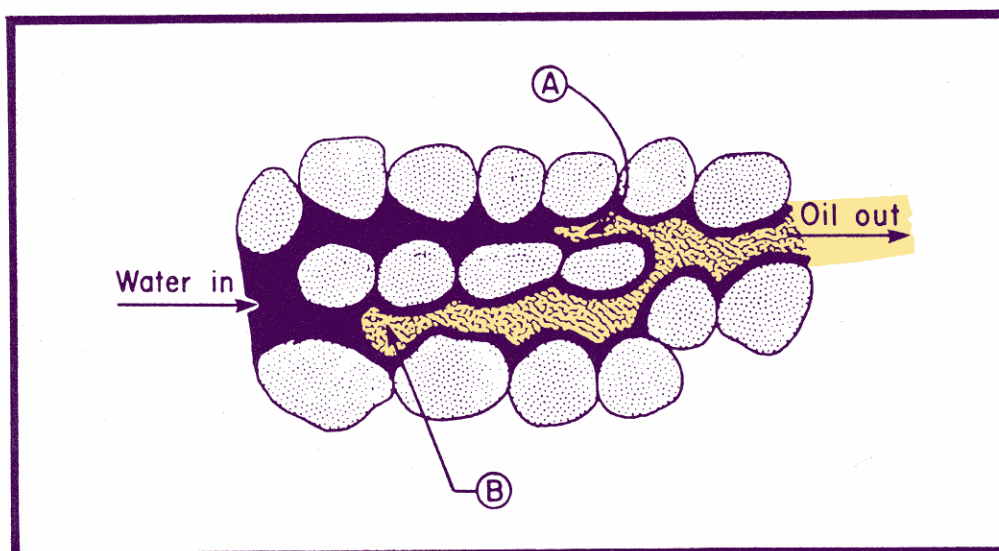


Fig. 5-16. Capillary forces cause water to move ahead faster in low permeability pore channel (A) when water is moving slow through high permeability pore channel (B). (Courtesy Journal of Petroleum Technology - June 1958).

During accumulation of hydrocarbon in the reservoir, some threshold pressure had to be overcome in order to permit the non-wetting oil to enter the water saturated pores.

These same capillary forces now aid the expulsion of oil from the tight and dead-end pores by inhibition of water along the surface of the grains, in a type of "counter flow".

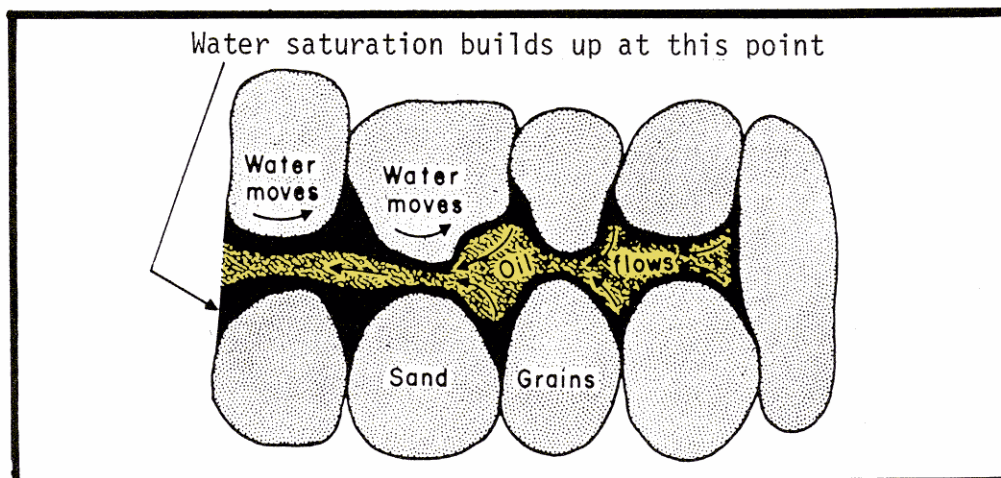


Fig. 5-17. Capillary pressure gradient causes oil to move out and water to move into a dead-end pore channel when sand is water-wet. (Courtesy Journal of Petroleum Technology - June, 1958).

H. Residual oil

Residual oil is left in the smaller channels when interfacial tension causes the thread of oil to break, leaving behind oil in droplets which tend to assume spherical form and when gradient pressure is not sufficient to deform the bubble enough to pass through the smaller diameter pore openings.

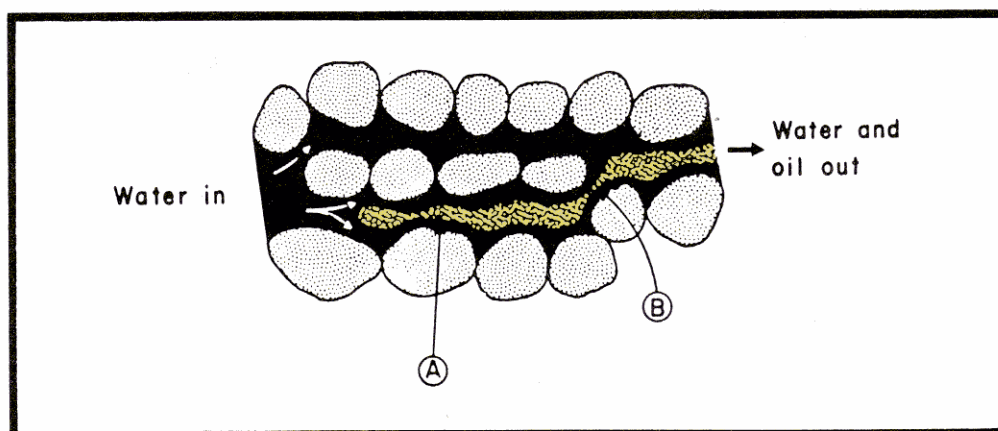


Fig. 5-18. As thread of oil gets smaller, interfacial tension increases in the film at restricted Points A and B, where film subsequently breaks. (Courtesy Journal of Petroleum Technology - June, 1958).

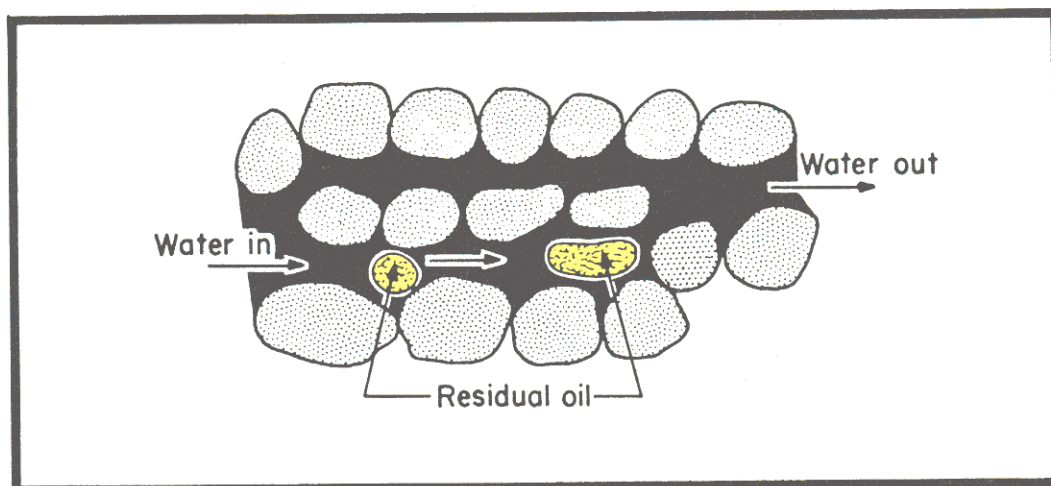


Fig. 5-19. Water drive leaves residual oil in sand because surface films break at restrictions in sand pore channels.
(Courtesy Journal of Petroleum Technology - June, 1958).

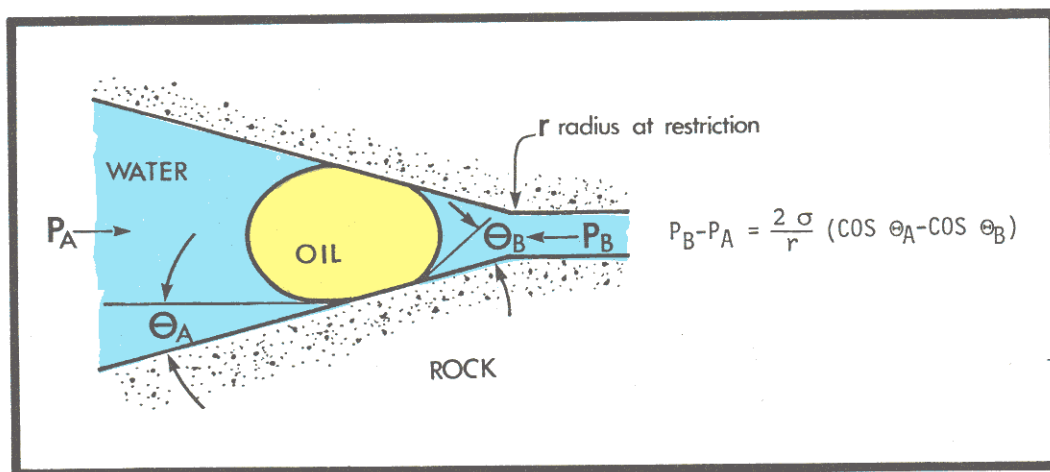


Fig. 5-20. Pressure to displace bubble through a restriction.

I. Relations between permeability and fluid saturations

Production of hydrocarbons inevitably involves simultaneous flow of two and three fluids in the reservoir rock. The presence of one fluid in the porous media impedes the flow of other phases.

- 1) Absolute permeability, covered in the preceding chapter, is a property of the rock and not of the fluid flowing through it. Absolute permeability is measured with a fluid which saturates 100% of the pore space.
- 2) Effective permeability - Is the permeability of a flowing phase which does not saturate 100% of the rock, e.g.

$$k_o = \frac{q_o \mu_o}{A} \times \frac{1}{dP_o/dx}$$

$$k_g = \frac{q_g \mu_w}{A} \times \frac{1}{dP_g/dx}$$

$$k_w = \frac{q_w \mu_w}{A} \times \frac{1}{dP_w/dx}$$

The effective permeability is always less than the absolute value of k for the rock.

The effective permeability of a fluid is a function of saturation. In complex porous media it is not a unique function of S_w and depends upon the capillary structure of the rock and the wetting characteristics as well as its saturation history, i.e the previous saturation.

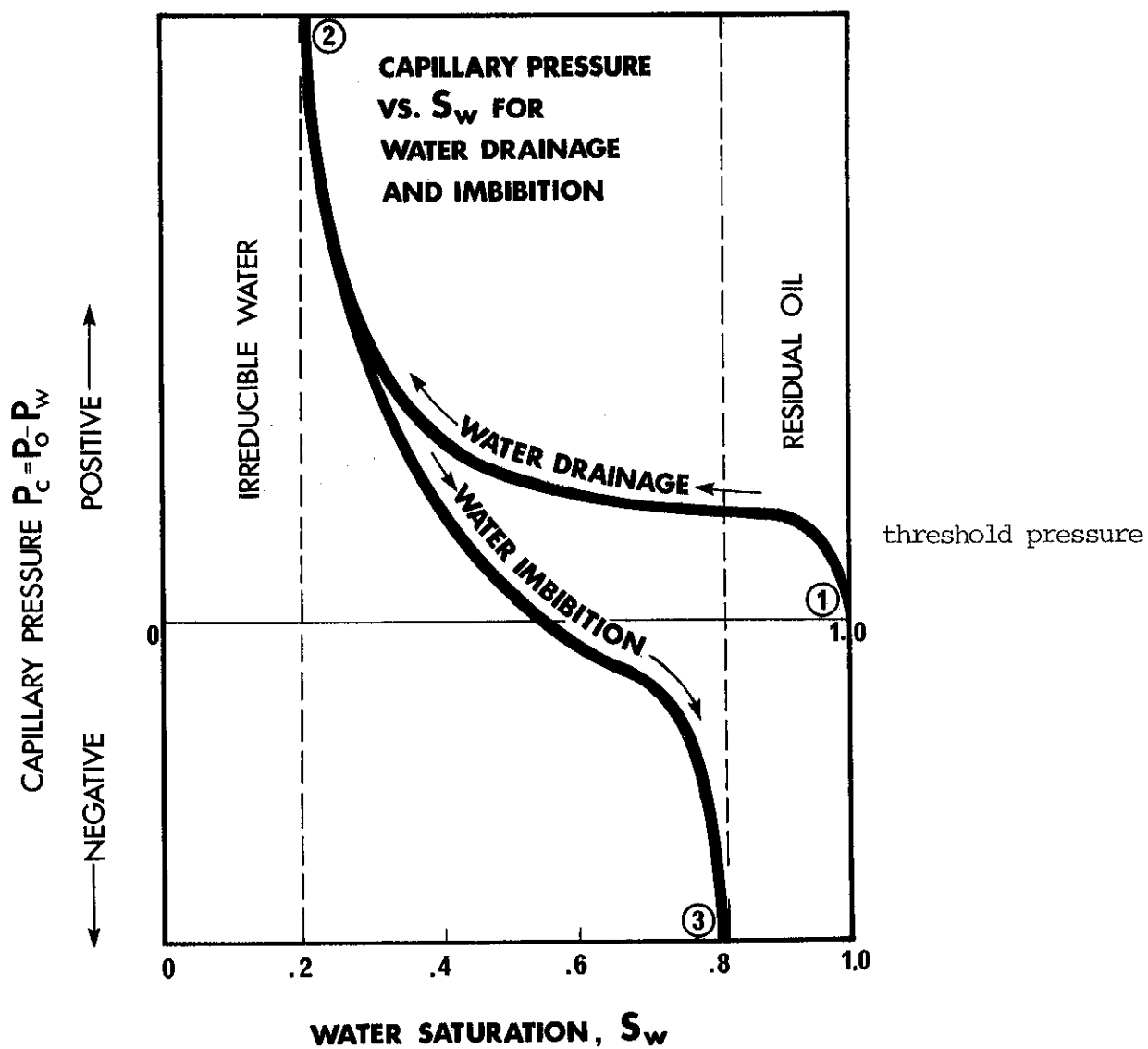
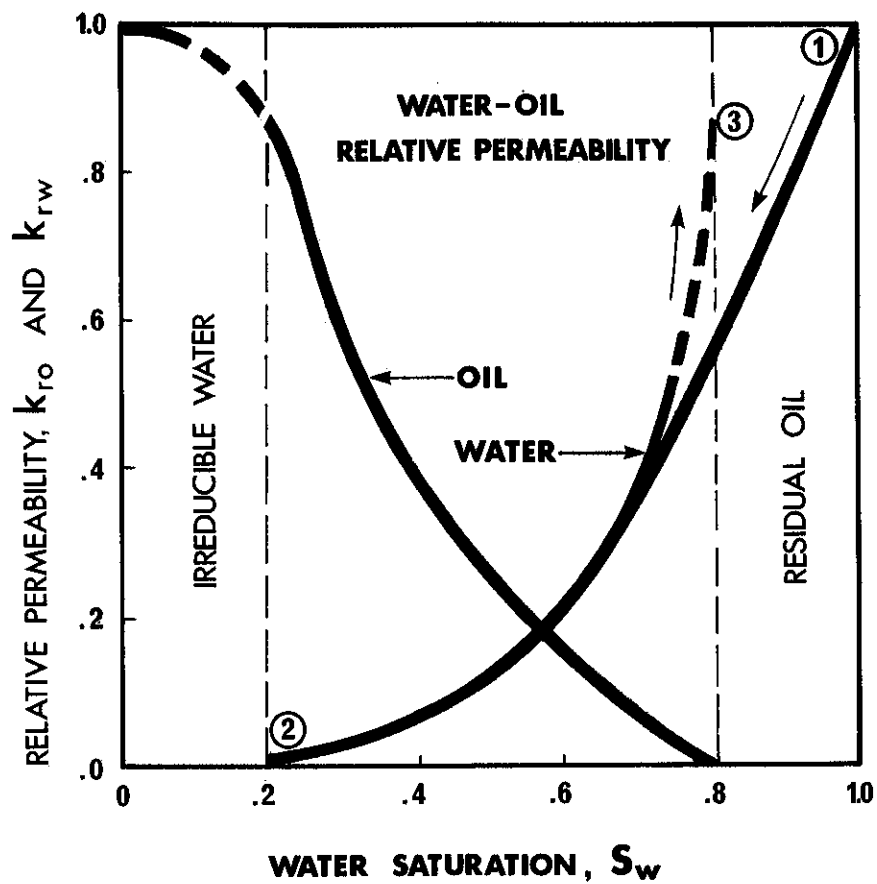
Relative permeability - is the ratio of effective permeability to absolute permeability :

$$k_{rw} = \frac{k_w}{k} \quad k_{ro} = \frac{k_o}{k} \quad k_{rg} = \frac{k_g}{k}$$

A typical set of oil/water relative permeability curves are shown on the next page, together with the corresponding capillary pressure relations. Both are plotted vs. water saturation to illustrate their relationship.

Starting with a 100% water saturated core at point (1) the threshold pressure must be exceeded before the non-wetting fluid (oil) can displace the wetting phase fluid, water from the matrix.

At higher displacement pressures increasing amounts of water are drained from the core until at (2) the irreducible water saturation is reached. At (2) the relative permeability to water becomes zero. Note that the relative permeability to oil at point (2) can not reach 1.0 as the irreducible water reduces the amount of pore volume to oil flow.



When water is imbibed into the core which now contains oil and water, the saturation of water increases up to the point (3), where the residual oil saturation is reached. The relative permeability to water can not reach a value of 1.0 because of the residual oil remaining in the pores.

3) Mobility ratio

The rates of oil and water production in the transition zone are governed by the viscosity ratio and effective permeability ratios of the fluids. Mobility ratio M , is defined as :

$$M = \frac{Q_w}{Q_o} = \frac{\frac{k_w}{\mu_w} \frac{AAP}{L}}{\frac{k_o}{\mu_o} \frac{AAP}{L}} = \frac{k_w/\mu_w}{k_o/\mu_o}$$

J. Relative Permeability - Saturation Correlations

In spite of the wide variety of pore structure in reservoir rocks, preferential wettabilities between fluids and rock surfaces, and fluid properties, normalized plots of relative-permeability ($k_o/k; k_g/k; k_w/k$) against saturation exhibit general similarities of form. It is, then, attractive to attempt to formulate theoretical, semi-empirical, or purely empirical relationships to assist in smoothing, extrapolating, extending (or even dispensing with) experimental measurements of effective permeability. This is particularly so since accurate, reliable, reproducible, experimental measurements are lengthy and troublesome, and the more rapid experimental techniques show generally poor reproducibility. The accuracy of approximate correlations may then be little worse than the accuracy of routine measurements.

Pore Models

If a porous medium consisted of bundles of capillary tubes, then successive increments of pressure would result in successively smaller capillary radii being invaded and flushed. The incremental volume invaded at each pressure increment would give the volume of capillary of the corresponding radius $\frac{(2\sigma \cos \theta)}{P_i}$, and the result could be termed a capillary size distribution.

The concept can be applied to porous media, but it should be remembered that the result obtained is a relation between the volume controlled by pore throats of a particular size, and not the volume of pores of a particular size.

Since the pore size distribution : saturation relation is governed by the sizes of pore throats, and these will be the predominant factor in determining the pressure drop in flow through the porous medium, it might be expected that there would be a strong relationship between pore size distribution and permeability. This is, in fact, generally the case, but since permeability in particular depends on continuity of pore space, it is not always possible to get an accurate estimate of permeability from capillary pressure and derived pore size distribution data. Such correlations as do exist, may give reasonable predictions of permeability for poorly to moderately consolidated sands, i.e. systems of relatively homogeneous pore structure, where the effects of cementation and consolidation will not necessarily affect the continuity of pore space.

Highly consolidated dual porosity systems may give very poor correlations of pore structure and permeability, since in this case, it is the continuity of the secondary porosity that controls permeability.

Pore Models for Permeability Prediction

Capillary tube models :

Poiseulles equation for flow through a single capillary is :

$$Q = \frac{\pi r^4 \Delta P}{8\mu L}$$

$$= \frac{V r^2 \Delta P}{8 \mu L^2}$$

where $V = \text{vol. of capillary} = \pi r^2 l$

r is related to capillary pressure through :

$$r = \frac{2 \sigma \cos \theta}{P_c}$$

Q = Flow rate
 L = Length of capillary
 μ = Fluid viscosity
 ΔP = Pressure gradient

Considering the medium to consist of a bundle of tubes of random radii, the total flow is :

$$Q = \frac{(\sigma \cos \theta)^2 \Delta P}{2 \mu L^2} \sum_0^n \frac{V_i}{(P_{ci})^2}$$

and equating this to Darcy's equation :

$$Q = \frac{KA \Delta P}{\mu L}$$

the expression for permeability results :

$$K = \frac{(\sigma \cos \theta)^2}{2 AL} \sum_0^n \frac{V_i}{(P_{ci})^2}$$

$AL = V_B = \text{Bulk volume of the medium}$

Expressing the capillary volume as the incremental change in saturation with capillary pressure, $V_i = S_i \Phi V_B$, and introducing numerical values for the standard mercury capillary pressure data (pressures in psi) :

$$K = 14,260 \phi \int_{S=0}^{S=1} \frac{ds}{(P_c)^2}$$

In order to bring observed results into reasonable agreement with calculated results, a fudge factor must be introduced - the divergence is attributed either to a longer path of travel than the nominal, or to departure of shape from the idealized capillary tube model, and is termed either a tortuosity or lithology factor :

$$K = 14,260 \phi \lambda \int_0^1 \frac{dc}{P_c^2}$$

If the capillary pressure data are replotted as $\left[\frac{1}{P_c}\right]^2$ against saturation, then the area under the curve gives the value of the integral. The value of λ is found to be about 0.2, but with a fairly wide variation between samples. Equivalent methods for this model have been reported by other authors (Burdine, Wyllie).

The idealized pore models previously described, have their greatest application in calculating relative permeabilities.

The drainage case is conceptually the simplest, and several simple idealized flow models lead to acceptable smoothing relations.

The inhibition case is more difficult to model, and gives generally less satisfactory results, but smoothing relations are not unacceptably inaccurate.

Correlations for Wetting Phase Permeabilities

. Drainage case

$$K_{rw} = (S_w^*)^a$$

$$a = 4 \quad \text{(Corey model)}$$

$$a = 10/3$$

$$S_w^* = \frac{S_w - S_c}{1 - S_c}$$

S_c = irreducible wetting phase saturation. An alternative correlation is :

$$K_{rw} = S_w^3 S_w^{* 3/2} \quad \text{(Pirson model)}$$

. Inhibition case

$$K_{rw} = (S_w^*)_{imb}^4$$

$$(S_w^*)_{imb} = (S_w^*)_{drainage} - \frac{1}{2} (S_w^*)_{drainage}^2$$

an alternative correlation is :

$$K_{rw} = S_w^4 \sqrt{S_w^*}$$

Correlations for Non-Wetting Phase Relative Permeability

. Drainage case

$$K_{rw} = (1 - S_w^*)^3 (1 + 2S_w^*)$$

or

$$K_{rnw} = (1 - S_w^*) (1 - S_w^{*\frac{1}{2}} S_w^{\frac{1}{2}})^{\frac{1}{2}}$$

. Inhibition case

$$K_{rnw} = \left[1 - \left(\frac{S_w - S_c}{1 - S_c - S_r} \right) \right]^2$$

S_r = irreducible non-wetting phase saturation.

Statistical Models

The assumption of lithological or tortuosity factors can be avoided by statistical models based on concepts of probability of pore continuity.

Dividing the pore volume (and therefore the pore area of a large plane face) into "n" equal classes, the porous medium is then considered to consist of two such faces joined at random. Assuming that flow takes place only through juxtaposed pore sequences, and that the smaller pore radius controls flow through any sequence, the permeability can be shown to be equivalent to :

$$K = \frac{\phi^{4/3}}{8n^2} \left[R_1^2 + 3R_2^2 + 5R_3^2 + \dots + (2n-1) R_n^2 \right]$$

where ϕ = porosity (fraction)

n = no. of pore classes

$R_1 > R_2 > R_3 > \dots > R_n$

The permeability is in sq. cms., and is converted to the usual units by :

$$\begin{aligned} 1 \text{ sq. cm.} &\approx 10^8 \text{ darcies} \\ &\approx 10^{11} \text{ millidarcies} \end{aligned}$$

Use of Calculated Permeability Data

In general, when cores are available, it is possible to get sufficient core plugs of adequate size for permeabilities to be measured experimentally. Occasionally it may happen that cores are too badly broken and irregular for good samples to be cut, or that cores are not available, but drill cuttings or sidewall samples of reasonable size may be useable to estimate pore size distribution data which may then be used to estimate permeabilities not directly measurable.

RESERVOIR DRIVE MECHANISMS

6

A. Oil Reservoirs

Oil can be recovered from the pore spaces of a reservoir rock, only to the extent that the volume originally occupied by the oil is invaded or occupied in some way. There are several ways in which oil can be displaced and produced from a reservoir, and these may be termed mechanisms or "drives". Where one replacement mechanism is dominant, the reservoir may be said to be operating under a particular "drive".

Possible sources of replacement for produced fluids are :

- Expansion of undersaturated oil above the bubble point
- Expansion of rock and of connate water
- Expansion of gas released from solution in the oil below the bubble point
- Invasion of the original oil bearing reservoir by the expansion of the gas from a free gas cap
- Invasion of the original oil bearing reservoir by the expansion of the water from an adjacent or underlying aquifer.

Since all replacement processes are related to expansion mechanism, a reduction in pressure in the original oil zone is essential. The pressure drops may be small if gas caps and aquifers are large and permeable, and, under favourable circumstances, pressures may stabilize at constant or declining reservoir offtake rates.

The compressibilities of undersaturated oil, rock and connate water are so small that pressures in undersaturated oil reservoirs will rapidly fall to the bubble point if there is no aquifer to provide water drive. So these expansion mechanisms are not usually considered separately, and the three principal categories of reservoir are :

Solution gas drive (or depletion drive) reservoirs

Gas cap expansion drive reservoirs

Water drive reservoirs

Frequently two or all three mechanisms (together with rock and connate water expansion) occur simultaneously.

B. Solution Gas Drive Reservoirs

If a reservoir at its bubble point is put on production, the pressure will fall below the bubble point pressure and gas will come out of solution. Initially this gas may be a disperse, discontinuous phase, but, in any case, gas will be essentially immobile until some minimum saturation - the equilibrium, or critical gas saturation, is attained.

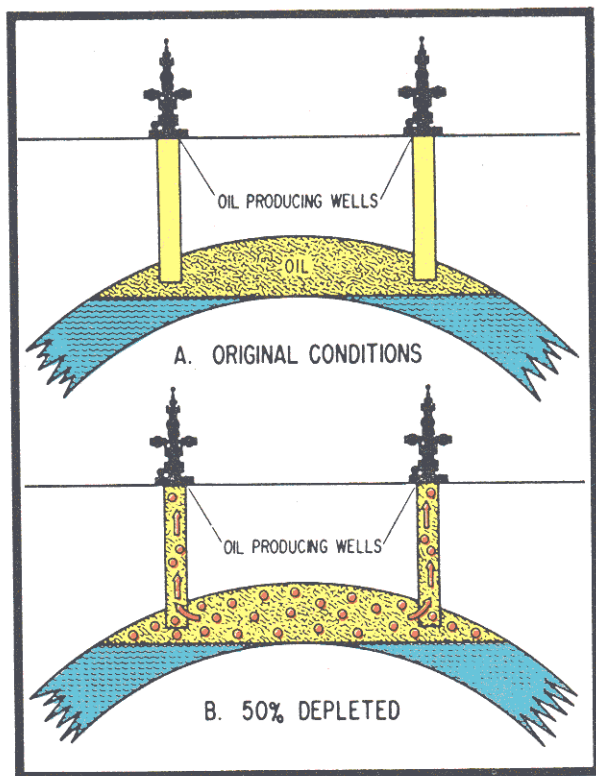


Fig. 6-1. Dissolved gas drive reservoir

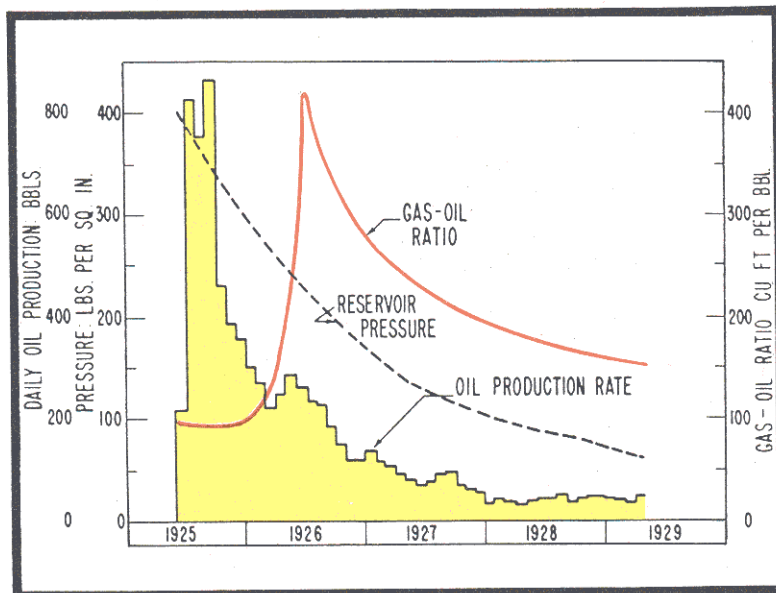


Fig. 6-2. Production data dissolved gas drive reservoir.
(Courtesy API, Drilling and Production Practices-1943).

The actual order of values for critical saturation are in some doubt, but there is considerable evidence to support the view that values may be very low - in the order of 1% to 2% of the pore volume. Once the critical gas saturation has been established gas will be mobile, and will flow under whatever potential gradients may be established in the reservoir - towards producing wells if the pressure gradient is dominant - segregating vertically if the gravitational gradient is dominant. Segregation will be affected by vertical permeability variations in layers, but is known to occur even under apparently unfavourable conditions.

Initially the gas-oil ratio of a well producing from a closed reservoir will equal solution GOR. At early times, as pressure declines and gas comes out of solution, but cannot flow to producing wells, the producing GOR will decline. When the critical gas saturation is established and if the potential gradients permit, gas will flow towards producing wells.

The permeability to oil will be lower than at initial conditions, and there will be a finite permeability to gas so that the producing gas oil ratio will rise. As more gas comes out of solution, and gas saturations increase, permeability to gas increases, permeability to oil diminishes and this trend accelerates.

Ultimately, as reservoir pressure declines towards abandonment pressure, the change in gas formation volume factor offsets the increasing gas to oil mobility ratio and the gas oil ratio trend is reversed; i.e. although the reservoir GOR may continue to increase, in terms of standard volumes, the ratio standard cubic ft/stock tank barrel may decline.

In addition to the effect of gas on saturation of, and permeability to, oil, the loss of gas from solution also increases the viscosity of the oil and decrease the formation volume factor of the oil.

C. Gas Cap Expansion Drive Reservoirs

The general behaviour of gas drive reservoirs is similar to that of solution gas drive reservoirs, except that the presence of free gas retards the decline in pressure. By definition the oil must be saturated at the gas oil contact, so that decline in pressure will cause the release of gas from solution, but the rate of release of gas from solution, and the build up of gas saturation and of gas permeability, will be retarded. At higher prevailing pressures, oil viscosities are lower, and provided that the free gas phase can be controlled, and not produced directly from producing wells, better well productivities and lower producing gas oil ratios can be maintained.

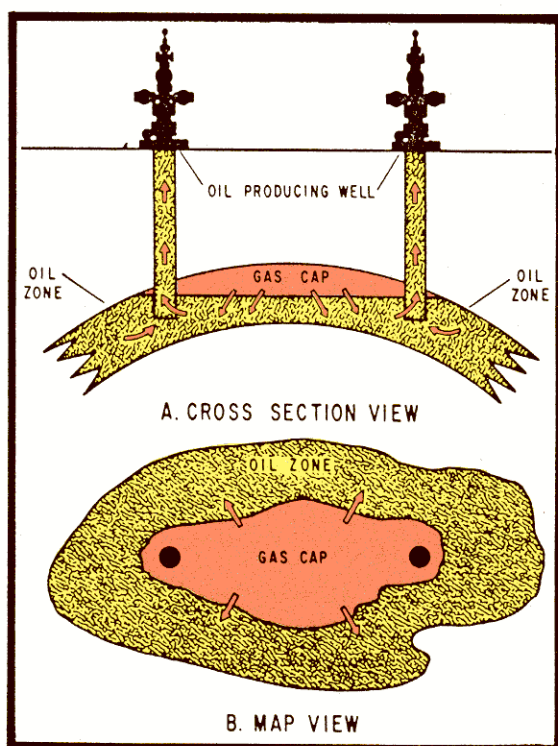


Fig. 6-3. Gas cap drive reservoir.

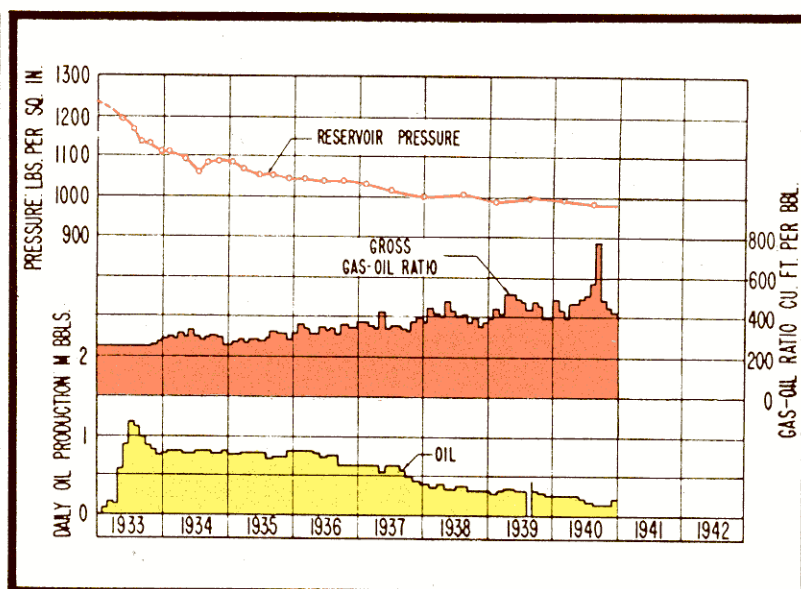


Fig. 6-4. Production data-gas cap drive reservoir.
(Courtesy API, Drilling and Production Practices - 1943)

Under residual conditions the stock tank oil left in place is S_o/B_o and the smaller this factor the greater will be the oil recovery.

Consequently the higher the pressure at abandonment, the greater the value of B_o , and the smaller this term becomes. In addition abandonment of wells and reservoirs depends primarily upon an "economic limit" - the rate of production required to pay for operating costs, and direct overheads - and an oil flow rate, which depends upon K_o/μ_o , which will be greater at any given saturation (and so given K_o) under pressure maintenance conditions due to the lower oil viscosity than under depletion conditions.

D. Water Drive Reservoirs

If a reservoir is underlain by, or is continuous with a large body of water saturated rock (an aquifer) then reduction in pressure in the oil zone, will cause a reduction in pressure in the aquifer. Although the compressibility of water is small ($\pm 3 \times 10^{-6} \text{ psi}^{-1}$) the total compressibility of an aquifer includes the rock pore compressibility ($\pm 5 \times 10^{-6} \text{ psi}^{-1}$) making the total compressibility in the order of $8 \times 10^{-6} \text{ psi}^{-1}$. The apparent compressibility of an aquifer can be substantially greater if some accumulation of hydrocarbons exist in small structural traps throughout the aquifer.

An efficient water driven reservoir requires a large aquifer body with a high degree of transmissivity allowing large volumes of water to move across the oil-water contact in response to small pressure drops.

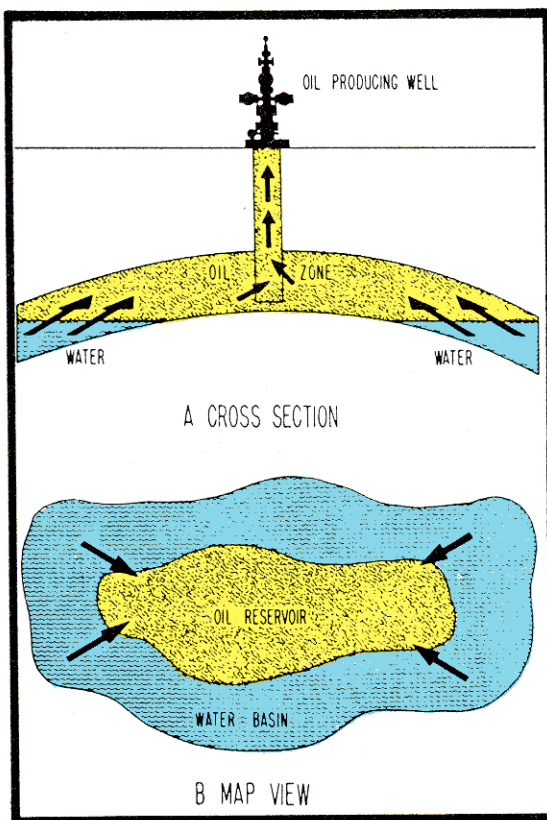


Fig. 6-5. Water drive reservoir.

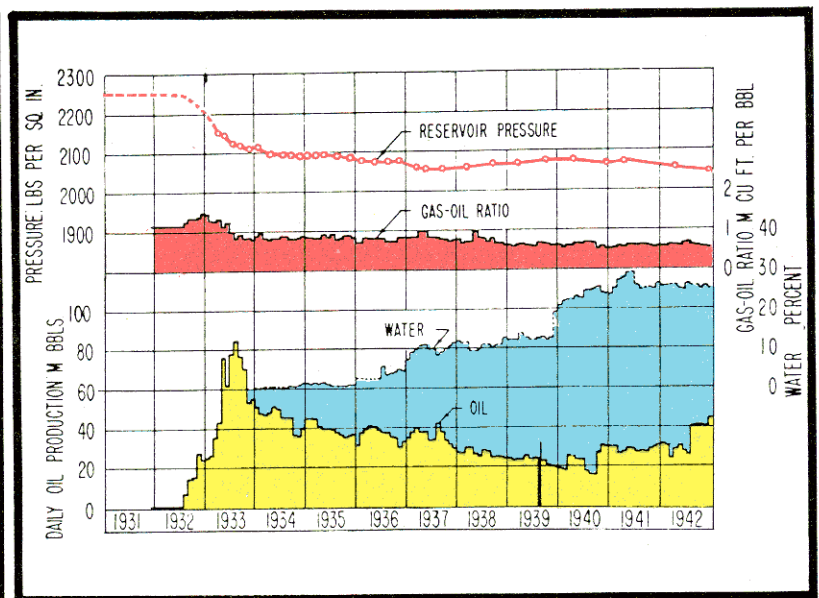


Fig. 6-6. Production data-water drive reservoir. (Courtesy API, Drilling and Production Practices - 1943).

This replacement mechanism has two particular characteristics - first there must be pressure drops in order to have expansion, and secondly, the aquifer response may lag substantially, particularly if transmissivity deteriorates in the aquifer.

A water drive reservoir is then particularly rate sensitive, and so the reservoir may behave almost as a depletion reservoir for a long period if offtake rates are very high, or as an almost complete pressure maintained water drive reservoir if offtake rates are low, for the given aquifer.

Because of the similarity in oil and water viscosities (for light oils at normal depths) the displacement of oil by water is reasonably efficient, and provided that localized channelling, fingering or coning of water does not occur, water drive generally represents the most efficient of the natural producing mechanisms for oil reservoirs.

As with gas cap drive reservoirs, the maintained pressures lead to lower viscosities and higher B_o values at any given saturation, reducing the saturation and minimizing the term S_o/B_o hence the stock tank oil left at any given economic limit.

While reservoir drive mechanisms may be classified into the three categories we have discussed, most often two or more of these mechanisms act simultaneously in a combination drive.

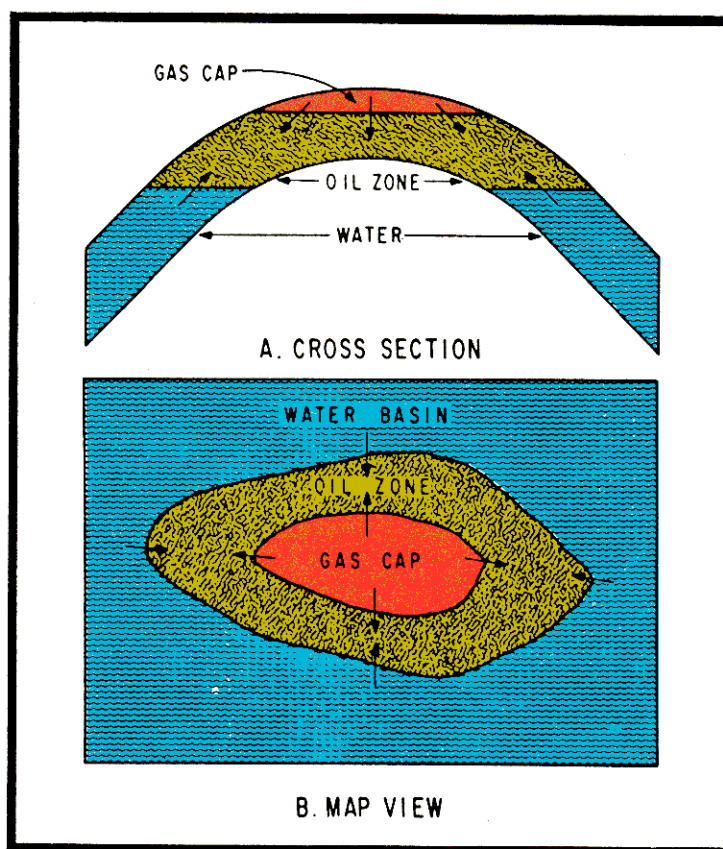


Fig. 6-7. Combination drive reservoir.

E. Discussion of recovery efficiency (including gravity segregation)

One mechanism, only briefly referred to, but which has an important role in several aspects of reservoir behaviour is that of gravity segregation the movement of phases countercurrent to each other, (generally of gas and oil) under the influence of the gravitational potential $g\Delta p$.

Considering the solution gas drive reservoir, the behaviour described earlier assumes essentially that gas saturations build up uniformly throughout the oil zone without any saturation gradients in the vertical direction. (Saturation gradients existing as a result of horizontal pressure gradients, i.e. the pressure drops near the well bore).

Under these conditions the expected recovery efficiency will depend on the economic limit for wells and could be as low as 2% - 3% for low permeability reservoirs with high viscosity, low gas oil ratio oils, and up to about 15% or so for high permeability reservoirs, normal GOR low viscosity oils, but will rarely exceed this range.

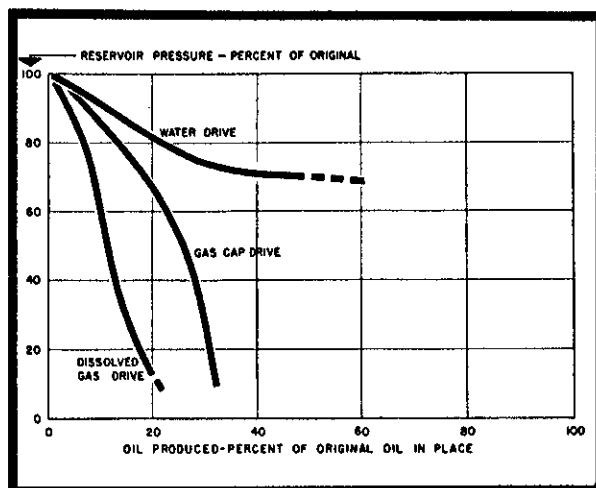


Fig. 6-8. Reservoir pressure trends for reservoirs under various drives. (Courtesy API, Drilling and Production Practices-1943).

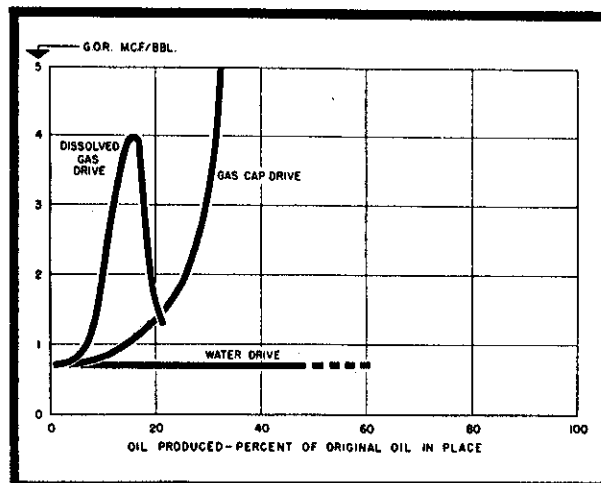


Fig. 6-9. Reservoir gas-oil ratio trends for reservoirs under various drives. (Courtesy API, Drilling and Production Practices - 1943).

If the vertical permeability to gas is non-zero however, there will be a vertical component of gas flow, under the gravitational potential, and gas will "segregate" in the reservoir, migrating to structurally high positions, with oil counterflowing downwards. This mechanism has two effects. Firstly the oil saturation in the lower parts of the reservoir is maintained at a value higher than the average oil saturation - so that permeability to oil is higher, and permeability to gas lower than for the "pure" solution gas drive case. The producing gas oil ratio is then lower than for solution gas drive alone.

Secondly, the lower producing gas oil ratio involves smaller gross fluid withdrawals than would otherwise be the case, so that the pressure decline at any given oil cumulative production will be smaller.

The segregated gas may form a secondary gas cap, and the later life of a reservoir may then be similar to that of a primary gas cap drive reservoir.

Under these conditions the recovery efficiency will be higher if the economic limit is low - possibly very much higher and may approach or even exceed the range 20% to 40% of oil in place.

Gravity drainage plays its greatest role in dual porosity systems with great contrast where almost complete segregation can take place in the secondary porosity system, and the producing wells produce throughout at solution gas-oil ratio. Gravity drainage is then the predominant mechanisms in draining oil to residual saturation in the secondary gas cap.

The recovery efficiency of water drive reservoirs will be governed by an economic limit, the limit in this case being dictated by water handling problems. Provided that water can be controlled reasonably, efficiencies of 30% to 40% would be expected and sometimes under extremely favourable conditions recovery efficiencies up to 50% might be achieved. (Ultimately, of course, calculating a recovery efficiency depends on knowing the initial oil in place, and an apparently high recovery factor might simply be the result of under-estimating oil in place).

WELL PERFORMANCE

7

Flow through non fractured formations is approximately radial, at least for a few hundred feet surrounding the well, therefore an idealized cylindrical model may be used to calculate flow rates and describe pressure distribution with good accuracy.

A. Nomenclature and model for ideal cylindrical flow

- Cylindrical reservoir with the well at its center
- Constant pressure source P_e , at the boundary
- Isotropic system - homogenous porous medium
- Well producing in open hole completion (no casing)
- Well producing from total bed thickness, h .

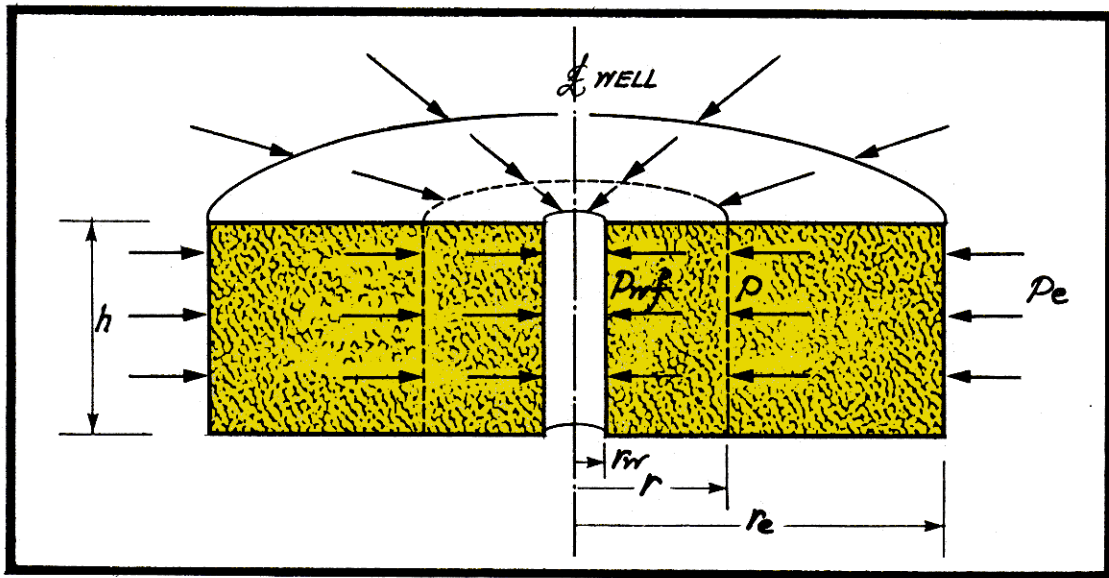


Fig. 7-1. Nomenclature for ideal cylindrical flow.

The cross section perpendicular to flow at r is $2\pi rh$, and the velocity at this section is

$$v = \frac{Q}{2\pi rh} \quad \text{flow rate} \quad (1)$$

From Darcy's definition of pressure loss

$$v = \frac{k}{\mu} \frac{dP}{dr} \quad (2)$$

combining (1) and (2)

$$dP = \frac{Q}{2\pi kh} \frac{dr}{r} \quad (3)$$

or integrating (3)

$$P = \frac{Q\mu}{2\pi kh} \ln r$$

if integrated

from $r = r_e$ at $r = r_w$

where $P = P_e$ and $P = P_w$

the result will be the rate equation

$$P \Big|_{P_w}^{P_e} = \frac{Q\mu}{2\pi kh} \ln r \Big|_{r_w}^{r_e}$$

if integrated

from $r = r_e$ at $r = r$

where $P = P_e$ and $P = P$

the result will be the pressure distribution

$$P \Big|_P^{P_e} = \frac{Q\mu}{2\pi kh} \ln r \Big|_r^{r_e}$$

$$Q_e - Q_w = \frac{2\pi kh (P_e - P_w)}{\mu \ln r_e/r_w}$$

$$P_e - P = \frac{Q\mu}{2\pi kh} \ln r_e/r \quad (4)$$

introducing (4) in (5)

$$Q = \frac{2\pi kh (P_e - P_w)}{\mu \ln r_e/r_w} \quad (5)$$

$$P = P_e - \frac{P_e - P_w}{\ln r_e/r_w} \ln r_e/r \quad (6)$$

RATE EQUATION *

PRESSURE DISTRIBUTION

The distribution of pressure vs. distance from the bore hole in the formation is shown in figure 7-2. Note that most of the pressure loss occurs within a few tens of feet from the well, and that pressure distribution is independent of layer permeability.

At very high flow rates, flow near the well becomes turbulent and pressure gradients become higher than predicted by Darcy's equation (6) which is valid only for laminar flow of slightly compressible (liquid) flow.

* Rate equation in practical oil field units :

$$Q = \frac{7.08 kh (P_e - P_w)}{\ln (r_e/r_w)}$$

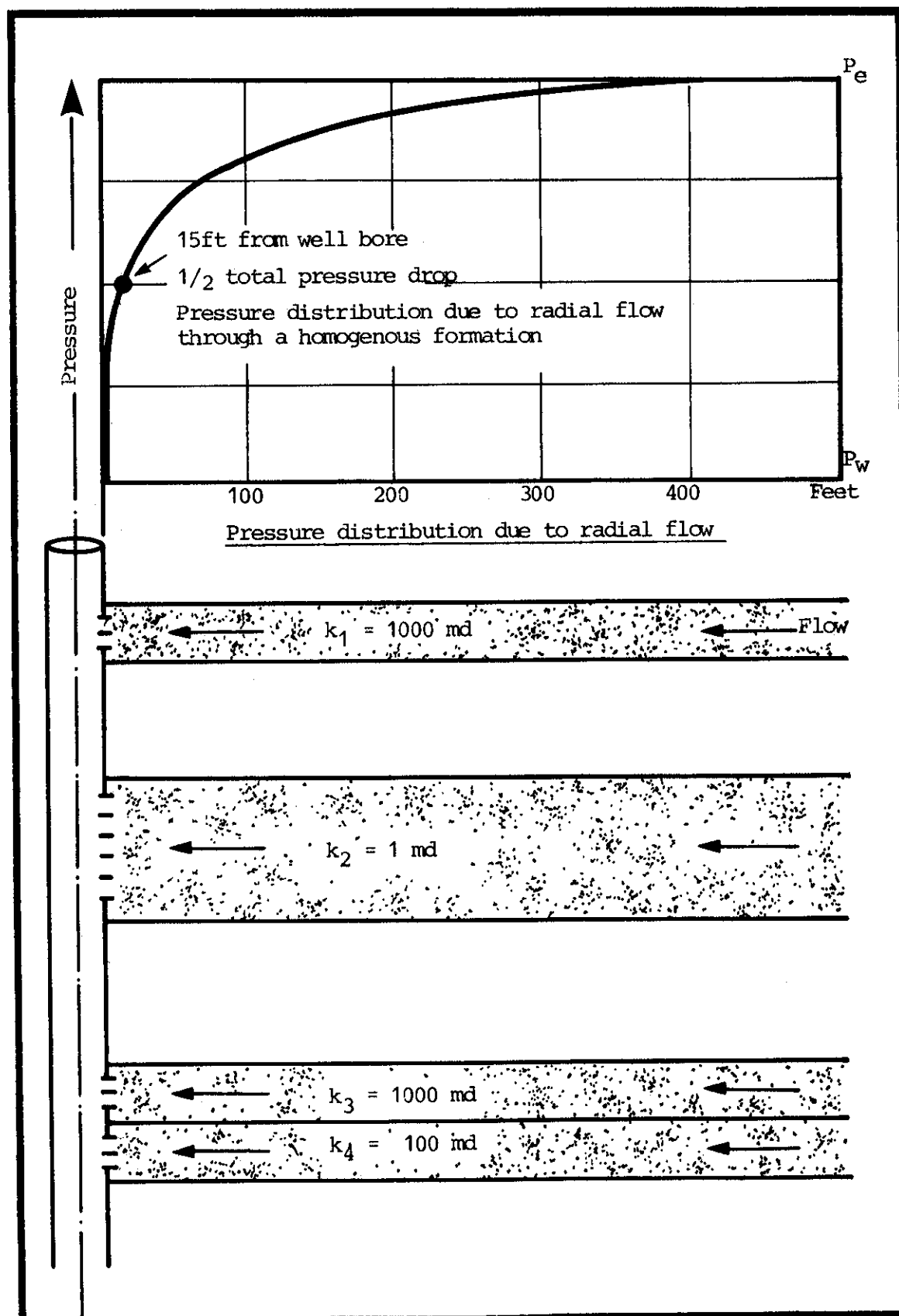


Fig. 7-2. Pressure distribution is identical for different permeability zones.

B. Radius of drainage

In the ideal case where wells produce at equal rates from a rectangular grid, drainage boundaries are symmetrical. Practically, flow close to the well is radial but due to formation heterogeneities and the influence of neighboring wells this radial pattern becomes distorted. The distortion of r_e has no real physical significance, since it enters only as a logarithmic expression either in the rate or in the pressure distribution.

Note in figure 7-4 how the drainage boundary becomes shewed where well 2 is producing at twice the rate of well 1.

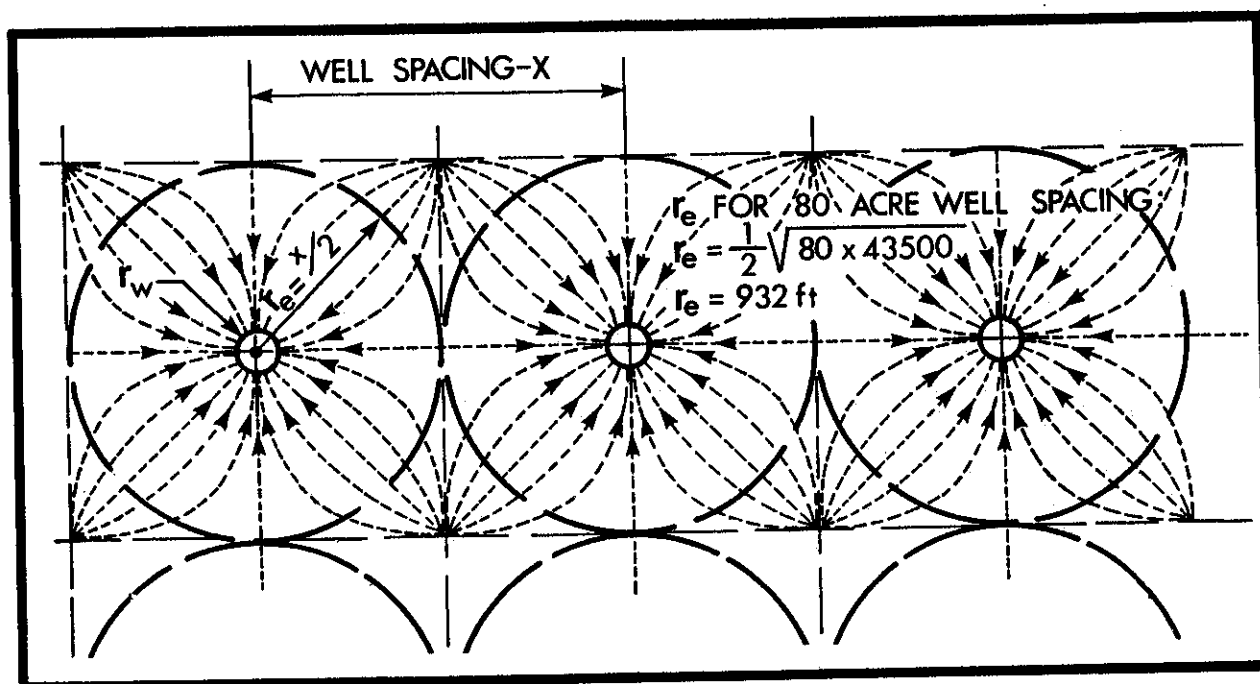


Fig. 7-3. Radius of drainage and boundaries in a rectangular reservoir.

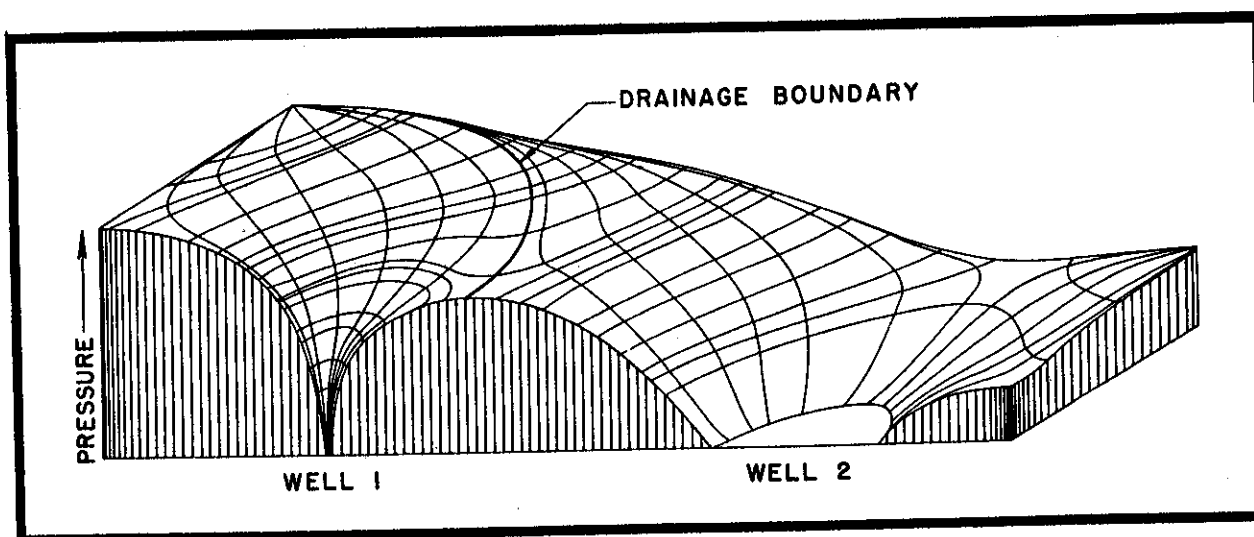


Fig. 7-4. Pressure distribution and drainage boundaries for wells producing at different rates.

For the purpose of making calculations with the Darcy radial flow* the radius of drainage can be taken as a number between 800 and 1000 ft. or 1/2 the well spacing. Note from the following example that the influence of r_e becomes negligible once that r_e is a few hundred times r_w , the well bore diameter :

$$\ln (r_e/r_w) = 7.901 \text{ where } r_w \text{ is 4" and } r_e = 900 \text{ ft.}$$

$$\ln (r/r_w) = 8.006 \text{ where } r_w \text{ is 4" and } r_e = 1000 \text{ ft.}$$

* The radius of drainage will be defined differently for the purpose of well transient testing in a later chapter.

C. Well pressure drawdown

For fluid to flow into the well, some difference in pressure must exist between the fluid in the reservoir and the well bore. This is called the drawdown pressure.

$$\text{Drawdown} = P_s - P_{wf}$$

D. Productivity index

Productivity index, J , is the ratio between production rate and total pressure drawdown.

The well productivity index is expressed as stock tank barrels of liquid per day per psi of drawdown pressure.

$$J = \frac{q}{P_s - P_{wf}} \text{ STB/D/psi} \quad (2)$$

Specific productivity index

The specific productivity index, J_s , is the liquid production rate (stock tank barrels) per day per psi of drawdown pressure per foot of net pay thickness.

$$J_s = \frac{q}{h(P_s - P_{wf})} \text{ STB/D/psi/ft.} \quad (3)$$

Where the formation and fluid parameters are known a formation productivity index might be calculated using the Darcy equation (1) rearranged in the form :

$$J = \frac{q}{P_s - P_{wf}} = \frac{7.08 kh}{\ln (r_e/r_w)} \text{ STB/D/psi} \quad (4)$$

This calculated productivity index corresponds to the undamaged formation with no casing and the pressure distribution would be as shown in fig. 7-5 on the left.

In reality, the formation might be highly damaged as shown on the right. A productivity index measured on this well would have a much lower value.

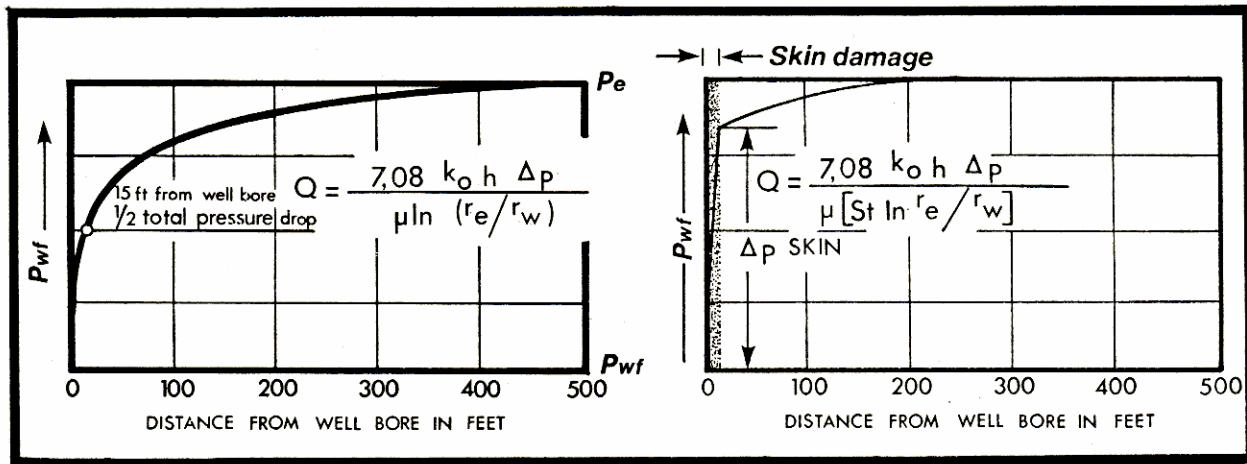


Fig. 7-5. Pressure distribution with and without formation damage.

E. Formation damage

A high pressure loss in the immediate vicinity of the formation face may be due to "well bore damage" caused by drilling processes. This damaged zone is commonly referred to as "skin" and the pressure loss as Δp_{skin} .

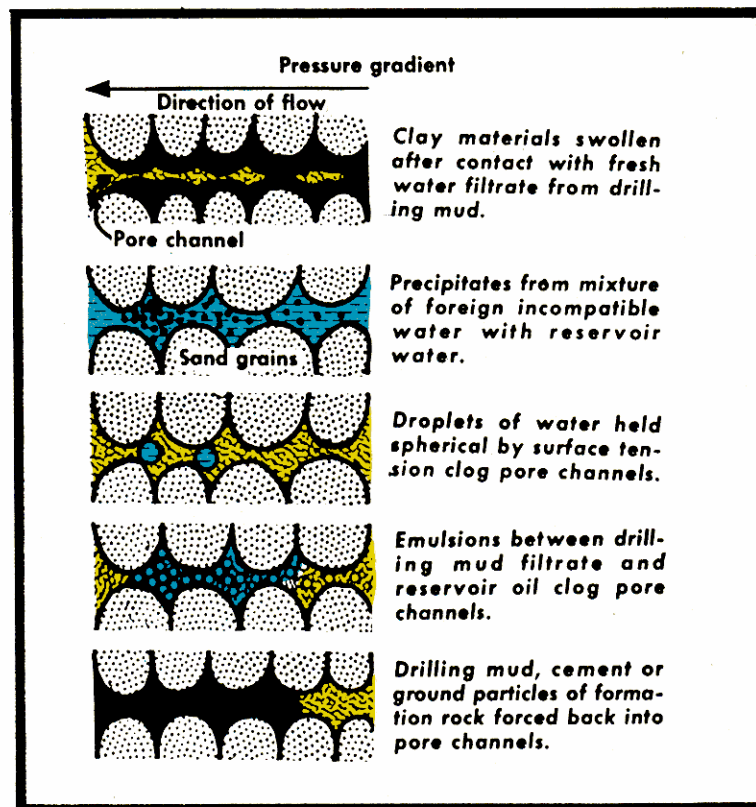


Fig. 7-6. Conditions causing formation damage.

Variations in permeability along the line of flow affects the pressure repartition. The result of skin damage is a redistribution of the pressure between P_e and P_{wf} as shown in figure 7-7 and a lower production rate.

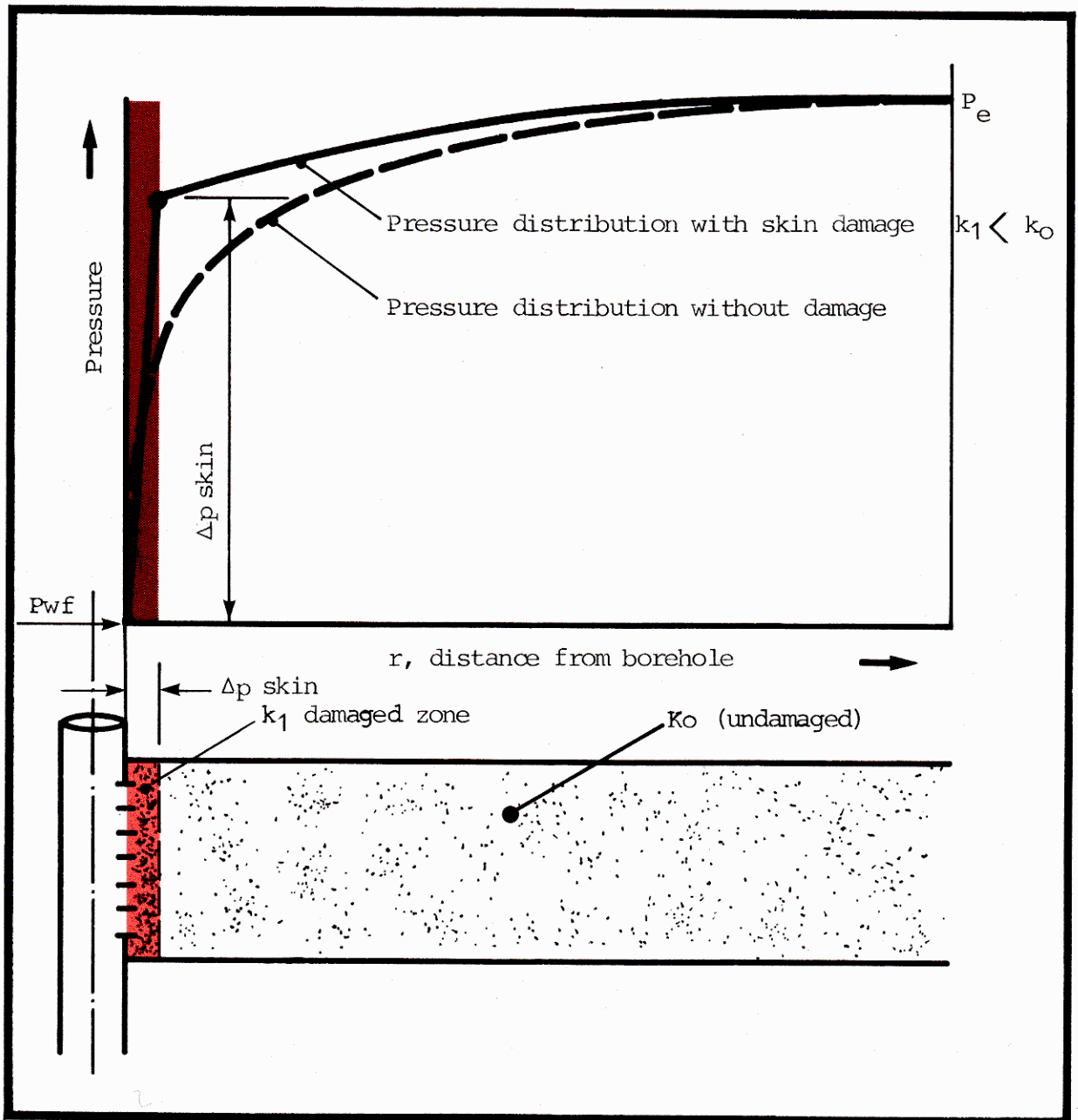


Fig. 7-7. Pressure distribution in a damaged formation.

F. Formation improvement

When the formation around the well has been altered by chemical treatment or hydraulically fractured, a low pressure gradient extends through the improved zone. This better pressure distribution between P_e and P_{wf} will result in an increase in the rate Q .

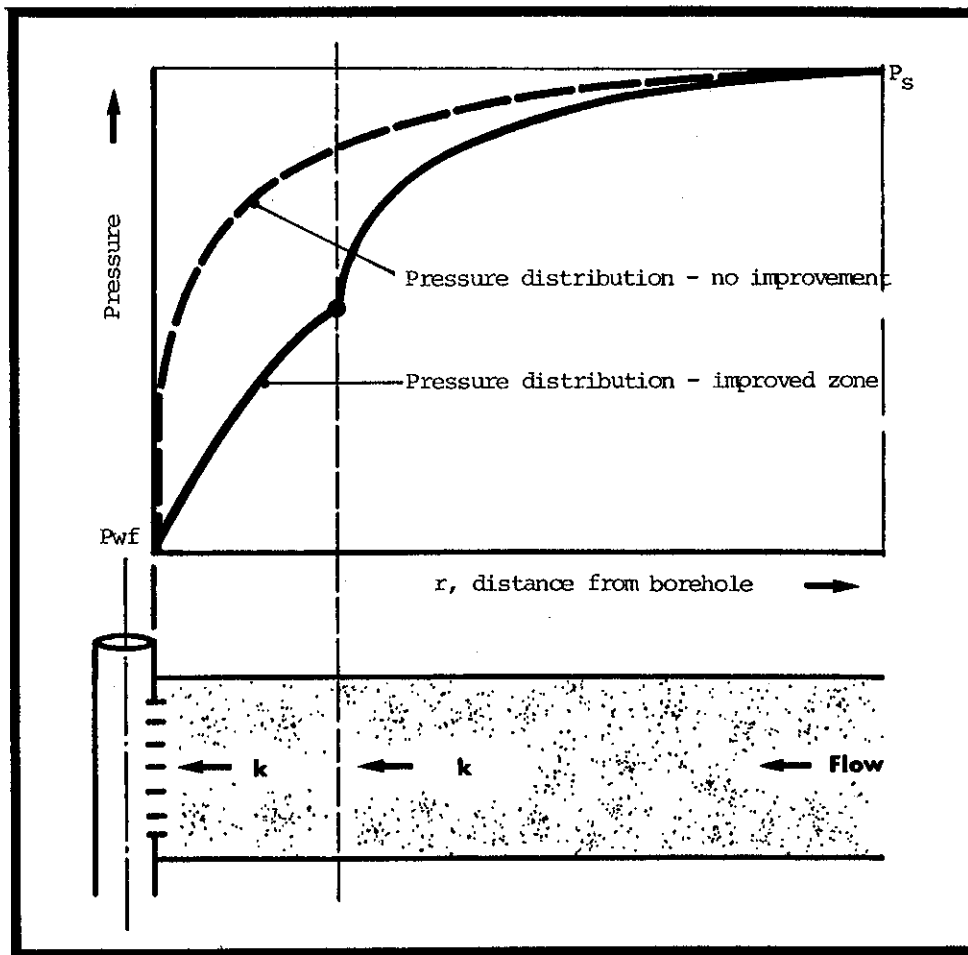


Fig. 7-8. Pressure distribution through an improved formation.

G. Skin factor

In the flow equation, the degree of damage or improvement is expressed in terms of a "skin factor", S , which is positive for a damaged formation and negative for an improved one.

S can vary from about -5 for a formation highly improved by hydraulic fracturing to $+$ for a well too damaged to produce.

The skin factor S , is entered in the denominator of the flow equation :

$$Q = \frac{7.08 kh (P_e - P_w)}{s + \ln r_e/r_w}$$

The pressure drop across the skin is given by :

$$\Delta P_{\text{skin}} = \frac{14.2 QB}{kh} s$$

H. Skin damage in perforated completions

The gun perforated casing completions, the lines of flow are distorted from a simple radial pattern as they approach the well bore and converge into the perforations.

Distortion from a radial flow pattern may be thought of as a "geometrical skin" and can be positive or negative depending on the efficiency of the perforating job. (see chapter 7 - appendix for practical application and charts).

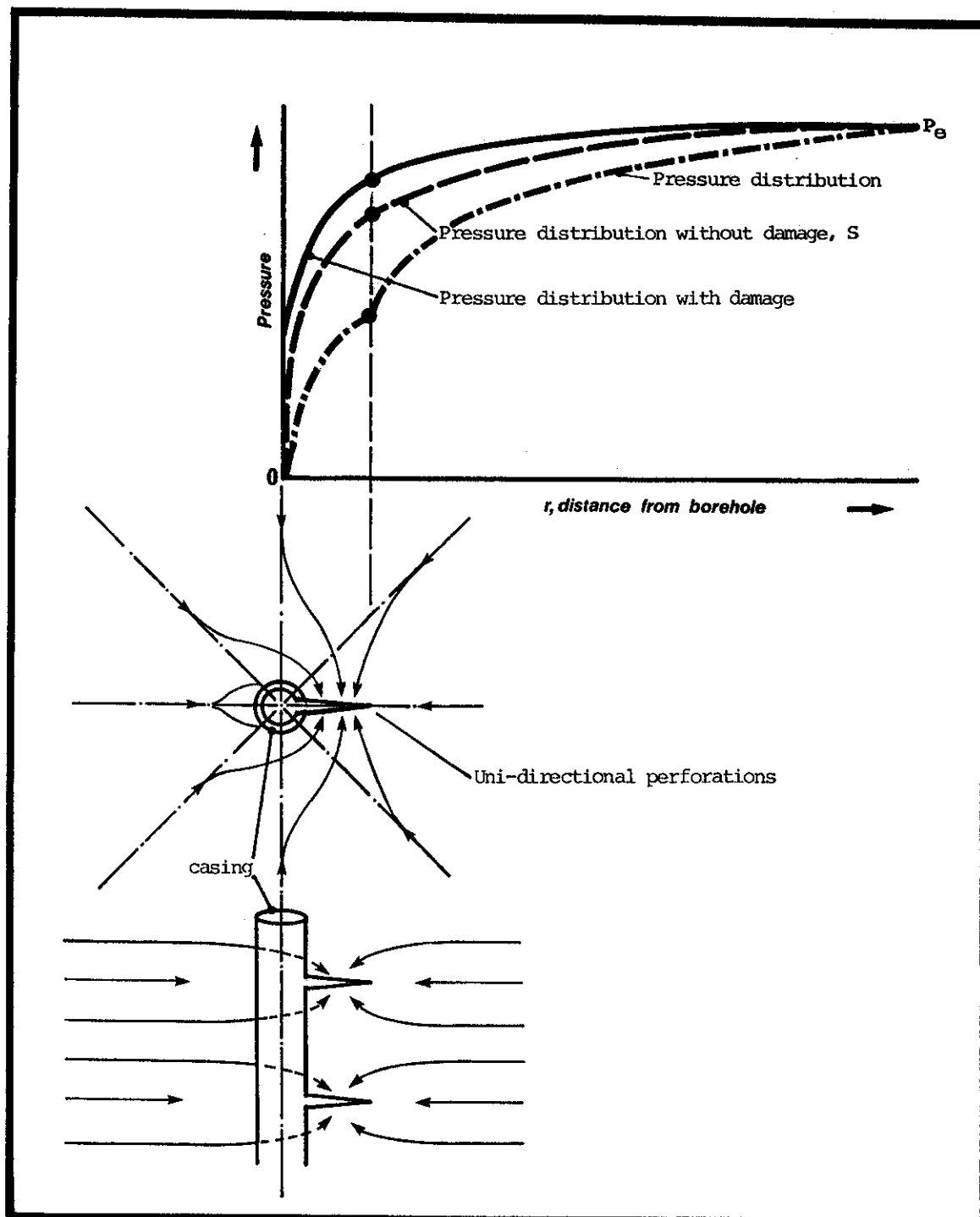


Fig. 7-9. Pressure distribution showing "perforating skin" damage - uni-directional perforations.

I. Inflow production relation - IPR

The inflow production relation shows the relation between well production rate q , and bottom hole pressure over the entire range of P_{wf} from zero to P_s . It is determined by producing the well at several different rates (including zero) and measuring the corresponding bottom hole pressures.

The slope $\frac{\Delta q}{\Delta p}$ of the IPR curve is the productivity index.

A straight line extrapolation of measured data points to intercept with the abscissa at $P_{wf} = 0$ gives the zone open flow potential. This is the flow rate that could be obtained if 1 atm is applied to the formation face.

If one were to plot the IPR curve using data points below the reservoir fluid bubble point, a departure from a straight line would be noted. The Darcy flow relation is linear only for non-compressible (liquid) flow.

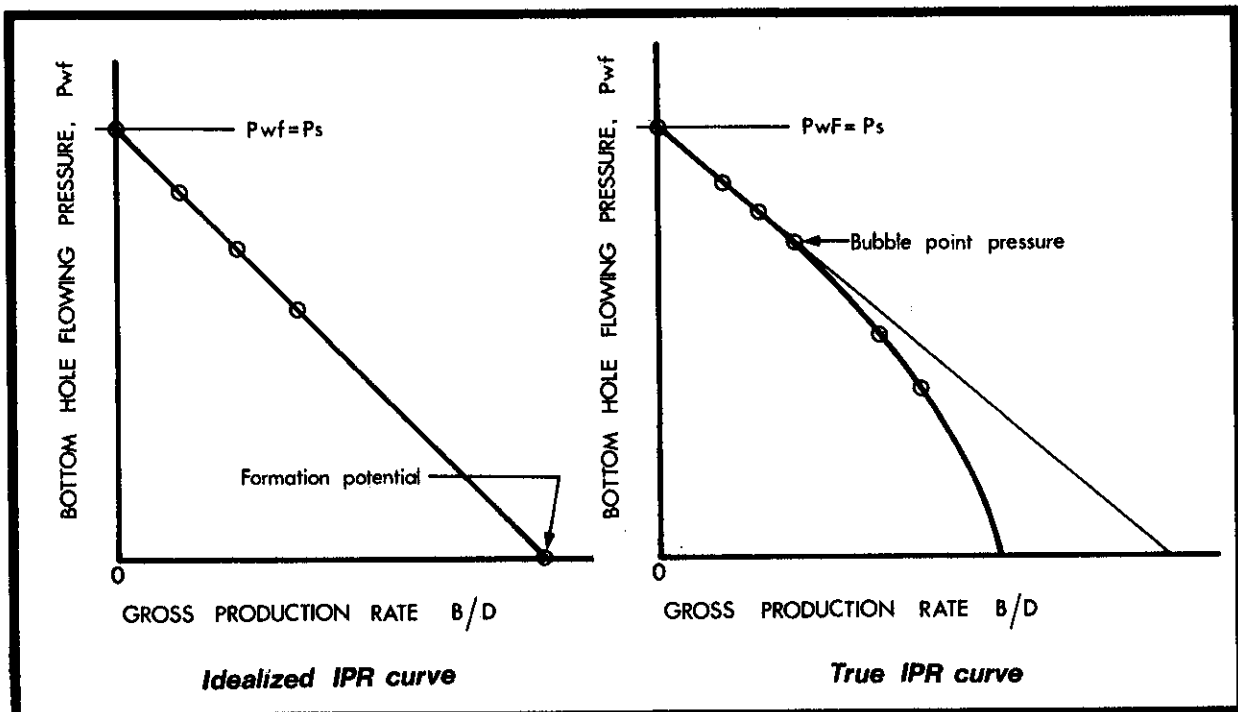


Fig. 7-10. Idealized and true IPR curves.

J. Evaluation of a formation treatment with IPR

A comparison of the IPR curve before and after a formation treatment is a measure of effectiveness of the treatment.

The figure on the left shows an increase from 500 to 700 B/D at the same bottom hole pressure. Formation improvement is indicated by a decrease in slope after treatment.

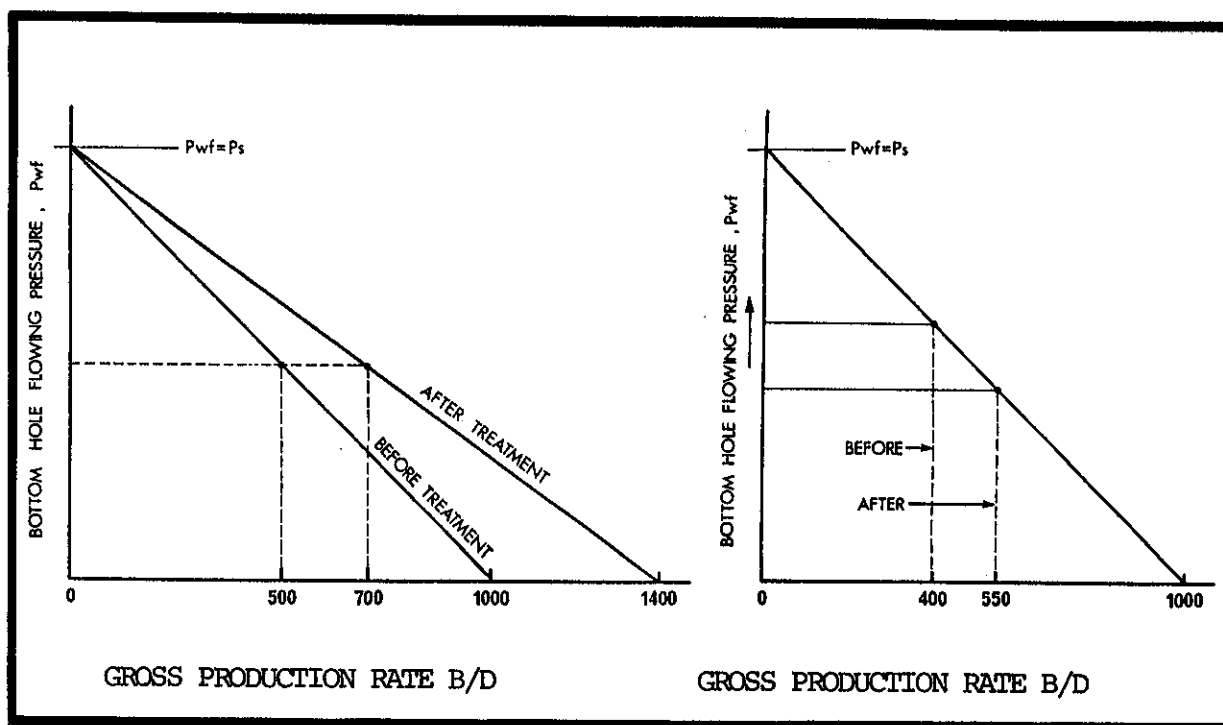


Fig. 7-10. Idealized and true IPR curves.

The figure at the right illustrates a case in which the production rate increase from 400 to 550 B/D is not due to formation improvement but possibly to some change in the flow string installation (better pump, optimum tubing etc.) which resulted in a lower bottom hole pressure.

K. Composite IPR of multi-zone completion

When an IPR curve is measured in the traditional manner by gauging total production rates into the surface tank while measuring the corresponding bottom hole pressures in a stratified reservoir where differences in permeability and/or formation pressure exist, a composite IPR is obtained.

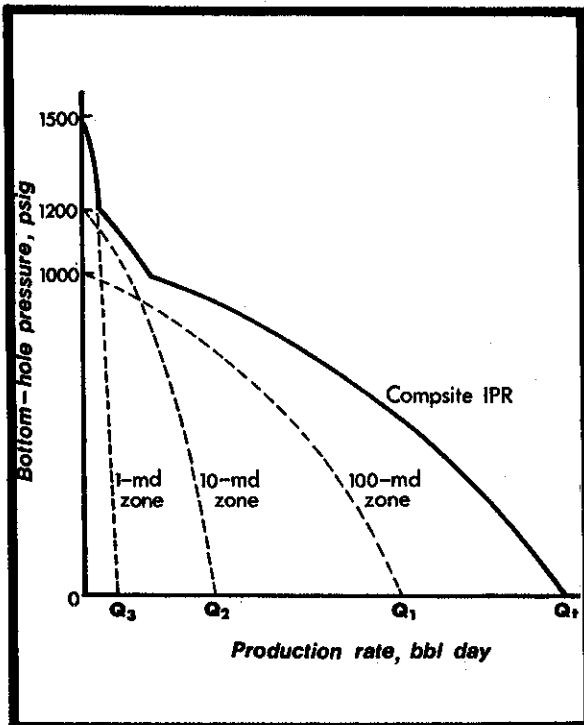


Fig. 7-12. Composite IPR for a stratified formation.

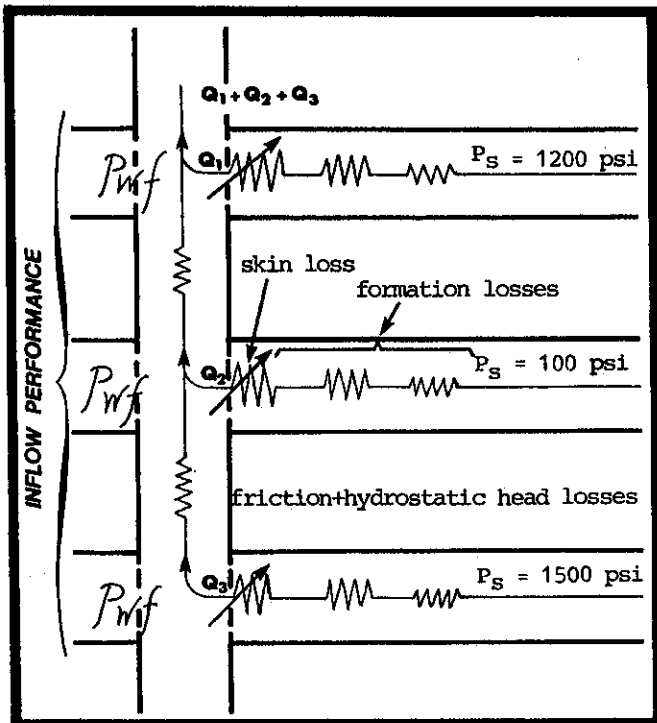


Fig. 7-13. Electrical analogy of composite inflow performance.

It can be seen that when the bottom hole pressure is slowly lowered, the highest pressure zone will begin to produce first. As the pressure is further reduced the remaining zones come into production. The production rate for each zone always depends on the product of the drawdown and the productivity index.

Individual zone flowing pressures are linked by the bore-hole and are affected by the hydrostatic and friction heads between the producing layers.

Individual zone flow rates and productivity indexes can be measured using flowmeter and pressure gauge passing over the intervals while producing at different surface rates.

L. Cross flow between zones

When a well is shut in at the surface or by plugging above the producing zones, an interflow will take place between the higher pressure and lower pressure zones.

The interflow between two zones of different pressures may be calculated graphically by plotting both IPR on the same grid after correcting for differences in hydrostatic pressure due to elevation.

As fluid produced from the higher pressure zone must equal the fluid injected into the lower pressure zone, the bottom hole flowing pressure will stabilize at level shown, found by extrapolating the low pressure curve to the left of the ordinate axis and finding the pressure at which the production from A equals the injection into B.

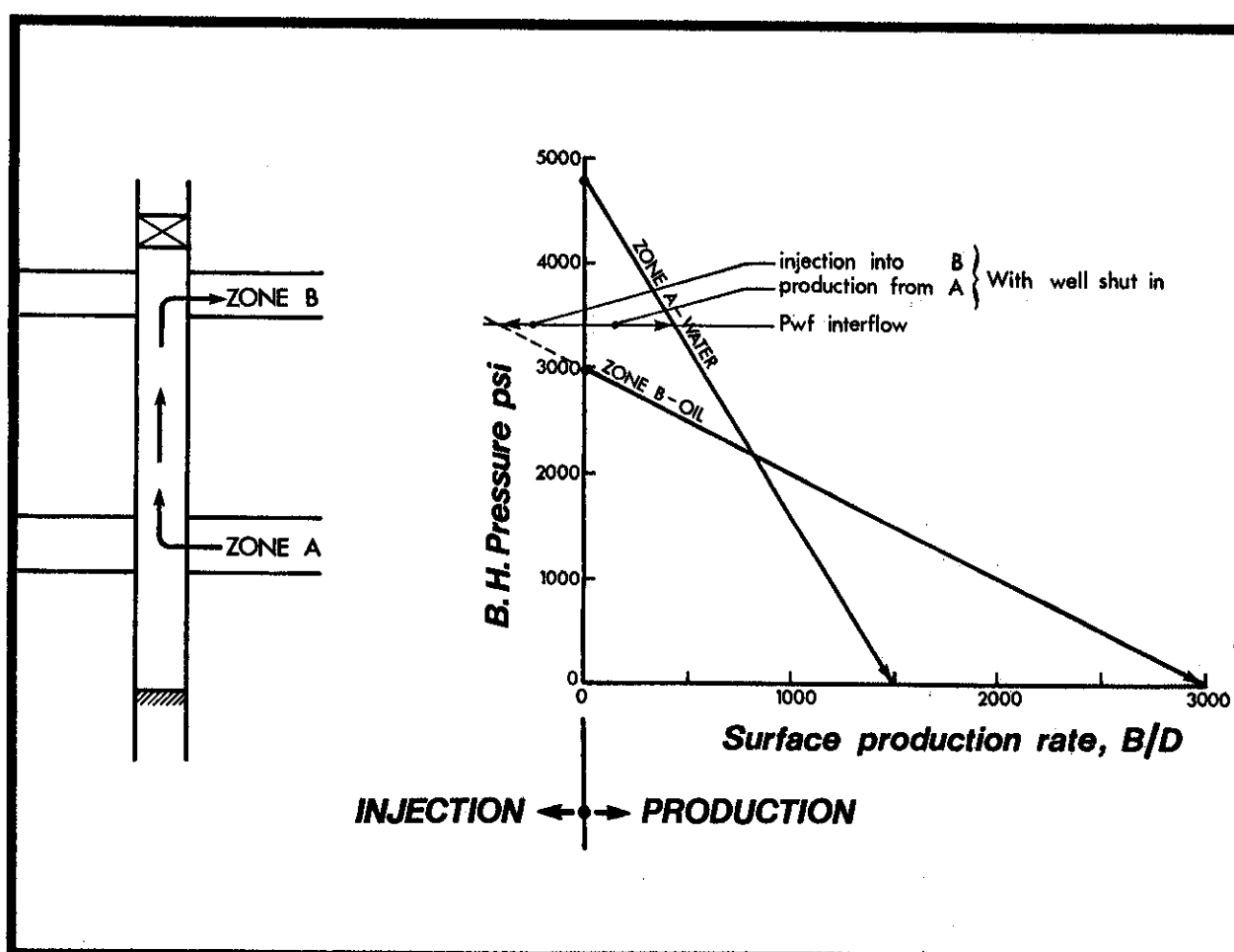


Fig. 7-14. Cross flow between zones - well shut in.

M. Water cut vs. production rate

If zone A is a high pressure water zone and B a lower pressure oil zone, curves of water cut vs. gross production rate or water cut vs. P_{wf} may be delivered from the IPR curves by calculating the flow from A and B at various bottom hole pressures. This water cut vs. P_{wf} is shown on the right.

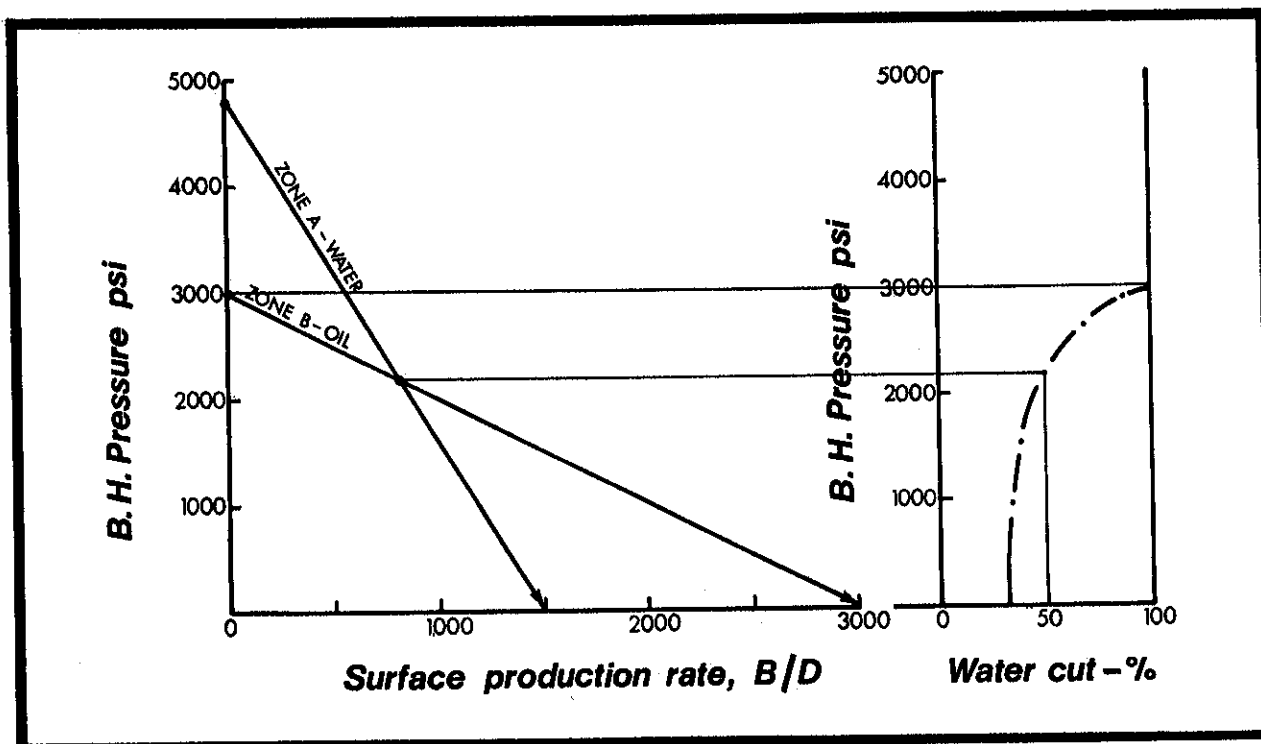


Fig. 7-15. IPR and water cut curves.

N. Performance of flowing oil wells

With the formation IPR, water cut, GOR behavior and fluid PVT properties established, the question arises whether or not the pressure drop along the length of the tubing string will permit flow to the surface and if so, at what rate will the well produce.

The pressure drop along the tubing string is the sum of the hydrostatic and friction head losses produced by the flow components - of these two the static head is the dominant term.

Gas evolving from solution with the oil on reduction of pressure in the tubing string plays an important role in lowering the average density of the column.

The two (and often three) phase mixtures found in the production tubing are characterized by several different flow regimes. The boundaries of these regimes are somewhat arbitrary and subjective but have recognisable patterns.

Bubble Flow : In this case bubbles of gas slip through the oil the gas phase is discontinuous, the liquid phase is continuous. Friction losses are small, but overall energy losses may be large with the gas doing little useful work on the oil while expanding.

Froth Flow/Slug Flow : At high velocities, or at higher gas oil ratios, gas bubbles are dispersed across the pipe cross section interfering to a degree where differential velocity between phases is minimal. Total energy losses are at a minimum. Froth flow is very unstable with liquid films being continuously broken and reformed, and it is possible to define a regime of slug flow where alternate slugs of liquid, with some dispersed gas, and gas with some dispersed liquid traverse the flow string.

Annular - Mist Flow : At lower pressures, high gas oil ratios and high gas velocities, the gas phase will become the continuous phase, with liquid distributed as an annular film, and as droplets in a mist. It is possible to have gas velocities so high that the annular film cannot exist, and the liquid phase is completely atomized. This subject is covered more rigorously in our Production Logging documentation.

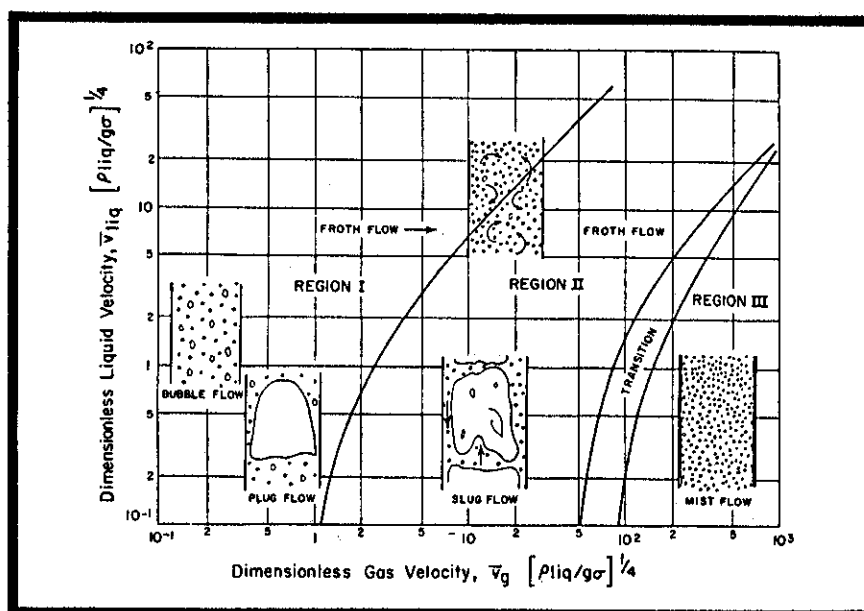


Fig. 7-16. Fluid configurations in various flow regimes.

1) Pressure losses in the vertical string

Poettman and Carpenter took a semitheoretical approach to the problem of calculating two phase pressure losses based on the energy equation. The assumptions made in this analysis are that the kinetic energy difference of the flowing fluid is negligible between the top and the bottom of the tubing and that the external work done by the fluid can also be neglected.

The irreversible energy losses W_f , are expressed as a friction factor term :

$$W_f = 4 f v^2 \frac{\Delta h}{2g D} \quad (9)$$

Using the above assumption the energy equation reduces to :

$$144 \frac{\Delta p}{\Delta h} = \bar{\rho} + \frac{\bar{K}}{\rho} \quad (10)$$

$$\text{in which } \bar{K} = \frac{f q^2 M^2}{(7.413 \times 10^{10} D^5)} \quad (11)$$

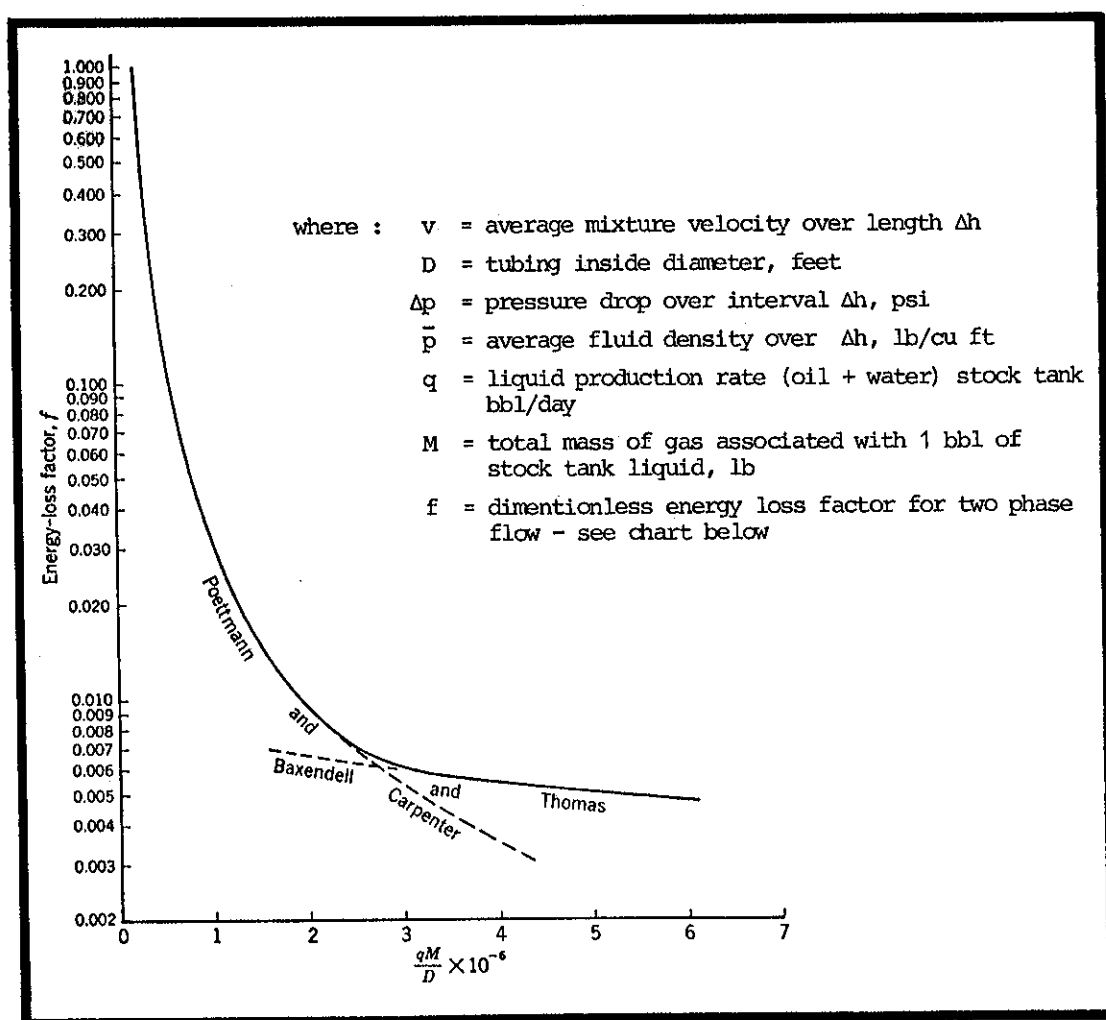


Fig. 7-17. Chart to find energy loss factor, f .

The vertical lift performance for a particular tubing size is developed by dividing the tubing into suitable increments of length $H_1, H_2, H_3...$ over which a pressure drop is calculated. Starting with an assumed bottom hole flowing pressure, the IPR tells us how much oil gas and water the formation will deliver, and with a knowledge of the fluids PVT properties and GOR relation over this interval, the pressure at H_2 is determined.

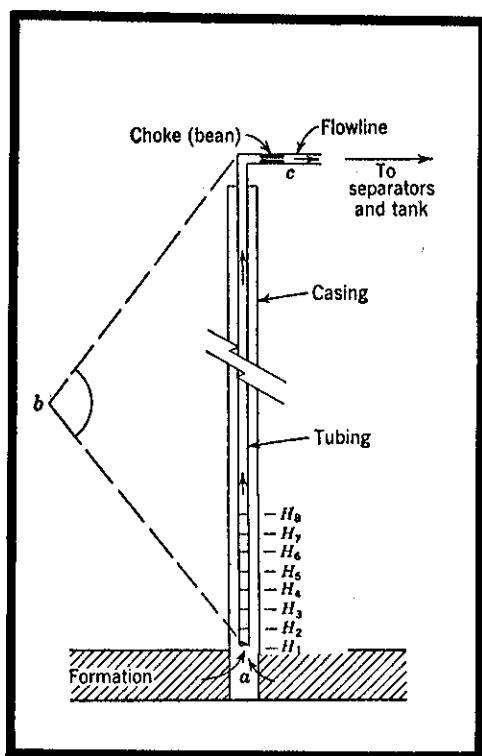


Fig. 7-18. Vertical lift performance.

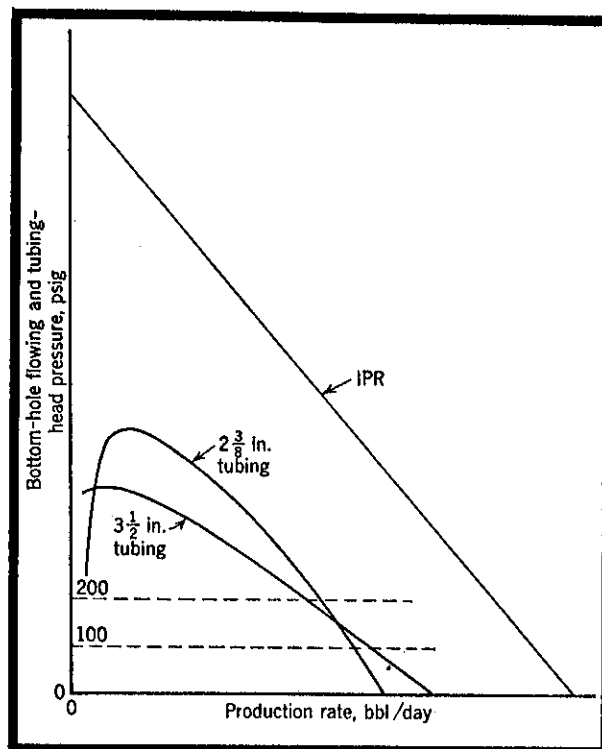


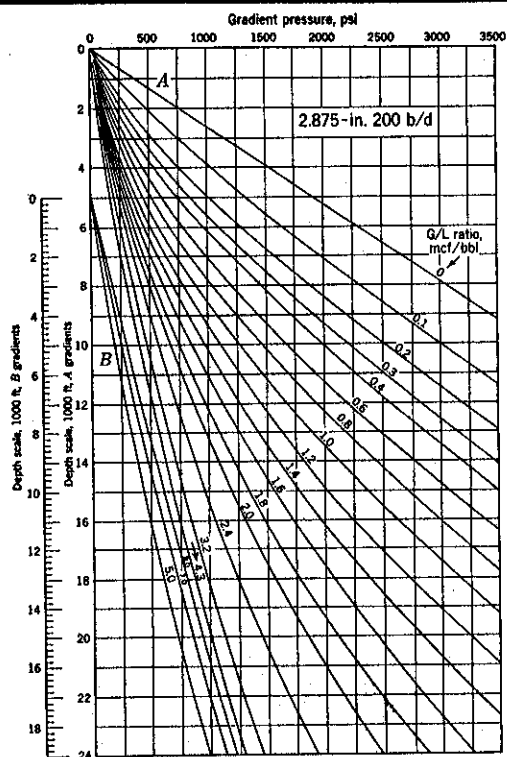
Fig. 7-19. Determination of optimum tubing size.

The calculation is repeated as many times as necessary until the pressure reaches 1 atm. A positive pressure at surface indicates that the well will flow naturally.

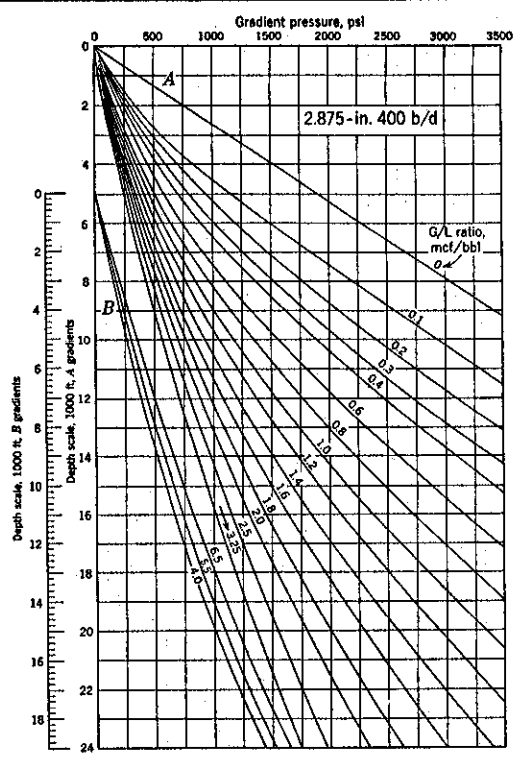
A complete tubing head pressure vs. production rate characteristic can be obtained by repetition of the process at a sufficient number of bottom hole pressures. Obviously, this method lends itself to machine computation and it is a simple matter to optimize tubing diameter and length by comparing a print out computed for several different completion strings.

Other investigators such as Gilbert took different approaches to estimate vertical lift losses. The results of these various studies are available in the form of families of pressure distribution curves which can be used together with the composite IPR to find simple graphical solutions to the overall performance of a flowing well.

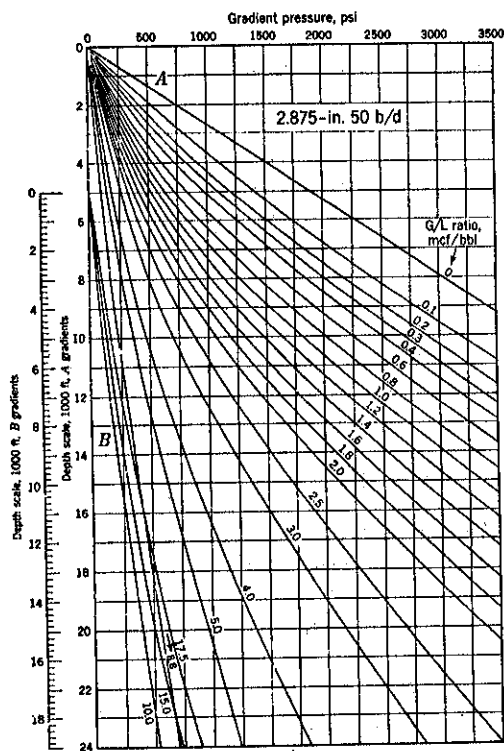
These pressure distribution charts such as shown on the right hand page, are available from Camco, Garrat, Brown and other suppliers of production equipment.



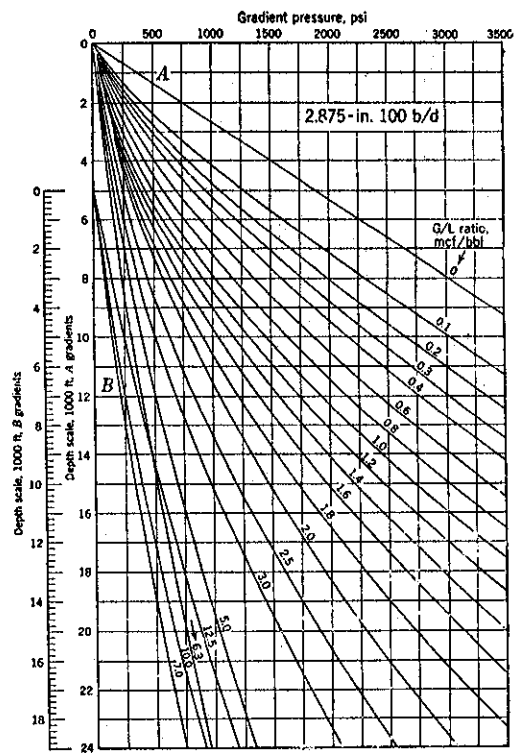
Approximate pressure-distribution curves for 2 $\frac{7}{8}$ -in. tubing: 200 bbl/day.
(From Gilbert, Courtesy API Drill. Prod. Practice.)



Approximate pressure-distribution curves for 2 $\frac{7}{8}$ -in. tubing: 400 bbl/day.
(From Gilbert, Courtesy API Drill. Prod. Practice.)



Approximate pressure-distribution curves for 2 $\frac{7}{8}$ -in. tubing: 50 bbl/day.
(From Gilbert, Courtesy API Drill. Prod. Practice.)



Approximate pressure-distribution curves for 2 $\frac{7}{8}$ -in. tubing: 100 bbl/day.
(From Gilbert, Courtesy API Drill. Prod. Practice.)

Fig. 7-20. Tubing flow pressure distribution tables.

2) Choke performance

Before the production leaves the well head, it passes through an orifice (often called a choke or bean) which serves to stabilize the optimum or desired rate against variations in flow line pressure.

The flow rate is determined only by the upstream pressure and choke size and is unaffected by fluctuations in the down stream pressure when flow through the choke exceeds sonic velocity. This condition is generally met when the upstream pressure is more than twice the downstream pressure.

Choke performance is given by the relation

$$P_{thf} = \frac{CR^{0.5}q}{S^2} \quad (12)$$

- where P_{thf} = tubing head pressure, psia
 R = gas liquid ratio, mcf/B
 q = gross liquid rate, B/D
 S = choke size, 1/64 inches
 C = constant of about 600

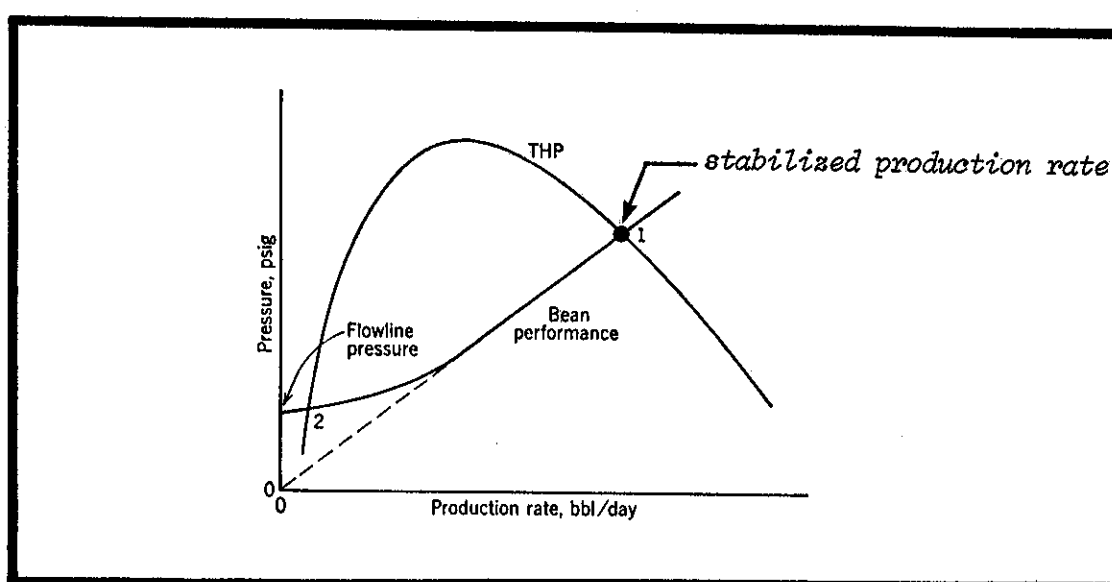


Fig. 7-21. Two possible production rates for a given size of choke.

The performance of one or more choke sizes may be superimposed over the flowing THP curve. The choke performance curve and the production rate intersect at 2 points. The lower intersection being unstable, stabilized production is at the higher rate.

0. Simulators - the single well model

The reservoir and well can be considered as coupled elements of a composite system where the performance of either element interacts and affects the overall system performance.

The system begins first, with the well and the characteristics of its associated reservoir volume, since it is evident that no well can produce more than the reservoir is able to deliver to the well.

Secondly, energy losses associated with the mass of produced fluids occur in the vertical pipe string.

Finally, the production must be delivered through a stabilizing choke to the surface facilities at a specified flow line pressure.

The performance of a well may be broken down into three separate elements for analysis :

- inflow production relation - IPR
- vertical lift performance
- choke performance

An electrical analogy, illustrating the inter-relation of elements for the case of a flowing well producing from three zones, is shown below :

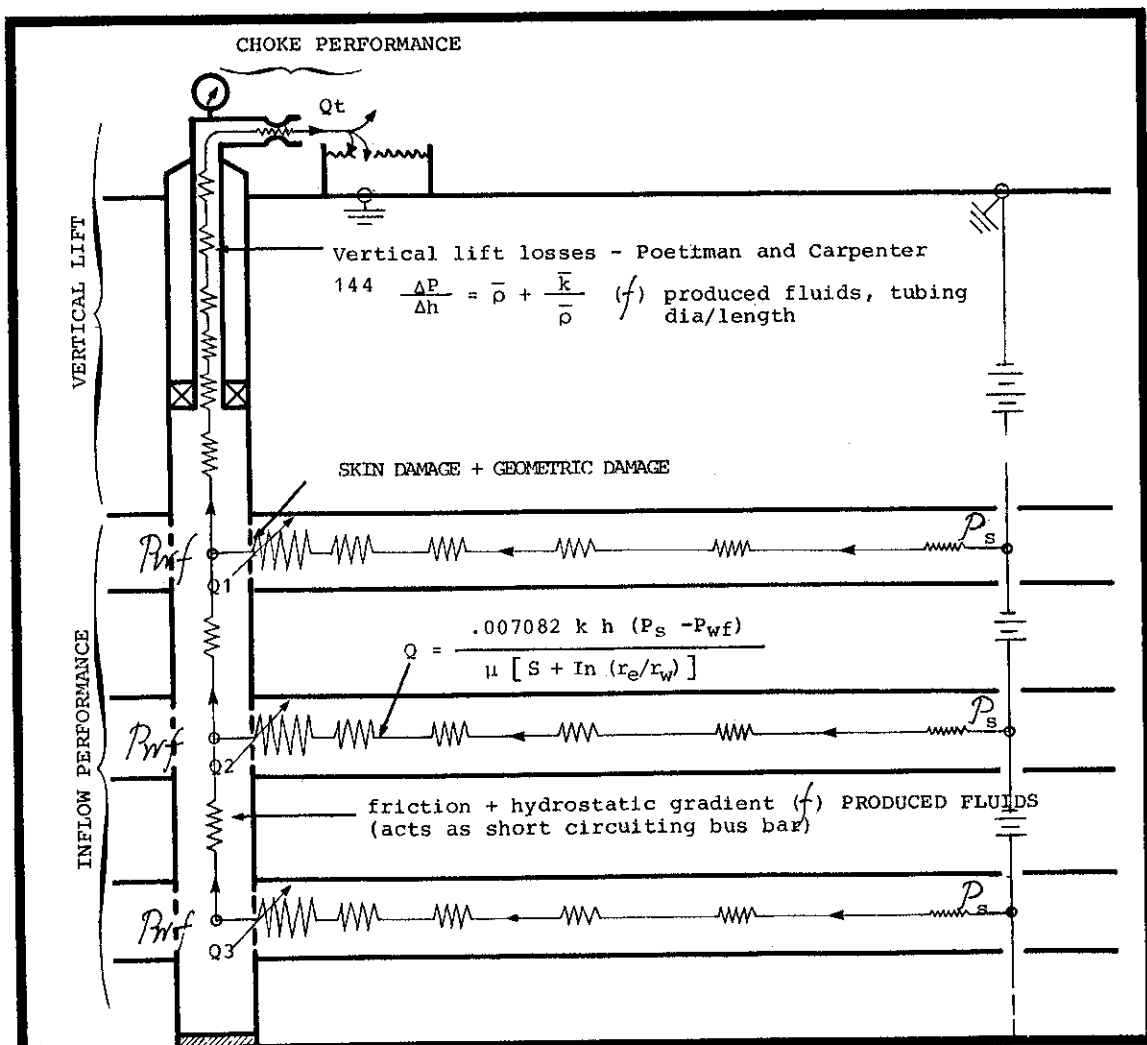


Fig. 7-22. Electrical analogy of a flowing well.

Single well simulator

Fluid movement, from the reservoir into the well-bore can be simulated by a system set up so that each zone or each layer of each zone is represented by a number of cross-sectional slices in a two dimensional R-Z coordinate system.

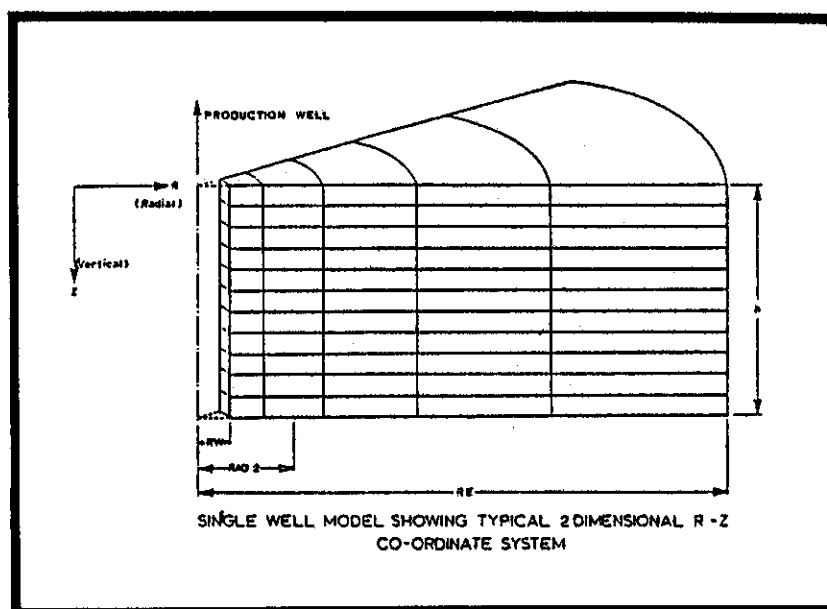


Fig. 7-23. Single well simulation radial grid.

The complete well model must account for zone interaction and for the pressure drop along the tubing and through the surface choke.

Single well simulators find numerous applications :

- To optimize size of tubular goods
- Avert cross flow - between layers
- Coning studies
- Interpretation of transient pressure behavior in build-up tests, curve matching
- History matching and prediction of reservoir pressure
- Input well data to larger scale complete reservoir simulators.

Chapter 7 - Appendix

Productivity ratio

The productivity ratio Q_p/Q_o is the ratio of production from a cased and perforated formation compared with the open hole production from the same conditions of pressure drawdown. Q_p/Q_o represents the efficiency of the completion.

Determination of Productivity Ratio

Figure 7-25 is a nomograph for finding the productivity ratio from borehole and perforation parameters. To use it, enter the nomograph from the upper left-hand side. All the dimensions are in inches. As an example, assume a 12" perforation in a 6" diameter borehole. Enter the nomograph on the upper left-hand corner where the perforation length is given as 12". This illustration follows the dashed line. The line crosses to the diagonal corresponding to the perforation diameter. One half inch is a reasonable approximation. The line next bends downward to the inset determining the effect of the damaged zone. If one assumes a 6" thick damage zone, one moves down to the 6" line. For a damaged zone whose permeability is 4/10 that of the virgin zone, (k_d/k_u), one measures, on the inset, the line off-set corresponding to this damage zone permeability (make $b'-c'$ equal to $b-c$). An assumption in constructing this nomograph is that the perforation penetrates through the damaged zone. The line is continued downward to the next set of curves. These correspond to the relative permeability of the crushed zone to the virgin formation, (k_c/k_u).

Cases are given for k_c/k_u from 0.1 to 1.0. From the intersection with 0.2, cross the graph to the section corresponding to the number of perforations per foot. Assume 4 shots per ft. From this point, we go up the curves incorporating the angular phasing. Assume 90 degrees phasing, so that from there one crosses and reads the productivity ratio for this case as 0.885.

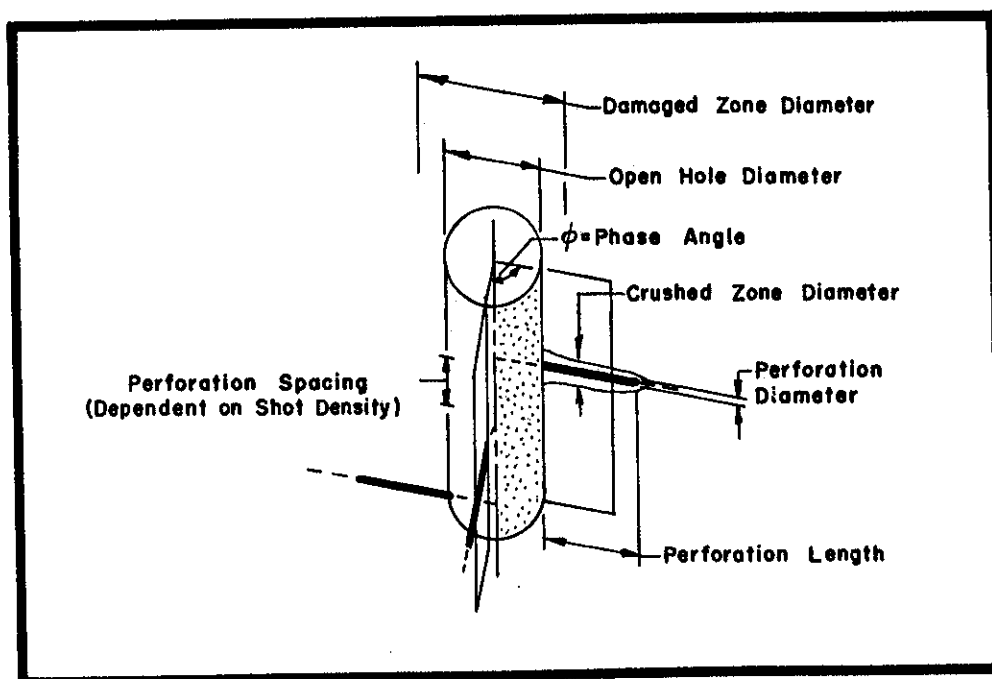


Fig. 7-24. Perforation geometry.

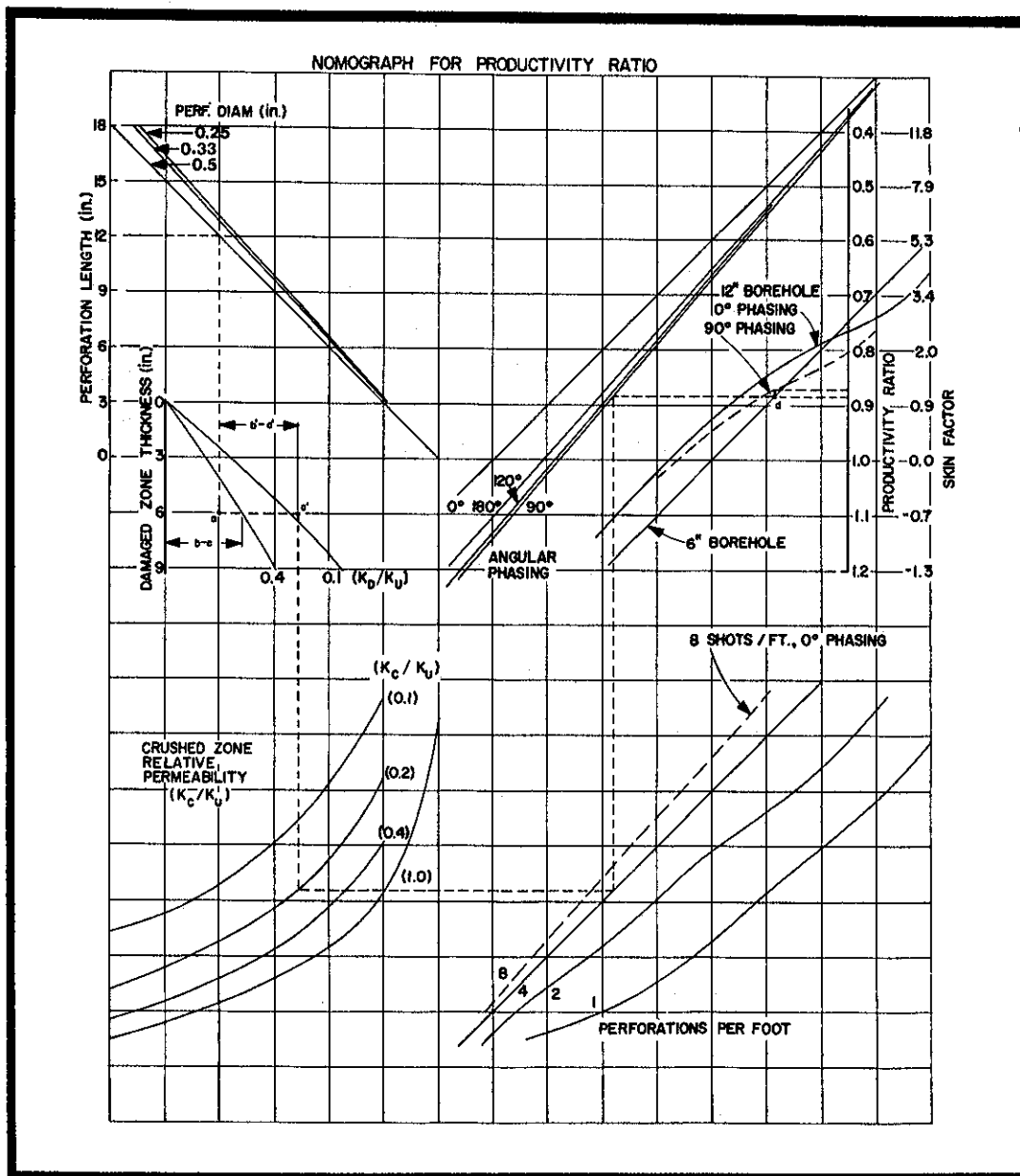


Fig. 7-25 - Nomograph for estimation of Productivity Ratio.

RESERVOIR ESTIMATES

8

A. Volumetric methods

Volumetric methods involve a determination of the bulk reservoir rock volume, average porosity and fluid saturations, from which the total reservoir hydrocarbon volume is calculated.

Recoverable reserves are then estimated by application of a suitable recovery factor and the formation/surface volume factor for the produced fluid.

$$\text{Recoverable oil} = \frac{V_b \times \phi \times (1-S_w) \times \text{R.F.}}{B_o}$$

where : V_b is the bulk reservoir volume

ϕ is the fractional porosity

$(1-S_w)$ is the hydrocarbon saturation

R.F. is the recovery factor

B_o is the formation volume factor (oil)

A recovery factor is approximated considering :

- laboratory measurement of oil displacement in cores $\frac{S_o - S_{or}}{S_o}$
- type of displacement mechanism involved
- correlation of sweep efficiency based on a similar reservoir.

Reservoir estimates are needed at various stages of a project

1) Geophysical exploration stages

Some order-of-magnitude estimate of the reserves which a structure might contain is necessary to rank various projects probability of economic success prior to making bids or possibly to relinquish undrilled acreage.

The first estimate is based on the volume of the structure determined from seismic maps supplemented by information on local geological trends which may indicate the thickness of porous beds which may be encountered.

By applying the common range of rock parameters, porosity (7 to 30%), water saturation (8 to 40%) and recovery factor (10 to 50%) a possible range of reserves that the structure might contain is estimated.

2) Exploration stage

With the drilling of a discovery well the uncertainty of encountering hydrocarbons is removed, and measured values for porosity and water saturation become available for the section of pay traversed.

Assuming that well log data corroborate the prior seismic data, now only the contour of the hydrocarbon/water contact (O.W.C.) is required to make a reasonable estimate for this stage.

3) Field development stage

As new wells are drilled the volume and geometrical distribution of the reservoir become even more accurately defined as well as the average reservoir porosity and saturation values.

On the other hand, fluid withdrawals and injections into the reservoir and the corresponding changes in fluid interfaces must be accounted for as the inventory of reserves is continuously upgraded.

Whether the accounting of hydrocarbon reserves is made by computer as in our "Field Studies" or manually, the procedures are the same in principle. Obviously, the trend in reservoir studies is toward numerical simulation on which not only the static inventory of reserves is kept, but which can predict the future behaviour of a field.

B. Calculation of the reserve

The gross reservoir rock volume enclosed by the structure above the hydrocarbon/water contact is calculated in the following steps :

- 1) A net sand isopach map, giving the contours of equal thickness of pay with the water contact assigned zero elevation contour is the most convenient basis for rock volume calculations.

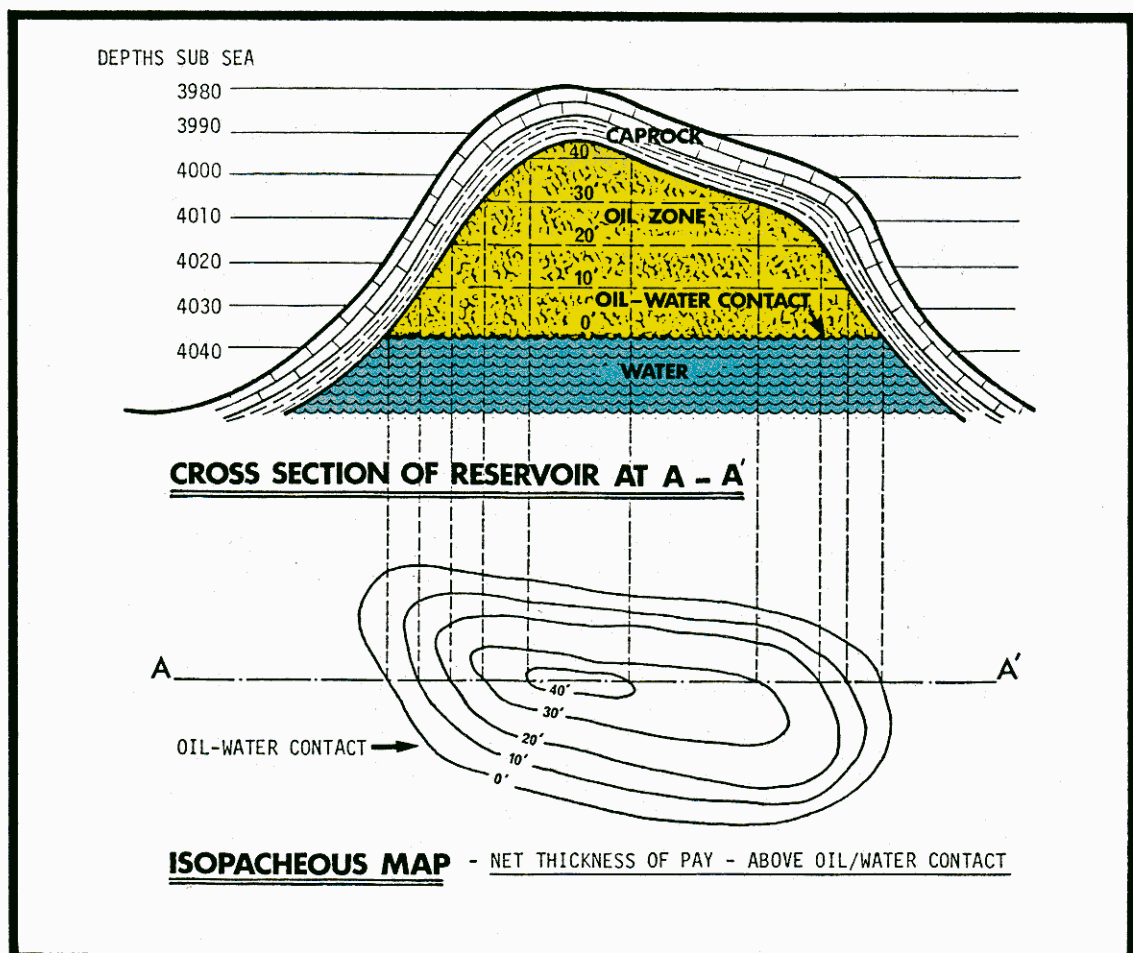


Fig.8-1. Isopachous map - Net thickness of pay - above oil/water contact

- 2) The area within each contour is determined by planimetering, and a plot prepared of area contained in each contour vs. depth.

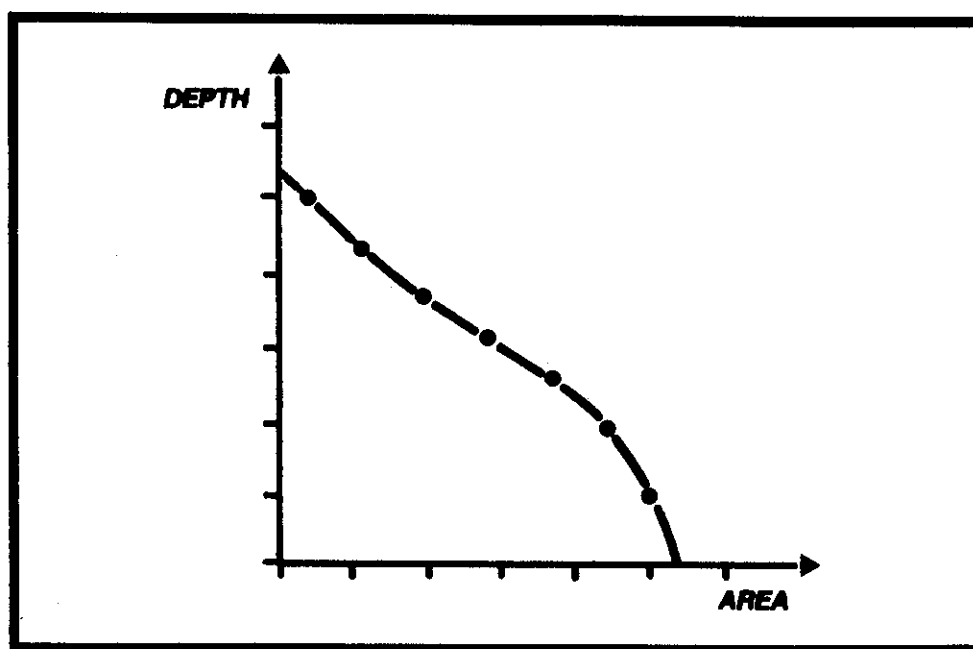


Fig. 8-2. Plot of depth vs. area contained within each contour.

- 3) The gross rock volume is $\sum A dh$ which may be found by planimetering again or by application of a numerical integration rule. In the Schlumberger field studies approach the volumetric reservoir distribution is calculated numerically and plotted by machine as isopach and isovolume maps.

- Pyramidal formula $\Delta V = \frac{h}{3} (A_n + A_{n+1} + \sqrt{A_n A_{n+1}})$

- Trapezoidal formula $\Delta V_b = \frac{h}{2} (A_n + A_{n+1})$

$$V_b = \frac{h}{2} (A_0 + 2A_1 + 2A_2 + \dots + 2A_{n-1} + A_n) + t_{av} \times A_n$$

C. Uncertainty in reservoir estimates (Volumetric method)

At an early stage in reservoir planning it is necessary to consider how departures from the available "best estimates" of the essential reservoir parameters will affect the viability of the project if the reserves are significantly greater or smaller than the "central estimate".

Monte Carlo method :

As the reserve is calculated from :

$$n = \frac{Ah \phi (1-S_w) R.F.}{B_o}$$

n = volume of the reserve

there will be an uncertainty in the accuracy of early contour maps, fluid interface locations and distribution of porosity, saturation and recovery factor variations throughout the reservoir.

If all the variables entering the equation are independent from each other, then the random distribution for each variable considering the most likely value and the probability distribution of the recoverable oil are generated.

It will be frequently true that all variables will not be independent. ϕ , h and S_w are highly correlated.

Water saturation and porosity may be broadly related, higher water saturations tending to occur in lower porosity, lower permeability intervals, and in thinner intervals a transition zone may affect the water saturation, while thicker intervals may develop better average porosities.

When this saturation occurs, one of the variables must be designated as the independent variable and must be selected first. The random variable so chosen will then define a limited range of values of the dependent variable.

e.g. Choose ϕ

If $\phi > 0.18$ then $0.10 \leq S_w \leq 0.22$

If $\phi < 0.18$ then $0.22 \leq S_w \leq 0.40$

Obviously this method requires digital computation, but standard library programmes are available.

An alternative method better suited to desk calculation, makes use of a number of values of each variable - 3 or 5 values to represent the probability distribution, e.g.

- 1) A very optimistic value (say 0.1 chance of yielding a low value)
- 2) An optimistic value (" 0.3 " " " " ")
- 3) Most likely value (" 0.5 " " " " ")
- 4) A pessimistic value (" 0.8 " " " " ")
- 5) A very pessimistic value (" 0.9 " " " " ")

All combinations of two parameters (say h and ϕ) are computed, (giving 25 products), and these are reduced to 5 by averaging successive groups of 5. The next parameter is then combined to yield a new suite of 25 values which are again reduced to 5. The process is repeated until all parameters are introduced, and a final range of 5 values, ranging from very pessimistic through the most likely to a very optimistic value, are then obtained.

These methods give a very much clearer idea of the possible spread of results, and divert attention from the potentially misleading "most likely" value, to other possibilities.

D. Field Integrated log analysis and reservoir mapping services

Schlumberger integrated log analysis and reservoir mapping service is a computerized method of handling log data on a field-wide basis. It has two main aims :

- 1.- To compare new recorded log data against established field norms in order to detect and correct (normalize) the data before it is assimilated. This is a quality control process.
- 2.- To machine compute and map reservoir parameters established from log data including the net hydrocarbons in place.

A computer plotted structural contour map is shown on the next page, superimposed over a posted map or grid used to establish the contours.

General procedure :

- 1.- Establish a field grid and enter the location of wells drilled on the grid. (A one km pattern is common in the Middle East).
- 2.- Enter the normalized numerical values for the parameter of interest (depth of top of the reservoir in the case illustrated) for each well.
- 3.- The computer establishes values at each grid node by interpolation and extrapolation of data from all of the wells gridded.
- 4.- The computer plots contours, interpolating between the values on the posted map.

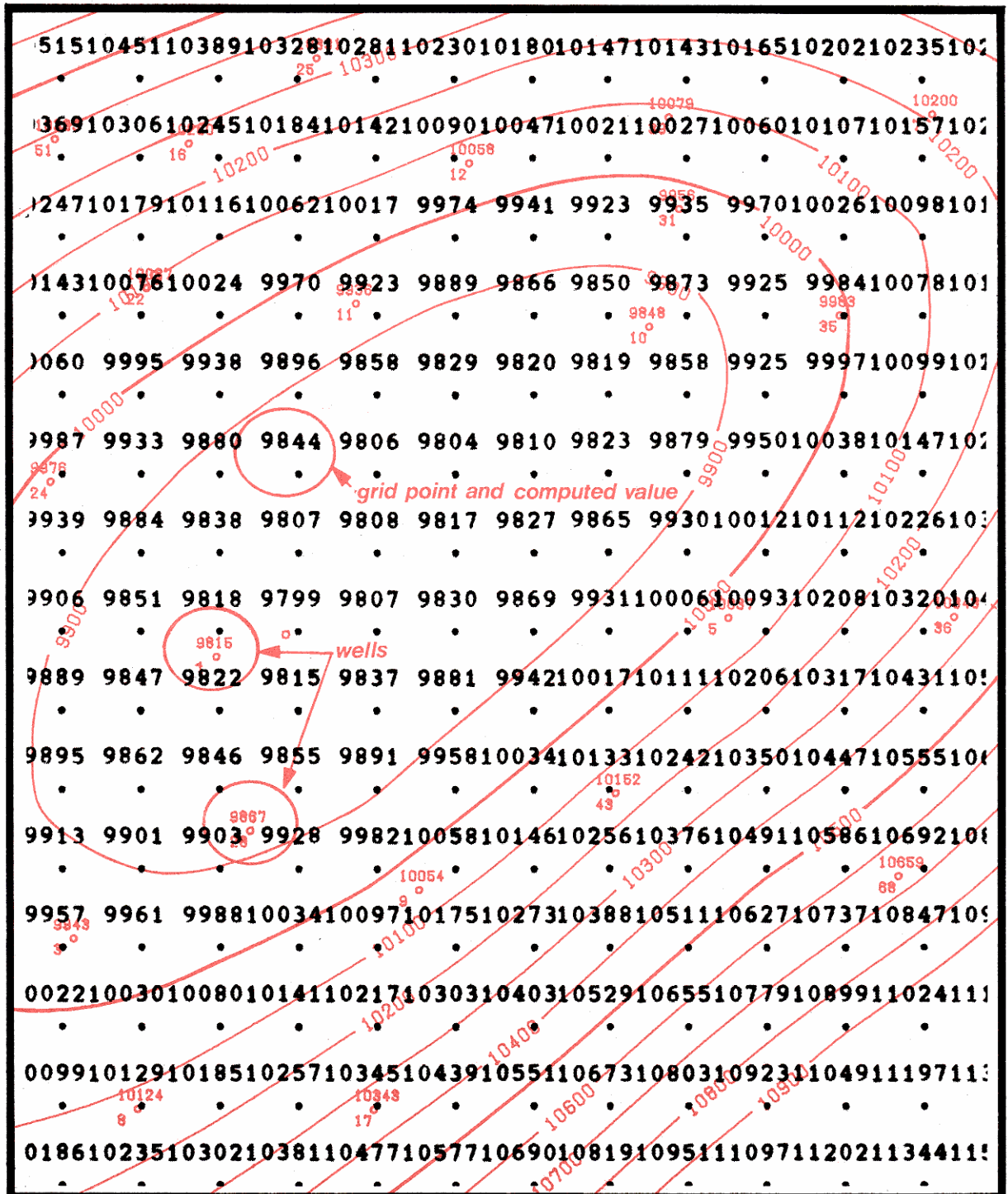


Fig. 8-3. Structural contour map superimposed over the posted map used.

1) Normalization of log data (Field Integrated Log Analysis)

Histograms* and cross plots for the formation under study obtained from each new well logged are compared with data established in "key wells" on which the standard plot profiles have been established by extensive comparison of log, core and well test data.

This comparison has two purposes, first as a log quality control and a means of recalibrating the log data if necessary, and secondly to recognize anomalous data trends due to time geological differences in a new well.

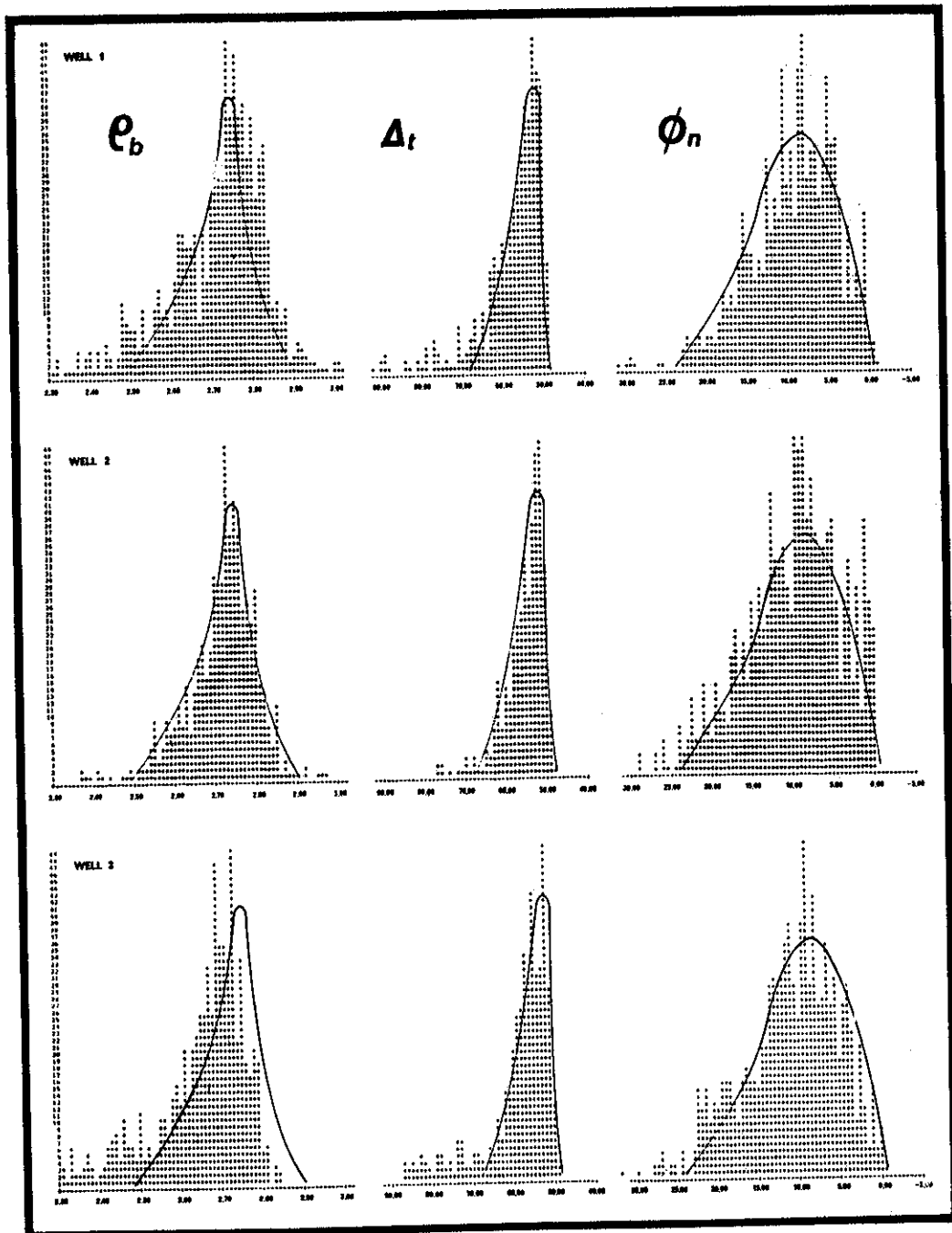


Fig. 8-4. P_b , Δt and ϕ_N histograms on three field wells.

* A histogram plots the occurrence of the same value of a parameter. It is an established method in the industry for comparison of core data.

Transform relations between log obtained porosity and permeability which have been modified for agreement of key well log, core and flow data are applied to the new well and a CPI is made giving normalized lithology, hydrocarbon type, fluid saturations, porosity and permeability for each 6" interval logged.

2) Reservoir Geometry and Mapping Services

For each interval the values of ϕ , k , and S_w are averaged for each well.

A lumped value for the same parameters but with appropriate limit and cutoff values applied is established by the computer for each grid coordinate and printed out.

Contour maps are derived by the computer by following and interpolating between points of equal value on the gridded data.

- structural map
- isopach map (gross thickness)
- isopach map (net pay with porosity cutoff)
- iso-porosity map (with porosity cutoff)
- iso-permeability map (with porosity and water saturation cutoff)
- iso net pay x porosity map (with porosity cutoff)
- iso net pay x permeability map (with porosity and water saturation cutoff)
- iso net pay x porosity x hydrocarbon saturation map

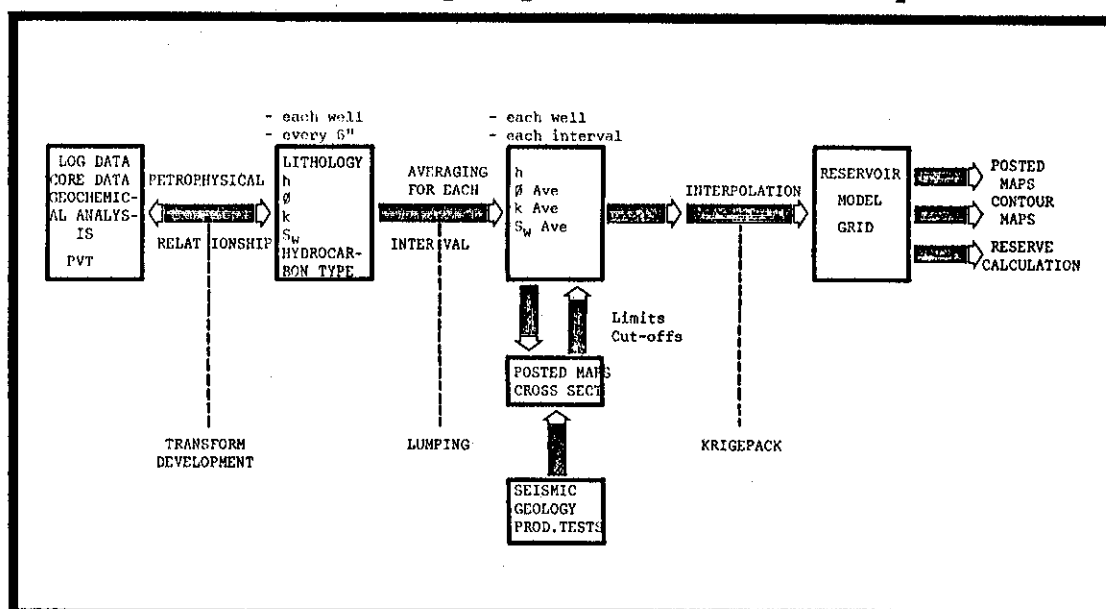


Fig. 8-5. Integrated log analysis and Reservoir geometry flow diagram

3) Monitoring fluid interfaces changes

To keep the reserves inventory up-to-date, a periodic monitoring of fluid interfaces, expansion of a gas cap or oil/water contact movement is required. In the past, uncased or plastic cased observation wells were used in the Middle East to monitor the above using resistivity tools. With the addition of TDT and GST tools, monitoring through casing is becoming standard practice.

The trend in reservoir studies is toward more complete numerical simulators which not only keep track of the inventory of reserves but can simulate dynamic reservoir behaviour of a field in response to potential gradients.

E. Reservoir estimates - material balance methods

As oil and gas are produced with an attendant decline in average reservoir pressure, influx of water and the expansion of the gas cap and reservoir liquids tend to offset these pressure changes.

The material balance relates the volumes of fluids withdrawn, injected and encroached and the corresponding pressures.

1) Material balance in gas reservoirs

Take a system of hydrocarbon filled volume V

$$\text{i.e. } V = V_b (1 - S_w) \phi$$

$V_b = \text{bulk rock volume}$

If this is filled with gas under the conditions

average pressure	P_i
average temperature	T
average deviation factor	Z_i

then the reservoir volume of gas referred to standard conditions (P_o , T_o , $Z = 1$) is given by the equation :

$$\frac{G P_o}{T_o \cdot 1} = \frac{P_i V}{Z_i T}$$

or

$$G = \frac{P_i V}{Z_i T} \frac{T_o}{P_o}$$

where G is the volume at standard conditions of the gas volume V contained in the reservoir.

At any subsequent time when the reservoir pressure has dropped, due to production of gas, to some value " P " (t) the contents at this time are given by :

$$G(t) = \frac{P(t) V T_o}{Z(p) T P_o}$$

and the cumulative production $G_p = G - G(t) = \frac{V T_o}{T P_o} \left[\frac{P_i}{Z_i} - \frac{P(t)}{Z(p)} \right]$

$$\begin{aligned} G(p) &= \frac{V T_o P_i}{T P_o Z_i} \left[1 - \frac{P}{P_i} \frac{Z_i}{Z} \right] \\ &= G \left(1 - \frac{P Z_i}{P_i Z} \right) \\ &= G - \text{constant} \times \frac{P}{Z} \end{aligned}$$

This is the equation of a straight line with cumulative production and P/Z as the variables, and with the initial gas in place as the intercept. Consequently a plot of cumulative production against P/Z extrapolated to $P/Z = 0$ yields the value of gas initially in place.

Alternatively, given values of P , Z and cumulative production at any time, the equation can simply be solved by substitution of values.

This equation will be valid only if there is no influx of water into the reservoir, with the decline in reservoir pressure. If decline in reservoir pressure induces a water encroachment then some part of the originally hydrocarbon filled volume will be occupied by the water, which has encroached.

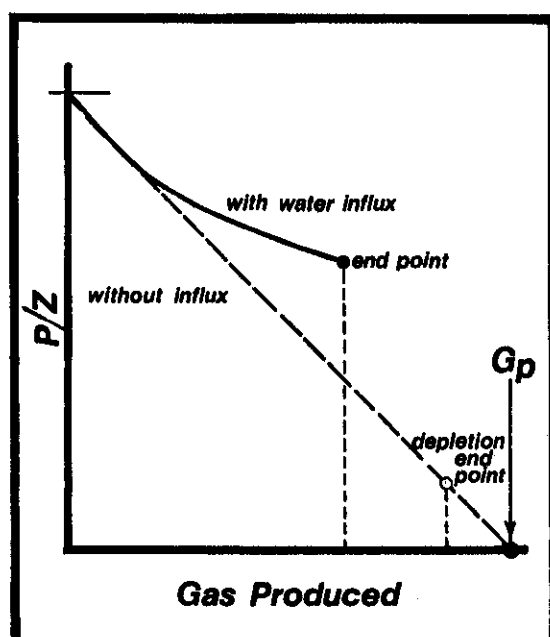


Fig. 8-6. Estimating initial gas in place.

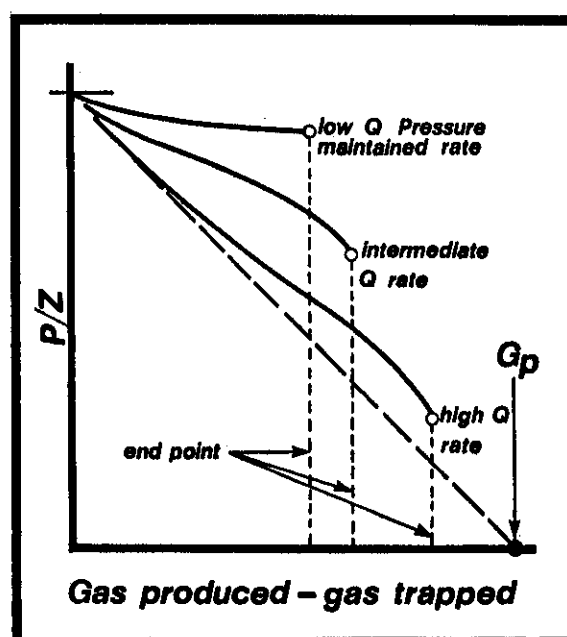


Fig. 8-7. Effect of production rate on recovery with water influx

For the case with water influx

$$G - G(t) = G(p) = \frac{V T_O}{T P_O} \left[\frac{P_i}{Z_i} - \frac{P}{Z} \right] + \frac{W_e}{B_g}$$

$$\text{since } B_g = \frac{Z T P_O}{P T_O}$$

$$\begin{aligned} G(p) &= \frac{V T_O P_i}{T P_O Z_i} \left[1 - \frac{P}{Z} \frac{Z_i}{P_i} \right] + \frac{W_e}{B_g} \\ &= G \left[1 - \frac{P}{Z} \frac{Z_i}{P_i} \right] + \frac{W_e}{B_g} \end{aligned}$$

The extrapolation of the line G_p against P/Z leads to an intercept at $P/Z = 0$ of

$$G_p = G + \frac{W_e}{B_g}$$

The gas in place will then be overestimated if the existence of water influx is undetected. (In fact, because of the higher abandonment pressure or reservoirs subject to water drive, the recoverable gas may be very substantially overestimated by this depletion analysis of water drive gas reservoirs). The residual gas saturation with water encroachment can be as high as 50% of the original gas saturation, and since the water influx tends to maintain reservoir pressure, the gas trapped may be at a relatively high pressure. The earlier figure shows the characteristic P/Z : cumulative plot.

For a gas reservoir with water drive, this terminates at an end point determined by the rate of gas offtake, relative to the rate of water encroachment. For a non-fractured homogeneous type reservoir subject to water influx, there is a potential advantage in rapid depletion of the gas reserve, since water influx is a time dependent function. Exploitation of the reserve by high rates of production, reduces reservoir pressures and brings the reservoir performance characteristic closer to that of a depletion system.

For fractured gas reservoirs (or any dual porosity type system), this beneficial effect of high rate withdrawals may not occur, since rapid advance of water through the high permeability system may lead to watering out of production wells at an early stage.

2) Generalized material balance relation for oil reservoirs

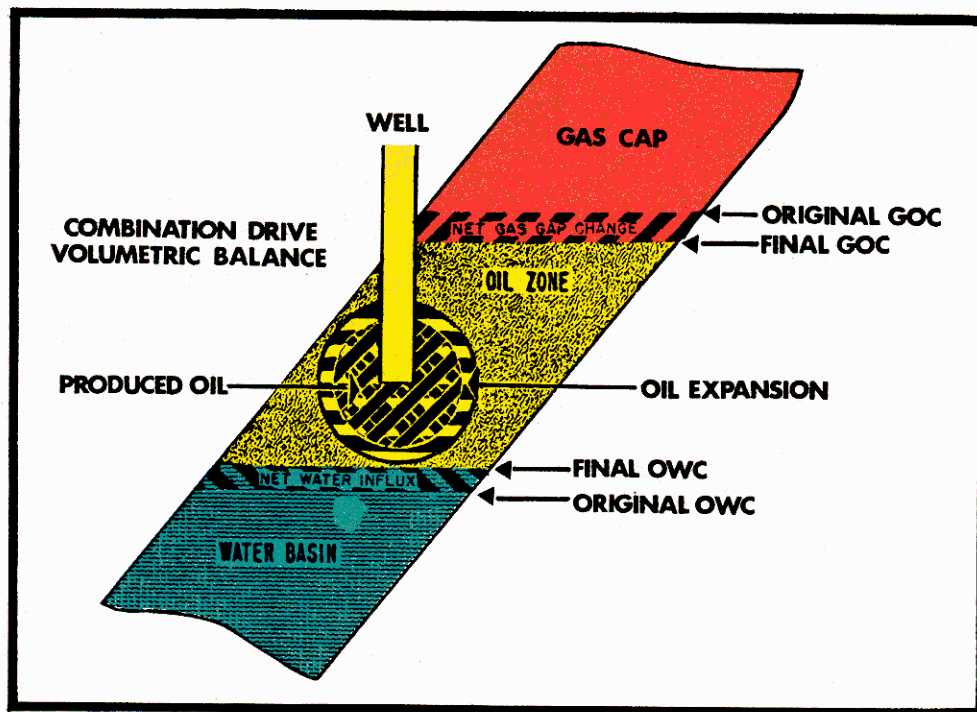


Fig. 8-8. Combination drive reservoir illustrating volumetric balance method.

When hydrocarbons are produced from the reservoir, the attendant pressure drop causes the remaining fluids to expand and water to encroach, compensating for the removed volume.

The generalized material balance relation below equates the volumes of oil, water and gas removed with expansion of the oil, free gas, and encroached water.

$$\left[\text{OIL ZONE EXPANSION} \right] + \left[\text{GAS CAP EXPANSION} \right] + \left[\text{WATER INFLUX} \right] = \left[\text{CUMULATIVE OIL PRODUCTION} \right] + \left[\text{CUMULATIVE GAS PRODUCTION} \right] + \left[\text{PRODUCTION WATER PROD.} \right]$$

$$N(B_t - B_{ti}) + \frac{NmB_{ti}(B_g - B_{gi})}{B_{gi}} + W_e = N_p B_t + N_p(R_p - R_{si}) + B_w W_p$$

where :

B_g , Gas formation volume factor

B_o , Oil formation volume factor

B_t , Total (two-phase) formation volume factor $B_t = [B_o + (R_{si} - R_s)B_g]$

B_w , Water formation volume factor

m , Ratio of initial reservoir free gas volume to initial reservoir oil volume

N , Initial oil in place

N_p , Cumulative oil produced

R_p , Producing gas-oil ratio

R_g , Solution gas-oil ratio

W_e , Cumulative water encroached

W_p , Cumulative water produced

i , Initial

Assumptions generally made are that the volume factors for solution gas and free gas from the cap are identical and that there is negligible release of gas from the produced water.

Terms for rock compressibility and connate water saturation will rarely be significant for gas or oil reservoirs with a gas cap. Terms for compressibility of rock pore volume may be included for oil reservoirs above the bubble point, where no free gas is present.

The equation can be solved for N , the oil in place, where the terms which include m , ratio of gas cap to oil volume, and W_e , the water influx can be determined independently or assumed to be zero.

$$N = \frac{N_p \left[B_t + (R_p - R_{si}) B_g \right] - (W_e - B_w W_p)}{B_t - B_{ti} + \frac{m B_{ti}}{B_{gi}} (B_g - B_{gi})} \quad \text{bbls}$$

Where there is no water influx or gas cap the corresponding terms are eliminated simplifying the equation for a dissolved gas drive to :

$$N = \frac{N_p \left[B_t + (R_p - R_{si}) B_g \right]}{B_t - B_{ti}} \quad \text{bbls}$$

For a gas cap drive where there is no water influx the material balance equation is :

$$N = \frac{N_p \left[B_t + (R_p - R_{si}) B_g \right] + B_w W_p}{B_t - B_{ti} + \frac{m B_{ti}}{B_{gi}} (B_g - B_{gi})} \quad \text{bbls}$$

As for a water drive where there is no gas cap :

$$N = \frac{N_p \left[B_t + (R_p - R_{si}) B_g \right] - (W_e - B_w W_p)}{B_t - B_{ti}} \quad \text{bbls}$$

a) Discussion of the accuracy of results

Pressure enters the material balance calculations as differences in the initial and present values of B_o-B_{oi} , $R_{si}-R_g$ and B_g-B_{gi} .

Accuracy of results depends heavily on the quality of fluid PCT, production and pressure data. Average reservoir pressure and pressure dependent PVT data B and R values must be accurately known to assure reliable results. It is not sufficient to use generalized correlations in place of PCT laboratory measurements on representative fluid samples - preferably taken with a PST type bottom hole sampler.

The material balance method of reservoir analysis becomes possible only after sufficient oil has been produced causing a significant drop in reservoir pressure.

Calculations improve in accuracy at later times in reservoir history when 5% or more of the oil has been produced and the value of the B_o-B_{oi} term becomes large.

a) Schilthuis steady state

$$W_e = k \int_0^t (P_i - P) dt$$

$$\frac{dW_e}{dt} = k (P_i - P)$$

b) Hurst modified steady state

$$W_e = c \int_0^t \frac{(P_i - P)}{\log dt} dt$$

$$\frac{dW_e}{dt} = \frac{c (P_i - P)}{\log dt}$$

c) Van Everdingen and Hurst unsteady state

$$W_e = B \Sigma_0^t \left[\Delta P Q(t_D) \right]$$

where :

W_e = water encroachment

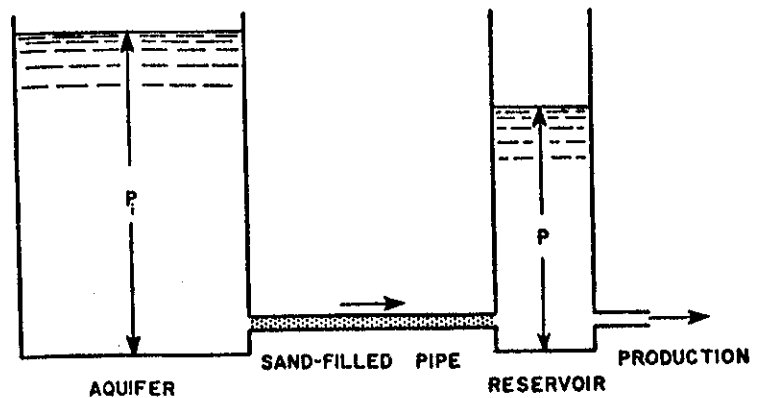
$\frac{dW_e}{dt}$ = rate of water encroachment

P = boundary pressure

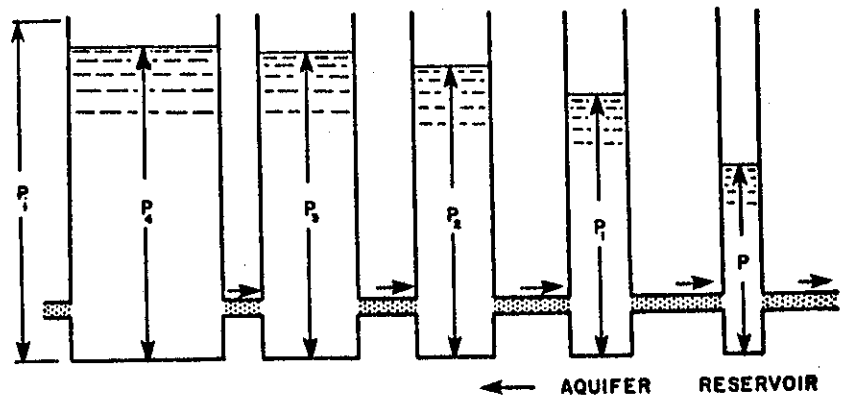
B, c, k = water influx constants

$P_i - P$ = pressure drop, psi

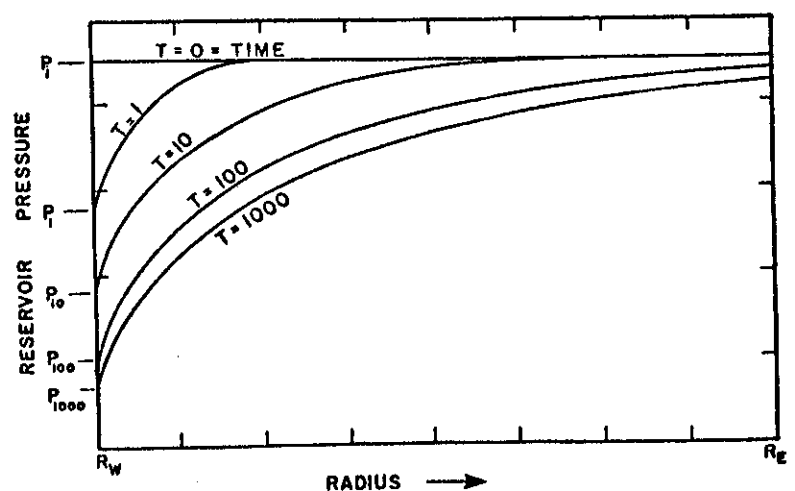
$Q(t_D)$ = dimensionless water influx



Hydraulic analog of steady-state water influx into a reservoir.



Hydraulic analog of unsteady state water influx into a reservoir.



Pressure distribution in an aquifer at several time periods, for a constant rate of water influx across a circumference of radius r_w .

Fig. 8-9. Water influx models.

b) Water influx

In contrast to the effects of water drive in gas reservoirs, the effect of water drive in an oil reservoir is to improve recovery.

Although some pressure drop is necessary in order to generate water influx, in a small accumulation subject to a very active water drive, the situation may arise where the water influx approaches the total of the offtake terms, and the material balance then becomes indeterminate as

$$N \simeq \infty$$

The extent that an aquifer can contribute driving energy depends on the degree of transmissivity between aquifer and reservoir and the size and nature of the aquifer. Many reservoirs overlay or are connected to aquifers along part or all of their periphery and connectivity can vary between virtually infinite and negligible. An aquifer may be large as to act as an infinite source or be small and enclosed by impermeable boundaries.

Values for encroachment W_e , and rate of encroachment dW_e/dt are necessary for prediction of reservoir performance. One of the water influx models shown in simplified form in figure 8-9 are used together with history matching studies to find the most suitable expression.

WELL TESTING & PRESSURE TRANSIENT ANALYSIS

9

The magnitude of capital outlay needed for permanent offshore facilities requires that the number of wells to be drilled, well spacing, location of drilling and production platforms be established at the earliest stage in field development.

Flowing tests are essential to verify productive capacity, determine gross reservoir parameters and reservoir limits as accurately as possible and they yield representative samples of the liquid hydrocarbons, gas and formation waters needed for the design of process facilities.

A. The DST (Drill stem test)

The DST or drill stem test is essentially a controlled blowout in which a limited amount of reservoir fluid is produced into the drill pipe through a DST tool. A DST is generally run in open hole to help determine the possibility of commercial production prior to a permanent completion of the well.

The DST tool consists of a packer to isolate the formation from the mud column, a test valve which can be opened and closed by manipulating the pipes, a reverse circulating sub which allows the produced fluids to be circulated out prior to pulling out, and a downhole clock-driven pressure recording device.

One hour of a strong blow will yield good test results. Several hours are needed in marginal cases but the usual practice is to try to flow all tests to the surface. The effluent is routed to a flare or burning pit.

Shown below are the typical DST tool strings used for different types of open hole tests. The double packer straddle tool tests zones between the packers while the single packer type tests formations below the packer.

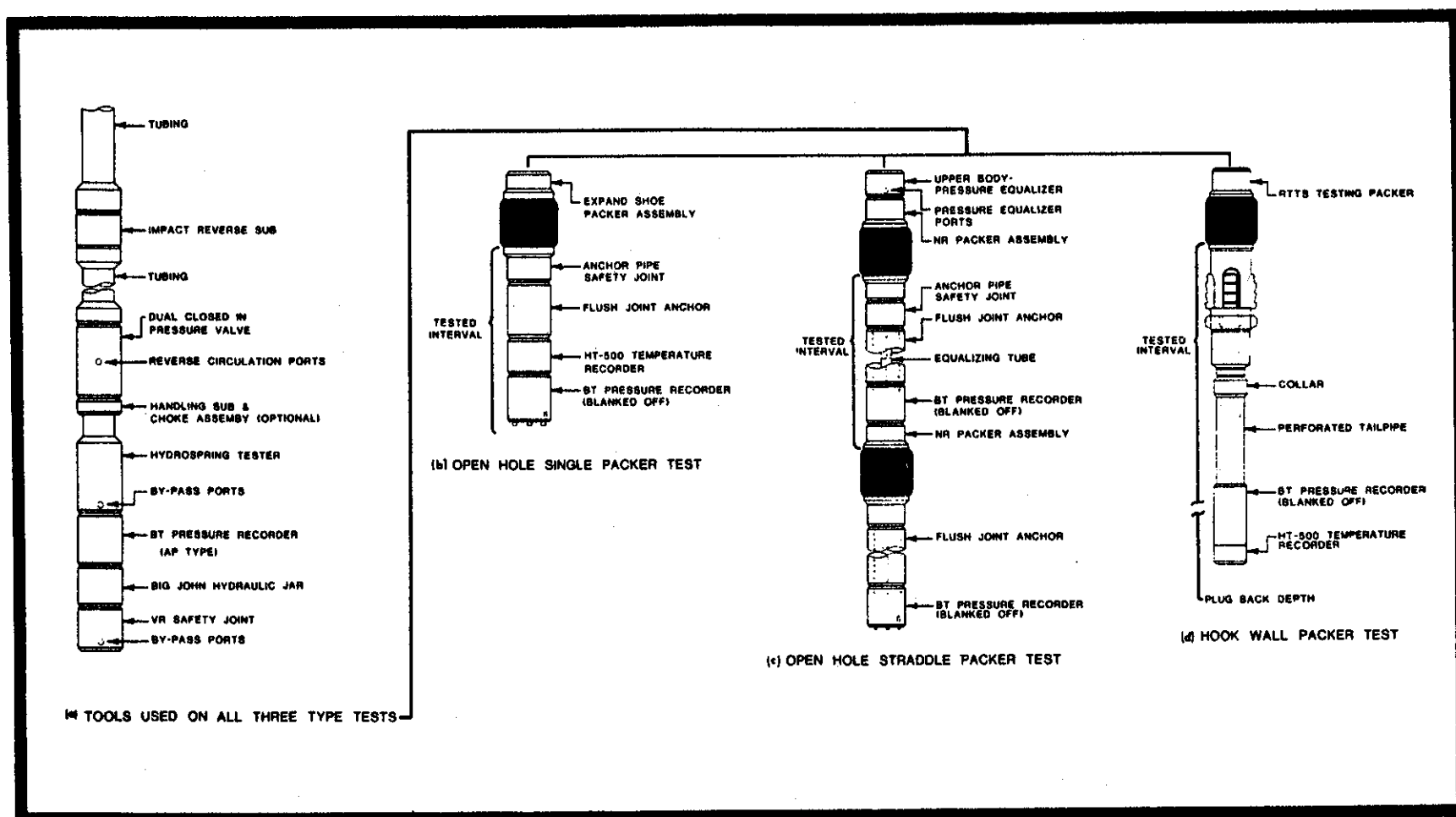


Fig. 9-1. Typical DST tools used for three types of tests. Upper assembly (left) is similar on all three test types.
After Edwards and Shryock - Courtesy Petroleum Engineer.

A surface operated test valve allows several cycles of flow and shut in.

The analysis of DST pressure data is similar to, and will be discussed together with, transient pressure analysis.

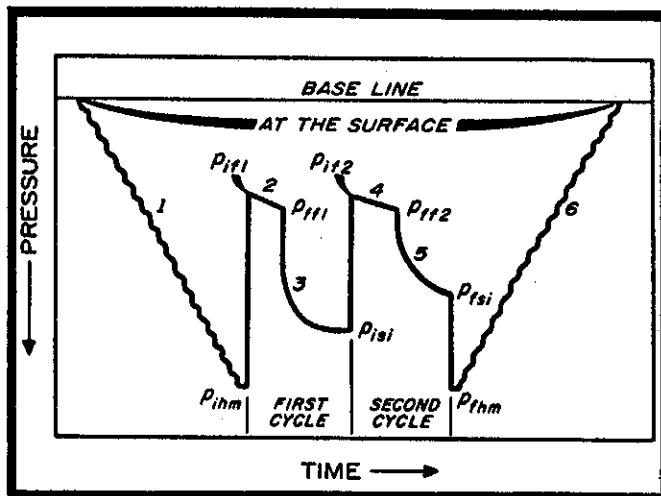


Fig. 9-2. Schematic of a DST chart :
 (1) going into hole: (2) initial flow period: (3) initial shut-in period: (5) final shut-in period: and (6) coming out of hole
 P_{ihm} = initial hydrostatic mud pressure: P_{if1} = initial flowing pressure in first flow period: P_{ff1} = final flowing pressure in first flow period: P_{isi} = initial shut-in pressure: P_{if2} = initial flowing pressure in second flow period: P_{ff2} = final flowing pressure in second flow period: P_{fsi} = final shut-in pressure: and P_{fhm} = final hydrostatic mud pressure

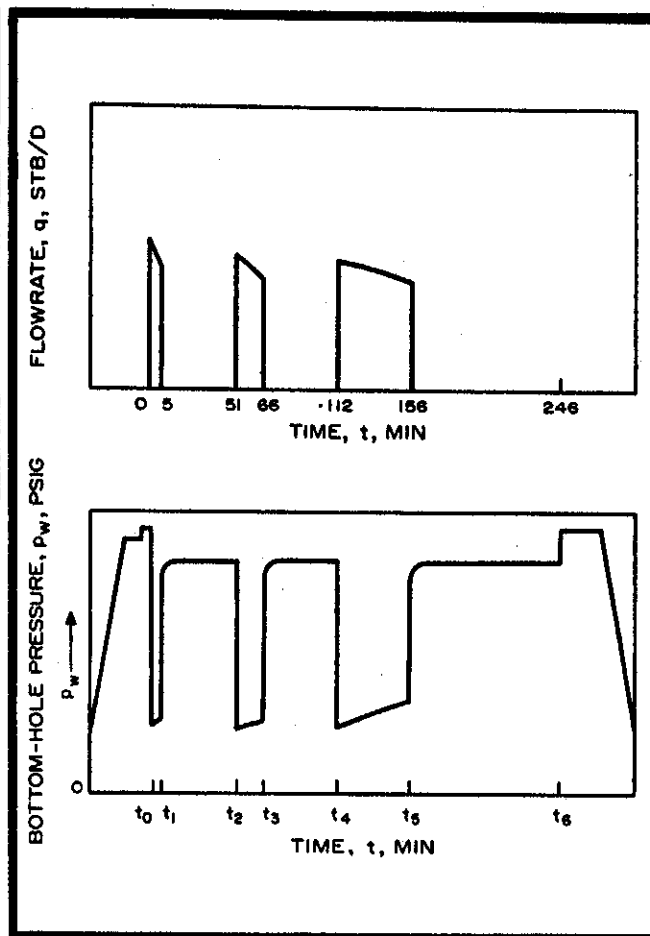


Fig. 9-3. Example of a three-cycle
drillstem test. After
McAlister, Nutter and Lebourg

Although other information may be obtained from a DST, the primary aims are :

- A representative sample of fluid
- To establish commercial flow capacity prior to completion
- Accurate measurement of reservoir pressure
- To obtain some information on formation continuity where permeability is not too high.

B. LTT (long term production test) of oil wells

The LTT, or long term production test, is carried out after the well has been permanently completed with its final casing or liner (if any). The production packer, tubing, safety valve or storm choke, and well head are all in place.

The production facilities may be permanent or temporary, but must have the capacity to separate and handle the full well flow. The produced oil is generally not burnt, but, if facilities to handle the associated gas are not adequate, the latter may be flared.

The practice is to monitor the bottom hole pressure with a subsurface pressure gage (surface reading Hewlett-Packard for high productivity wells where possible) along with continuous monitoring of the oil and gas flow rates.

Oil flow rates are measured by :

- orifice meter readings
- positive displacement meter readings
- tank level dips

Gas flow rates will generally be measured by orifice metering.

Test objectives :

- Determine exact nature of produced fluids.
 - . PVT tests to be performed on recombined samples
- Define well productivity
 - . IPR curve for oil wells
 - . Deliverability curve and open flow potential for gas wells
- Evaluate characteristics of the producing formation
 - . Static formation pressure
 - . Formation flow capacity (kh)
- Evaluate formation damage
 - . Determine if acidizing or other treatment is needed
 - . Control results of the treatment operation

Test procedure for highly productive oil wells :

- Cleaning up period - a few to 24 hours
- Initial shut in period - twice clean up period
- Flowing period - 1 to several days
- Final shut in period - same duration as flow period.

Where the well IPR is to be determined a multiple flow rate test must be made. In this case each flowing period should be long enough to reach "steady" conditions with respect to the well bore.

The IPR was discussed in the previous chapter and buildup will be covered in transient test analysis.

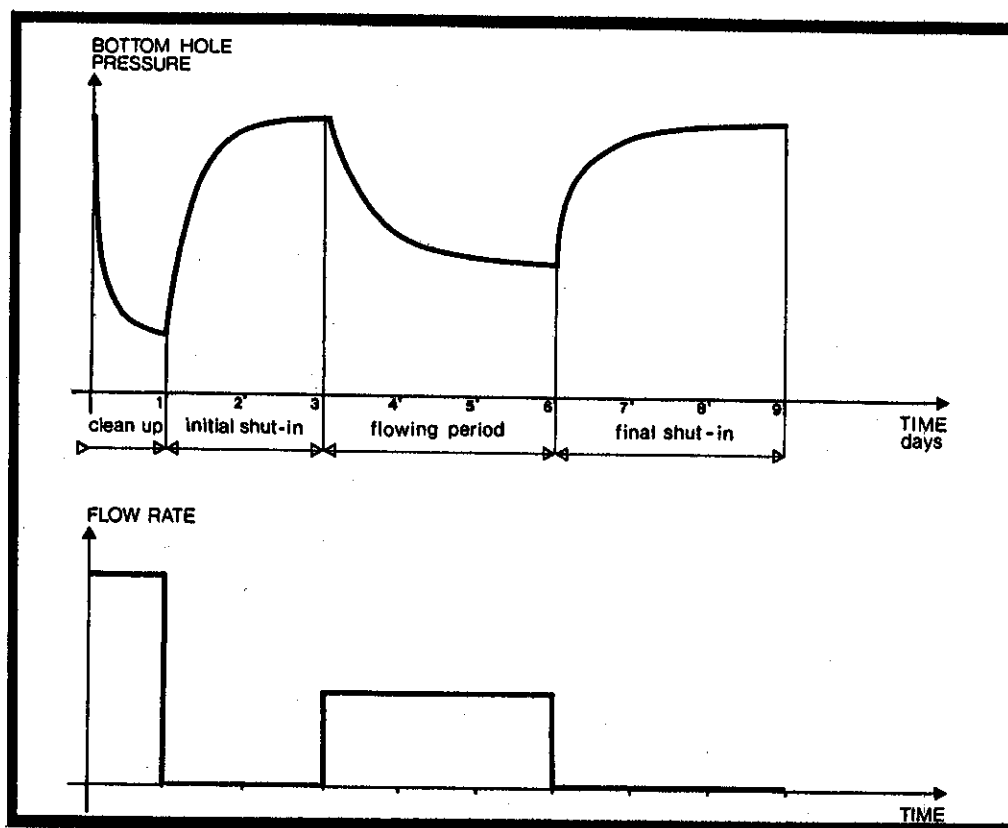


Fig. 9-4. Idealized diagrams of flow and pressure during an oil well test.

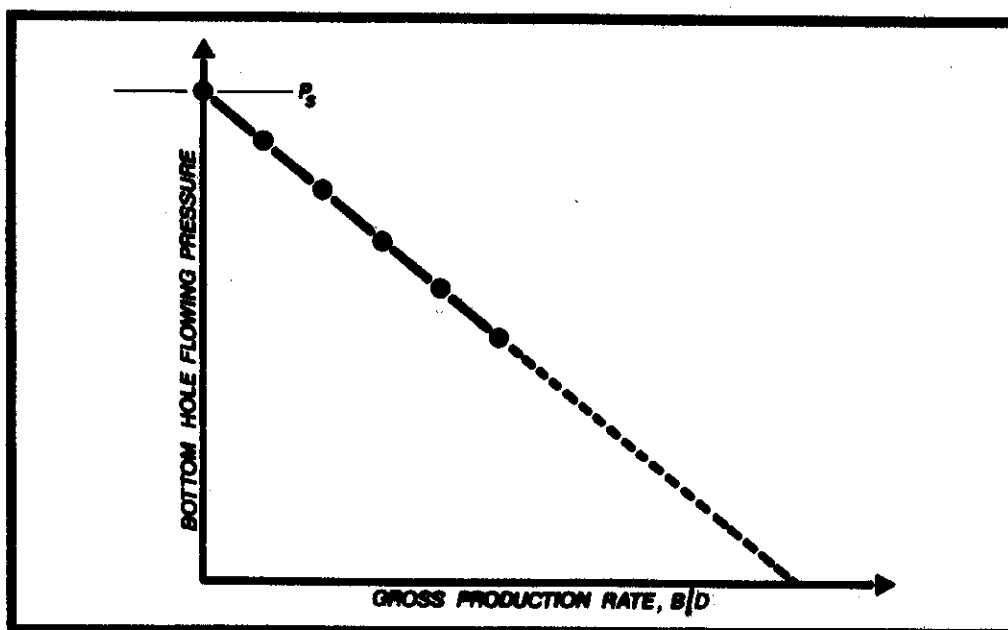


Fig. 9-5. Results of a multiple rate test are presented as a plot of P_{wf} vs. gross liquid production rate.

C. Testing procedures for high capacity gas wells :

Gas wells with an open flow potential of over 50 MMCFD are classified as high productivity wells. For these wells the back pressure test is the standard means of evaluating the productive capacity.

The well is usually cleaned up for a few to 24 hours and closed in for an equal period prior to testing.

In the back pressure test, bottom hole pressures and the corresponding surface flow rates are measured during a series of four different flow periods. The flow rate is increased in steps of equal time duration without shutting the well in between. Each flow period is about 4-8 hours duration, the time needed for stabilization often taken when the tubing head pressure variation is less than 2 psi/hour. The final shut in period is usually between 12 and 24 hours.

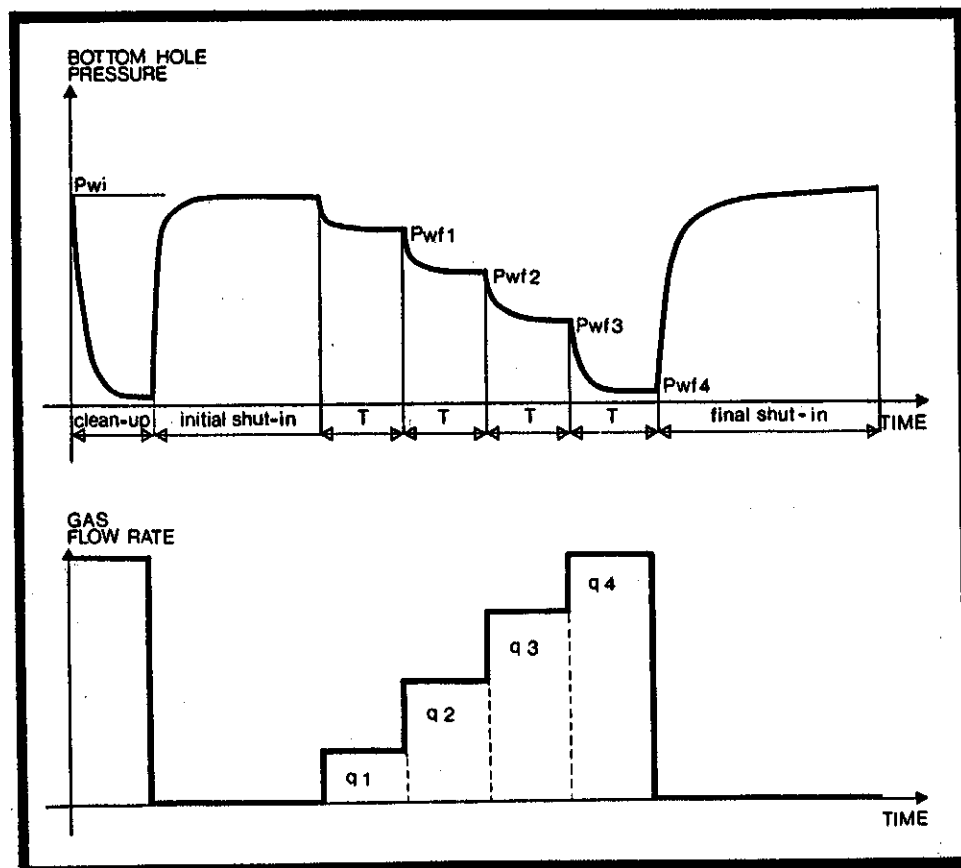


Fig. 9-6. Pressure and flow diagrams of a gas well back pressure test.

The results of a back pressure test are presented as a plot of surface production rate vs. $P_s^2 - P_{wf}^2$ on a log-log grid (as shown below).

Open flow potential is found by extrapolation of the performance line to P_s^2 , the flow rate which would occur when $P_{wf} = 0$.

Finding P_g is made by analysis of the pressure build up curve and is covered later in this chapter.

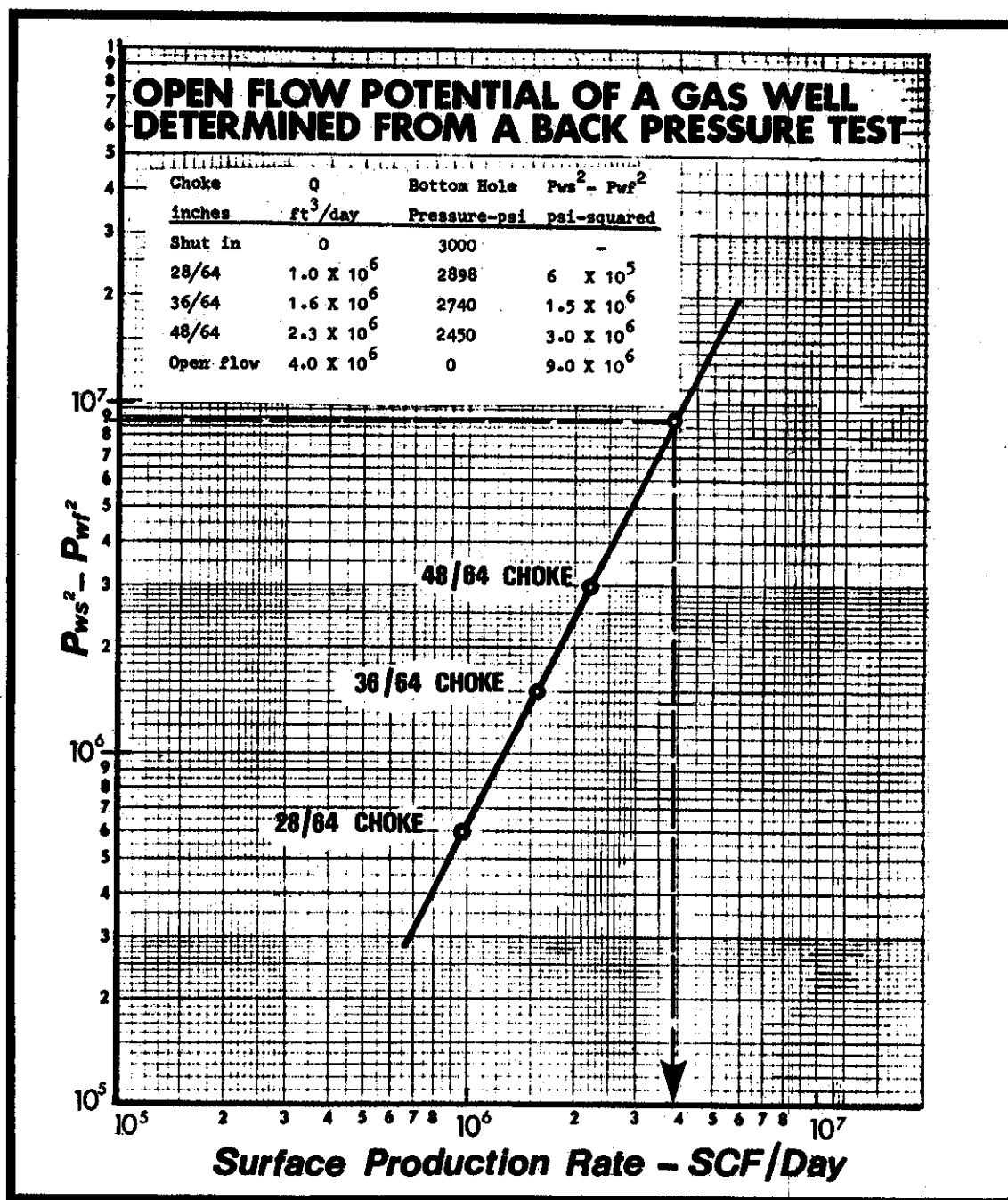


Fig. 9-7. Plot showing results of a gas well back pressure test.

Isochronal test procedures :

For gas wells where the stabilization time would be too long to use the back pressure test, an isochronal test technique may be used.

The modified isochronal test consists of flowing the well at four different rates for periods of equal duration. Between two flowing periods the well is shut in for a time equal to the test time.

The last flow period is extended until stabilized conditions 1 psi/hr tubing head pressure change are reached; then the well is shut in for an extended build up period of one to three days.

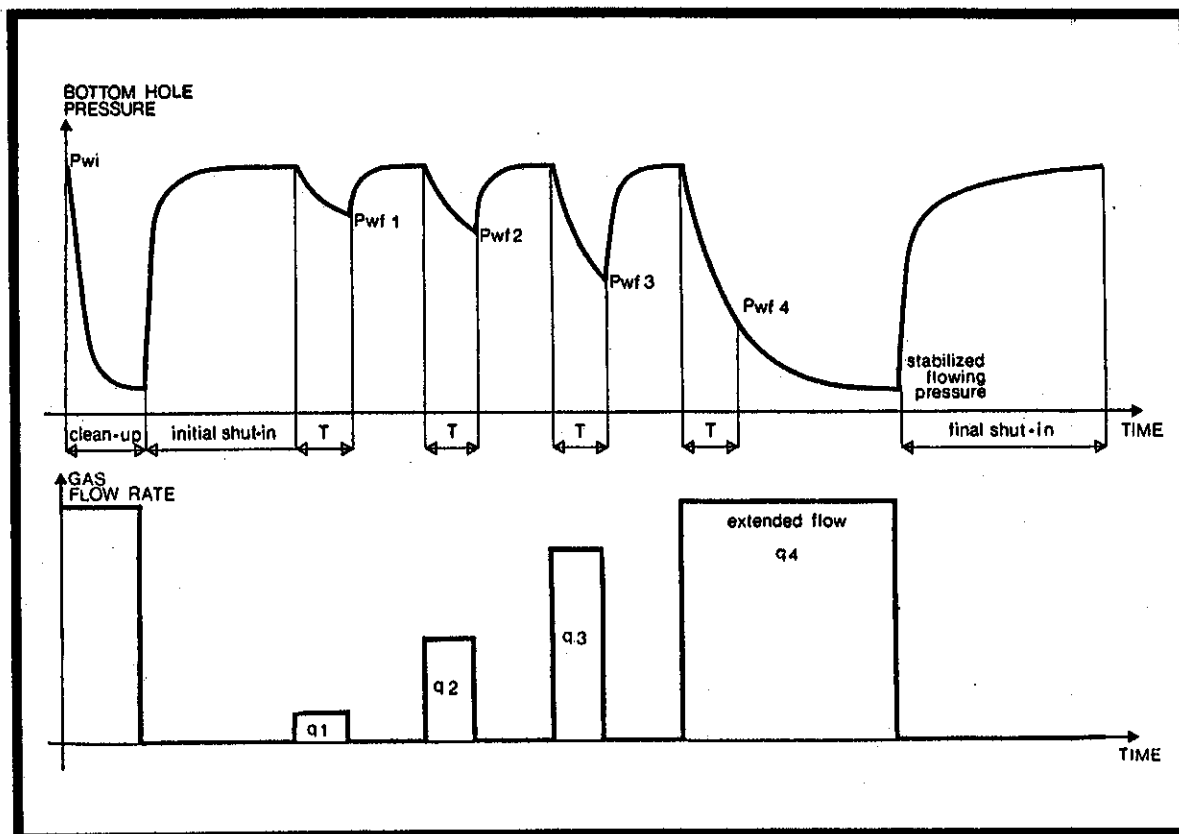


Fig. 9-8. Pressure and flow diagrams of a modified isochronal test of a gas well.

The data, Q vs. $P_S^2 - P_{wf}^2$ taken after 1/4 hr, 1/2 hr, 1 hr, 2 hrs etc., are plotted on log-log paper for each flow rate. On the extended test a point is plotted for stabilized flow near the end of the extended flow period.

Lines connecting data points for 1/4 hr, 1/2 hr and 5 hrs will be parallel but have a slope related to the productive capacity. A line of this slope passed through the final extended flow data point can be extrapolated to $P_S^2 - P_{wf}^2$ (when $P_{wf} = 0$) yielding the open flow potential.

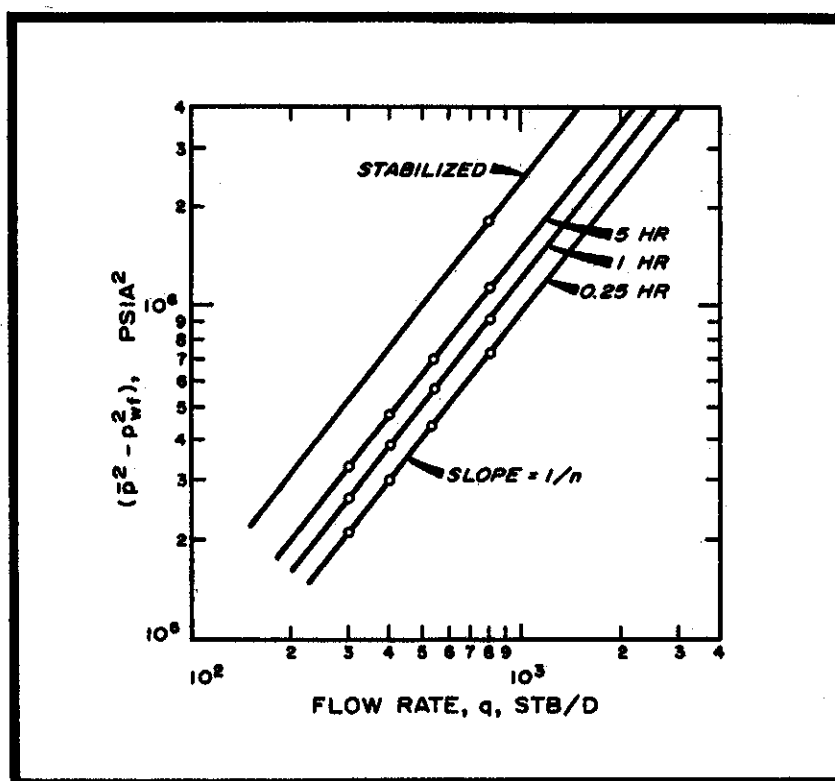


Fig. 9-10. Plot showing results of modified isochronal test data.

D. RFT - The wireline formation tester

Our Repeat Formation Tester is a wireline tool to measure formation pressures and to obtain formation fluid samples in the uncased well prior to completion. Two fluid samples of 1 or 2-3/4 gallons (up to 12 gallons for the second sample) plus any number of formation pressures are obtained per trip in the well.

The RFT has much in common with the DST however it must be kept in mind that the DST sample is larger and tests a zone while the RFT is essentially a point measurement. Where invasion from drilling fluids is severe and the mobility ratio $\left(\frac{k_o/u_o}{k_{mf}/u_{mf}} \right)$ favors filtrate movement, the RFT sample will be highly contaminated. On the other hand, the strength of the RFT is that pressures at a great number of points in the formation can be determined accurately, reliably, and safely at comparatively moderate cost.

Information obtained from pressure data :

- Determination of reservoir pressures
- Identification of formation fluids by establishing pressure gradients
- Location of gas/oil and oil/water contacts informations traversed by the bore hole
- Extrapolation of gradients to deduce fluid interfaces remote from the bore hole (in discovery or exploration wells before the original pressure distribution is disturbed by production).
- Identify producing units in partially depleted reservoirs
- Estimate gas/oil or oil/water contacts or discontinuities between wells
- Permeability indications.

The applications of RFT are discussed in more detail in the Appendix, Chapter 11.

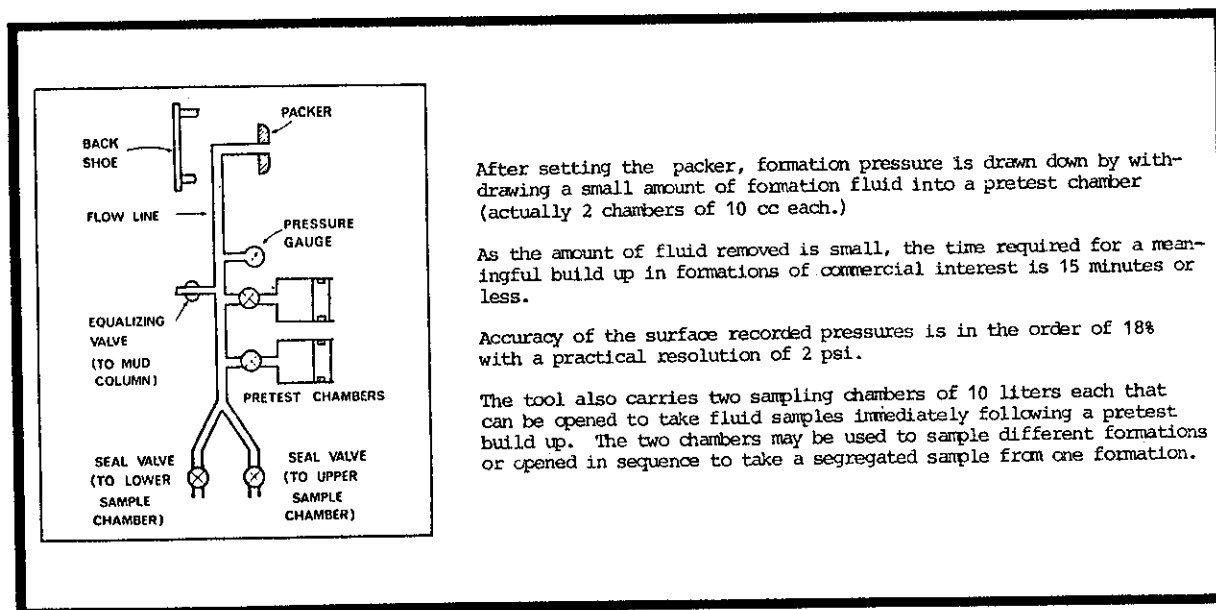


Fig. 9-11. Schematic diagram and tool functioning.

E. Transient test techniques and analysis

Any step change in the production rate of a well causes a pressure disturbance to be propagated radially outward in the formation at a rate determined by the hydraulic diffusivity, $\frac{k}{\phi c \mu}$, of the formation and fluid and is independent of the magnitude of the change causing the disturbance.

The phenomenon is analogous to the observation that the velocity of ripples caused by throwing a pebble into a pond is independent of the size of the stone.

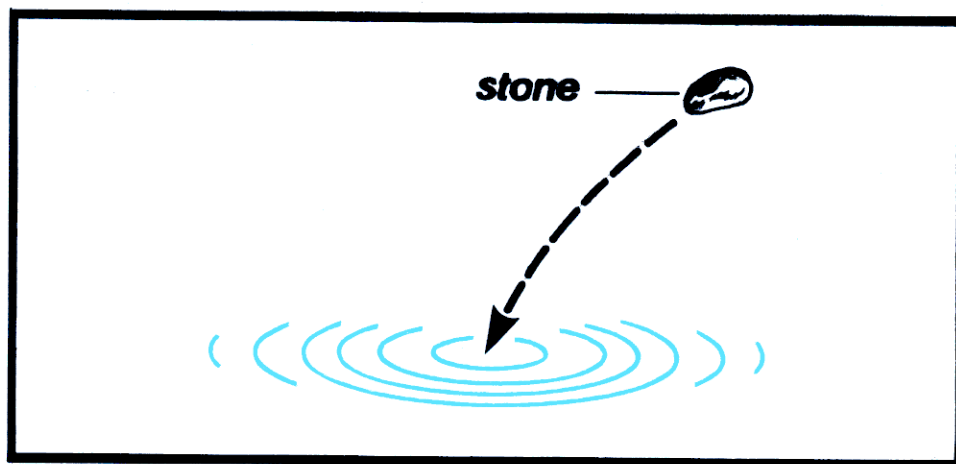


Fig. 9-12. Propagation of waves in a pond is analogous to propagation of a pressure wave through formation.

An analysis of the pressure changes in the well during the transient period can yield information on the properties of the reservoir at some distance from the wellbore. Transient pressure analysis of DST, LTT and RFT data may be analysed to find :

- permeability of gross reservoir, k_o or k_g
- reservoir heterogenities (faults, pinchouts)
- static reservoir pressure
- formation damage or skin.

Two types of pressure transient tests are used :

1) Pressure drawdown test

After the well has been shut in for a long enough period to establish static pressure conditions, the well is opened and produced at a steady rate while the pressure fall off is observed with a bottom hole gauge.

2) Pressure build-up test

After flowing the well long enough to establish quasi-steady state conditions, the well is closed in while the pressure build-up is observed with a bottom hole gauge.

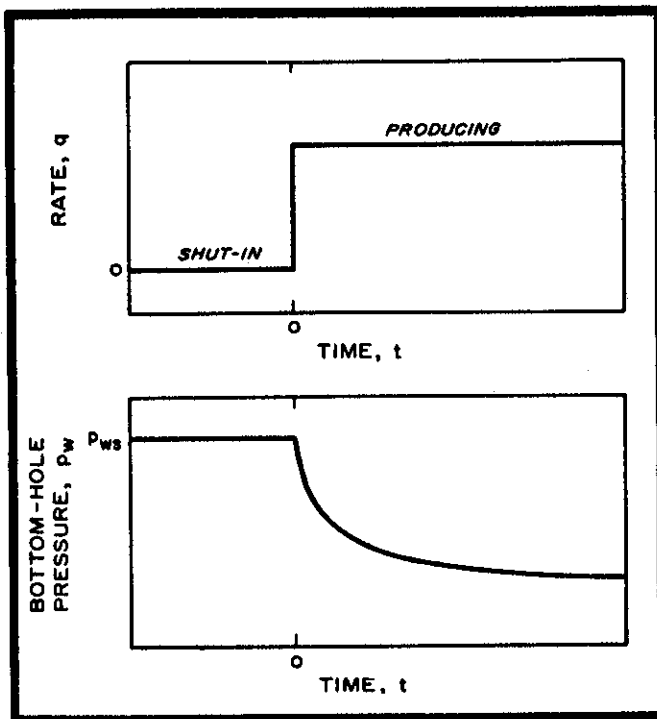


Fig. 9-13. Idealized rate schedule and pressure response for drawdown testing.

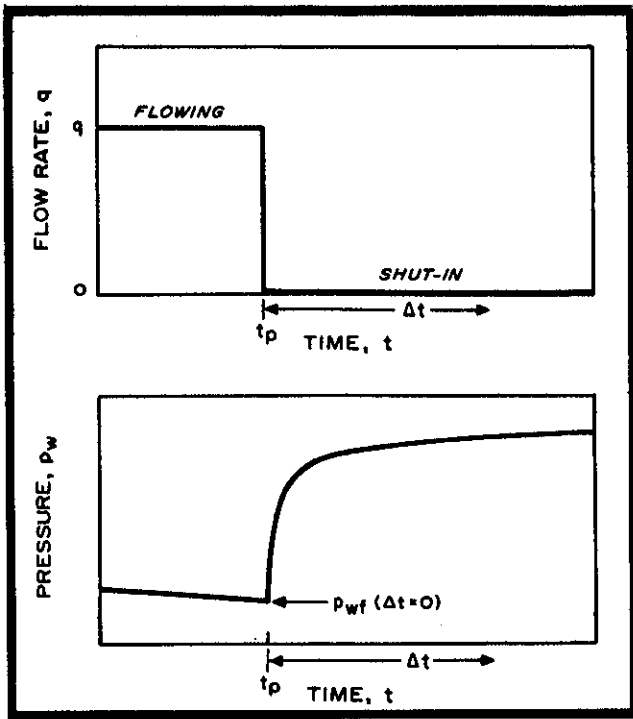


Fig. 9-15. Idealized rate and pressure history for a pressure build-up test.

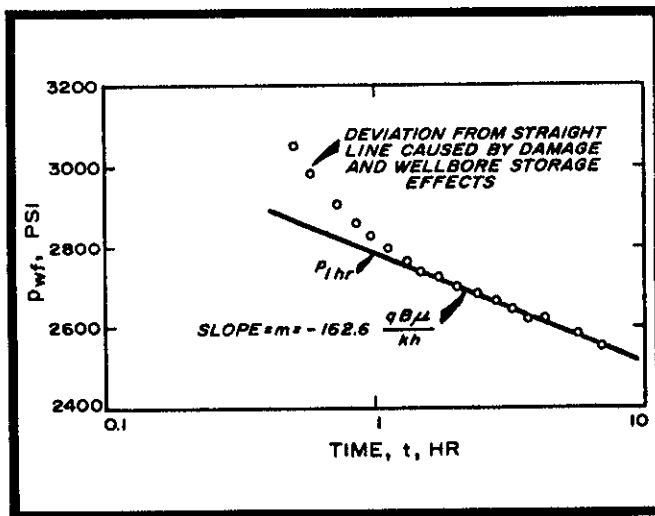


Fig. 9-14. Semilog plot of pressure drawdown data for a well with wellbore storage and skin effect.

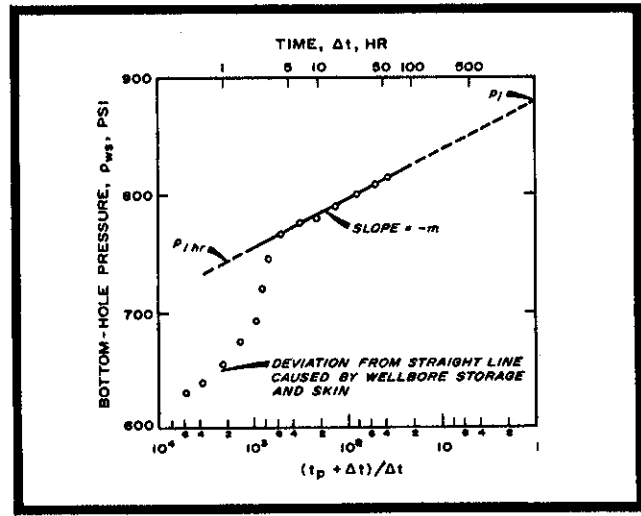


Fig. 9-16. Horner plot of pressure build-up data showing effects of wellbore storage and skin.

The physical significance of well behaviour during the drawdown period is easier to grasp than the case of build-up and will be treated first.

Transient test analysis is based on solutions to the differential equations describing fluid flow through porous media* during the infinite acting period which is generally met in practical situations at early transient times.

Pressure build-up testing finds wider applications than the drawdown testing, first because the shut in is free from the influence of skin effect, secondly because the calculation of P_s , the static reservoir pressure, is more straightforward and accurate. The drawdown method is used most commonly in LIT, DST and RFT analysis.

* Diffusivity equations for fluid flow through porous media

Liquid flow (low fluid compressibility)

$$\frac{2}{r^2} \frac{P}{r} + \frac{1}{r} \frac{P}{r} = \frac{1}{0.0002637} \frac{\phi \mu c_t}{k} \frac{P}{t}$$

Gas flow (high fluid compressibility)

$$\frac{2}{r^2} \frac{P^2}{r} + \frac{1}{r} \frac{P^2}{r} = \frac{\phi \mu}{k P} \frac{P^2}{t}$$

The above equations assume :

- horizontal single phase flow
- constant viscosity and compressibility
- homogenous isotropic formation
- negligible inertial and gravity forces
- pressure gradients are small

F. Drawdown behaviour

A pressure disturbance, caused by a step increase in production rate from zero to Q , is propagated radially outward. Beyond this disturbance, which is also the radius of drainage, no appreciable pressure change may be noted.

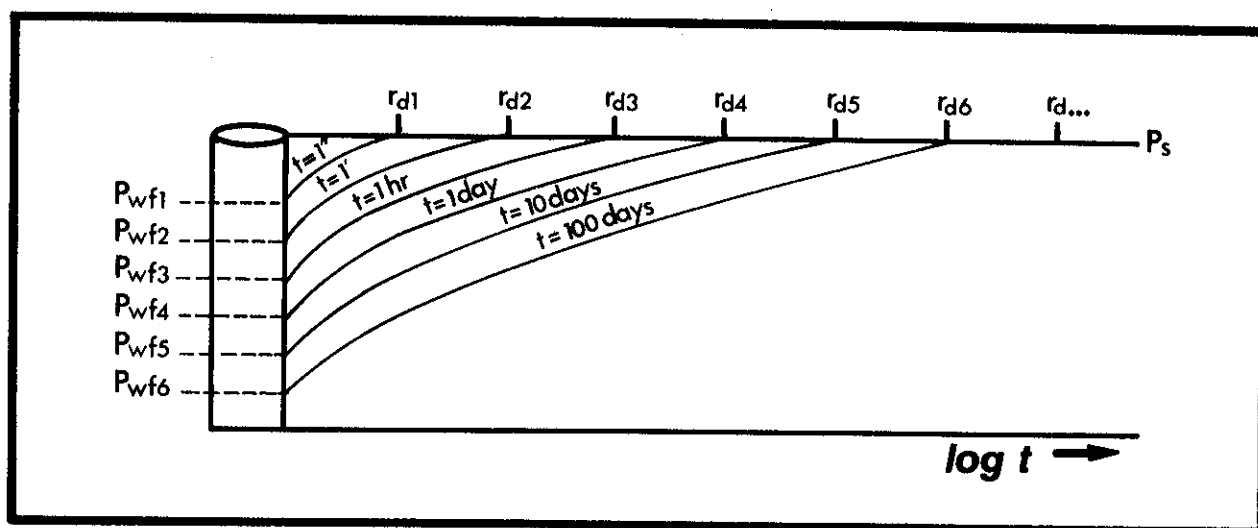


Fig. 9-17. Propagation of a pressure disturbance vs $\log t$.

The velocity of pressure wave propagation through porous rock is controlled by $\frac{k}{\phi c \mu}$, called the hydraulic diffusivity.

The radius of drainage, or the distance the pressure wave has traveled in a time t , after flow was initiated is given by :

$$r_d = 0.029 \sqrt{\frac{kt}{\phi c \mu}} \quad \text{where : } t = \text{time, hours} \\ r_d = \text{radius of drainage, feet} \\ \text{other units as per nomenclature}$$

As withdrawal continues at a constant rate the well pressure continues to decline. P_{wf} vs. $\log t$ will plot as a straight line on semilog grid.

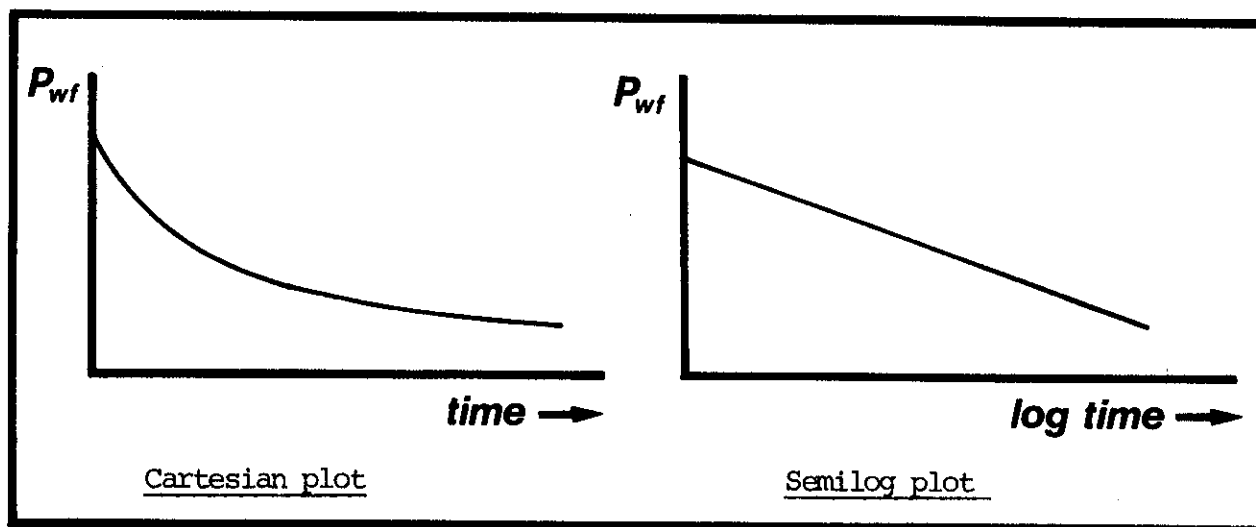


Fig. 9-18. Plots of well flowing pressure vs. time.

Boundary conditions and plot of P_{wf} vs $\log t$

During early times all pressure transients behave as a single well in an infinite reservoir. At later times, the effects of surrounding wells, reservoir boundaries and aquifers are observed in the pressure behaviour of the well under test.

Three different boundary conditions are considered in the figure below :

- infinite reservoir
- bounded cylindrical reservoir
- constant pressure outer boundary

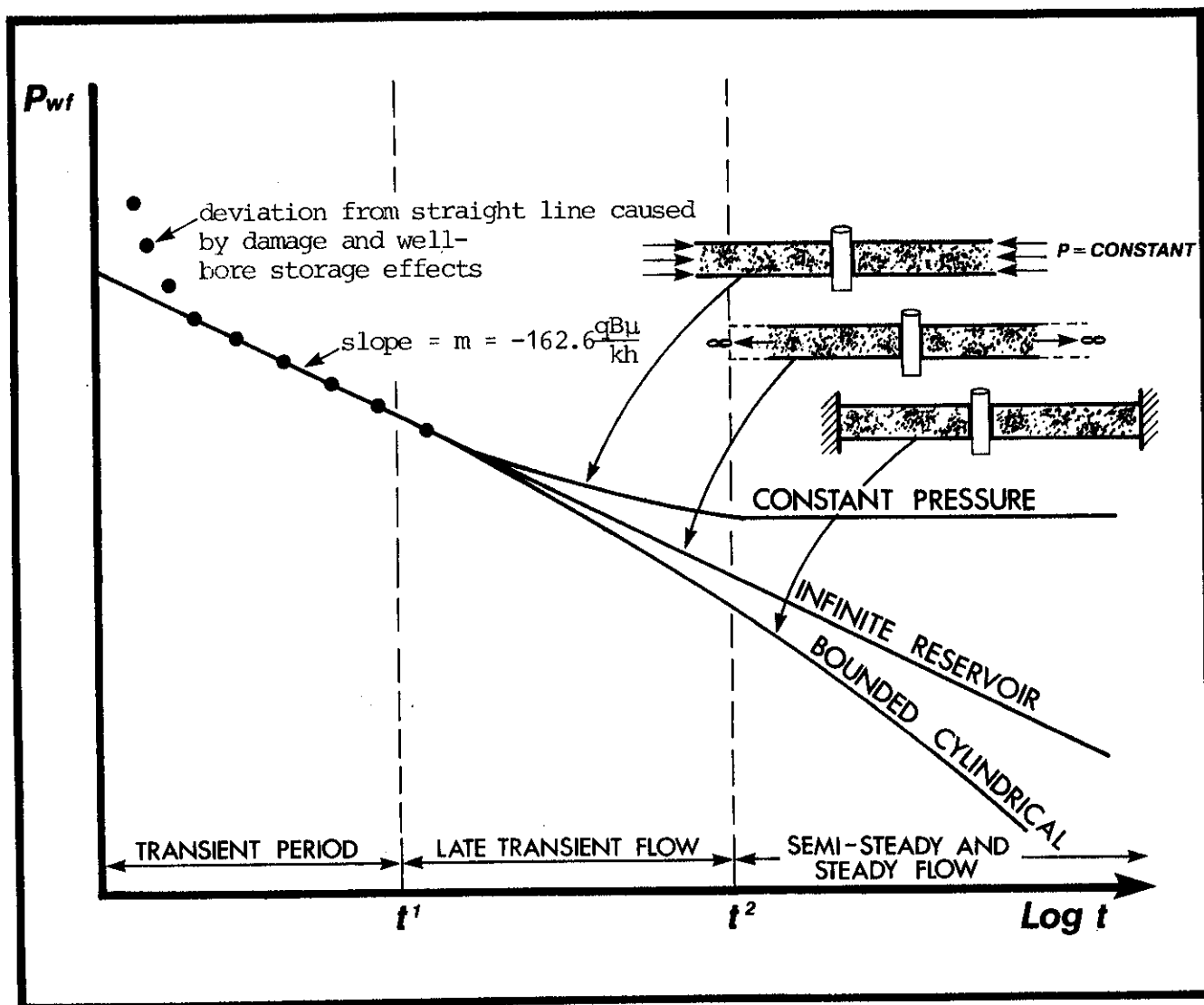


Fig. 9-19. Plot of P_{wf} vs. $\log t$ - different model reservoirs.

a) Bounded cylindrical reservoir

When the pressure disturbance encounters a closed barrier the well pressure continues to decline, but at a higher rate than if the boundary were not encountered.

The slope of this curve is :

$$\frac{P_{wf}}{t}$$

b) Constant pressure outer boundary

If a replenishable source is encountered such as a strong water drive or if well production is balanced by injection at the outer boundary the well pressure will stabilize to a constant value.

The slope of this curve becomes :

$$\frac{P_{wf}}{t}$$

c) Infinite reservoir

As fluid withdrawal continues at a constant rate, the disturbance continues to move outward into the infinite reservoir. The well pressure declines along a straight line when plotted vs. $\log t$.

The slope of this curve is :

$$\frac{P_{wf}}{t} = \frac{Q \mu}{4\pi kh} \cdot \frac{1}{2,246 \alpha/\pi_w^2 t} = \frac{Q \mu}{4\pi kh} \frac{1}{t_D}$$

G. Pressure build-up analysis

Pressure build-up is the most widely form of transient testing methods.

Every build-up test is preceded by a constant flow period, during which a high, stabilized flow is achieved. In practice, this flow period may vary from over several days or months in a producing well, to hours in the DST, or minutes in the RFT test.

The well is then shut in and the pressure recorded and the pressure allowed to build up, as shown in the idealized diagram below. At any time greater than t_p , build-up pressure obtained is a result of the superposition of pressure drawdown at time t (for rate Q) and build-up effect for the rate $(0-Q)$.

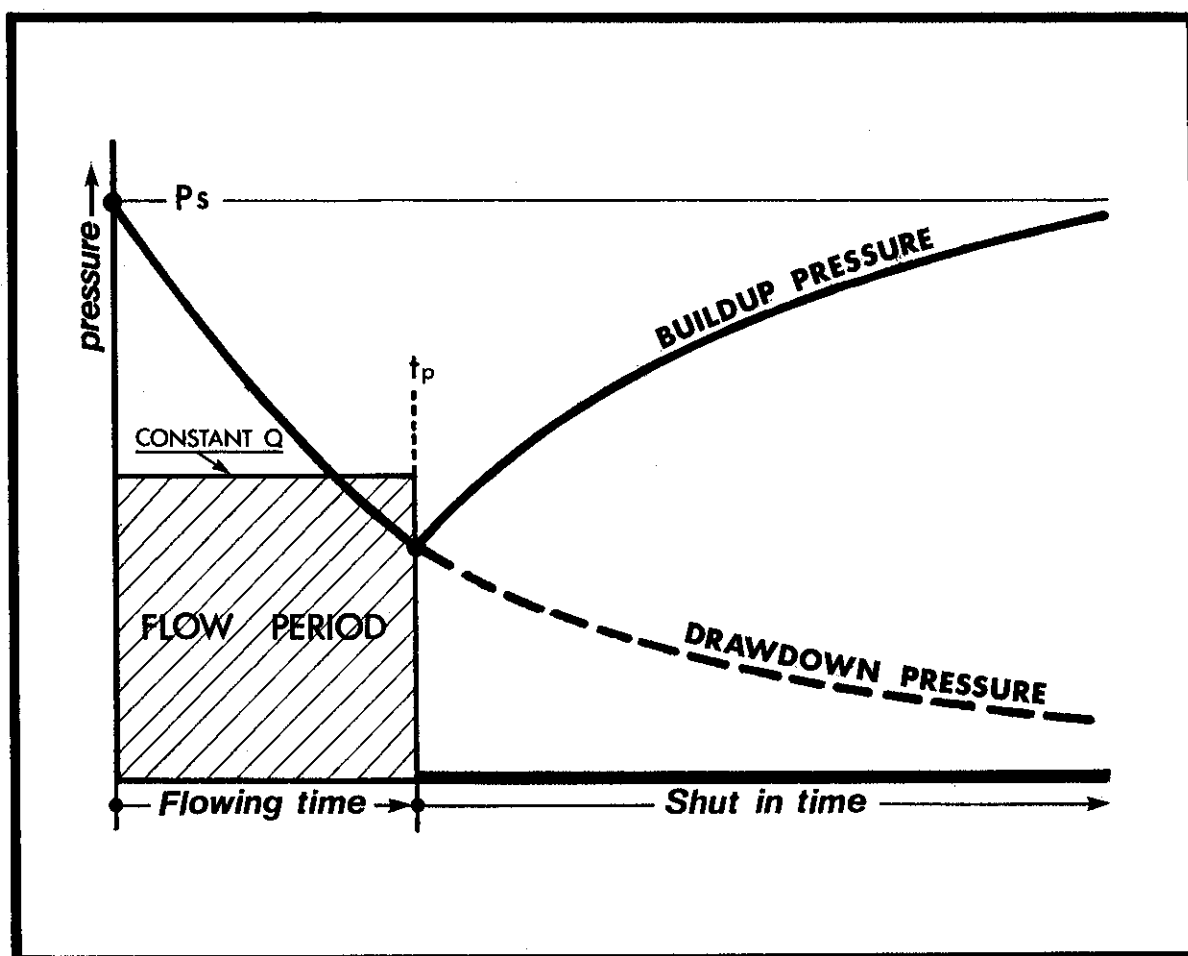


Fig. 9-20. Idealized flow rate and pressure vs. time, Cartesian coordinates.

Two classical plots of the build-up data are possible :

- 1) The Horner plot, in which P_{ws} is plotted vs $\log \frac{t + \Delta t}{t}$
 t is the time of production before shut in and Δt is the time following shut in when the pressure point being plotted is read off.
- 2) The MDH (Miller, Dyes, Hutchinson) method, a plot of P_{ws} vs $\log t$, the time after shut in.

Both plot as a straight line in the infinite acting period and show deviations at early time resulting from skin damage and wellbore storage and boundary effects at long times. The Horner plot gives better definition of slope in the infinite acting period than the MDH and extrapolates to P^* which is close to P_i , the initial formation pressure when flowing times are short as in the case of a DST or RFT. The MDH finds application in build-up analysis of finite reservoirs following long production periods where P^* found by the Horner's method leads to a pressure somewhat higher than the true P_i . The MDH method is given at the end of this chapter.

The aim of build-up analysis is determination of :

- effective formation permeability (k_o or k_g)
- static formation pressure, P_s
- formation damage or skin effect, S
- productivity ratio
- reservoir heterogenities (faults, pinchout etc.)

1) Horner's method

The pressure build-up equation in infinite reservoir conditions as described by Horner :

Oil wells

$$P_{ws} = P_i - \frac{162.6 q B_{\mu}}{kh} \log \frac{t + \Delta t}{\Delta t}$$

Gas wells

In a gas well, the difference is that B_g cannot be taken as a constant and :

$$B_g = \frac{ZT P_o}{T_o} = .02829 \frac{ZT}{\frac{P_i + P_{ws}}{2}}$$

Introducing B_g in the Horner equation and taking into account that gas flow rates are measured in SCF/D, the Horner equation for gas buildup becomes :

$$P_{ws}^2 = P_i^2 - 1637 \frac{Q \mu ZT}{kh} \log \frac{t + \Delta t}{\Delta t}$$

where Q is MSCF/D

Note : When the difference in $P_{ws}-P_i$ is small, e.g. 500 psi, an average value of B_g may be taken for mid point pressure and B_g assumed to be constant. The Horner analysis may then be made as for liquids without significant loss in accuracy.

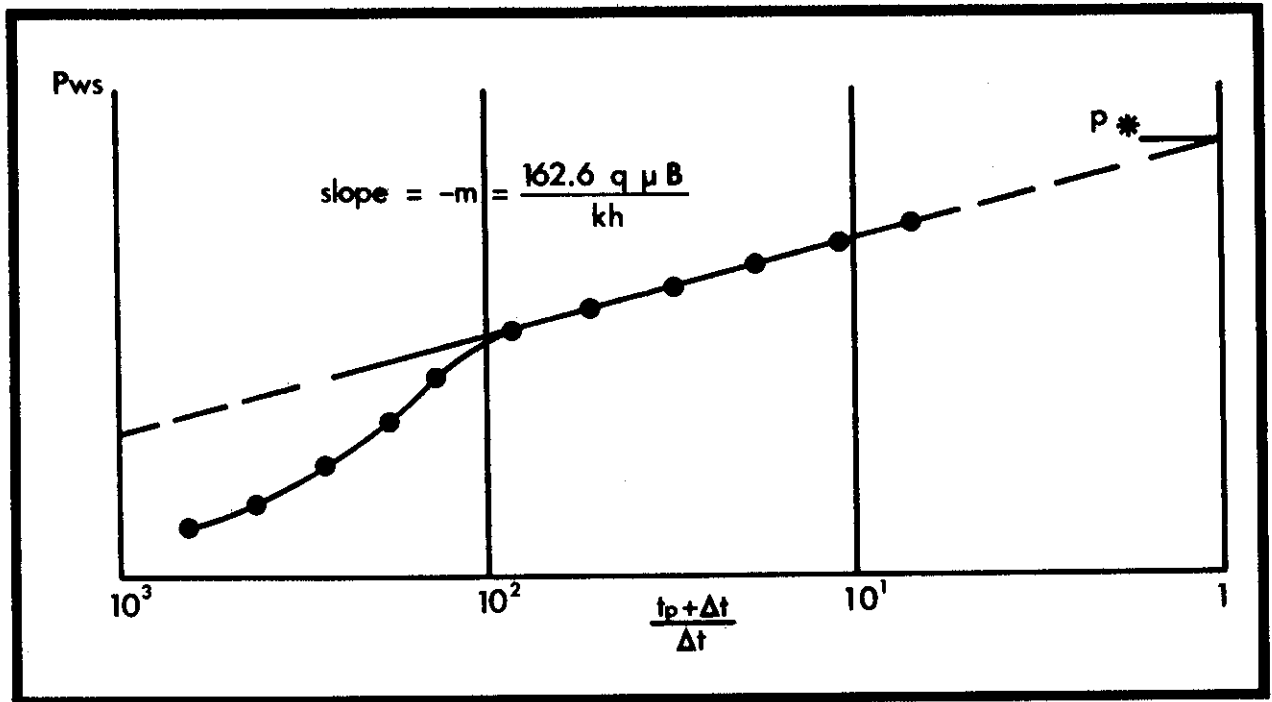


Fig. 9-21. The Horner plot.

a) Permeability determination

In the infinite acting zone the slope of the build-up curve in psi/cycle is related to permeability by :

$$-m = \frac{162.6 q \mu B}{kh} \quad (\text{for oil well})$$

$$-m = \frac{1637 \mu q Z T}{kh} \quad (\text{for gas well})$$

b) Static reservoir pressure determination

Extrapolation of the straight line portion of the curve to $\frac{t + \Delta t}{\Delta t} = 1$

will intercept at the build-up pressure of an infinite reservoir

This condition exists at $\lim_{\Delta t} \frac{t_p + \Delta t}{\Delta t}$ or when $\frac{t_p + \Delta t}{\Delta t} = 1$.

As stated previously this extrapolation gives acceptable results when t_p is relatively short as in the DST or RFT build-up. Where the well has been produced for a long period of time before shut in, P^* may be less accurate.

c) Determination of formation damage or skin effect

An estimation of skin may be made by extrapolating the straight line back to $\Delta P_{ws} = 1$ hour and reaching $P_{1h} - P_{wf}$ from the plot.

This value is used in the relation below to find S, the dimensionless pressure drop due to skin effect.

$$S = 1.151 \frac{P_{1h} - P_{wf}}{m} - \log \frac{k}{\phi c r_w^2} + 3.23$$

where : S = dimensionless pressure drop due to skin effect

P_{wf} = bottom hole pressure prior to shut in, psi

P_{1h} = bottom hole pressure - after one hour shut in
read from extrapolated straight line portion
of build-up curve, psi

r_w = well radius, feet

This equation is essentially a comparison between the permeability near the wellbore and the permeability deeper in the formation.

When S is positive, it is the result of formation damage.

When S is negative, formation is improved as by hydraulic fracturing.

The pressure drop at the wellbore due to skin effect is calculated by :

$$\Delta p = 0.87 \times 5 \times m \quad \text{in psi}$$

For gas wells, the above equations may be used to calculate skin and

Δp skin if P_{ws} vs. $\log \frac{t_p + \Delta t}{\Delta t}$ was used to calculate m and k.

2) MDH (Miller, Dyes and Hutchinson) method for finite reservoirs

Where finite conditions prevail or the well has been produced for a long period of time to reach the semi-steady or steady state flowing conditions. The Horner's method should not be used to obtain the static reservoir pressure. The general procedure of the MDH method is :

a) Plot P_{ws} vs. $\log \Delta t$

b) Calculate $kh = \frac{162.6 \mu QB}{m}$ (as for Horner's method)

c) Calculate dimensionless time Δt_D :

$$\Delta t_D = \frac{0.000264 k \Delta t}{\phi \mu C r_e^2}$$

Δt is the end point of straight line portion

r_e external radius of boundary which should be assumed according to the well spacing or just estimated

d) With Δt_D and chart fig. 9-23 define Δp_D

e) Calculate the reservoir pressure :

$$P = P_w(\Delta t) + \frac{m}{1.15} \Delta p_D$$

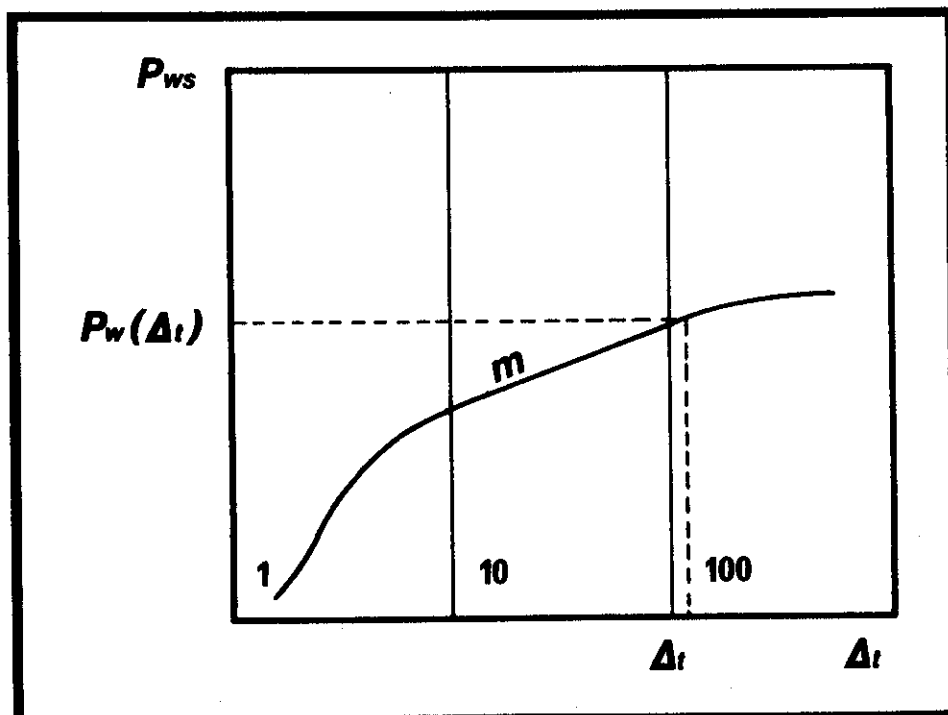


Fig. 9-22. MDH Interpretation method plot.

If the proper straight line portion was chosen, the calculated value from equation in (e) above should be between 10^{-2} and 10^{-1} .

If the calculated value does not fall between these values, then another slope must be selected and a new "K" and " Δt_D " calculated.

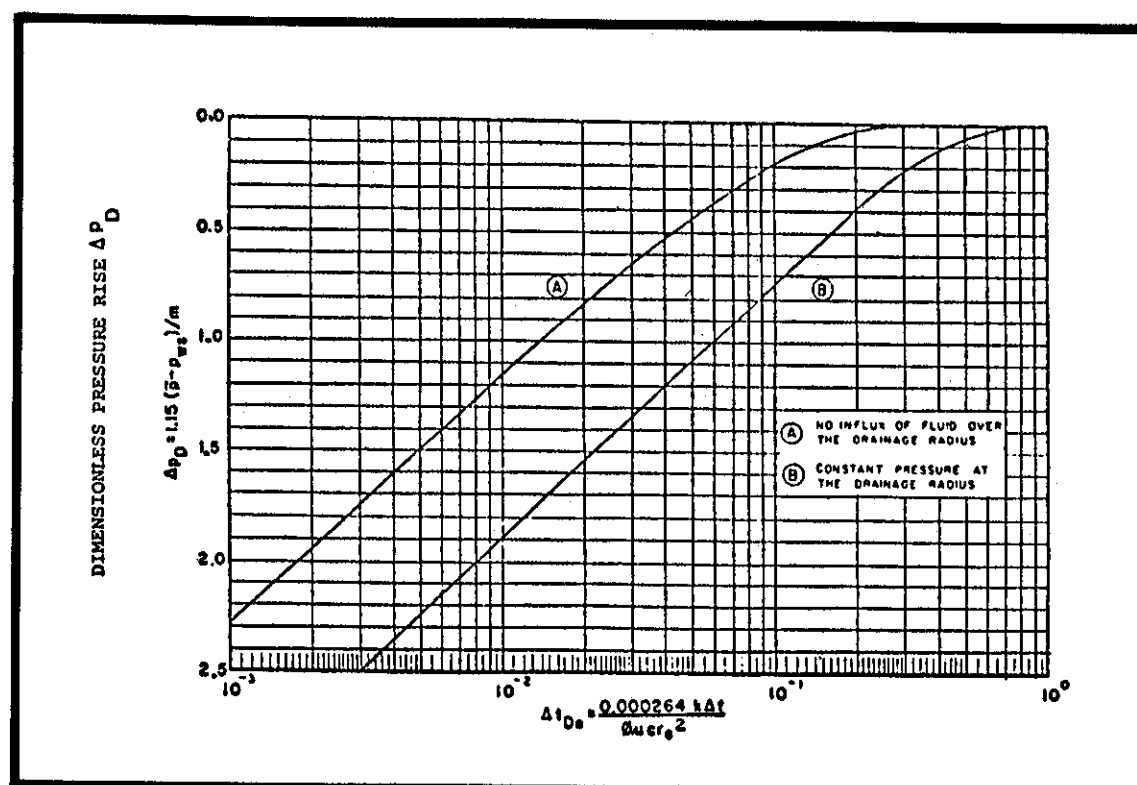


Fig. 9-23. Dimensionless shut-in time.

H. Remarks concerning the slope and shape of pressure drawdown curves

- 1) Slope of the infinite acting section portion of the curve and kh

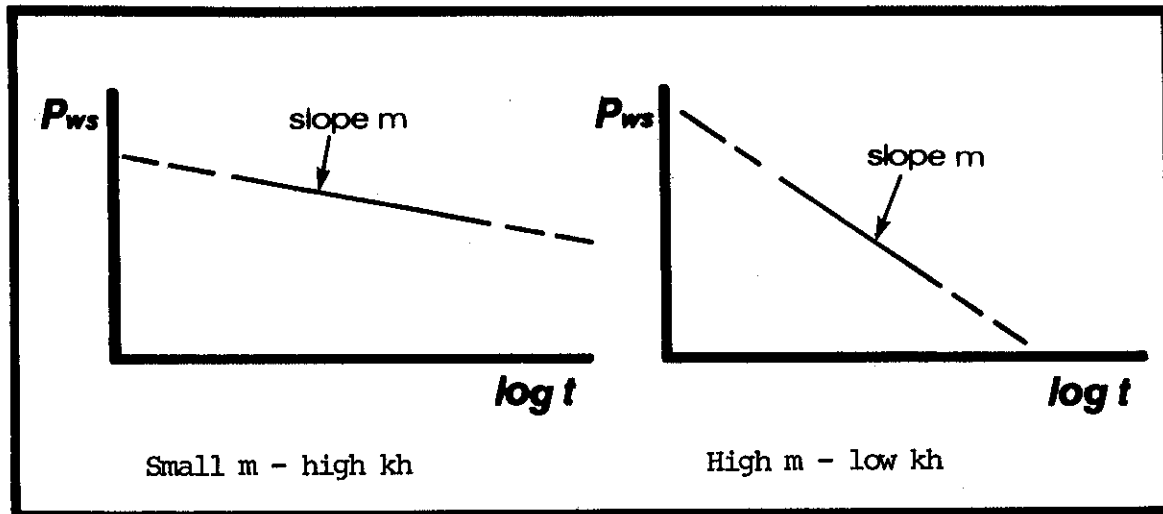


Fig. 9-22. Slope of drawdown curve in high and low kh formation.

- 2) Boundary at t'

An increase in slope by a factor of approximately two is an indication that a barrier has been encountered and that flow after time t' is from cylindrical zone π not 2π . The radial distance to barrier at time $= t'$ may be calculated from the radius of drainage equation :

$$r_d = 0.029 \frac{kt}{\phi \mu c}$$

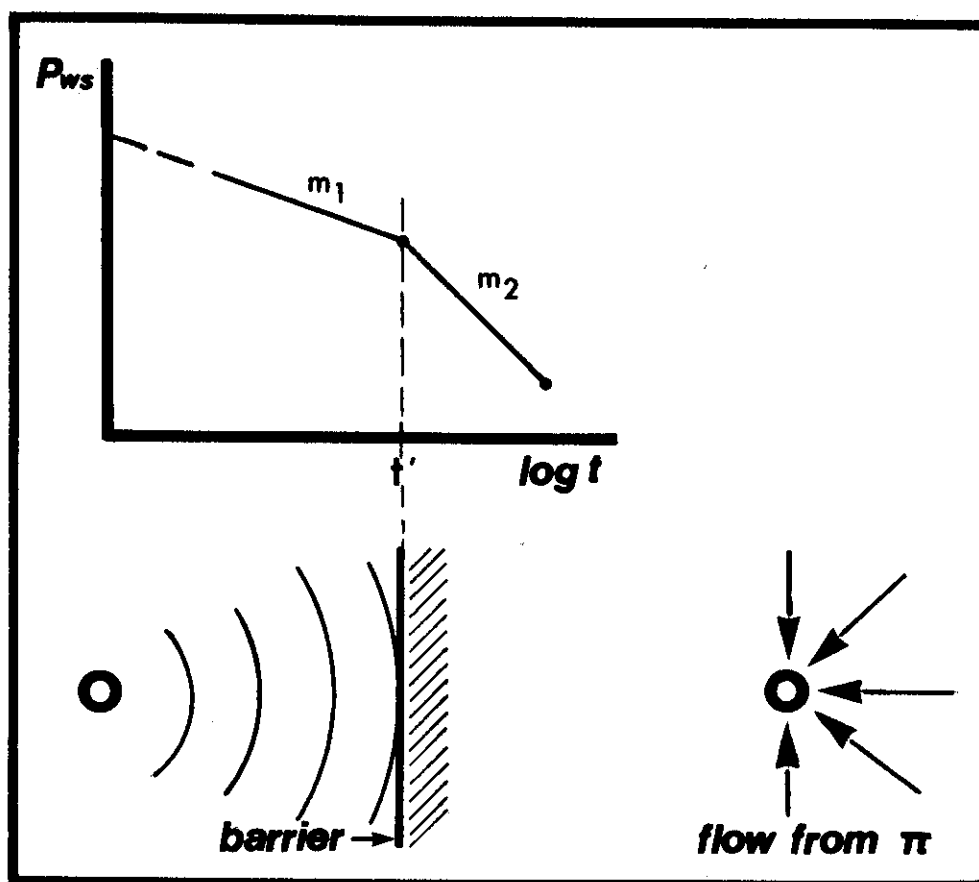


Fig. 9-23. Reservoir boundary encountered after time t' .

3) Change in slope at t'

Where $m_1 > m_2$ indicates an increase in permeability at t' . There are various possibilities :

- a) indication that a fracture has been reached
- b) increase in bed thickness h , as in non-continuity of a scale bed.

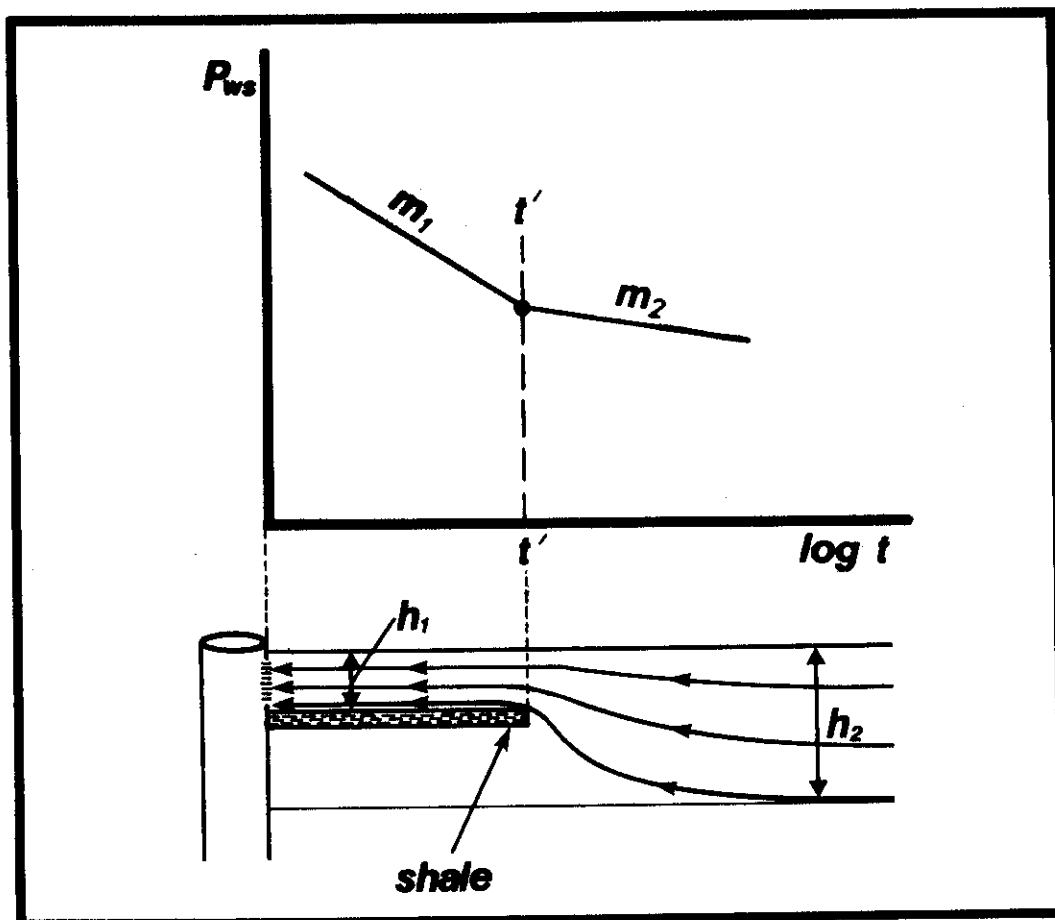


Fig. 9-24. Change in slope indicates change in kh after time t' .

FRACTURED RESERVOIRS

10

A. Introduction

A fractured reservoir is a dual porosity system consisting of primary intergranular matrix interlaced by a network of channels comprising the fracture network.

If the fracture system is extensive, and has considerable surface area contact with the matrix, oil is easily transferred into the fracture system from where it is delivered to the producing wells with very little loss of pressure. Thus a fractured reservoir is capable of surprising performance as compared with a conventional reservoir of similar matrix porosity and permeability.

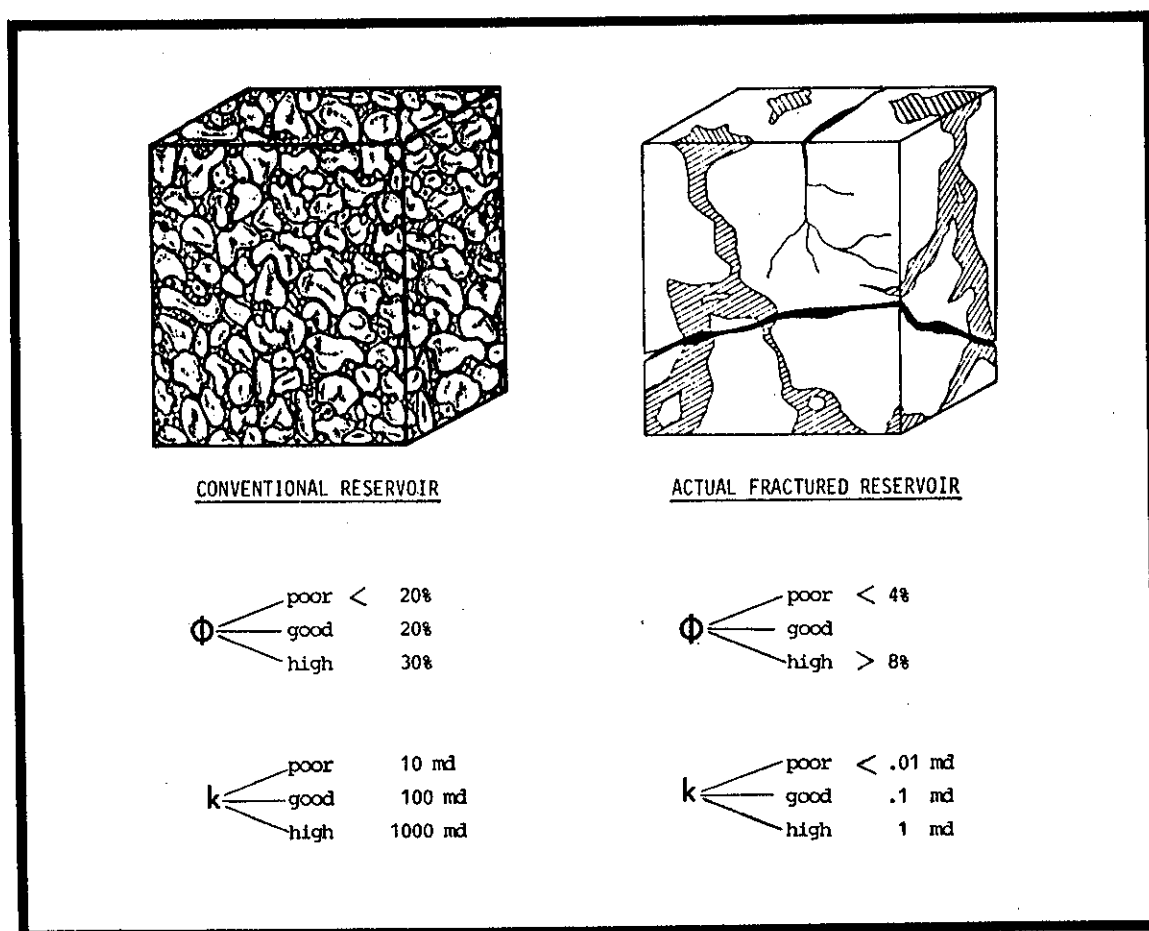


Fig. 10-1. Comparison of matrix porosity and permeability of conventional and fractured reservoirs.

B. A physical description of a fractured reservoir

The essential characteristic of a fractured reservoir is a network of fractures oriented in both horizontal and vertical directions extending throughout the reservoir. This assures tremendous contact area of the fracture channels with the matrix and almost unrestricted movement of fluids in any direction - figure 10-2.

A formation with localized fractured areas or with hydraulically produced fractures in the vicinity of the wells does not perform as an unconventional reservoir.

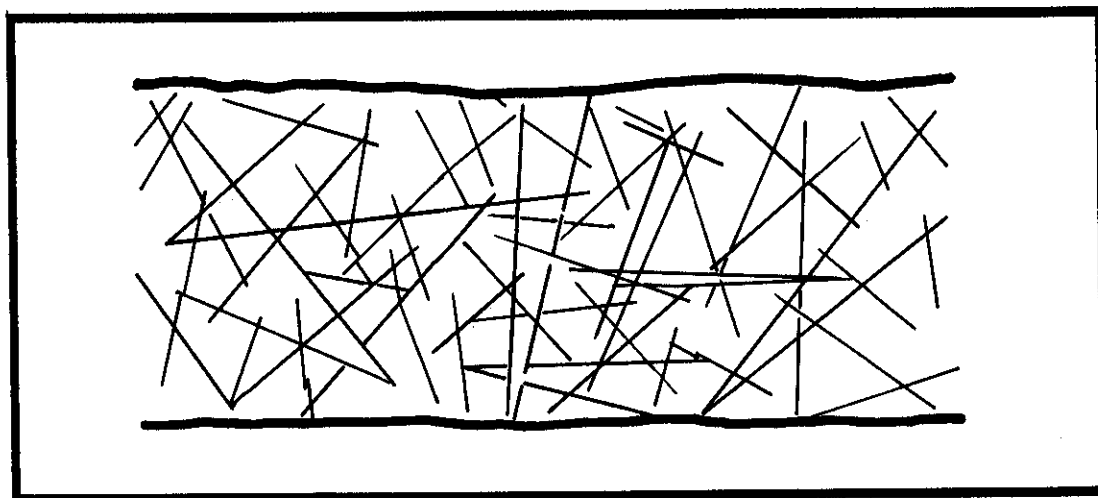


Fig. 10-2. Fractures must be oriented in intersecting planes and extend throughout the reservoir for the reservoir to exhibit unconventional performance.

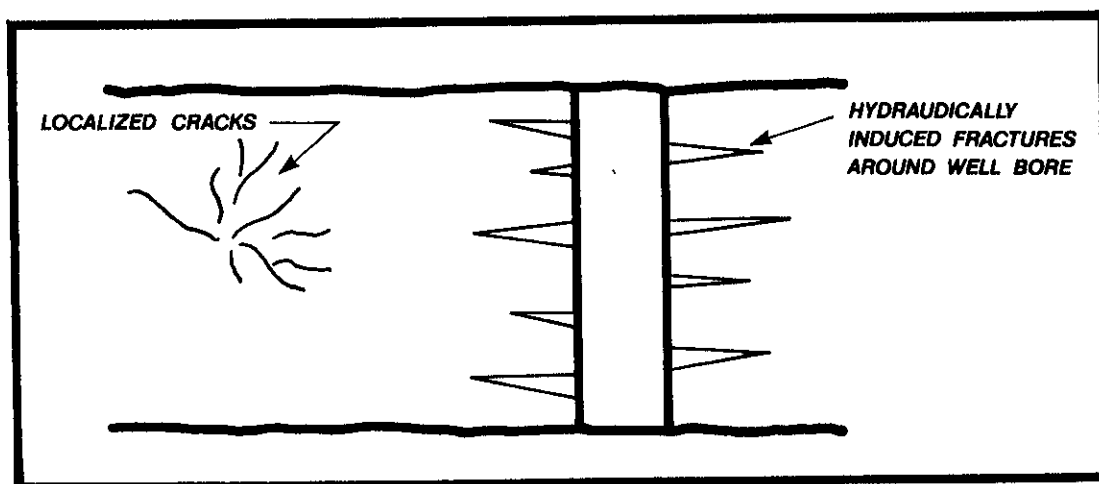


Fig. 10-3. Localized or mechanically induced fractures do not achieve fractured reservoir performance.

C. A comparison of conventional and fractured reservoir performance

1) Productivity index and pressure drawdown

The productivity index in a low permeability conventional reservoir is around 5 STD/D/psi, while in a fractured reservoir of similar matrix permeability the productivity index is usually over 10 STB/D/psi and often reaches 100 or higher.

Figure 10-4 compares the pressure drop within a typical fractured formation with the pressure drop of a conventional formation producing at equal rates.

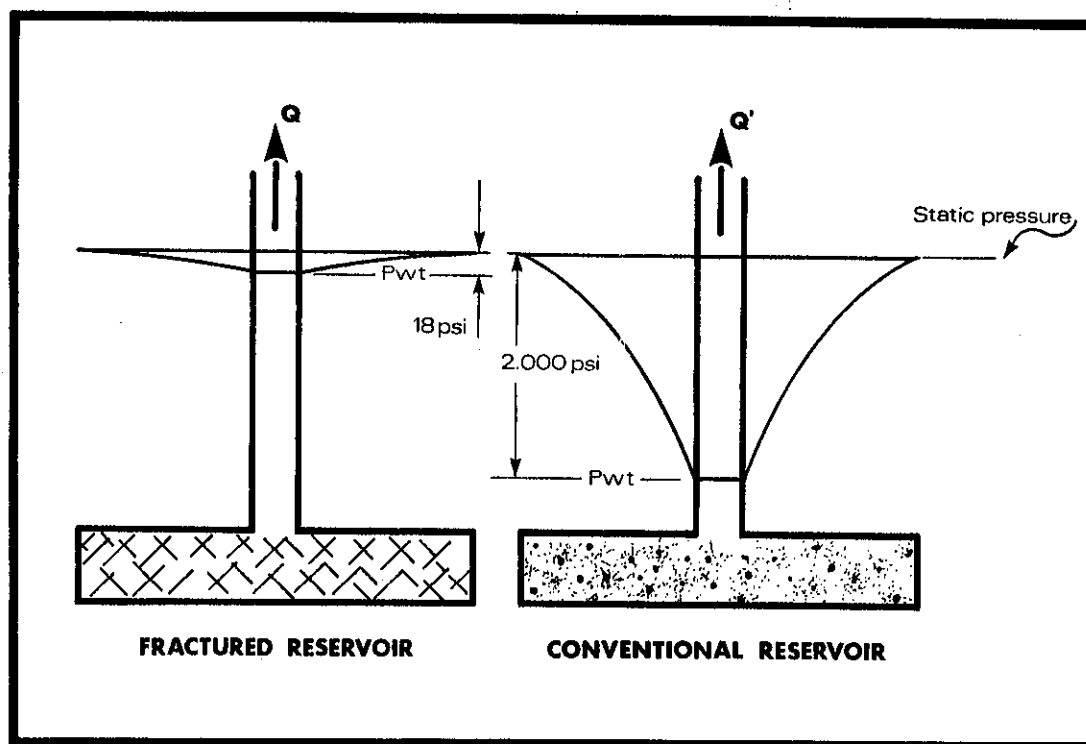


Fig. 10-4. Comparison of pressure drawdowns for typical fractured and conventional reservoirs producing at equal rates.

2) Producing GOR

Producing gas-oil rate is substantially lower in a fractured reservoir during reservoir depletion compared with GOR of a conventional reservoir. This is mainly due to the tendency of the gas released as a result of reservoir pressure decline to move up through the fractures toward the gas cap. As consequence, the gas moving toward the well will be very much reduced - fig. 10-5, and consequently GOR will be low.

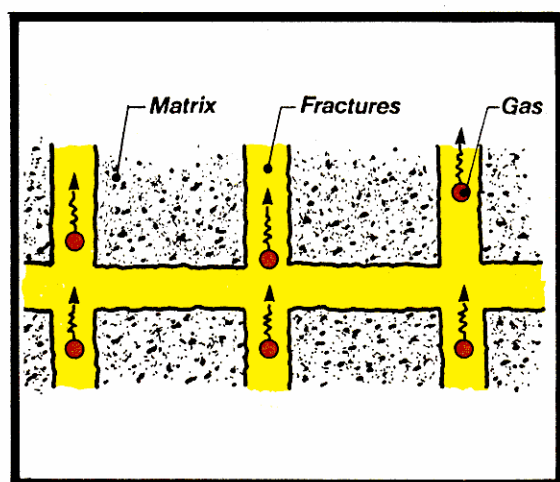


Fig. 10-5. Mechanism of gas segregation in a fractured reservoir

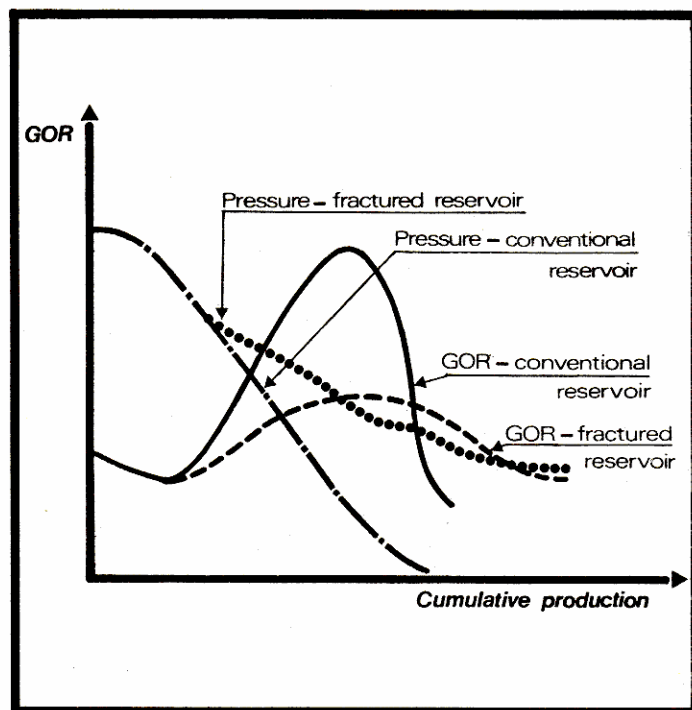


Fig. 10-6. Gas-oil ratio and pressure trends for solution gas drive conventional and fractured reservoirs

3) Pressure decline

Pressure declines at a substantially lower rate during depletion of a fractured reservoir than in the conventional reservoir, see fig. 10-5. This more efficient behaviour is the result of a natural "pressure maintenance" caused by "migration" of liberated gas through the fracture system to form a gas cap, and the performance (of a dissolved gas drive) in a fractured reservoir can approach that of an equivalent conventional reservoir in which 80% of the produced gas is reinjected in the reservoir. That is, a fractured reservoir shows a capability of a self-conservation of its energy.

4) Fluid interfaces and transitions - fig. 10-6

The absence of the transition in the gas/oil or in the oil/water zone. A comparison in the figure of the next page shows that transitional zones in a conventional reservoir do not exist in a fractured reservoir. In fractured reservoirs, there is little communication between matrix "blocks" since they are separated by fractures. Fluid interfaces on fractured reservoir scale takes place only within the fractures network and clearly delineates the two fluids contact without any transition zone.

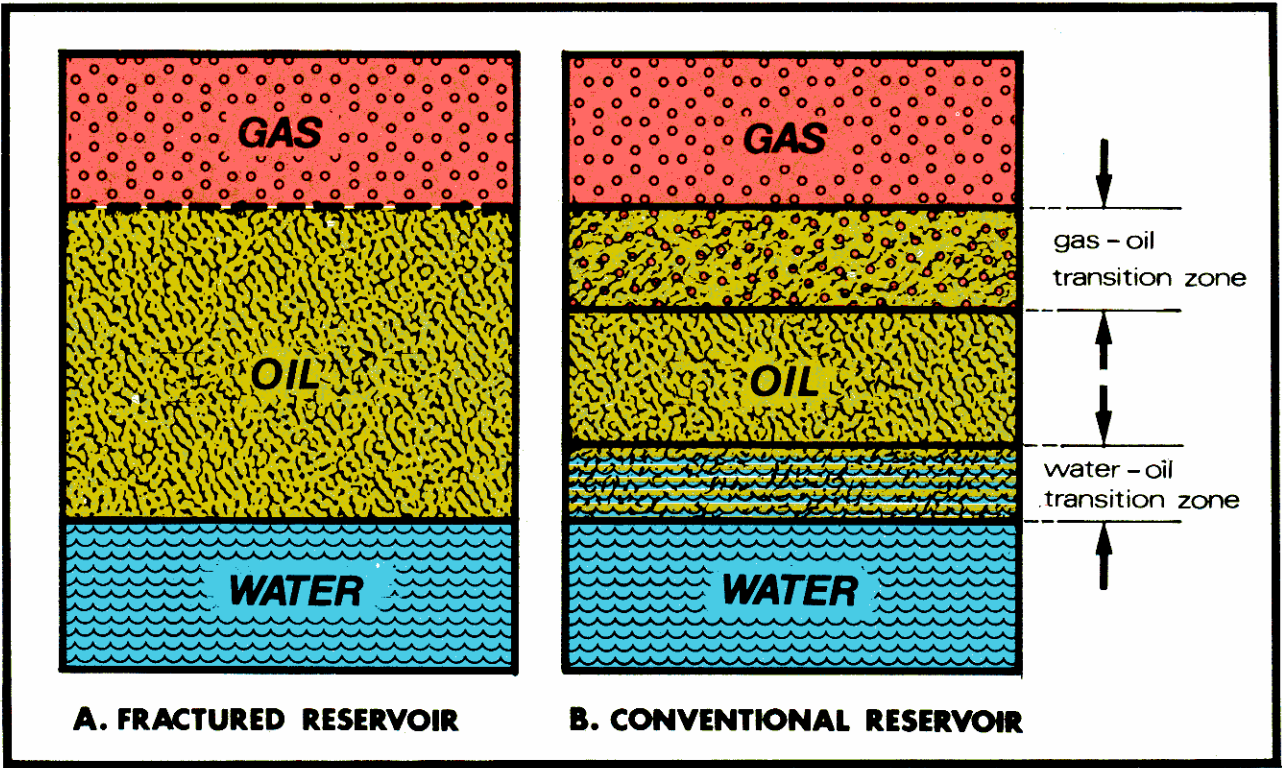


Fig. 10-7. The transition zone in conventional and fractured reservoirs.

5) Water cut - figure 10-8

Water cut in the fractured reservoir is essentially a function of production rate while in the conventional reservoir it depends on the conditions causing the breakthrough, in both cases coning and displacement processes.

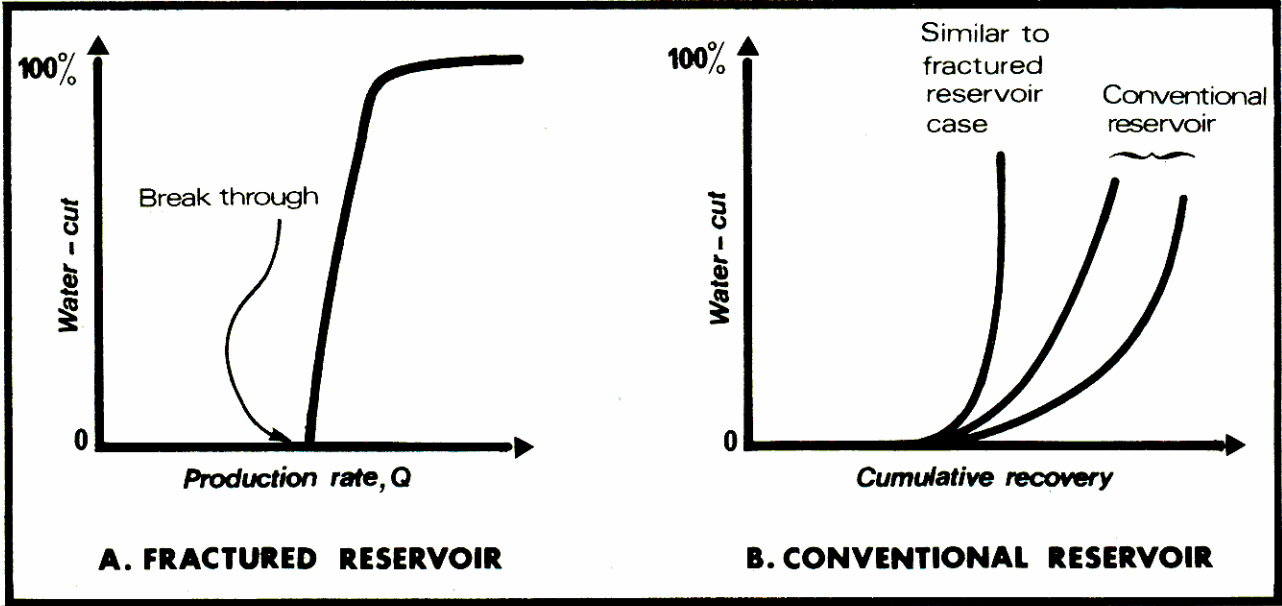


Fig. 10-8. Water-cut in the fractured and conventional reservoirs.

In a fractured reservoir the water-cut increases suddenly from 0 to 100% if well rate is higher than critical rate.
 In a conventional reservoir the water-cut increases slowly from 0 to 100% due to condition of displacement - uniformity of permeability distribution viscosity ratio, etc.

6) Recovery

The familiar parameters ϕ , S_w and relative permeability relations k_g/k_o vs. S_g , k_o/k_w vs. S_o do not significantly affect recovery from the fractured reservoir. Gravity drainage is the dominant producing mechanism and recovery is estimated from the fracture block dimensions and capillary pressure curve of imbibition and drainage.

D. Idealized model of a fractured reservoir

An idealized model consisting of cubic matrix blocks separated by orthogonal network of channels is sometimes used to model the fractured reservoir.

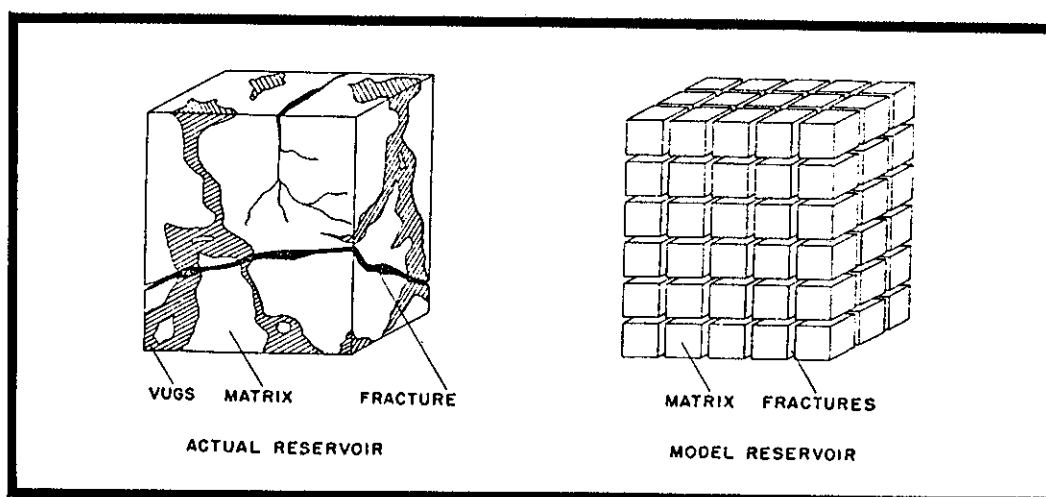


Fig. 10-9. An idealized model of a fractured reservoir

The volume of the matrix block is determined by the intersections of the fracture planes which surround it. As will be demonstrated later, the height of the matrix blocks and the capillary pressure/saturation relations are of primary importance in determining recovery.

The presence of fissures or fractures which start or terminate within the matrix block do not change its dimensions - figure 10-6.

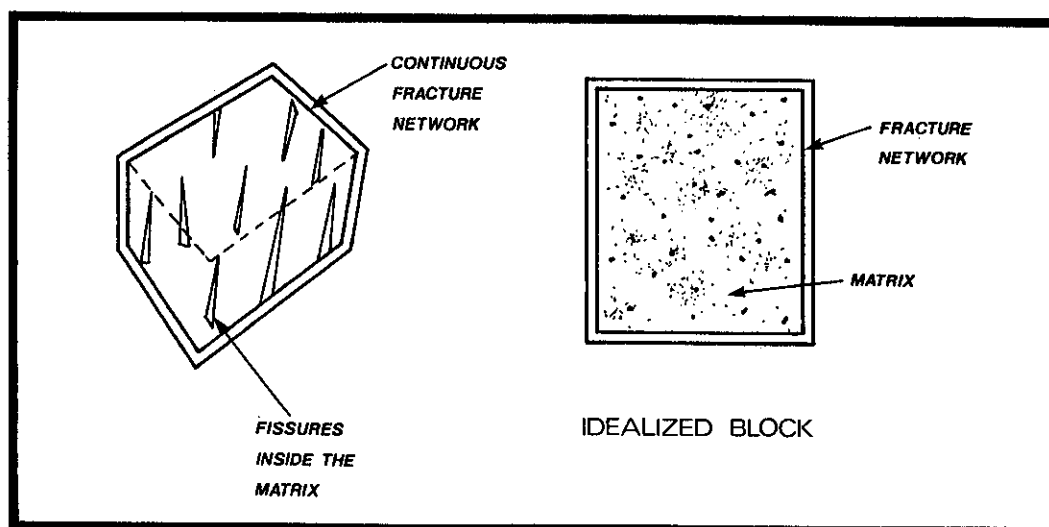


Fig. 10-10. Matrix block dimensions are determined by intersecting fracture planes

E. Description of the fracture process

The fracturing process is the result of : shearing forces where the movement of the rock is parallel to the fractures, or is the result of the tension - compression forces and in this case the walls of fracture will move apart. Genetically, fractures can be structural and tectonic, as the result of one or other type of geological events. In the case of structural fractures the fractures are associated with structural features as faults, thrusting etc., and in case of tectonic events with folding, overthrusting etc. the tectonic fractures are considered of "first order" if these are cutting through several layers but, if confined to only one layer, are considered "second order".

Fracture dimensions also influence the distribution of fractures in "macro-fractures" and "microfractures" the latter often are similar to fissures.

And finally the fractures can be "open" or "closed". Fractures may be plugged by mineral precipitations of the circulating water.

1) Fractures parameters

Fractures in general are expressed quantitatively by 3 basic data :

- fracture opening
- fracture orientation
- fracture density

2) Fracture opening

It represents the distance between the two walls of a fracture and in general indicates average values in the range of 10-30 μ m.

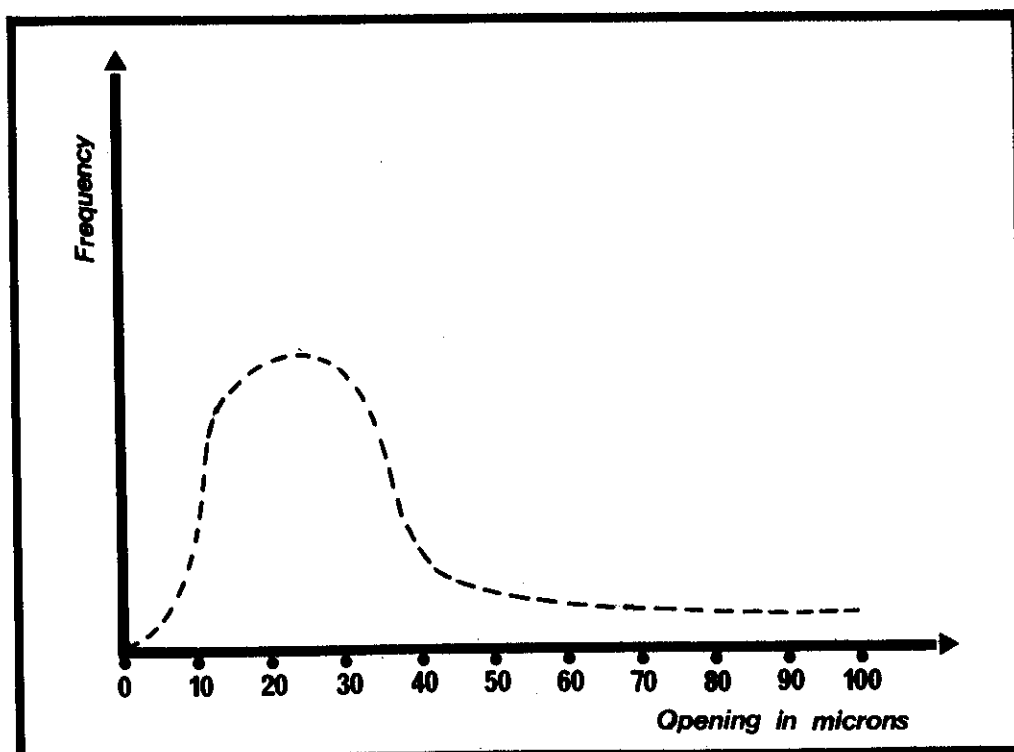


Fig.10-11. Frequency vs size of fracture openings

3) Fracture orientation

Fracture strike and direction (azimuth) can be obtained by correlating measurements made on cores relative to formation dip, with a dipmeter log.

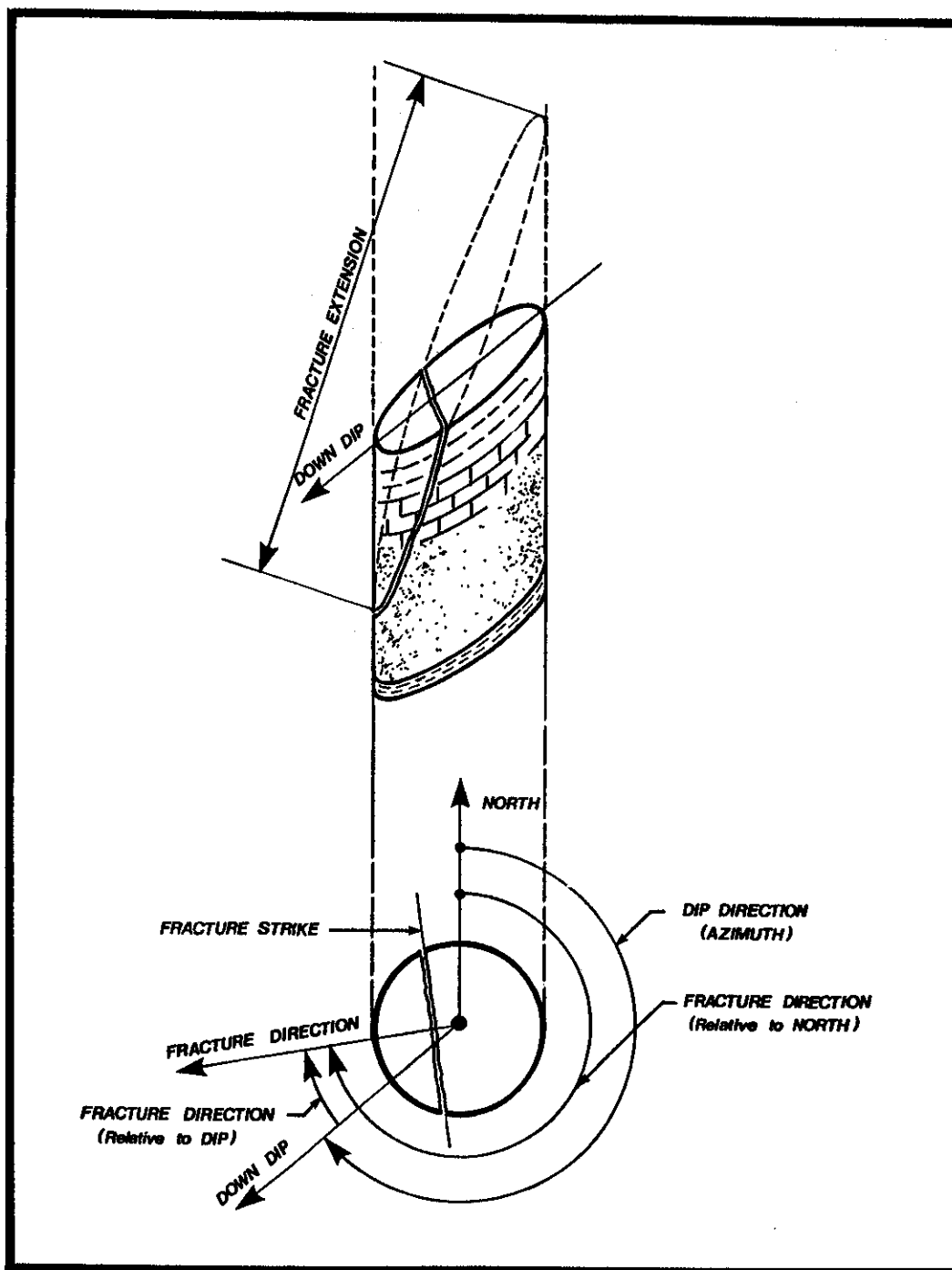


Fig. 10-12. Nomenclature for fracture orientation

F. Porosity and permeability

The porosity of the matrix is not changed because the rock is fractured and the fractures themselves contribute only a very small fraction of the bulk rock porosity, yet the permeability of the fractures is very high compared with matrix permeability. Typical ranges of k and ϕ are :

	k	ϕ
MATRIX	1 m D	8 to 35%
FRACTURE	1000 to 1000,000 m D	0.01 to 1%

The result is that the storage capacity of the reservoir is essentially in the matrix while the movement of the fluids towards the well is mainly through the fracture network. The flow is then the result of two processes :

- the matrix liquid flows toward the fractures feeding them with a rate depending on matrix permeability, the fracture-matrix surface contact area, pressure drop, etc.
- the liquid in the fracture network is transported to the well through these channels. This explains the small pressure drop in the reservoir, and high productivity index, the fluid flow toward the well is done only through highly permeable fractures.

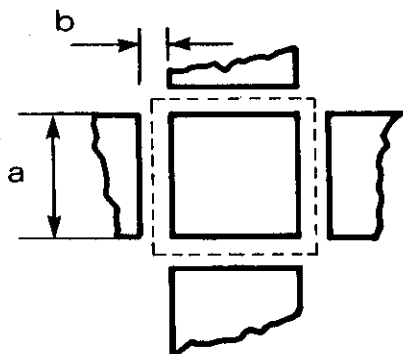
1) Determination of porosity

Classical procedures as described in chapter 4 are used to measure the matrix porosity.

$$\phi_m = \frac{\text{Volume of matrix pores}}{\text{bulk volume}}$$

The fissure porosity is substantially more difficult to evaluate - it is expressed as a ratio between the fracture volume and the bulk volume. The method is evident from the following example :

If the reservoir is assumed as an ideal system of orthogonal cubes the porosity will be given by the ratio.



$$\phi_f = \frac{6 a^2 b / 2}{(a+b)^3} \approx \frac{3b}{a}$$

since $b \ll a$

If the block has .1 m and $b \approx 40\mu = 4 \times 10^{-5}$ m then

$$\phi_f = \frac{3 \times 4 \times 10^{-5}}{1} = 12 \times 10^{-4} = 0.12\%$$

Porosity is also related with fracture permeability through the equation

$$\phi_f = 12 \frac{k_f \text{ (Darcy)}}{b^2 \text{ (cm}^2\text{)}} \approx 10^{-2} \frac{k_f \text{ (mD)}}{b^2 \text{ (microns)}}$$

where permeability is the average value of matrix and fractures. The result when $b \approx 10$ microns and $k_f \approx 100$ mD

$$\phi_f \approx 0.01\%$$

Fracture porosity may be evaluated by well test data if using the equation,

$$\phi_f = \frac{1}{577.9} \frac{J \mu_o B_o f_s^2 \log r_e/r_w}{h}$$

where : J = productivity index, $m^3/\text{day}/\text{bar}$

μ_o = oil viscosity, cp

f_s = areal fracture density, m/m^2

h = bed thickness, m

B_o = oil volume factor

2) Permeability determination

Fracture permeability expresses resistance to fluid flow through the matrix and fracture system, per bulk unit of reservoir rock.

Fracture permeability may be estimated by evaluating two parameters, the matrix permeability and the intrinsic fracture permeability.

- a) Matrix permeability - is the resistance to flow through the matrix and is measured on an unfractured formation core sample using the classical Darcy equation :

$$k = \frac{Q \mu L}{A \Delta p}$$

- b) Intrinsic fracture permeability - is the resistance to flow through a single fracture and is calculated from the thickness of the fracture openings (b , microns) measured on cores.

$$k_{if} = \frac{b^2}{12}$$

The flow rate through n fractures of l length for a pressure drop of $\Delta P/l$ may be defined by analogy with Darcy's law for porous media.

Fracture flow

$$Q = n \frac{b^3 l}{12 \mu} \frac{\Delta P}{l}$$

Porous media flow

$$Q = \frac{s k_f}{\mu} \frac{\Delta P}{l}$$

Fracture permeability thus defined is

$$k_f = \frac{n}{s} \frac{b^3 l}{12} = \frac{b^3}{12}$$

and since

$$\phi_f = \frac{nbl}{s} \quad \text{and} \quad k_{if} = \frac{b^2}{12}$$

the result is that

$$k_f = k_{if} \phi_f$$

$$\text{or} \quad k_{if} = k_f / \phi_f$$

G. Production Mechanisms in the Fractured Reservoir

A section through an idealized fractured reservoir is shown in figure 10-13. As depletion progresses, the attendant pressure decline causes enlargement of the gas cap at the top and encroachment of water from the bottom, into the oil zone.

When pressure falls below bubble point, a gasing zone is created within the oil column that progressively moves downward with time.

Several distinct zones can now be recognized :

- a secondary gas cap expanding downward into the oil zone
 - a water invaded zone at the lower part of the reservoir
 - a gasing zone in oil where $P < P_b$
 - the lower portion of the oil zone remains undersaturated
- 1) In the gas invaded zone oil is displaced by the gas accumulate in the upper portion of the reservoir and expanding downward through the fractures surrounding oil filled matrix blocks-(1) and (2). Fig.10-14.

The production mechanism involved is totally different from a conventional reservoir, since it is essentially dominated by the gravity-drainage relationship. The basic parameters are :

- difference in density ($\gamma_o - \gamma_g$)
 - threshold capillary pressure at which gas (non-wetting) displaces the oil
- 2) In the gasing zone the blocks are surrounded by oil filled fractures. Gas liberated from the oil remains within the matrix block until $S_g > S_{gcr}$, then begins to migrate into the fracture system.

The production mechanisms in the gasing zone are :

- expansion $S_g < S_{gcr}$. block (4)
- expansion + gravity segregation $S_g > S_{gcr}$. block (3)

The expansion of immobile gas governs oil displacement while $S_g < S_{gcr}$. - block (4).

When $S_g > S_{gcr}$, the gas begins to move :

- if the gas segregates rapidly from the oil and escapes from the block, the gravitational mechanism predominates.
- if the gas segregates slowly and moves along with the oil a solution gas mechanism predominates.

Note : The latter mechanism has a relatively limited effectiveness and is important only in the case of a rapid reservoir depletion.

- 3) In the undersaturated zone the matrix block is oil saturated surrounded by oil filled fractures and the production mechanism, block (5), expansion of the undersaturated liquid.

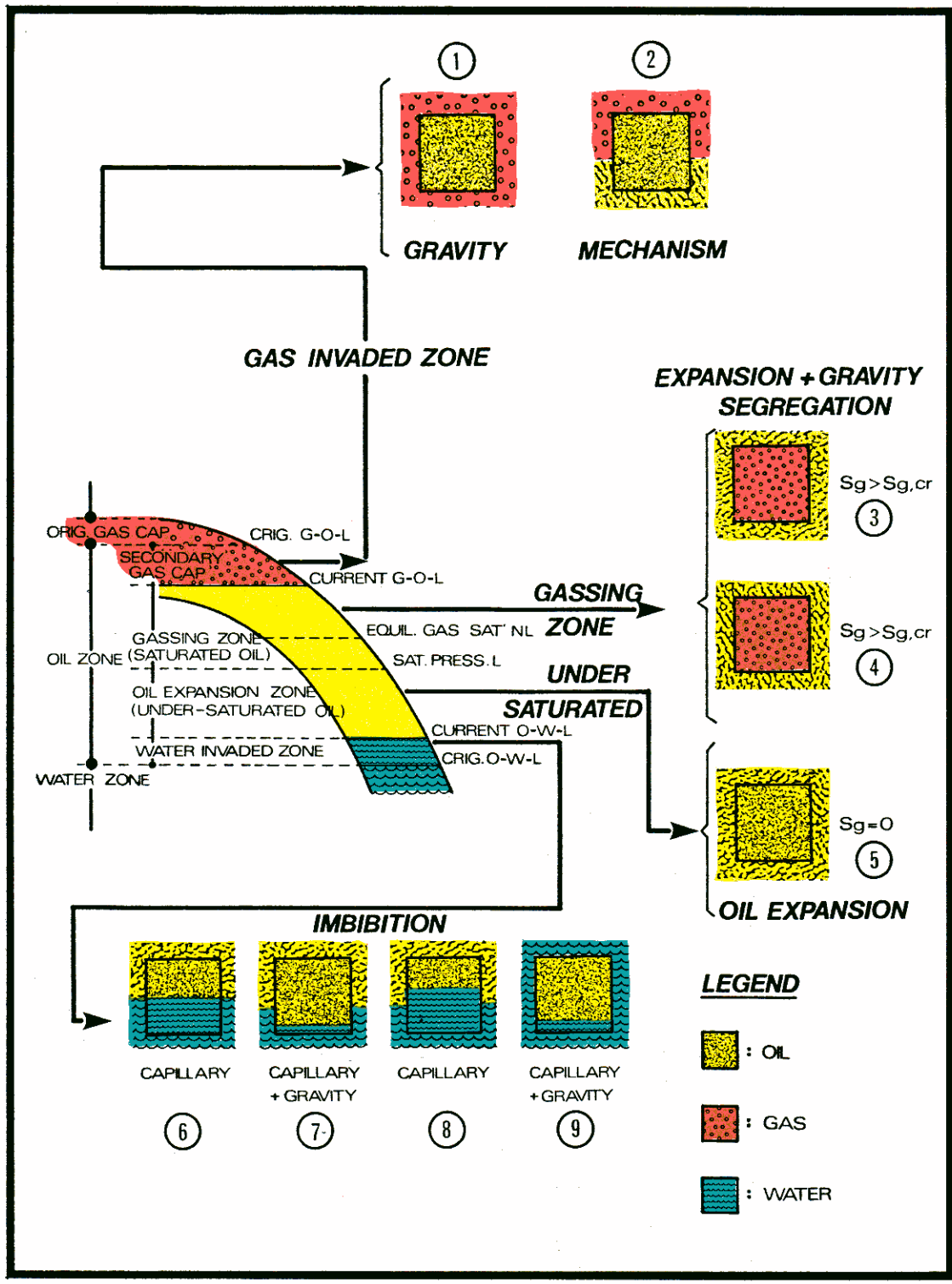


Fig. 10-13. Mechanisms of production in the fractured reservoir.

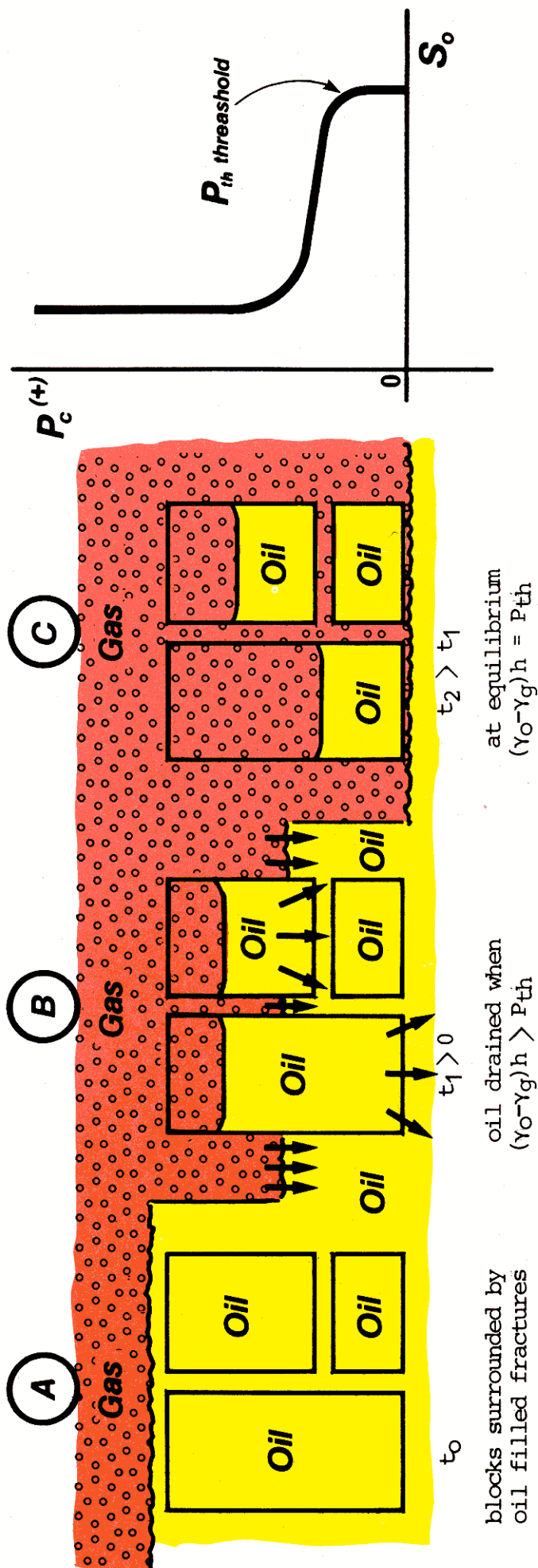


Fig. 10-14. Oil drainage from different height blocks by gravity mechanism

- (A) Oil saturated blocks surrounded by oil filled fractures.
- (B) Gas-oil contact in fractures moves rapidly down - oil drained when $(\gamma_o - \gamma_g)h > P_{th}$
- (C) Blocks surrounded completely by gas in fracture system - amount of oil remaining after equilibrium is established depends on P_c vs S_o relation., $(\gamma_o - \gamma_g)h = P_{th}$

- 4) In the water invaded zone oil is displaced by water moving upward through the fractures surrounding the oil filled matrix blocks. The production mechanism is : capillary inhibition + gravity inhibition.

Referring to figure 10-13 :

- in block (6) when the level of water in fractures = oil level in matrix the mechanism is capillarity.
- in block (7) when the level of water in fracture > oil level in matrix the mechanism is capillarity + gravity inhibition.
- in block (8) when the level of water in fractures = oil level in matrix the mechanism is capillarity.
- in block (9) when water surrounds block completely, mechanism is capillarity + gravity.

H. Discussion of Displacement Mechanisms

- 1) Drainage mechanism - see figure 10-14.

As the gas cap expands downward through the fractures surrounding oil filled matrix blocks, gas will begin to enter the matrix when the column of gas in the fractures is greater than the threshold height. Oil will continue to be displaced until equilibrium is reached when

$$(\gamma_o - \gamma_g)h = P_{th}.$$

Note that the amount of oil recovered depends on the height of the block, the threshold pressure, and the shape of the capillary pressure curve.

- 2) Inhibition mechanism

As illustrated in figure 10-15, A, B, and C recovery efficiency in the water encroached zone is controlled by the shape of the composite capillary pressure curve.

A.- Water saturation increases in the matrix blocks above the oil-water contact in the fractures. An amount of oil (shaded area) equal to $1 - (S_w - S_{wir})$ can be displaced by capillary mechanism at $P_c = 0$ if given sufficient time.

B.- Oil drainage lags behind a rapidly rising oil-water contact in the fractures.

C.- In a total immersed block water imbibes by a combination of gravity (shaded area) and capillary effects.

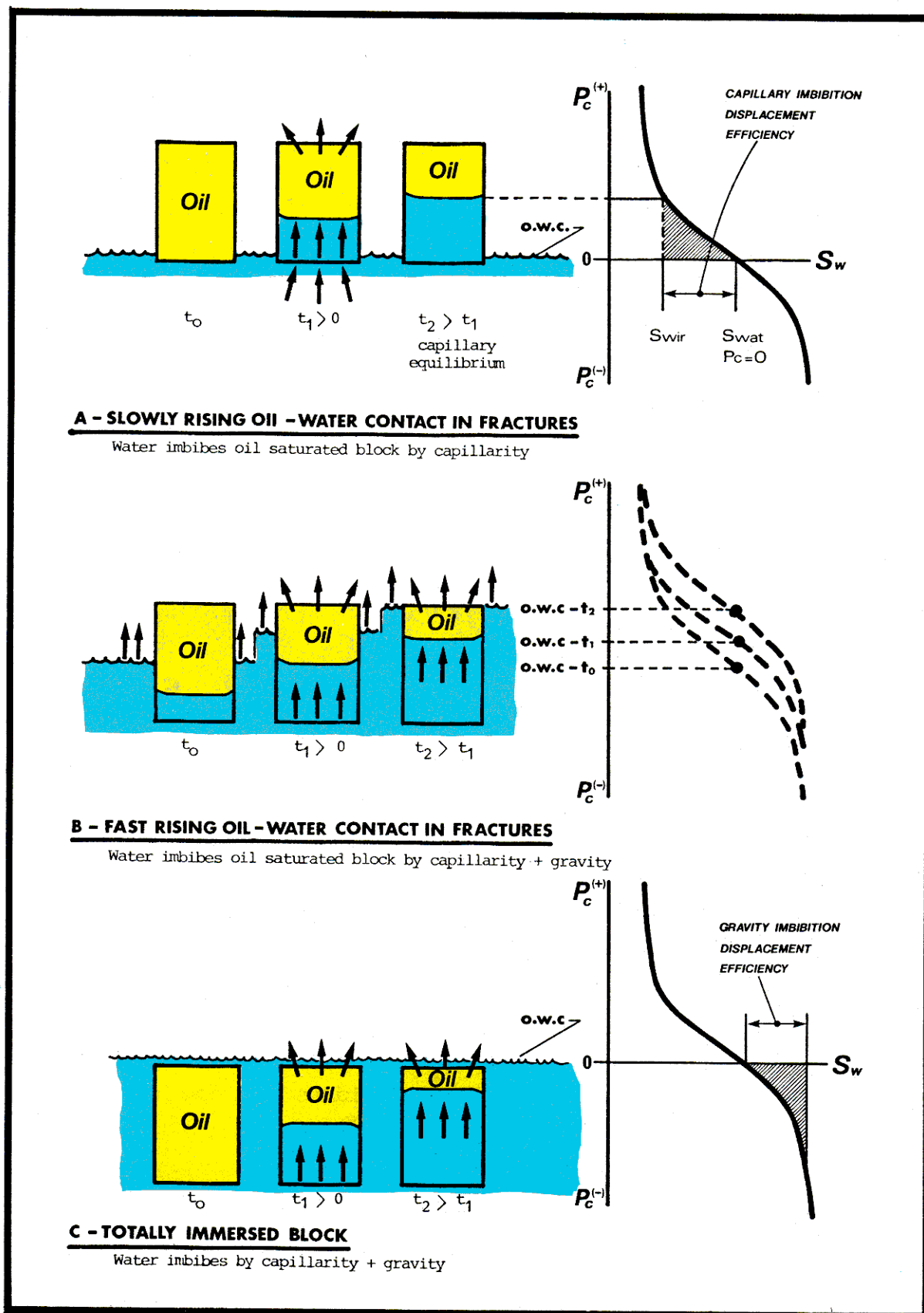


Fig. 10-15. Imbibition mechanisms

I. Steady state flow towards the well

The relation between production rate and drawdown pressure is established by measuring surface production at several rates, including zero, while recording the corresponding bottom hole pressures.

A characteristic plot of Q vs. ΔP (see figure 10-16) shows a linear relationship if the flow in the fractures is laminar, up to some critical rates Q_{cr} . For high flow rates above Q_{cr} , flow is turbulent and the relation becomes increasingly non-linear.

In turbulent conditions flow is described by the equation :

$$\Delta P = A Q + B Q^2$$

Where ΔP is the laminar flow term and BQ^2 the additional pressure drop in turbulent conditions. The BQ^2 term becomes more important as Q increases, while AQ term prevails at low rate.

To evaluate the parameters of above equation it may be written :

$$\frac{\Delta P}{Q} = A + B Q$$

When the pressure and flow data $\frac{\Delta P}{Q}$ vs. Q are plotted the slope of the resulting curve gives the parameter B and the intercept with $Q = 0$ gives the parameter A .

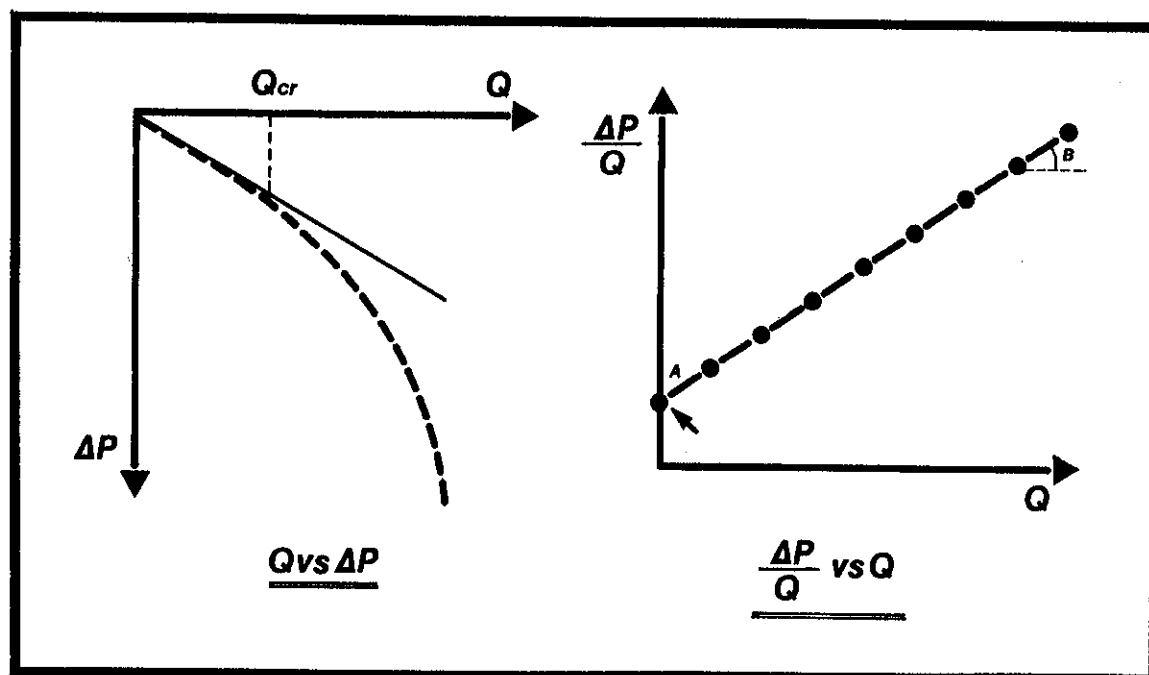


Fig. 10-16. Steady state flow relations in the fractured reservoir.

Analytically the equation can be expressed by :

$$\Delta P = \frac{\mu B_o}{2\pi kh} Q \ln \frac{r_w}{r_w} + \Sigma S + \beta \frac{Q B_o}{4\pi^2 h^2} Q^2 \left(\frac{1}{r_w} - \frac{1}{r_e} \right)$$

where the coefficient of turbulence β is given by :

$$\beta(1/\text{ft}) = \frac{4.16 \times 10^{10}}{k^{1.34} (\text{mD})}$$

so that

$$A = \frac{\mu B_o}{2\pi kh} \ln \frac{r_e}{r_w} + \Sigma S \quad \text{and} \quad B = \beta \frac{Q B_o}{4\pi^2 h^2} Q^2 \left(\frac{1}{r_w} - \frac{1}{r_e} \right)$$

A similar equation was used and verified on Iranian wells where

$$A = 0.00715 \frac{\mu B_o}{b^3} \log \frac{r_e}{r_w}$$

and

$$B = 0.015 \frac{Q B_o^2}{r_w^2 + b_w^2} \left(1 + \frac{0.083}{b_w} \right)$$

where : μ = viscosity, poises

b = average fracture width in the formation, inches

b_w = fracture width in well bore, inches

An empirical equation for skin effect which has given good results is :

$$\Delta P_{\text{skin}} = 2 B Q^2$$

J. Transient Flow

The objective in interpreting transient pressure behavior is to estimate reservoir parameters :

- permeability, k
- permeability thickness product, kh
- damage around the well bore
- radius of drainage
- fracture porosity, density, and block dimensions

Of the various methods used to analyze transient behavior in fractured reservoirs the most useful are :

- Warren and Root method - a classical approach based on analysis of an idealized model
- Pollard method - a simpler, semi-empirical method which has given good results in fractured limestones of Venezuela.

1. Warren and Root method

This method assumes a reservoir formed by parallelepiped matrix blocks containing the primary porosity and separated by an orthogonal system of fractures through which all flow to the well takes place.

The mathematical basis for the Warren and Root method is discussed in the appendix of this chapter.

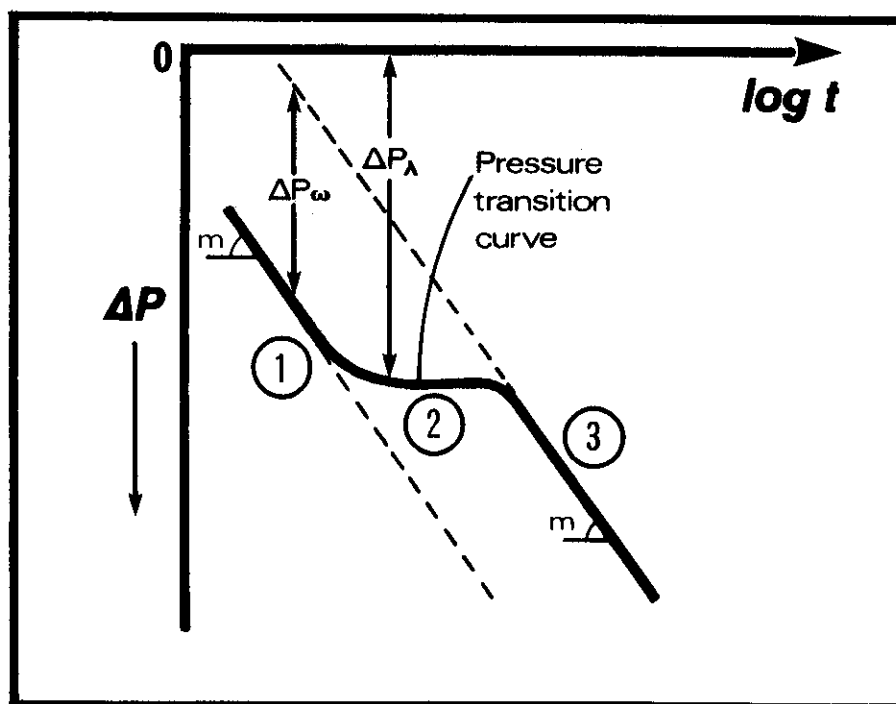


Fig. 10-17. Warren and Root drawdown plot.

Fig. 10-17 is a drawdown plot of P_f vs. $\log t$ showing two parallel lines (1) and (3), separated by a pressure transition curve (2).

During early drawdown times, pressure drop is confined essentially to the fracture system (segment (1)) and P_f vs. $\log t$ falls on a straight line; then as the pressure in the fractures is further depressed, the matrix begins to supply the fractures with fluid and the pressure, P_f , remains virtually constant - segment (2). At later times a pseudo steady-state is created between the matrix blocks which supply the fluids to the fractures and the pressure decline P_f vs. $\log t$ - segment (3) assumes a constant slope, m , equal to initial slope.

The Warren and Root method is most useful where a strong contrast exists between matrix and fracture, ϕ and k and when matrix blocks are large. Where the network of fractures is very dense or the contrast between matrix and fracture porosities is small the formation performs as a homogeneous media, $\Delta P_w \rightarrow 0$, and no transient pressure sector is observed.

The Warren and Root plot is used to :

- determine kh of the fracture network from slope, m
- evaluate ϕ_m and ϕ_f , the storage capacity of the matrix and fracture through the equation :

$$w = 1^{-2,3} \Delta P_w / m$$

$\frac{\Delta P_w}{m}$ being the pressure drop between two parallel straight lines and $\frac{1}{m}$ the slope (Fig. 10-17). And further the relative capacity storage is expressed by :

$$w = \frac{\phi_f C_f}{\phi_m C_m + \phi_f C_f}$$

evaluate the blocks dimensions through interflow parameter,

$$\lambda = a \frac{k_m}{k_f} r_w^2$$

where

$$a = \frac{4n(n+2)}{\alpha^2}$$

considering $n = 3$ flowing directions and solving the two equations for block dimension evaluation, the result is,

$$\alpha^2 = 60/a = 60 \times \frac{k_m r_w^2}{k_f \lambda}$$

Since λ is obtained from equation :

$$\lambda = 0.56 (1-w)^1$$

Where both ΔP_λ and m are known from Fig. 10-17. In addition k_m is measured on cores and k_f from slope m .

Example : If $\lambda = 10^{-6}$, $k_m = 0.1$ mD, $k_f = 10$ D, $R_w = 10$ cm. the matrix block dimension is :

$$\alpha = \left(60 \frac{k_m}{k_f} \frac{r_w^2}{\lambda} \right)^{\frac{1}{2}} = \left(60 \frac{10^{-4}}{10} \times \frac{10^2}{10^{-6}} \right)^{\frac{1}{2}} = 2.44 \text{ m}$$

The results show that the model of Warren and Root is applicable only when the blocks are very large and permeability of fractures is high.

2. Pollaird method

This empirical method assumes that the transient behaviour of a fractured reservoir is influenced by coexistence of three zones : matrix, fractures network and fracture around the wellbore. In a pressure drawdown or build-up it is possible to write,

$$\Delta P_{\text{total}} = \Delta P_{\text{matrix fractures}} + \Delta P_{\text{fractures}} + \Delta P_{\text{skin effect}}$$

or as a function of time

$$\Delta P(t) = A_1 t^{-\alpha_1} + A_2 t^{-\alpha_2} + A_3 t^{-\alpha_3}$$

From the curve resulting from variation of ΔP vs time, we obtain the constants A_1 , A_2 , A_3 , α_1 , α_2 , α_3 .

Procedure

From recorded data p, t , plot the diagram $\log \Delta P$ vs. t to obtain a curve (C_1), in the fig. 10-18.

The last part of the curve for late times shows the behaviour of the matrix. The linear part can be extrapolated to give a straight line (SL_1) which has a slope a_1 and an ordinate A_1 at $t = 0$, expressed by :

$$\Delta P_{\text{matrix}} = \log A_1 + a_1 t$$

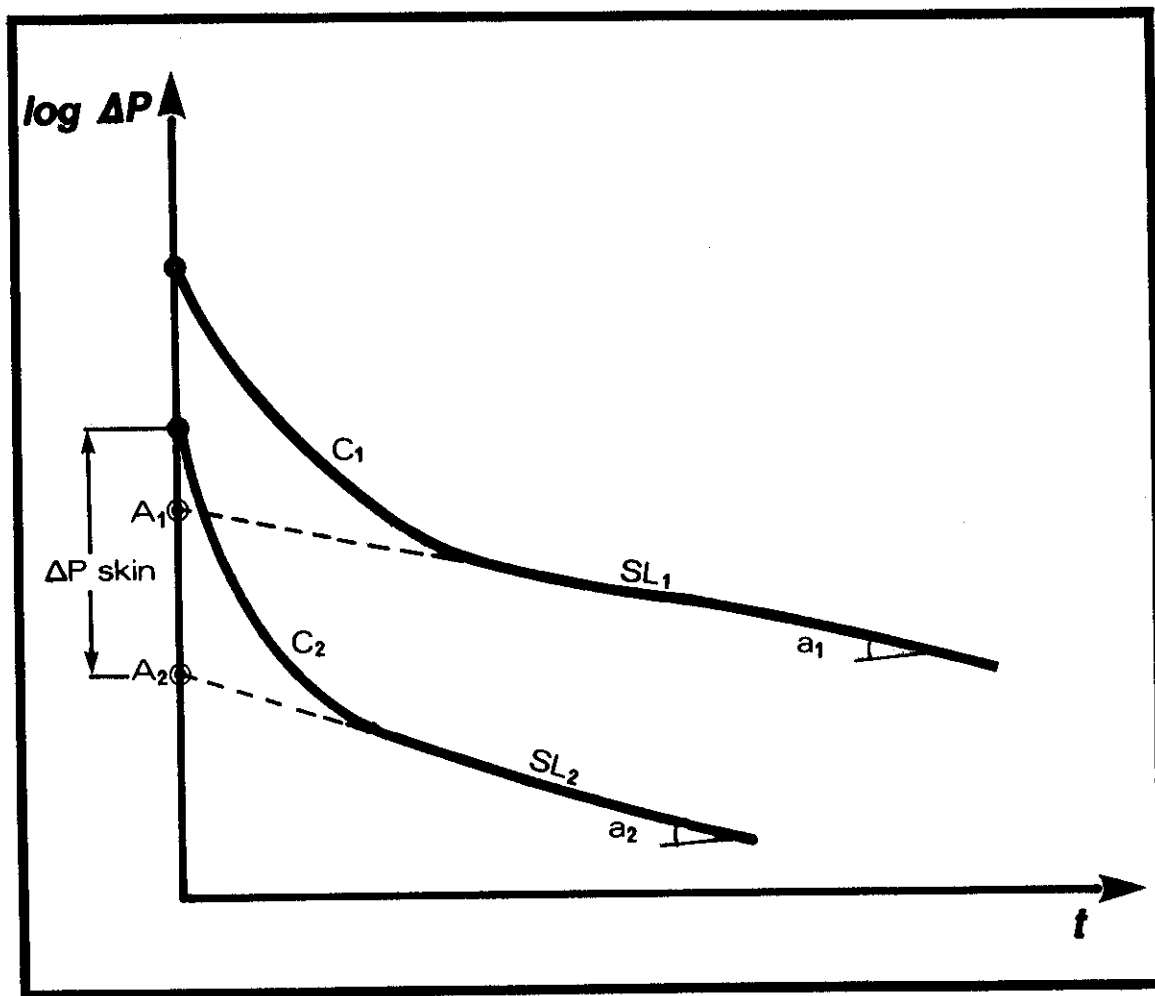


Fig. 10-18. Pollaird plot - $\log \Delta P$ vs. t

From the difference between the curve (C_1) and (SL_1) data a differential pressure curve (DSC) may be plotted - Fig. 10-18. This data is expressed by :

$$\Delta P(t) - \Delta P_{\text{matrix fractures}} = A_2 1^{-a_2 t} + A_3 1^{-a_3 t}$$

The straight line portion of this curve (SL_2) shows the pressure drop in the fractures, the slope a_2 , if extrapolated will give ordinate A_2 at $t = 0$.

Finally, the skin in matrix and fracture is represented by the difference in pressure between straight line and curve.

$$\Delta P_{\text{skin}} = (C - SL_2)_{t=0}$$

K. Appendix to Chapter 10

- 1) Mathematical derivation of Warren and Root model to analyse fractured reservoirs.

$$\frac{k_f \chi}{\mu} \frac{\partial^2 P_f}{\partial \chi^2} + \frac{k_f \psi}{\mu} \frac{\partial^2 P_f}{\partial \psi^2} = \phi_m C_m \frac{\partial P_m}{\partial t} + \phi_f C_f \frac{\partial P_f}{\partial t}$$

The expression represents the equality between fluid moved in the fractures (left hand terms) with the variation of mass supplied by matrix and fractures (right hand terms).

In addition to this equation the fluid exchange between matrix and fractures is expressed by :

$$\phi_m C_m \frac{P_m}{t} = a \frac{k_m}{\mu} (P_f - P_m)$$

This equation shows that the expanded fluid from the matrix (left hand term) is equal to fluid which flows through matrix-fracture face in the fracture network (right hand term) as a result of the pressure drop between fracture and matrix. The term a is associated with the matrix geometry.

For an infinite reservoir producing at a constant rate the equation is expressed by :

$$\Delta P = 162.6 \frac{q_{\mu B}}{kh} \left[\log t_D + 0.351 + 0.435 \operatorname{Ei} \left(\frac{-\lambda t_D}{w(1-w)} \right) - 0.435 \operatorname{Ei} \left(-\frac{\lambda t_D}{1-w} \right) + 0.87S \right]$$

(In practical API field units)

$$\omega = \frac{\phi_f C_f}{\phi_m C_{pm} + \phi_f C_{pf}}$$

$$t_D = \frac{2.637 \times 10^{-4} k_f \chi^2}{(\phi_m C_{pm} + \phi_f C_{pf}) \mu r_w^2}$$

$$\lambda = 4n(n+2) \left(\frac{r_w}{a}\right)^2 \frac{k_m}{k_m + k_f} \frac{\phi_m C_{pm} + \phi_f C_{pf}}{\phi_m C_{pm}}$$

where : C, k, n, a are compressibility, permeability, number of planes defining the fracturing, block height and indices m and f referring to matrix and fractures.

In estimation

$$C_{em} = C_o + \frac{C_{pm} + S_{wi}C_w}{1 - S_{wi}}$$

$$C_{ef} \cong C_o$$

Remarks on Warren and Root method

For small t values the pressure drop equation reduced to :

$$\Delta P(t) = - \frac{162,6 \text{ q}\mu\text{B}}{kh} \left[\log t_D + 0.351 - \log w + 0.87S \right]$$

and for large t values :

$$\Delta P(t) = - \frac{162,6 \text{ q}\mu\text{B}}{k a} \left[\log t_D + 0.351 + 0.87S \right]$$

Example of estimation of matrix block height from core and test data :

If production test results show a value $k_f = 10 \text{ mD}$, and from the examination of cores an average fracture opening of $b = 20 \mu$, it is possible to evaluate the fracture porosity.

$$\phi_f = 10^{-3} \frac{k_f \text{ (mD)}}{b^2 \text{ (microns)}} = 10^{-3} \times \frac{100}{400} = 0,0.25\%$$

height, a of the idealized cubic block is :

$$\frac{3b}{a} = \phi_f \quad \text{and} \quad a = \frac{3b}{\phi_f}$$

$$a = \frac{3 \times 20 \times 10^{-5}}{0,0.25 \times 10^{-2}} = 24 \text{ cm}$$

APPENDIX

11

A. Nomenclature

Practical oilfield units and nomenclature are used in this booklet except where otherwise indicated.

Practical oilfield units-symbols and subscripts:

A = drainage area of well, sq ft	P _{iw} = bottom-hole injection well pressure, psi
B = formation volume factor	P _{wf} = bottom-hole flowing (or pumping) pressure, psi
c = compressibility, psi ⁻¹	P _{lhr} = pressure read from linear portion of pressure buildup curve at 1-hour closed-in time, psi; also refers to pressure read from linear portion of drawdown test curve, two-rate flow test curve, or pressure falloff curve, at 1-hour test time
c _f = effective formation (rock) compressibility, psi ⁻¹	p* = pressure obtained when linear portion of pressure buildup curve, p _{ws} vs log (Δt + Δt)/Δt, is extrapolated to (t + Δt)/Δt = 1; corresponds to pressure obtained after infinite closed-in time in an infinite reservoir, psi.
c _t = total compressibility, psi ⁻¹	\bar{p} = average pressure, psi
d _t = diameter of tubing, in.	Δp _{skin} = pressure drop in "skin" region next to wellbore, psi
D = non-Darcy flow constant, (B/D) ⁻¹	q = production rate of well, B/D at surface conditions
g = acceleration due to gravity	r _e = external boundary radius, ft
h = formation thickness, ft	r _w = wellbore radius, ft
i = injection rate, B/D at surface conditions	R = universal gas constant
I = injectivity index, B/D-psi	R _s = gas solubility in oil, bbl/bbl
J = productivity index, B/D-psi	R _{sw} = gas solubility in water, bbl/bbl
k = formation permeability, md	S = saturation, fraction of pore space
m = absolute value of slope of linear portion of pressure buildup of flow test curve, psi/log ₁₀ cycle	
M = mobility ratio, (k/μ) ₁ /(k/μ) ₂	
M = molecular weight of a gas	
p _e = external boundary pressure at radius r _e , psi	
p _i = initial reservoir pressure, psi	
p _{sc} = pressure at standard conditions, psi	
p _t = tubing-head injection pressure at time of closing in, psi	
p _w = bottom-hole pressure, psi; in two-rate flow tests and in all injection tests, p _w is the pressure at time of change in rate	

t = time of flowing, hours
 Δt = closed-in time, hours
 $\Delta t'$ = flowing (or injection) time after change in rate, hours
 T = absolute temperature, $^{\circ}R$
 T_{sc} = absolute temperature at standard conditions, $^{\circ}R$
 u = volumetric rate of flow per unit cross-sectional area
 V_g = oil volume
 V_o = oil volume, bbl
 V_p = pore volume, bbl
 W_i = cumulative water injection, bbl
 z = gas deviation factor (compressibility factor, $z = pV/nRT$)
 μ = viscosity, cp
 ρ = density, gm/cc (in injection well analysis)
 ϕ = porosity, fraction

Subscripts

i = initial
 o, w, g = oil, water, gas; w also refers to well when used with p and r
 os, ws, gs = oil, water, gas at standard conditions
 $or, gr,$ = oil and gas at residual conditions
 sc = standard conditions
 t = total; refers to tubing when used with d or p

B. CONVERSION FACTORS BETWEEN PRACTICAL OILFIELD UNITS, METRIC SI
AND OTHER MEASURES

SI symbols shown in parenthesis in the right hand column

MULTIPLY	BY	TO OBTAIN
LENGTH		
angstrom	1.0 *E-10	metre (m)
centimetre	3.280 840 E-02	foot
centimetre	3.937 008 E-01	inch
centimetre	1.0 *E-02	metre (m)
centimetre	1.0 *E+01	millimetre (m)
fathom	1.828 800 *E+00	metre (m)
foot	3.048 *E-01	metre (m)
foot	3.048 *E+01	centimetre (cm)
foot	3.048 *E+02	millimetre (mm)
foot	1.2 *E+01	inch
inch	2.540 *E-02	metre (m)
inch	2.540 *E+00	centimetre (cm)
inch	2.540 *E+01	millimetre (mm)
inch	8.333 333 E-02	foot
kilometre	6.213 712 E-01	mile [U.S. statute]
metre	3.937 008 E+01	inch
metre	5.468 066 E-01	fathom
metre	3.280 840 E+00	foot
metre	1.093 613 E+00	yard
metre	6.213 712 E-04	mile [U.S. statute]
microinch	2.54 *E-02	micrometre (µm) [micron]
micrometre [micron]	1.0 *E-06	metre (m)
micrometre [micron]	3.937 008 E+01	microinch
mile [U.S. statute]	1.609 344 *E+03	metre (m)
mile [U.S. statute]	1.609 344 *E+00	kilometre (km)
mile [U.S. statute]	5.280 *E+03	foot
millimetre	3.280 840 E-03	foot
millimetre	3.937 008 E-02	inch
yard	9.144 *E-01	metre (m)

AREA		
acre	4.046 856 E-01	hectare (ha)
acre	4.356 *E+04	foot ²
acre	4.046 856 E+03	metre ² (m ²)
centimetre ²	1.550 003 E-01	inch ²
centimetre ²	1.076 391 E-03	foot ²
foot ²	2.295 684 E-05	acre
foot ²	9.290 304 *E+02	centimetre ² (cm ²)
foot ²	9.290 304 *E-02	metre ² (m ²)
foot ²	1.44 *E+02	inch ²

* Exact value

MULTIPLY	BY	TO OBTAIN
----------	----	-----------

AREA (CONTINUED)

foot ²	9.290 304 *E+04	millimetre ² (mm ²)
hectare	1.0 *E+04	metre ² (m ²)
hectare	2.471 054 E+00	acre
hectare	1.076 391 E+05	foot ²
hectare	1.0 *E-02	kilometer ² (km ²)
inch ²	6.451 6 *E+00	centimetre ² (cm ²)
inch ²	6.451 6 *E-04	metre ² (m ²)
inch ²	6.451 6 *E+02	millimetre ² (mm ²)
inch ²	6.944 444 E-03	foot ²
millimetre ²	1.076 387 E-04	foot ²
millimetre ²	1.550 003 E-03	inch ²
mile ²	6.4 *E+02	acre
mile ²	2.589 988 E+06	metre ² (m ²)
metre ²	2.471 054 E-04	acre
metre ²	1.550 003 E+03	inch ²
metre ²	1.076 391 E+01	foot ²
metre ²	1.195 990 E+00	yard ²
yard ²	8.361 274 E-01	metre ² (m ²)

VOLUME

acre-foot	7.758 368 E+03	barrel
acre-foot	4.356 *E+04	foot ³
acre-foot	3.258 515 E+05	gallon
acre-foot	1.233 482 E+03	metre ³ (m ³)
barrel [API]	1.288 931 E-04	acre-foot
barrel [API]	1.589 873 E+05	centimetre ³ (cm ³)
barrel [API]	1.589 873 E+02	litre (l)
barrel [API]	1.589 873 E-01	metre ³ (m ³)
barrel [API]	5.614 583 E+00	foot ³
barrel [API]	4.2 *E+01	gallon
barrel [API]	9.701 999 E+03	inch ³
centimetre ³	6.289 981 E-06	barrel [API]
centimetre ³	3.531 466 E-05	foot ³
centimetre ³	2.641 721 E-04	gallon
centimetre ³	6.102 374 E-02	inch ³
foot ³	1.781 076 E-01	barrel [API]
foot ³	2.831 685 E+04	centimetre ³ (cm ³)
foot ³	7.480 520 E+00	gallon
foot ³	1.728 *E+03	inch ³
foot ³	2.831 685 E+01	litre (l)
foot ³	2.831 685 E-02	metre ³ (m ³)
gallon	2.380 952 E-02	barrel [API]
gallon	3.785 412 E+03	centimetre ³ (cm ³)
gallon	3.785 412 E+00	litre (l)
gallon	3.785 412 E-03	metre ³ (m ³)
gallon	2.310 001 E+02	inch ³
gallon	1.336 806 E-01	foot ³
gallon [U.K.]	1.200 950 E+00	gallon [U.S.]
inch ³	1.030 715 E-04	barrel [API]
inch ³	4.329 003 E-03	gallon

MULTIPLY	BY	TO OBTAIN
----------	----	-----------

VOLUME (CONTINUED)

inch ³	1.638 706 E+01	centimetre ³ (cm ³)
inch ³	1.638 706 E-02	litre (l)
inch ³	1.638 706 E-05	metre ³ (m ³)
inch ³	5.787 037 E-04	foot ³
inch ³	1.638 706 E+04	millimetre ³ (mm ³)
litre	1.0 *E+03	centimetre ³ (cm ³)
litre	1.0 *E-03	metre ³ (m ³)
litre	6.289 811 E-03	barrel [API]
litre	3.531 466 E-02	foot ³
litre	2.641 720 E-01	gallon
litre	6.102 373 E+01	inch ³
metre ³	1.0 *E+06	centimetre ³ (cm ³)
metre ³	1.0 *E+03	litre
metre ³	8.107 131 E-04	acre-foot
metre ³	6.289 811 E+00	barrel
metre ³	3.531 466 E+01	foot ³
metre ³	2.641 720 E+02	gallon
metre ³	6.102 376 E+04	inch ³
metre ³	1.307 951 E+00	yard ³
millimetre ³	6.102 376 E-05	inch ³
yard ³	7.645 549 E-01	metre ³ (m ³)

VELOCITY, ACCELERATION, TIME

centimetre/second	1.181 102 E+02	foot/hour
centimetre/second	1.968 504 E+00	foot/minute
centimetre/second	3.280 840 E-02	foot/second
centimetre/second	6.0 *E-01	meter/minute
foot/hour	8.466 667 E-03	centimetre/second
foot/hour	8.466 667 E-05	metre/second (m/s)
foot/hour	5.08 *E-03	metre/minute
foot/hour	1.666 667 E-02	foot/minute
foot/minute	5.08 *E-01	centimetre/second
foot/minute	3.048 *E-01	metre/minute
foot/minute	5.08 *E-03	metre/second (m/s)
foot/minute	6.0 *E+01	foot/hour
foot/second	3.048 *E+01	centimetre/second
foot/second	1.828 8 *E+01	metre/minute
foot/second	3.048 *E-01	metre/second (m/s)
kilometre/hour	6.213 712 E-01	mile/hour
kilometre/hour	5.399 E-01	knots [International]
knots [International]	1.852 E+00	kilometre/hour
knots [International]	1.151 E+00	mile/hour
mile/hour	4.470 4 *E+01	centimetre/second
mile/hour	8.8 *E+01	foot/minute
mile/hour	1.466 667 E+00	foot/second

MULTIPLY	BY	TO OBTAIN
----------	----	-----------

VELOCITY, ACCELERATION, TIME (CONTINUED)

mile/hour	1.609 334 *E+00	kilometre/hour
mile/hour	4.470 4 *E-01	metre/second (m/s)
metre/minute	1.666 667 E+00	centimetre/second
metre/minute	3.280 840 E+00	foot/minute
metre/minute	1.968 504 E+02	foot/hour
metre/minute	5.468 067 E-02	foot/second
metre/second	3.280 840 E+00	foot/second
metre/second	1.181 102 E+04	foot/hour
metre/second	1.968 504 E+02	foot/minute
foot/second ²	3.048 *E-01	metre/second ² (m/s ²)
metre/second ²	3.280 840 E+00	foot/second ²
day	2.4 *E+01	hour
day	1.44 *E+03	minute
day	8.64 *E+04	second (s)
minute	6.944 444 E-04	day
minute	1.666 667 E-02	hour
minute	6.0 *E+01	second (s)
second	1.157 407 *E-05	day
second	2.777 778 E-04	hour

VOLUMETRIC FLOW RATE

barrel/day	1.840 131 E+00	centimetre ³ /second
barrel/day	1.589 873 E-01	metre ³ /day (m ³ /d)
barrel/day	6.624 472 E-03	metre ³ /hour
barrel/day	3.899 016 E-03	foot ³ /minute
barrel/day	2.916 667 E-02	gallon/minute
barrel/day	6.624 472 E+00	liter/hour
foot ³ /minute	1.699 011 E+03	liter/hour
foot ³ /minute	4.719 474 E-04	metre ³ /second (m ³ /s)
foot ³ /minute	2.564 749 E+02	barrel/day
foot ³ /second	2.831 685 E-02	metre ³ /second (m ³ /s)
gallon/minute	3.428 571 E+01	barrel/day
gallon/minute	1.428 571 E+00	barrel/hour
gallon/minute	1.336 806 E-01	foot ³ /minute
gallon/minute	2.271 247 E+02	liter/hour
gallon/minute	6.309 020 E-05	metre ³ /second (m ³ /s)
gallon/minute	5.450 993 E+00	metre ³ /day
liter/hour	1.509 554 E-01	barrel/day
liter/hour	5.885 776 E-04	foot ³ /minute
liter/hour	2.4 *E-02	metre ³ /day

MULTIPLY	BY	TO OBTAIN
----------	----	-----------

VOLUMETRIC FLOW RATE (CONTINUED)

litre/minute	3.531 466 E-02	foot ³ /minute
litre/minute	2.641 720 E-01	gallon/minute
litre/second	1.585 032 E+01	gallon/minute
metre ³ /second	5.434 396 E+05	barrel/day
metre ³ /second	2.118 880 E+03	foot ³ /minute
metre ³ /second	3.531 466 E+01	foot ³ /second
metre ³ /second	1.585 032 E+04	gallons/minute
metre ³ /minute	2.641 720 E+02	gallons/minute
metre ³ /day	6.289 811 E+00	barrels/day
metre ³ /day	3.531 466 E+01	foot ³ /day
metre ³ /day	2.452 4 07 E-02	foot ³ /minute
metre ³ /day	1.834 528 E-01	gallon/minute
metre ³ /day	4.166 667 E+01	litre/hour
metre ³ /day	4.166 667 E-02	metre ³ /hour

VISCOSITY, PERMEABILITY

centipoise	1.0 *E-03	pascal-second (Pa.s)
centipoise	1.0 *E-02	dyne-second/centimetre ²
centipoise	2.088 543 E-05	pound-force-second/foot ²
centistoke	1.0 *E-06	metre ² /second (m ² /s)
centistoke	1.0 E+00	centipoise/(gm/cm ²)
metre ² /second	1.0 *E+06	centistoke
metre ² /second	1.0 *E+04	stoke
pascal-second	1.0 *E+03	centipoise
pascal-second	1.0 E+01	poise
pound-force-second/foot ²	4.788 026 E+01	pascal-second (Pa.s)
poise	1.0 *E-01	pascal-second (Pa.s)
stoke	1.0 *E-04	metre ² /second (m ² /s)
darcy	9.869 23 E-13	metre ³ (m ²)
darcy	9.869 23 E-09	centimetre ²
darcy	9.869 23 E-01	micrometre ² (µm ²)
darcy	1.0 *E+03	millidarcy
millidarcy-foot	3.008 142 E+04	micrometre ² -metre

MASS

grain [avoirdupois]	6.479 891 E-02	gram (g)
gram	1.543 236 E+01	grain
gram	1.0 *E-03	kilogram (kg)
gram	3.527 397 E-02	ounce
gram	2.204 622 E-03	pound

MULTIPLY	BY	TO OBTAIN
----------	----	-----------

MASS (CONTINUED)

kilogram	1.0 *E+03	gram
kilogram	3.527 397 E+01	ounce
kilogram	2.204 622 E+00	pound
kilogram	6.852 178 E-02	slug
kilogram	9.842 064 E-04	ton [long]
kilogram	1.102 311 E-03	ton [short]
kilogram	1.0 *E-03	ton [metric]
ounce	2.834 952 E+01	gram (g)
ounce	2.834 952 E-02	kilogram (kg)
pound	7.0 *E+03	grains
pound	4.535 924 E-01	kilogram (kg)
slug	1.459 390 E+01	kilogram (kg)
ton [long 2240 pounds]	1.016 047 E+03	kilogram (kg)
ton [short 2000 pounds]	9.071 847 E+02	kilogram (kg)
ton [metric]	1.0 *E+03	kilogram (kg)

DENSITY

gram/centimetre ³	1.0 *E+03	kilogram/metre ³ (kg/m ³)
gram/centimetre ³	6.242 797 E+01	pound/foot ³
gram/centimetre ³	8.345 405 E+00	pound/gallon
gram/centimetre ³	3.612 730 E-02	pound/inch ³
kilogram/metre ³	1.0 *E-03	gram/centimetre ³
kilogram/metre ³	6.242 797 E-02	pound/foot ³
kilogram/metre ³	1.002 242 E-02	pound/gallon
pound/foot ³	1.601 846 E-02	gram/centimetre ³
pound/foot ³	1.601 846 E+01	kilogram/metre ³ (kg/m ³)
pound/foot ³	1.336 805 E-01	pound/gallon
pound/gallon	1.198 264 E-01	gram/centimetre ³
pound/gallon	1.198 264 E+02	kilogram/metre ³
pound/gallon	7.480 520 E+00	pound/foot ³

FORCE

dyne	1.0 *E-05	newton (N)
dyne	2.248 089 E-06	pound-force
kilogram-force	9.806 650 *E+00	newton (N)
kilogram-force	2.204 622 E+00	pound-force
newton	1.0 *E+05	dyne
newton	1.019 716 E-01	kilogram-force
newton	2.248 089 E-01	pound-force
newton	3.596 942 E+00	ounce-force
ounce-force	2.780 139 E-01	newton (N)
pound-force	4.448 222 E+00	newton (N)
pound-force	4.535 925 E-01	kilogram-force

MULTIPLY	BY	TO OBTAIN
PRESSURE AND PRESSURE GRADIENT		
atmosphere, normal	1.013 25 E+00	bar
atmosphere, normal	3.389 95 E+01	feet of water, 4 deg C
atmosphere, normal	2.992 E+01	inches of Hg, 32 deg F
atmosphere, normal	7.6 *E+02	millimetres of Hg, 0 deg C
atmosphere, normal	1.013 25 E+05	pascal (Pa)
atmosphere, normal	1.469 60 E+01	pound/inch ²
bar	9.869 23 E-01	atmosphere, normal
bar	1.019 716 E+00	kilogram-force/centimetre ²
bar	1.0 *E+05	newton/metre ² (N/m ²)
bar	1.0 *E+05	pascal (Pa)
bar	1.450 377 E+01	pound/inch ²
centimetres of Hg at 0° C	1.333 22 E+03	pascal (Pa)
centimetres of Hg at 0° C	1.933 67 E-01	pound/inch ²
dyne/centimetre ²	1.0 *E-01	pascal (Pa)
dyne/centimetre ²	1.450 377 E-05	pound/inch ²
inches of Hg at 60 deg F		pascal (Pa)
inches of Hg at 60 deg F	4.898 E-01	pound/inch ²
feet of water at 4 deg C	2.988 98 E+03	pascal (Pa)
feet of water at 4 deg C	4.335 15 E-01	pound/inch ²
kilogram-force/centimetre ²	9.806 650 *E-01	bar
kilogram-force/centimetre ²	9.806 650 *E+04	pascal (Pa)
kilogram-force/centimetre ²	1.422 334 E+01	pound/inch ²
kilogram-force/metre ²	9.806 650 *E+00	newton/metre ² (N/m ²)
kilogram-force/metre ²	9.806 650 *E+00	pascal (Pa)
kilogram-force/metre ²	2.048 161 E-01	pound/foot ²
kilogram-force/metre ²	1.422 334 E-03	pound/inch ²
newton/centimetre ²	1.450 377 E+00	pound/inch ²
newton/metre ²	1.0 *E-05	bar
newton/metre ²	1.0 *E+00	pascal (Pa)
newton/metre ²	1.450 377 E-04	pound/inch ²
newton/metre ²	1.019 716 E-01	kilogram-force/metre ²
newton/millimetre ²	1.450 377 E+02	pound/inch ²
pascal	9.869 23 E-06	atmosphere, normal
pascal	1.0 *E-05	bar
pascal	1.019 716 E-01	kilogram-force/metre ²
pascal	1.0 *E+00	newton/metre ² (N/m ²)
pascal	2.088 543 E-02	pound/foot ²
pascal	1.450 377 E-04	pound/inch ²
pound/foot ²	4.882 429 E+00	kilogram-force/metre ²
pound/foot ²	4.788 026 E+01	pascal (Pa)
pound/foot ²	6.944 444 E-03	pound/inch ²

MULTIPLY	BY	TO OBTAIN
----------	----	-----------

PRESSURE AND PRESSURE GRADIENT (CONTINUED)

pound/inch ²	6.804 60 E-02	atmosphere, normal
pound/inch ²	6.894 757 E-02	bar
pound/inch ²	7.030 697 E-02	kilogram-force/centimetre ²
pound/inch ²	6.894 757 E-01	newton/centimetre ²
pound/inch ²	6.894 757 E+00	kilonewton/metre ²
pound/inch ²	6.894 757 E+03	newton/metre ² (N/m ²)
pound/inch ²	6.894 757 E-03	newton/millimetre ²
pound/inch ²	6.894 757 E+03	pascal (Pa)

ENERGY AND WORK

Btu [International table]	1.055 056 E+03	joule (J)
Btu [International table]	2.518 021 E-01	calorie [Kg, mean]
Btu [International table]	7.781 693 E+02	foot-pound
Btu [International table]	2.930 711 E-01	watt-hour
calorie [Kg, mean]	4.190 021 E+03	joule (J)
calorie [Kg, mean]	3.971 372 E+00	Btu [International table]
calorie [Kg, mean]	3.090 400 E+03	foot-pound
calorie [Kg, mean]	1.560 808 E-03	horsepower-hour
calorie [Kg, mean]	4.190 020 E+03	newton-metre
calorie [Kg, mean]	1.163 894 E+00	watt-hours
foot-pound	1.285 067 E-03	Btu [International mean]
foot-pound	1.355 818 E+00	joule (J)
foot-pound	3.235 826 E-04	calorie [Kg, mean]
joule (J)	9.478 170 E-04	Btu [International table]
joule (J)	2.386 623 E-04	calorie [Kg, mean]
joule (J)	7.375 621 E-01	foot-pound
joule (J)	2.777 778 E-04	watt-hour
joule (J)	1.0 *E+00	watt-second
watt-hour	3.6 *E+03	joule (J)

POWER

Btu/HR [International table]	2.930 711 E-01	watt (W)
foot-pound/hour	3.766 161 E-04	watt (W)
foot-pound/minute	3.030 303 E-05	horsepower
foot-pound/minute	2.259 697 E-02	watt (W)
foot-pound/second	1.818 182 E-03	horsepower
foot-pound/second	1.355 818 E+00	watt (W)
horsepower [550 ft-lbs/s]	7.456 999 E-01	kilowatt (KW)
horsepower	5.50 *E+02	foot-pounds/second
horsepower	3.3 *E+04	foot-pounds/minute
horsepower [electric]	7.46 *E+02	watt (W)
kilowatt	1.341 022 E+00	horsepower [550 ft-lbs/s]
watt	2.655 224 E+03	foot-pound/hour
watt	4.425 372 E+01	foot-pound/minute
watt	1.341 022 E-03	horsepower [550 ft-lbs/s]

MULTIPLY	BY	TO OBTAIN
----------	----	-----------

LENGTH

watt watt	1.340 483 E-03 3.412 141 E+00	horsepower [electric] Btu [International table]
--------------	----------------------------------	--

TEMPERATURE

TO CONVERT	SOLVE	TO OBTAIN
------------	-------	-----------

celsius degree	$K = ^\circ C + 273.15$	Kelvin (K)
celsius degree	$F = 1.8^\circ C + 32$	Fahrenheit degree
Fahrenheit degree	$C = (^\circ F - 32) / 1.8$	Celsius degree
Fahrenheit degree	$R = ^\circ F + 459.67$	Rankine degree
Rankine degree	$K = ^\circ R / 1.8$	Kelvin (K)

The SI unit of temperature is the degree Kelvin (written K without a degree symbol) and defined so the triple point of water is 273.16 exactly

C. MISCELLANEOUS OIL FIELD CONVERSIONS

MULTIPLY	BY	TO OBTAIN
<u>TEMPERATURE GRADIENT</u>		
°C/100 metres	5.486 4 E+01	°F/100 feet
°F/100 feet	1.822 7 E-02	°C/100 metres
<u>CONCENTRATION</u>		
grains/gallon	1.714 E-02	grams/liter
grains/gallon	1.712 E+01	parts per million
grains/gallon	1.429 E+02	pounds per million gallon
pounds/million gallon		grains/gallon
pounds/million gallon	1.1982 E-01	parts per million
<u>GAS-OIL RATIO</u>		
m ³ /m ³ at 15°C and 1 atm	1.801 175 E-01	scf/B at 60°F, 14.65 psia
scf/B at 60°F, 14.65 psia	5.551 931 E+00	m ³ /m ³ at 15°C and 1 atm
<u>GAS-VOLUME</u>		
m ³ at 15°C and 1 atm	3.549 373 E+01	scf at 60°F and 14.65 psia
scf at 60°F and 14.65 psia	2.817 339 E-02	m ³ at 15°C and 1 atm

GIVEN	USE FORMULA	TO OBTAIN
<u>OIL GRAVITY</u>		
°API	$\frac{141.5}{131.5 + ^\circ\text{API}}$	sp.gr. @ 60°F
sp.gr. @ 60°F	$\frac{141.5}{\text{sp.gr. @ } 60^\circ\text{F}} - 131.5$	°API
<u>GAS GRAVITY</u>		
gas density (gm/cc) at 60°F, 14.7 psia	$\frac{\text{gas density (gm/cc)}}{.00122}$	gas specific gravity
gas density (lbs/cu.ft.) at 60°F, 14.7 psia	$\frac{\text{gas density (lbs/ft}^3\text{)}}{0.762}$	gas specific gravity
	$\frac{\text{gas mol. weight}}{28.966}$	gas specific gravity

QUANTITY	MAGNITUDE	UNIT
PHYSICAL CONSTANTS AND VALUES		
Triple point of water	273.16 exactly 0.01 exactly 491.688 exactly 32.018 exactly	K °C °R °F
Absolute zero	0.00 exactly -273.15 exactly 0.00 exactly -459.67 exactly	K °C °R °F
Gas constant (R)	8.3143 8.3143 E+07 10.732	J·mol ⁻¹ K ⁻¹ erg·(gm mole) ⁻¹ K ⁻¹ psi·ft ³ (lb mole) ⁻¹ °R ⁻¹
Maximum density of water	999.973 0.999 973 62.426 1	kg·m ⁻³ g·cm ⁻³ lb _m ·ft ⁻³
Density of water at 60°F (15.56°C, 288.71 K)	999.014 0.999 014 62.366 4	kg·m ⁻³ g·cm ⁻³ lb _m ·ft ⁻³
Water gradient at 60°F (15.56°C, 288.71 K)	9,796.98 979.698 0.433 100	Pa·m ⁻¹ dyne·cm ⁻³ psi·ft ⁻¹
Standard atmosphere	1.013 25 E+05 1.013 25 E+06 14.695 9	Pa dyne·cm ⁻² psi
Density of air at 1atm, 60°F (15.56°C, 288.71 K)	1.223 2 1.223 2 E-03 0.076 362	kg·m ⁻³ g·cm ⁻³ lb _m ·ft ⁻³
Earth's gravitational acceleration, g	9.806 650 980.665 0 32.174 05	m·s ⁻² cm·s ⁻² ft·s ⁻²
g _c	1.000 000 1.000 000 32.174 05	kg·m·N ⁻¹ sec ⁻² g·cm·dyne ⁻¹ sec ⁻² lb _m ·ft·lb _f ⁻¹ s ⁻²
π	3.141 593	
e	2.718 282	
1/n(10)	2.302 585	
γ (Euler's constant)	0.577 215 66	
°API	141.5 γ(60°F)	-131.5